Universitat de Barcelona
Facultat de Química
Departament de Química Física

Theoretical Study of Phospholipid Membranes: the Complex Role of Cholesterol and Lipid Unsaturation

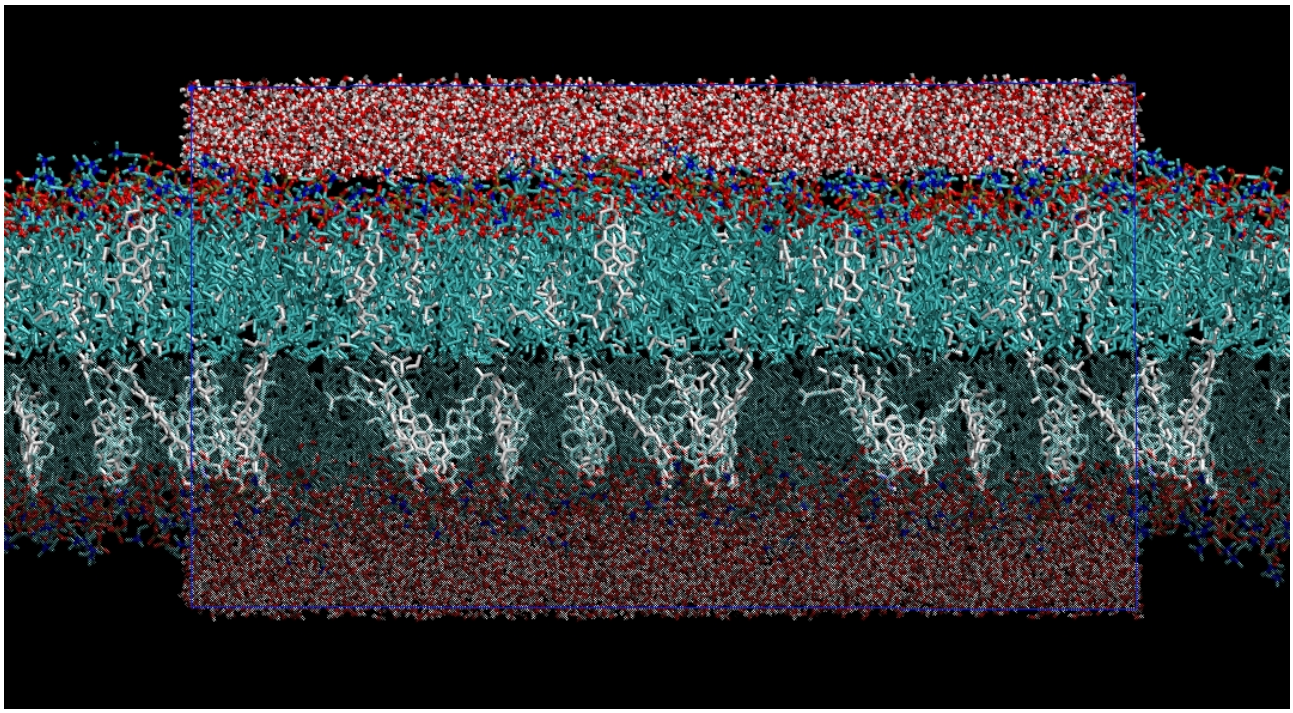

Hector Martínez-Seara Monné

Doctoral Thesis

Barcelona, maig del 2010

Universitat de Barcelona
Facultat de Química
Departament de Química Física

"Ciència i tecnologia de col·loides i interfases"
Programa de doctorat del bienni: 2003–2005

Theoretical Study of Phospholipid Membranes: the Complex Role of Cholesterol and Lipid Unsaturation

Memòria per optar al títol de
Doctor per la Universitat de Barcelona,
presentada per
Hector Martínez-Seara Monné

Barcelona, 7 de maig del 2010

Director:
Dr. Ramon Reigada Sanz
Departament de Química Física
Facultat de Química, UB

Director:
Dr. Francesc Sagués Mestre
Departament de Química Física
Facultat de Química, UB

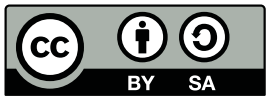

Attribution – Share Alike

You are free:

To Share – alter, transform, build upon this work, copy, distribute and transmit the work

Under the following conditions:

Attribution – You must attribute the work in the manner specified by the author or licensor (but not in any way that suggests that they endorse you or your use of the work).

Share Alike – If you alter, transform, or build upon this work, you may distribute the resulting work only under the same or similar license to this one.

With the understanding that:

Waiver – Any of the above conditions can be waived if you get permission from the copyright holder.

Other Rights – In no way are any of the following rights affected by the license:

- Your fair dealing or fair use rights;
- The author's moral rights;
- Rights other persons may have either in the work itself or in how the work is used, such as publicity or privacy rights.

Notice – For any reuse or distribution, you must make clear to others the license terms of this work. The best way to do this is with a link to the web page http://creativecommons.org/licenses/by-sa/3.0/.

A la meva estimada
iaia Rosa

Acknowledgements

Fer una Tesi, en el meu cas, és el somni de tota una vida. Un camí que va començar tot just quan era un infant. Molts volien ser bombers, policies o mestres, però jo ho tenia clar: volia ser doctor. Si bé en aquell moment no entenia del tot el significat d'aquesta paraula, sí que intuïa que era quelcom important.

Aquesta idea, és clar, no s'originà directament del meu encara immadur cervell, ni tampoc del meravellós entorn muntanyenc on vaig créixer. Més aviat va sorgir del respecte que, com tot nen, sentia per certes persones del meu entorn. Si he de destacar algú, tres persones, a les quals professo admiració, tingueren en mi una incidència cabdal.

La primera i sens dubte la més important fou mon pare. Les nostres interminables converses, debats i discussions sobre tot allò digne de dir-ne quelcom no tan sols han forjat el que sóc, sinó que també van despertar en mi la necessitat de saber. Així doncs li vull agrair de tot cor la seva paciència, no tan sols pel munt de preguntes contestades una i altra vegada, sinó també pel dia a dia en tants i tants dies d'estreta convivència.

La segona en ordre cronològic seria la meva tieta Matilde. Potser perquè va ser de les primeres persones amb qui vaig sentir que la nostra comunicació era d'adult a adult, potser per la seva manera de gaudir del dia a dia, potser per altres raons que no puc ni tan sols arribar a comprendre, però la veritat és que ha sigut capaç d'influir de manera decisiva en la meva percepció d'allò que m'envolta. A ella li dec sens dubte el meu interès per la natura i, per tant, es mereix el meu més sentit agraïment. Sense ella la realització d'aquesta tesi no hagués sigut el plaer que ha estat.

La tercera, i no per això menys important, va ser la meva tieta Tere. No hi ha prova més contundent de la meva admiració que la necessitat constant, a poc que es presenta l'ocasió, de dir a tothom que tinc una tieta professora de matemàtiques a la universitat. Potser perquè en certa manera allò de les matemàtiques té quelcom místic. Potser perquè va ser capaç de fer-me entendre el teorema de Steinitz. Potser perquè en el fons em meravellava que una persona pogués demostrar totes aquelles coses. Potser perquè la seva forma metòdica de fer les coses evitava allò que a mi sempre em passa, cometre errades ximples. En el fons el motiu tant se val. El resultat és que volia ser com ella: volia ser doctor. Així que no puc fer més que expressar-li el meu etern agraïment ja que sense ella no hauria pogut acceptar aquest repte del qual estic orgullós.

Les dues altres persones responsables directes de la consecució d'aquesta Tesi han estat

els meus Directors. Al Francesc li vull agrair la difícil decisió de confiar en mi i haver-me donat l'oportunitat de pujar al carro de la ciència. També vull ressaltar que per a mi és un exemple a seguir. En els molts anys que he estat fent aquesta Tesi, puc dir que és un pencaire com pocs. Quan el líder d'un grup és així, no es pot esperar menys que la excel·lència en el grup que dirigeix. Al Ramon li vull agrair la paciència, molta paciència, amb mi i amb el nostre projecte. Ell sap i jo també que les coses no han estat sempre fàcils. Més encara, la majoria de moments bons de què hem gaudit han estat precedits per dies de nervis i plors. Per això mil gràcies, ho hem aconseguit.

I would like to express my eternal gratitude to Tomasz Róg, my closer collaborator and often wise adviser. I would also like to thank Ilpo Vattulainen and Mikko Karttunen for their scientific and financial contribution to this project.

Voldria agrair a l'extint "Ministeri de ciència i tecnologia", avui "Ministeri d'indústria, turisme i comerç", demà Déu dirà, la seva generosa contribució que ha permès per quatre anys que no sàpiga com respondre a la pregunta de: Estudies o treballes? També vull agrair el seu suport de la xarxa europea SIMBIOMA, la "Aalto University School of Science and Technology" i la "Tampere University of Technology".

També vull donar les gràcies a aquells que han participat en el procés d'elaboració d'aquesta Tesi: Isabel Pastor, Antonio Via, Lorna Stimson, Vera Moshina, Sergi Monteagudo, l'excel·lent col·lectiu de persones que constitueix el departament de Química Física i molts altres que segur m'he descuidat.

Finalment un fort agraïment a la família i amics. Sou el més valuós tresor que tinc i tindré en aquesta vida.

Part I

Doctoral Thesis

Overview of Contents

Contents

List of Figures

List of Tables

List of Publications

This Thesis consists of this Manuscript and the following publications:

[I] H. Martinez-Seara, T. Róg, M. Pasenkiewicz-Gierula, I. Vattulainen, M. Karttunen, and R. Reigada. "Effect of Double Bond Position on Lipid Bilayer Properties: Insight through Atomistic Simulations". *J. Phys. Chem. B*, Vol. 111, No. 38, pp. 11162–11168, 2007.

[II] H. Martinez-Seara, T. Róg, M. Pasenkiewicz-Gierula, I. Vattulainen, M. Karttunen, and R. Reigada. "Interplay of Unsaturated Phospholipids and Cholesterol in Membranes: Effect of the Double-Bond Position". *Biophys. J.*, Vol. 95, No. 10, pp. 3295–3305, 2008.

[III] H. Martinez-Seara, T. Róg, M. Karttunen, I. Vattulainen, and R. Reigada. "Why is the *sn*–2 Chain of Monounsaturated Glycerophospholipids Usually Unsaturated whereas the *sn*–1 Chain Is Saturated? Studies of 1–Stearoyl–2–oleoyl–*sn*–glycero–3–phosphatidylcholine (SOPC) and 1–Oleoyl–2–stearoyl–*sn*–glycero–3–phosphatidylcholine (OSPC) Membranes with and without Cholesterol". *J. Phys. Chem. B*, Vol. 113, No. 24, pp. 8347–8356, 2009.

[IV] H. Martinez-Seara, T. Róg, M. Karttunen, R. Reigada, and I. Vattulainen. "Influence of cis double-bond parametrization on lipid membrane properties: How seemingly insignificant details in force-field change even qualitative trends". *J. Chem. Phys.*, Vol. 129, No. 10, p. 105103, 2008.

[V] H. Martinez-Seara, T. Róg, M. Karttunen, I. Vattulainen, and R. Reigada. "Cholesterol induces specific spatial and orientational order in cholesterol/phospholipid membranes". Under revision.

[VI] T. Róg, H. Martinez-Seara, N. Munck, M. Oresic, M. Karttunen and I. Vattulainen. "Role of Cardiolipins in the Inner Mitochondrial Membrane: Insight Gained through Atom-Scale Simulations". *J. Phys. Chem. B*, Vol. 113, No. 11, pp. 3413–3422, 2009.

During the execution of the work included in this Thesis the author has also been involved in several projects not included in this Thesis. The resulting publication can be found below:

- J. Claret, J. Crusats, R. Albalat, J. Ignés-Mullol, H. Martinez-Seara, R. Reigada, and F. Sagués. "Travelling waves in two-dimensional smectic-C domains". *Eur. Phys. J. E*, Vol. 21, pp. 111–116, 2006.

List of Abbreviations

Abbreviation	Details
ACF	Auto Correlation Function
Card	Cardiolipin
CHOL	Cholesterol
DCHOL	Flat Cholesterol Without out Off-plane Methyl Groups
DOPC	1,2–dioleoyl–*sn*–glycero–3–phosphatidylcholine
DLPC	1,2–dilauroyl–*sn*–glycero–3–phosphatidylcholine
DSPC	1,2–distearoyl–*sn*–glycero–3–phosphatidylcholine
DVPC	1,2–divacenyl–*sn*–glycero–3–phosphatidylcholine
OSPC	1–oleoyl–2–stearoyl–*sn*–phosphatidylcholine
Phd	Glycero–Phospholipid
PhdA	Glycero–Phosphatic Acid deriravite lipid
PhdCho	Glycero–Phosphatidylcholine deriravite lipid
PhdEtn	Glycero–Phosphatidylethanolamine deriravite lipid
PhdGly	Glycero–Phosphatidylglycerol deriravite lipid
PhdIns	Glycero–Phosphatidylinositol deriravite lipid
PhdSer	Glycero–Phosphatidylserine deriravite lipid
POPC	1–palmitoyl–2–oleoyl–*sn*–phosphatidylcholine
POPE	1–palmitoyl–2–oleoyl–*sn*–phosphatidylethanolamine
SL	Sphingolipid
SM	Sphingomyelin
SOPC	1–stearoyl–2–oleoyl–*sn*–phosphatidylcholine
T_m	Melting Temperature
χ_c	Cholesterol Molar Fraction
χ_c^*	Cholesterol Molar Fraction Solubility Limit

CHAPTER 1

Membranes

1.1 General Description

A membrane can be defined as a quasi-two dimensional physics object that separates two media, while remaining permeable only to specific components under adequate driving forces.

According to their origin, membranes can be classified as biological or artificial. Biological membranes constitute the boundary between a cell and its surroundings (plasma membrane), and also separate different organelles and compartments of the cell. Biological membranes deal with several critical tasks. The most important is to separate the cell from the environment; the breakage of the plasma membrane, the one surroundings the cell, always leads to its death. They are semipermeable and control the traffic of different substances across them by passive or active mechanisms. Characteristic mechanical properties exhibited by membranes enhance their usage as attachment platforms for many enzymes. They are also fundamental to maintain the resting cell potential. The plasma membrane is also the attaching point of the cytoskeleton and, if present, the extracellular wall. In cooperation with other cellular components it can be responsible for the cell movement.

Since biological membranes are complex, model membranes are often used to study their generic and fundamental properties and their dependence on, for example, a particular lipid or surfactant composition. They are artificial membranes designed to mimic biological ones. Their theoretical and numerical study is the main goal of this Thesis.

1.2 Historical Background

The history of membranes dates back to the XVII century when Robert Hooke discovered the cell [Hook65]. We had to wait until 1855 when Carl Nägeli noticed the presence of the plasma membrane, and named it. Later observations between 1895 and 1902 by Ernest Overton suggested the Meyer-Overton rule, which is widely used to predict the potency of anaesthetics [Katz94]. The Meyer-Overton rule states that the permeability across the membrane is directly correlated to the solubility of the crossing particles into lipids. According to this,

they proposed that the thin-layer surrounding the cell has to be composed of lipids.

The first glimpse of the cell membrane's structure came in 1925 when Evert Gorter and F. Grendel completed their acclaimed experiment [Gort25] with ghost erythrocyte membranes. They compared the calculated superficial area of the cell with the superficial area of a Langmuir monolayer obtained from the lipids extracted from the cell membrane. The data obtained showed that the area of the monolayer was approximately twice the one of the cell. Consequently, they proposed that the plasma membrane has to be a **bimolecular layer**.

> ...the chromocytes [erythrocytes] of different animals are covered by a layer of lipoids [lipids] just two molecules thick...every chromocyte is surrounded by a layer of lipoids, of which the polar groups are directed to the inside and to the outside [of the cell] in much the same way as Bragg (1) supposes the molecules to be oriented in a 'crystal' of a fatty acid, and as the molecules of a soap bubble are according to Perrin (2). On the boundary of the two phases, one being the watery solution of hemoglobin, and the other the plasma, such an orientation seems a priori to be the most probable one.(Gorter and Grendel, 1925, p.439)

The following advances in understanding membranes and their physical properties were closely related to the development of highly innovative instrumentation techniques. In the mid-1930s, F. O. Schmitt found that the rotation of polarized light by myelin sheaths suggested the presence of proteins in membranes. The first attempt to incorporate proteins into the membrane description was made by Danelli and Davson in 1935 [Dani34] with the **Paucimolecular** or **Davson-Danielli** membrane model. They proposed that proteins may be unwrapped on top of the lipid bilayer with their side chains inserted into the apolar core of the bilayer and their polar linkages projected into the water phase. As a result, their model consists of a lipid bilayer capped on the inside and the outside by proteins and with protein-lined pores to account the easy movements though membranes by small molecules. This model was the basis of many others for more than 30 years and supported by many experiments, such as observations from electron microscopy [Genn89].

In 1970, the fluid nature of biomembranes was foreseen by David Frye and Michael Edidin. They followed mouse and human surface antigens by indirect fluorescent antibody technique [Frye70]. Furthermore, sequential extraction experiments of human erythrocyte membranes performed in 1972 by Tanner and Boxer proved that most membrane proteins could not be removed by extraction with salt [Tann72]. Thus they concluded that membrane proteins are strongly attached to the membrane. These experimental observations led to the announcement of the famous **fluid mosaic** model by S. Jonathan Singer and Garth L. Nicolson in 1972 [Sing72]. According to this model, both proteins and lipids are free to diffuse in the bilayer, implying a random organization. This revolutionary view also described the membrane as a fluid-like lipid bilayer where membrane proteins are not only attached to the surface (*peripheral*) but also embedded (*integral* and *transmembrane*) in the fluid lipid matrix. This dynamic view of the membrane sharply contrasts with the static view of the **Davson-Danielli** model and agrees with the rapid diffusion of proteins measured by Frye.

Despite the great heuristic value in understanding the membrane topology achieved by the **fluid mosaic** model, it presents several inaccuracies due to its simplicity. The implicit randomness of the model is its major weakness [Jaco95]. Already before the 90's, some heterogeneities in the membrane concerning either protein and lipid were reported

[Stie73, Isra80, Edid94]. For example, the lateral mobility of cell membrane glyco-proteins was often found to be restricted [Edid94, Damj95]. Based on these results Kusumi and colleagues proposed the **membrane-skeleton fence** model [Kusu93, Kusu96] where the existence of a mesh (probably originated from the cytoskeleton [Sako94]) is invoked to explain the restriction of the protein diffusion. In the case of lipids , the predominant evidence that supports this fact was the discovery that a fraction of the cell membrane lipids were insoluble under treatment with non-ionic detergent (triton X-100) at low temperatures [Brow92, Brow97]. This finding lead to the **lipid raft** model published by Simons and Ikonen in 1997 [Simo97]. This theory proposes the existence of domains enriched in cholesterol, sphingolipids and specific proteins, called lipid rafts. The role of these submicrometer scale domains has been proven to be critical in many cellular processes in mammalian cells [Brow98, Edid03, Simo04].

Finally, in 2003 Vereb et al. proposed a modified version of the fluid mosaic model of Singer and Nicolson: the **dynamically structured mosaic** model [Vere03]. It tries to unify the old view given by fluid mosaic model with, at that time, new experimental observations. This is achieved by shifting the view from the fluidity to emphasize the mosaicism. This model claims that the forces needed for the observed domain formation are not only based on lipid-lipid, protein-protein, and protein-lipid interactions but also in some supra-membrane effectors such as the cytoskeleton and extracellular matrix. This model achieves a more realistic description of biomembranes.

Current understanding of cellular membranes remains incomplete. The complex relation between membrane composition, structure and functionality remains unresolved. Moreover, how the cell regulates membrane behavior is mainly unknown [Zhan08]. This encourages, day after day, scientists all over the world to unravel different aspects of membranes.

1.3 The Structure of Membranes

Membranes are thin (<10 nm) layers that cells use to constitute different compartments and mainly consist of proteins and lipids. The basic structure of a membrane is given by the amphiphilic nature of the constituent lipids. The term 'amphiphilic' describes a chemical compound possessing both hydrophilic (polar) and hydrophobic (apolar) properties. These molecules try to be in contact to the aqueous environment with their polar headgroup while the apolar part tends to minimize it. The self-assembling capabilities of these moieties lead to lyotropic stable phases or aggregates [Isra91, Cook06], see some of them in Fig. 1.1. In all of them, cell membranes correspond to the bilayer configuration, see Fig. 1.2.

1.3.1 Membrane Constituents: "Building Blocks"

Most of the mass of a biological membrane is mainly composed of lipids and proteins, although the exact proportion depends on the studied membrane. Protein content varies from 25 to 75% in weight, although lipids are the components that form most of a membrane's surface area [Silb67, Korn69, Sing72]. The typical ratio in animal cells is about 50% in weight [Davi03]. The immense diversity and proportions of lipid and protein molecules present in biological membranes substantially complicates the study of the relationship between their composition and functionality. To investigate this problem, the knowledge about the structure of the different involved moieties is needed. So far, a strategy based on functional groups has proven

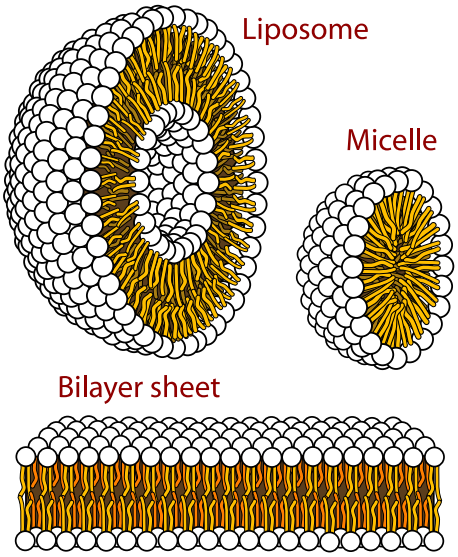

Figure 1.1: Cross section of various structures that phospholipids can adopt in an aqueous solution. The circles are the hydrophilic heads and the wavy lines correspond to the fatty acyl chains. Adapted from [Ruiz07b].

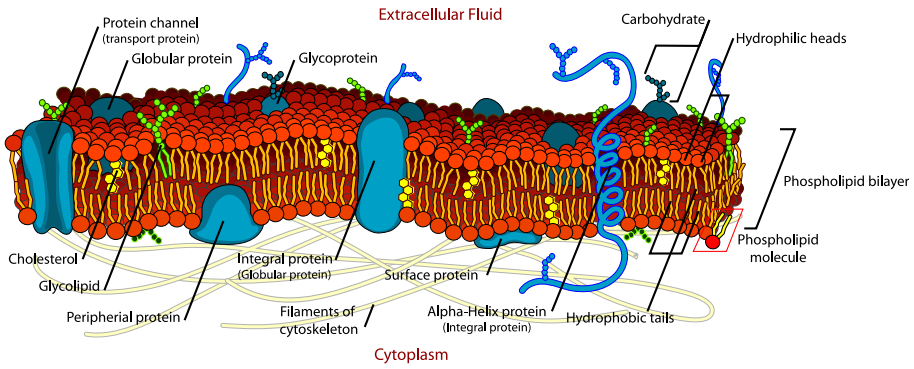

Figure 1.2: Schematic representation of the cell membrane structure. Adapted from [Ruiz07a].

to be successful in order to bring some order to this complex issue. This approach allows us to group moieties with structural similarities that leads to similar specific functionalities.

1.3.1.1 Major Structural Lipids

The fraction of the genetic code devoted to the synthesis of lipids is about 5% resulting in thousands of lipid moieties and forming the biomembranes [Meer05, Sud07, Meer08]. Accepting the hypothesis that cells have evolved to improve their functionality, most of these molecules should have a well defined function. Some of them, however, might correspond to evolutionary fossils [Horr99]. Another reason for lipid diversity can be attributed to the lack of synthetical selectivity and the existence of several precursors. In any case, it is clear that the selection of its lipid components confers the cell membrane a delicate control over its functionality.

Lipids of interest in this section are constituted by the linkage of smaller molecules, see Fig 1.3. Fatty acids, glycerol, phosphoric acid, sphingosine and sugars are some of these molecules.

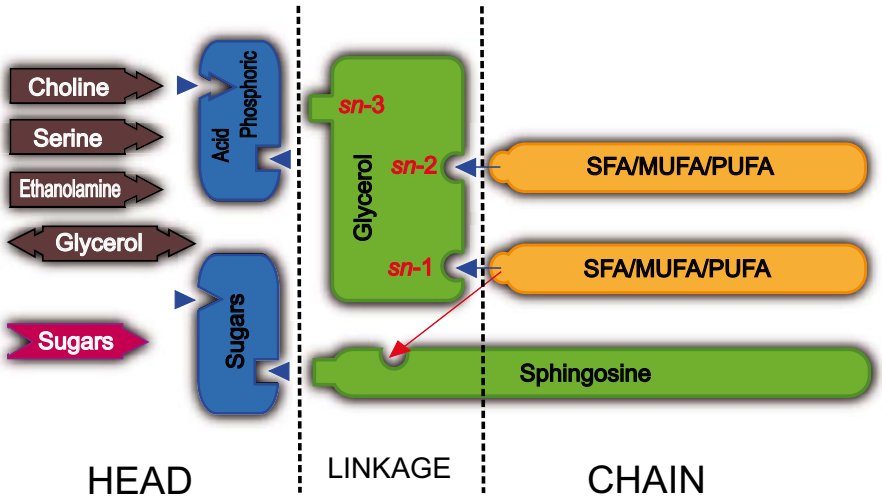

Figure 1.3: Conceptual model of the membrane lipids by attachment of "Building Blocks" and their functional regions. Where SFA=Saturated, MUFA=Monounsaturated and PUFA=Polyunsaturated fatty acids.

Phospholipids (Phd), glycolipids and sphingolipids (SL) constitute the three major classes of these lipids in biomembranes. Their hydrophobic backbone is mainly constituted by long fatty acids, sphingosine or similar molecules. They provide the hydrophobic core of the membrane and are rarely in contact with the surrounding water. Their length is variable and usually system dependent, but with normal values range from C_{14} to C_{22} [Olss97], unusual lengths as long as C_{36} have been found in phospholipids in photoreceptor retina membranes [Avel87]. An additional important feature of the chains is their unsaturation level. Sphingomyelins rarely present any additional unsaturation apart from the sphingosine one, a common example can be found in palmitoyl-SM. Other lipids may have double bonds (up to 6), i.e. DOPC or DLPC, although saturated chains are also frequent, i.e. DPPC or DSPC. Asymmetric composition of each chain is also rather common, e.g. POPC or SOPC. The major role of the double bond is to maintain the fluidity of the membrane [McEl82, Lewi88], although it may be indirectly involved in cell signaling and protein functionality. In higher organisms a large fraction of the membrane lipid chains are unsaturated [Hulb03] with *cis* double bonds. Remarkable findings by Hulbert show an inverse correlation between the size of the birds and mammals, and the concentration of double bonds in cell membranes [Hulb03]. The size seems to be also correlated with the presence of monounsaturated chains and inversely correlated with the presence of polyunsaturated ones [Hulb03]. One of the main issues addressed in this Thesis deals with the importance of phospholipid unsaturation on different membrane properties.

The linkage of the fatty acids to the headgroups occurs in nature by esterification of two fatty acids in two adjacent positions [*sn*–2 (β), *sn*–1 (γ)] of a glycerol molecule (the so-called glycerol-based lipids), or by amide linkage between the sphingosine alcohol and a fatty acid

(sphingolipids). Attached to these structures can be additionally found either a sugar by a glycosidic linkage [Reno89] or a esterified phosphoric acid. They constitute the heads of glycolipids and phospholipids, respectively. Sphingolipids can be seen as phospholipids or glycolipids with a sphingosine or related alcohol backbones. The acid phosphoric generally has other molecules esterified simultaneously to the glycerol or sphingosine. The variety of them is indeed quite large. Choline and ethanolamine are common examples. Others like serine, inositol and glycerol are typical for glycerol-based lipids, while sugars of different complexity are usually found in sphingolipids. In any case, the resulting headgroup is substantially hydrophilic. The presence of net charge, charge distribution, cross sectional area, volume, hydration level, presence of acceptor/donor atoms for hydrogen bonds, are just a few of the large number of distinctive structural properties of the resulting headgroups. All these possibilities generate large diversity of membrane lipids.

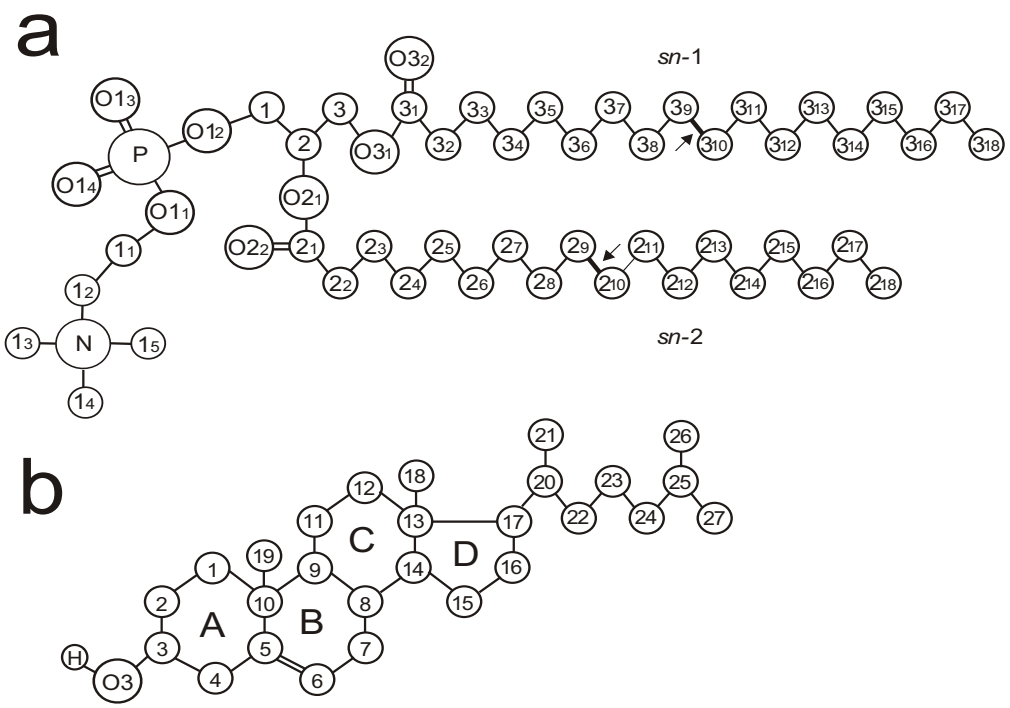

Figure 1.4: (a) Molecular structure of DSPC and (b) cholesterol molecules with numbering of atoms. In panel (a) the arrows indicate the locations of the double bonds in DOPC. In both panels, the chemical symbol for carbon atoms, C, is omitted.

Some of the lipid properties can be deduced from their shapes. A very important structural class is formed by glycerol-based lipids with a phosphatidylcholine headgroup (PhdCho). They show a high tendency to form planar bilayers because the voluminous headgroup results in a global cylindrical shape, see Fig. 1.4. They usually possess a *sn*–2 *cis*-unsaturated chain which favors membrane fluidity. Instead, glycerol-based lipids with a phosphatidylethanolamine headgroup (PhdEtn) present a global conical shape due to their smaller headgroups. Additions of PhdEtn lipids into PhdCho bilayers cause curvature stress into the membrane and processes like budding, fission and fusion are facilitated by this kind of "cone-shaped" lipids [Mars07]. Sphingolipids are another important class of structural

lipids having a cylindrical shape. Their chains are generally saturated and larger than in PhdChos, so they form thicker and more ordered bilayers.

In addition to the shape, another important feature of a lipid is the charge of the headgroup. They can be either neutral or charged. Normally, neutral lipids are zwitterionic, e.g. PhdCho and PhdEtn. Natural charged lipids are mostly monovalent and negatively charged, e.g. PhdSer, PhdIns, PhdA. Only few, highly specific lipids are divalent (-2 e), e.g. cardiolipins (Card), or more, e.g. lipid A. The study of the effect of cardiolipins on lipid membranes is addressed in chapter 8.

1.3.1.2 Cholesterol

Cholesterol is a major constituent of mammalian cell membranes [Meer08]. Due to its relevance and roles in the structural and dynamic properties of cell membranes it deserves a full section for itself [Vanc00, Rog09b]. The coincidence between the surge of eukaryotic cells and the appearance of the cholesterol as a membrane component has been suggested [Bloo91]. Cells are provided with a complete set of tools to tightly self regulate its cholesterol content [Simo00], and malfunctions in these regulations are related to several illnesses [Simo02, Taba02].

The structure of cholesterol as a lipid is peculiar, see Fig. 1.4. Three six–membered rings (*A*, *B*, *C*) plus one five–membered ring (*D*) attached in *trans* configuration constitute its flat-rigid steroid backbone, which is responsible of its ordering abilities. Two methyl groups between rings *A*-*B* and *C*-*D* sharing the same side of the steroid plane (rough face) expand the functionality of the backbone. Several works, have confirmed the utility of these two off-plane methyl groups, and dismissed the possibility of being evolutionary fossils [Rog07a, Mart08b, Mart09]. This issue, constitutes an important part of the work presented in this Thesis. The interaction of these methyl groups and the sterol plane with the acyl chains of the phospholipid components of a bilayer is exhaustively investigated in this work. Furthermore, the presence of a double bond in the *B* ring between atoms C5 and C6 has also been determined to be essential [Xu05]. The 1,5-dimethylhexane chain bounded to the *D* ring completes the hydrophobic core. This chain enhances the membrane stability [Suck76, Crai78, Suck79, Ruja86, Vemu89, Shou90]. Hydrophilic behavior is provided by the 3-β-hydroxyl group in *A* ring. It determines the cholesterol orientation in the bilayer by its interaction with the polar headgroups of other lipids [Mart08b] by hydrogen bonding although direct interaction with water cannot be excluded. The most important role of cholesterol is related to its influence to determine the physical properties of membranes: fluidity, lipid chain ordering, bending rigidity, permeability [Rog09b], see also Sec. 1.4. Some of these properties will be analyzed in this Thesis for cholesterol-containing lipid membranes.

Promotion of particular lipid configurations and lateral nanoscale organization are also important topics concerning cholesterol containing membranes. Their origin might be found in the different interactions of cholesterol with saturated and unsaturated lipids, see Sec. 1.4 and Sec. 1.5.

1.3.1.3 Membrane Proteins

Proteins are polymeric structures constituted by different aminoacid combinations [Davi03]. Proteins which are related to the membranes can be classified into two categories according

the level of interaction with the membrane. On the one hand, *peripheral* proteins are loosely attached to the membranes and can be easily dissociated using mild treatments. On the other hand, *integral* proteins, being normally >70% of the total number of the membrane proteins [Sing72]. They are embedded into the membrane and in some cases traversing it, the so-called *transmembrane* proteins, see Fig. 1.2. The dissociation of those membrane proteins requires more energetic agents as detergents, bile acids, protein denaturants or organic solvents. These proteins strongly affect the membrane properties and, in turn, the membrane influences the protein conformation and functionality. They normally have a globular shape with an elevated α-helix content [Ke65, Lena66, Wall66, Fost71] as a hydrophobic core that constitutes the backbone. This optimizes the free energy of the protein by minimizing the contact of the apolar residues with the solvent. In contrast, the surface in contact with the solvent is full of polar aminoacids. They present an amphiphilic structure [Wall66, Warr70] that fixes the proteins in one particular orientation and layer making flip-flop improbable [Sing72].

1.3.2 Lipid Composition

It is well known that membrane functionality is tightly coupled to composition. Proteins and lipids, substantially differ from membrane to membrane not only in their proportion but also in their moieties. On the one hand, the presence of different protein moieties is conceptually easy to justify. On the other hand, it is more difficult to justify the large amount (hundreds, thousands) of lipid moieties that may form a cell membrane. The lipid composition of biological membranes (lipodomics) remains to be an active field of study, see Table 1.1. Composition range for each moiety changes widely between different kinds of cells. In eukaryotic membranes a larger fraction of lipids are Phds [Dewe71], and from them more than 50% in weight are PhdChols. Other important phospholipids classes are PhdEtn, PhdSer, PhdIns and PhdA, whereas others are more cell specific. Mammalian cells have cholesterol (up to 40% of molar lipid content) and SL, the later especially in the outer plasmatic layer as SM or Glycosphingolipids [Li07, Tafe07]. Yeast cells possess ergosterol instead of cholesterol [Hain01]. Plants contain a substantial amount of Glycolipids. Bacterial membranes are radically different: the presence of PhdChos and SLs is negligible, whereas the major structural lipids are PhdEtn, PhdSer and PhdGly. They also contain unique lipids, e.g. Card which can also be found in mitochondria [Daum85].

Another level of complexity is found in different cell organelles. Each organelle membrane has a particular composition [Meer08]. The local and specific synthesis of lipids on each organelle and the selective transport between them are the major reasons for this. An additional source of complexity comes from the fact that different compositions are found in each layer of a given cell membrane. In addition to the local synthesis and specific transport, the underlying mechanisms of lipid asymmetry are multiple. First, the different natural flipping ability of lipids, governed mainly by the size, charge, and polarity of the headgroup [Stec02, Lope05, Angl07, Papa07]. Second, the presence of specific translocation mechanism which can be ATP-independent, especially in membranes where lipids are synthesized [Kol04, Pomo06, Dale07, Papa07], or ATP-dependent, like in the Golgi apparatus [Grah04, Pomo06, Dale07]. Third, the local ability to attach specific moieties in a given leaflet.

The specific lipid type (PhdCho, PhdEtn, PhdSer, SL...) proportions of a given membrane is genetically encoded [Gold69] and it is regulated by many processes involving lipid synthesis

Compound	Mye	Ret	Plas	Mito	Bac	Chlo
Protein	22	59	60	76	75	48
lipids	78	41	40	24	25	52
PhdCho	7.5	13	6.9	8.8		
PhdEtn	11.7	6.5	6.5	8.4	18	
PhdSer	7.1	2.5	3.1			
PhdIns	0.6	0.4	0.3	0.75		
PhdGly					4	
Card		0.4		4.3	3	
SM	6.4	0.5	6.5			
Glycolipid	22.0	9.5	Trace	Trace		23
CHOL	17.0	2.0	9.2	0.24		
Total Phd	33	27	24	22.5	25	4.7
% Phds of total lipid	42	66	60	94	>90	9

Table 1.1: Membrane composition: Percentage of total weight of membrane. Adapted from [Davi03].Abbreviations: Mye=Myelin (bovine); Ret=Retinal rod; Plas=Plasma membrane (human erythrocyte); Mito= Mitochondrial membranes; Bac=E. colib (inner and outer membranes); Chlo= Chloroplasts

and transport. Lipid transport between different membranes or cell compartments involve complex mechanisms as lateral diffusion through membrane continuities, budding and fusion of membrane vesicles in the secretory and endocytic pathways, monomers traffic assisted by soluble and membrane proteins, etc. Full understanding of cell lipid homeostasis and the connection between composition, structure and functionality is one of the biggest challenges in cell biology [Zhan08].

The distribution of different acyl chains among the lipid classes of the cell membranes is also vast [Olss97]. Phase behavior [Koyn98], permeability [Math08], structural and mechanical properties of the membrane are directly affected by the lengths and degree of unsaturation of the acyl chains. Their occurrences are also genetically encoded, although they can vary in order to adapt to the environment [Stub84, Garb95, Webe96, Iske98]. This contrast with the fraction of lipid types (PhdCho, PhdEtn, PhdSer, SL...) found in a membrane that is rather fixed [Gold69, Smit82, Olss96]. In general, SLs present long and saturated chains, whereas the PhdChos present a wider distribution of chains with different degrees of unsaturation and lengths. The presence of saturated (DPPC, DSPC) or unsaturated (DOPC) symmetric PhdChos is biologically relevant, although the most common PhdChos moieties present a saturated chain in *sn*–1 (normally 16:0 or 18:0) and an unsaturated one in *sn*–2 [Olss97]. In case *sn*–2 chain is only monounsaturated, it has been found that derivatives of the oleic acid (18:1c9) (Fig. 1.4) are the most common. This particular chain interestingly present its double bond just in the middle what has been probed to be a non fortuitous characteristic in chapter 4.

1.4 Thermodynamics of Lipid Membranes

The large variety of lipid moieties present in biological membranes makes the study of their phase behavior a rather complicated task. To study this problem, the phase stability of synthetic model membranes with an increasing complexity in lipid composition can be performed. First, pure lipid bilayers that generally display the existence of two mesomorphic phases known as L_α and gel states. The gel phase is found at low temperatures and corresponds to a solid (crystalline) state where the lipid acyl chains are fully extended with all their C-C bonds in the *trans* conformation and packed together parallel to each other. The L_α state appears at high temperatures and corresponds to a fluid (liquid-crystalline) phase where the lipid acyl chains present the occurrence of rotational gauche isomers (120° rotation about the C-C bonds) accompanied by a more disordered behavior. The physical properties of both phases are rather different. The gel phase shows lower lateral and rotational lipid diffusions [Suga05], smaller area per lipid and thicker [Dimo00, Rawi00, Meck03] and more rigid bilayers [Kobe98, Tris02] than the fluid L_α state.

The transition between the gel and the fluid states in lipid bilayers is first-order and it is usually called the main or melting transition. It occurs at temperature T_m that depends on the nature of the headgroup, the length of the acyl chains and the number and position of double bonds in the acyl chains. In general, lipids with short and unsaturated acyl chains have a low T_m (low-melting lipids) whereas lipids with large and saturated acyl chains have a high T_m (high-melting lipids).[Koyn98]

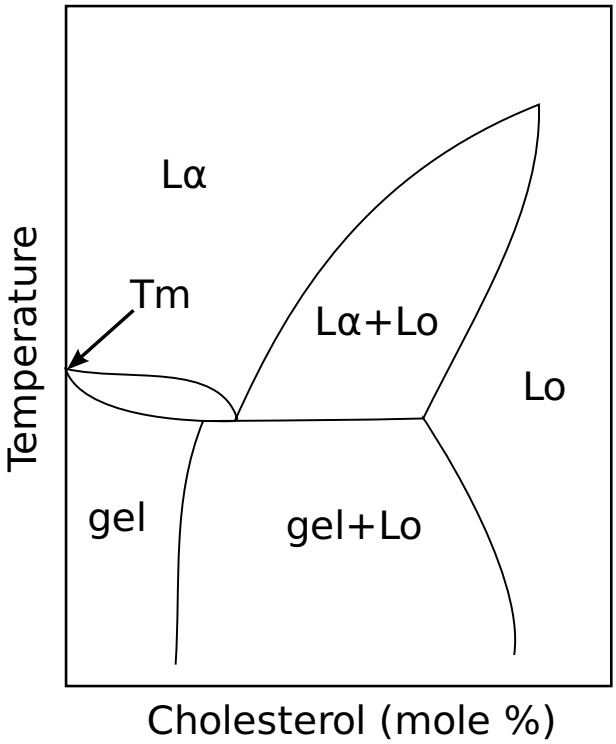

Figure 1.5: Phase diagram of a binary membrane. Adapted from [Vist90].

Addition of cholesterol to lipid bilayers induces strong modifications in their phase behavior, see Fig. 1.5. The main effect is the appearance of a new phase, the liquid ordered (L_o) state, between the two previous gel/L_α phases, smearing out the lipid main transition. The presence

of the rigid steroid part of the cholesterol molecule orders the acyl chains of the lipids around it [Habe77, Oldf78, Jaco79, Blum82, Corn83, Vist90] and therefore induces a condensing ordering effect when introduced in a fluid-phase lipid bilayer. On the contrary, when added to a gel bilayer, its fluidity is strongly increased [Kuo79]. The L_o phase is still rather liquid (lateral [Rube79, Lind81, Alec82] and rotational [Corn83] lipid diffusion are not significantly restricted), but the bilayer becomes more rigid [Need88], more ordered, thicker [Hui83] and less permeable [Deme72] than in the L_α phase. All these features correspond to fundamental physical properties of eukaryotic cell membranes, revealing the important role of cholesterol in these systems [Davi79, Davi80a, Mara82, Ranc82, Bloo88].

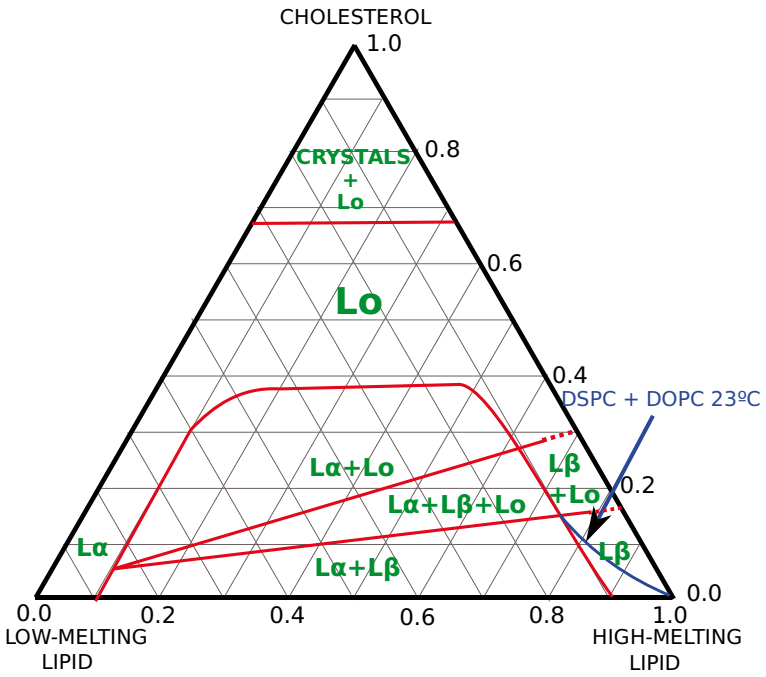

Figure 1.6: Phase diagram of a ternary membrane. Adapted from [Feig09].

A better understanding of the phase behavior of biological membranes is provided by the phase diagrams of ternary model bilayers composed of a low-melting lipid (for example an unsaturated phospholipid), a high-melting lipid (for example a saturated sphingolipid) and cholesterol. An example of such phase diagram is provided in Fig. 1.6, and others can be found in Refs. [Veat03, Veat05b, Veat05a, Feig06, Zhao07a, Feig09]. Different coexistence regions appear in the diagram and the most relevant in the biological context corresponds to the L_α/L_o region. In this zone, liquid disordered domains rich in low-melting (unsaturated) lipids and liquid ordered domains rich in high-melting (saturated) lipids and cholesterol, coexist [Veat03, Veat05b, Veat05a, Feig06, Zhao07a, Feig09].

1.5 Lipid Arrangements: Lateral Structures

The properties of lipid membranes are largely determined by the collective behavior of the interacting lipid species, so not only the global membrane composition but the lateral distribution of the different lipid components needs to be known to understand such behavior. In cholesterol-containing model lipid bilayers (as models to approach biological membranes) the

specific interaction between lipid molecules, including cholesterol, has been extensively studied and four different scenarios can be considered: a random lipid distribution, the formation of regular spatially arranged structures, the formation of lipid-cholesterol complexes and the generation of segregated domains with different composition [Von 78], see Fig. 1.7. The last three options can be of applicability in the biological context and will be summarized in the following subsections.

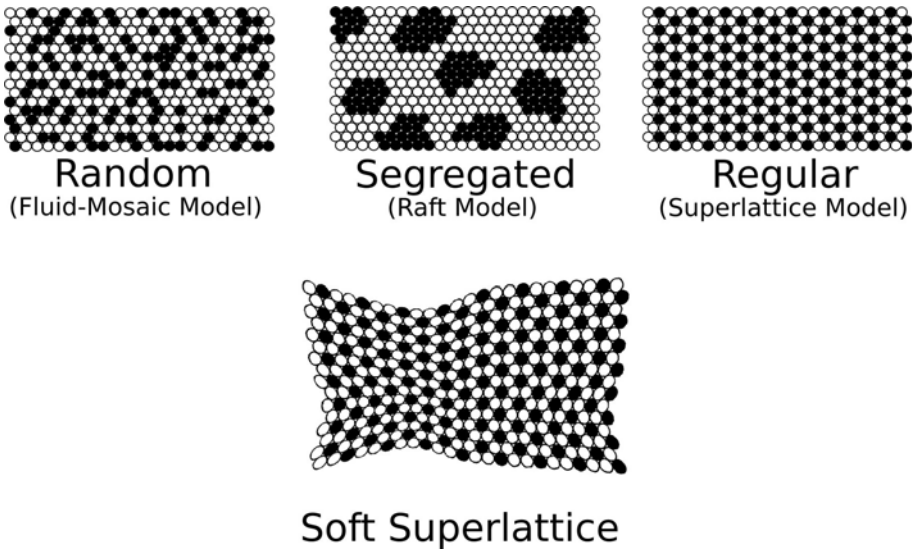

Figure 1.7: Models for lateral lipid organization in membranes. Each ball color accounts for a particular lipid moiety. For example, in cholesterol binary mixtures they will be a Phd/SL and cholesterol. In the raft model balls not only account for a given Phd/SL (black balls stand for high-melting lipids and white balls for low-melting lipids) but simultaneously show the cholesterol content which is higher in the black ones. Adapted from [Some09].

1.5.1 Superlattice and Umbrella Models

The **Superlattice** model suggests spatially-extended regular organization of lipids in membranes. Such arrangements do not cover the whole membrane surface, but instead, regions with a random distribution coexist with regularly arranged domains in a dynamic equilibrium [Chon94b]. Coexistence of different regular arrangements may also occur. Moreover, membrane superlattices have to be understood as a compressible and dynamic soft meshes with no long-range positional order, see Fig. 1.7. It has been suggested that the lattice deformability is a direct consequence of the compressibility of the lipids due to their inner flexibility.

Different experimental results suggest the existence of superlattices in binary lipid bilayers. For example, the fluorescence intensity emitted by Pyrene-labeled Phds which depends on their collision does not increase homogeneously with the mole fraction of one of the two lipid components [Some85, Tang92, Chon94b]. Instead, dips or kinks are observed at particular concentrations. They are probably caused by the formation of better packed structures at those concentrations. Similar observations were gathered by IR spectroscopy and fluorescence while measuring POPC membranes with increasing amounts of POPE [Chen97]. Information is also available for membranes containing charged lipids with zwitterionic ones, like Card [Berc81, Berc84, Senn05, Lupi08] or fatty acids [Cevc88, Lohn91] in a PhdCho matrix. The

existence of particular compositions, where abnormal behaviors are observed in all these experiments, constitutes the core of the **Superlattice** model.

Theoretical models based on geometric and symmetry arguments predicting the observed critical compositions have been developed [Some99]. Most of them rely on a maximization of the separation between the minority lipids in the lipid matrix constituted by the majority lipids. The reason for such a maximization can be found in the minimization of the perturbations created by the minority lipid in the membrane, or simply due to effective repulsion between two minority lipids. The possible driven forces can involve charge-charge repulsion, complementary shapes, steric strain, headgroup rotational entropy, dipolar interactions or hydrophobic effect. Finally, theoretical models suggesting the compatibility of the superlattice formation with the presence of proteins allow the extension of the **Superlattice** model to real biological membranes [Some99]. Excellent reviews on this issue can be found in Refs. [Some99, Some09].

More related to the biological context, superlattice arrangements are also suggested in cholesterol-containing lipid bilayers [Virt95, Ali07, Chon09]. In these systems, the **Superlattice** model is complemented and expanded by the **Umbrella** model [Huan99]. This model suggests that the mismatch between the small cholesterol headgroup and its large hydrophobic structure determines the relation between lipid and cholesterol molecules. The small headgroup of the cholesterol molecule cannot protect its apolar backbone from water, and therefore, the direct exposure of cholesterol to water lead to an unfavorable contribution to the free energy [Priv88, Levy98]. Consequently, cholesterol associates preferentially with membrane components that are able to shield it from the water [Huan02, Ali07]. Components with choline groups like Phds of SLs with larger crosssectional area in their headgroups with respect to their chains are good candidates. For the same reason, configurations with two or more adjacent cholesterols, where no shielding is provided, results in non-favorable arrangements. In conclusion, cholesterol molecules tend to avoid direct contacts with other cholesterol and prefer to be placed below the polar headgroups of other lipids, that act as "umbrellas".

The **Umbrella** model has been proven to be a powerful predicting tool, especially when Monte Carlo simulations are combined with it [Huan99]. For example, the model is able to explain the existence of a solubility limit of cholesterol in Phd membranes, $\chi_c^* \sim 66,7 mol\%$ and to characterize it spatially. It also justifies the substantial drop in χ_c^* observed for PhdEtns by means of the head/chain crosssection areas ratio of the lipid. The substantially smaller headgroup of PhdEtns respect to PhdChos results in a worst shielding of cholesterol. Similar arguments are used to explain the relative independence of χ_c^* from the chain length as it does not disturb substantially the head/chain ratio. The **Umbrella** model also provides a mechanism that explains the formation of different regular distributions at some critical concentrations. It also provides the driving force to explain the preferential interaction of cholesterol with saturated lipids in the following manner. Every *cis* double bond added to the acyl chains decreases the lipid's lateral compressibility, and therefore, the head/chain ratio is decreased for unsaturated moieties compared to saturated ones thus reducing their shielding capabilities. The explanation about the increase of the acyl order and the decrease of the membrane permeability, when cholesterol is present, is also derived. Cholesterol wants to hide from water by placing itself in the acyl chain region beneath the polar headgroup of the lipids. Therefore, cholesterol molecule effectively pushes the chains restricting their rotational and lateral movements promoting more ordered *trans* configurations. All theses effects correspond

to the well known cholesterol condensing effect. Finally, the **Umbrella** model proposes a possible driving force for raft formation, see Sec. 1.5.3. Both high-melting (saturated) and low-melting (unsaturated), provide coverage of cholesterol from water. Association of high-melting (saturated) lipids with cholesterol is more favorable as the entropic effect due to the straighten of the lipid chain is lower for saturated compared to unsaturated moieties.[Ali07]

1.5.2 Condensed Complex Model

Early experiments with monolayers of phospholipids and cholesterol display the typical effects of non-ideal liquid mixtures, the condensing effect being one of the most relevant. To account for these effects, McConnell [Radh99b, Radh99a, McCo03] proposed the **Condensed Complex** model. According to this model, phospholipids react reversibly with cholesterol to form complexes following

$$CHOL + R \leftrightarrows COMPLEX, \tag{1.1}$$

where R is a reactive lipid that corresponds to a high-melting (saturated) phospholipid. The complex occupies a smaller area than the sum of its individual components separately, so it explains the condensing effect produced by cholesterol when introduced in a two-dimensional fluid phase of a saturated lipid.

The **Condensed Complex** model describes the phase behavior of ternary mixtures in monolayers [Veat03, Veat05a]. High-melting (saturated) and low-melting (unsaturated PhdCho) lipids are usually miscible, but once cholesterol is added coexistence of liquid phases appears [Diet01, Sams01, Veat03, Veat05a], see Sec. 1.4. This immiscibility is suggested to be determined by the partial miscibility of the formed complexes with the unreactive (unsaturated) lipid [McCo05, Radh05]. Therefore, the model proposes the coexistence of four species (cholesterol, reactive lipid, unreactive lipid and complex) where a negative interaction between the complex and the unsaturated lipid is invoked.

The nature of the complex is unclear. Several attempts to find the stoichiometry have been performed [Gers78, Pres82]. Although some values have been proposed (e.g. 2:1 for SM and cholesterol [Radh01]), no conclusive values exist. Recently the definition of complex has been softened to fit into the current available experimental data [Radh05]. It is suggested that condensed complexes has not to be identified with highly specific and static molecular structures. Condensed complex formation has been suggested to be compatible with the superlattice structures [Radh00, McCo05].

Although interesting and versatile, several critics to this model have recently appeared. Most of them are based on the fact that complexes have never been experimentally isolated or structurally described by any available theoretical technique [Vand94, Huan99, Niel99, Smon99]. Additionally, the applicability of this proposal in the biological context is debated since the low lateral pressure range where complex formation successfully applies in monolayers ($<$20 mN/m) substantially differs from the lateral pressure in membranes ($\sim$35 mN/m) [Some09]. A good review of the study of condensed complexes in vesicle bilayers can be found in Ref. [Radh05].

1.5.3 Lipid Rafts

The treatment of membranes from erythrocytes, later extended to other cell types, with Triton X-100 at 277 K, a non-ionic detergent, yields detergent-resistant membrane fragments [Yu73]. Reported compositions of these fragments showed to be rich in saturated lipids (especially SLs), cholesterol, and specific proteins, whereas the solubilized parts of the membrane were rich in unsaturated lipids [Yu73]. On the other hand, as commented in Sec. 1.4, cholesterol showed an unique ability for promoting the formation of the L_o phase in coexistence with the L_α phase. Based on these two findings the **raft** hypothesis was formulated by Simons and Ikonen in 1997 [Simo97]. It proposes the existence of functional liquid ordered domains (lipid rafts) rich in cholesterol and high-melting lipids (e.g. SLs) surrounded by a more disordered fluid phase composed by low-melting lipids (e.g. unsaturated Phds) [Simo97, Brow98].

The study of lipid rafts is rather complicated since they develop at very small scales, within the tens to few hundreds nanometers range [Ande02]. Most knowledge about lipid raft organization in living cells comes from fluorescence and electron microscopy. Imaging membrane lipid organization at length scales smaller than 300 nm remains still unavailable. Although recently, imaging mass spectrometry has shown the potential to fill this resolution gap [Grov06, Kraf06] the raft field is now at a technical impasse because the experimental methods to study biomembranes at the characteristic raft length and time scales are still being developed. Current research on lipid rafts is mainly focused on the outer plasma membrane of mammalian cells, although electron microscopy also suggests analogous aggregation of putative raft molecules in the inner leaflet [Prio03, Plow05]. It is not clear, however, how the raft phenomenon is coupled between outer and inner leaflets [Deva04, Alle06].

GPI-anchored proteins are generally found in detergent-resistant membrane fragments and therefore included into the raft components category. Notice that GPI-anchored proteins contain saturated lipids as anchoring fragments which accommodate better with the ordered phases such as presented by rafts [Schr94]. Some proteins are only partially found in detergent-resistant membrane fragments [Edid03, Munr03, Simo04] and others are excluded [Simo97, Simo04]. This suggests that rafts are responsible for the sorting of specific proteins and, therefore, they are involved in signal transduction and other important cellular functions [Brow00, Doug05]. Evidence of functional lipid-lipid, lipid-protein clusters in living cell membranes exist [Edid03, Simo04, Kusu04, Mayo04]. They rely on movements of proteins [Varm98, Cott04, Simo04] and differential partitioning of fluorescent probes [Gaus03]. Furthermore, they have been found to be important in several cellular processes including: lateral segregation of cell components, protein selection, immune response [Simo02], signal transduction [Full04], endo- and exocytosis [Sala04, Schu04], intracellular trafficking [Helm04], apical sorting [Full04] and regulation of the activity of membrane proteins. In this context, a deeper understanding is crucial for tackling several diseases.

The original raft model has been updated. The simplistic hypothesis that stable and freely diffusing lipid rafts exist in plasma membranes is being replaced by a more complex scenario. Recent observations suggest a hierarchical picture of an active lipid organization at different length scales that are exploited for distinct functions [Kusu04]. On the one hand, the existence of small, transient lipid ordered domains may induce short-lifetime protein interactions necessary to facilitate specific biochemical reactions in the membrane. On the other hand, larger and stabilized rafts, resulting from the coalescence of small

and temporary domains, may be required for protein trafficking, endocytosis and signaling. Such a picture opens new and challenging perspectives that revise the raft hypothesis to take into account the dynamic nature of lipid assemblies at the surface of living cells [Subc03, Kusu04, Mayo04, Shar04].

1.6 Experimental Techniques

Knowledge of biological membranes is incomplete, yet progressing, because of the development of experimental techniques. The vast time and space scales within which membrane processes occur remain problematic. The complexity of biological membranes (thickness, heterogeneity, number of moieties and highly coupled processes) has not deterred the membrane community. A selection of experimental techniques related to this work is briefly detailed below.

1.6.1 Spectroscopy

1.6.1.1 Fluorescence

Fluorescence is luminescence originated from photonic absorption-emission using molecular singlet states. A requirement for using fluorescence spectroscopy in a system is to have a chromophore group. This constitutes the main drawback of the technique as membrane components, excluding proteins, do not naturally contain chromophores. The high sensitivity of this technique allows small enough additions of chromophores without significant perturbation of the system properties. Typical probes for lipid membranes are 1,6-diphenyl-1,2,5-hexatriene (DPH), 1-(4-trimethylammoniumphenyl)-6-phenyl-1,3,5-hexatriene
(TMA-DPH), p-toluene sulfonate and *trans*-parinaric acid.

Among all methods based on fluorescence, the "steady-state and time-resolved anisotropy" provides important information about membranes fluidity, order parameters and rotational movement of the fluorescent probe [Kino77, Lipa80], which are related to the molecular environment. This technique covers time scales from picoseconds to nanoseconds. Additional techniques like Fluorescence Recovery After Photobleaching (FRAP or FRP) [Vaz89, Vaz90, Vaz91], and Fluorescence Correlation Spectroscopy (FCS) [Eige94, Alme95, Korl99] allow the study of lateral diffusion processes. Both are confocal microscopy techniques, and their sensitive range covers from milliseconds to seconds on a 500 nm diameter focus, which is enough to calculate lipid diffusion rates. In addition to the dynamic information they also provide information about the confinement of the probe by the surrounding lipids [Lipa80]. In FRAP, fluorescent molecules are permanently bleached at a region of interest in the sample, so the rate of fluorescence recovery provides a measure of how quickly fluorescent molecules move into the bleached region. FCS, on the other hand, measures the fluorescence in stationary state. In this case, the registered fluctuations in the fluorescence correspond to fluorophore movements in and out the focus [Elso01].

Another interesting fluorescence technique applied to membranes is Förster Resonance Energy Transfer microscopy (FRET). This technique requires two molecules: one acting as a donor, excited traditionally, and the acceptor which is excited by energy transfer of the donor in its exited state. FRET occurs when donor and acceptor fluorophores have sufficiently large spectral overlap, favorable dipole-dipole orientation, proximity of 1–10 nm, and large enough

quantum yield [Lako99]. It has been used to determine clustering in membranes, e.g. by labeling ligand-receptor complexes [Lako99].

1.6.1.2 Electron Paramagnetic Resonance

Electron Paramagnetic Resonance (EPR) can be used to study the structure and dynamics of biological macromolecules such as proteins, and the behavior of lipid assemblies. This technique has numerous advantages including high sensitivity and it provides access to an exceptional variety of structural and dynamical properties [Hubb68, Tour70, McCo71a]. Unfortunately, only few macromolecules have natural paramagnetic centers. Thus, various types of spin labels have to be introduced into the native systems.

Compared to fluorescence probes, spin labels are much smaller and better localized in the cross-membrane profile. Spin labels are usually stable nitroxide free radicals, which give a characteristic EPR spectrum. The three-line hyperfine structure splitting for these systems is anisotropic and varies with the orientation of the magnetic field relative to the nitroxide axes [Mars81]. Different types of nitroxide spin labels are used for labeling in cell membranes. The most commonly used ones are fatty acids, usually steric acid, derivatives with an oxazolidine ring, where the nitroxide group is flanked by quaternary carbon atoms [Stim07]. Additionally, an oxazolidine ring can be attached to various carbons in the steric acid chain.

The motion of the nitroxide reflects the motion of the labeled part of the molecule, which in turn provides information about the local environment at a given depth in the membrane. These probes provide specific information about the internal structure of bilayers [McCo71a, Ge98], as well as unique data on oxygen distribution and diffusion in membranes [Subc89, Subc91], and hydrophilicity profiles along the membrane normal [Subc94]. It also allows for evaluation of flipping ratios of lipids [McCo71b] and discrimination between phases [Subc07]. Recently, it has been also used to trace raft domains [Simo97].

1.6.1.3 Nuclear Magnetic Resonance

Nuclear Magnetic Resonance (NMR) should be a priori an excellent technique to characterize biological membranes. The native occurrence of active atoms and the non-destructive nature of the technique support this idea. In principle, it provides access to structural and dynamical information. The ordered nature of membranes substantially complicates the output by broadening and overlapping the signals [Boci78].

NMR uses the magnetic properties of certain nuclei, e.g. ^{1}H, ^{2}H, ^{13}C, ^{31}P whose energy levels split under the influence of magnetic field. By irradiating the sample while applying a magnetic field, spectra of resonance frequencies in the radio frequency range can be obtained. The resolution of the spectra is directly proportional to the strength of the magnetic field. An important feature of this technique is that resonance frequencies are modified by the proximity of other magnetic nuclei. These nuclei can be in the same molecule or in certain cases in adjacent molecules when the molecular movement is restricted.

The interpretation of NMR spectral parameters for a partially ordered system with a complex local motion is complicated. In the gel phase, where molecular movements are slow and restricted, a broad and featureless spectrum is obtained. This is a consequence of the non-averaging of the inter- and intramolecular static dipolar interactions in the NMR timescale. As the local motions become significantly less restricted and faster, as in L_α phase,

better resolved spectra are obtained [Jame75, Wenn77]. However, even in the L_α phase the restricted motions result in incomplete averaging of the magnetic and electric second-rank tensor interactions. This leads to first order effects resulting in a general broadening [Boci78] and also to the appearance of quadrupolar splittings in the ^{2}H NMR spectra [Wenn77]. From the analysis of the first order effects molecular ordering can be extracted.

Introduction of perdeuterated or specifically deuterated lipids and probes allows the analysis of the quadrupolar splittings to obtain parameters characterizing the molecular ordering. For example, the order parameter associated to a bond between a carbon and deuterium atoms (C-D) in a lipid, S_{CD}, can be extracted from:

$$S_{CD} = \frac{1}{2}\langle 3\cos^2\theta - 1\rangle = \frac{4}{3}\left(\frac{h}{e^2qQ}\right)\Delta\nu, \tag{1.2}$$

where θ is the angle between the magnetic field and the bond, e^2qQ/h=170 kHz is the static quadrupole coupling constant for the C-D bond (eq and eQ are electric quadrupole moments for C and D nuclei and h is the Planck constant) and $\Delta\nu$ spectral lines separation [Seel74].

The motion of the acyl chains might be also extracted by measuring NMR spin-lattice relaxation times, T_1. For example, in the case of the C-D bond, the spin-lattice relaxation rate is given by:

$$\frac{1}{T_1} = \frac{3\pi}{10}\left(\frac{e^2qQ}{\hbar}\right)^2 [J(\omega_D) + 4J(2\omega_D)], \tag{1.3}$$

where ω_D is the Larmor frequency of the deuterium, and $J(\omega)$ is the spectral density of the second rank orientative autocorrelation function, $C_2(t)$. The relation can be expressed as follows:

$$J(\omega) = \int_0^\infty C_2(t)\cos(\omega t)\,dt, \tag{1.4}$$

$$C_2(t) = \frac{1}{2}\langle 3[\vec{\mu}(t)\cdot\vec{\mu}(0)]^2 - 1\rangle, \tag{1.5}$$

where $\vec{\mu}$ is the unit vector along the C-D bond [Lind01a, Mash01].

The usage of NMR is not only limited to the properties described above. A good example is, for instance, the calculation of diffusion rates extensively used in this work.

1.6.2 Small-Angle Scattering

Scattering techniques are based on the deviation of the radiation when it passes through an optically heterogeneous material. Since membranes are not crystalline, no resolved diffraction patterns can be extracted. Instead, the use of scattering techniques, in particular Small-Angle Scattering (SAS), provides important structural information. This technique is based on the deflection of a beam of particles away from its initial trajectory by the interaction of structures larger than the wavelength used. This deflection is produced at small angles, normally 0.1°–10°. Two kind of techniques base on the radiation type are normally used to study membranes: Small-Angle X-ray Scattering (SAXS) with wavelength between 0.1–0.2 nm [Kuuc08a] and Small-Angle Neutron Scattering (SANS). Both provide similar or complementary outputs

[Kuuc08a]. The information provided by these techniques is condensed in the structure factor that can be expressed as:

$$F(q) = \sqrt{\frac{I(q)P_{LC}(q)}{P_{TS}(q)}}, \tag{1.6}$$

where I(q) is the obtained experimental intensity, P_{LC}(q) is the Lorentz correction (equal to q for oriented bilayers and q^2 for unilamellar vesicles), and P_{TS}(q) describes the sphericity and polydispersity [Penc06] which is constant for oriented bilayers. q is the modulus of the scattering vector.

The form factor can be directly correlated with the transversal electronic (or neutron scattering length for SANS technique) distribution in the membrane by the following relation [Kuuc08b]:

$$|F(q)|^2 = \left(\int_{D/2}^{-D/2} \Delta\rho(z) \cos(qz)\, dz \right)^2 + \left(\int_{D/2}^{-D/2} \Delta\rho(z) \sin(qz)\, dz \right)^2, \tag{1.7}$$

where, z is the direction perpendicular to the membrane, and $\Delta\rho(z) = \rho(z) - \rho_w$, and it corresponds to the electron (or neutron scattering length for SANS technique) density profiles of the membrane and the bulk water respectively. D stands for height of the analyzed cell in the z direction. By modeling the form factor one can access several structural parameters of the membrane including thickness, area per lipid or volume per lipid [Kuuc08a], and perform a direct comparison with data obtained from numerical simulations.

1.6.3 Differential Scanning Calorimetry

Differential Scanning Calorimetry (DSC) is a thermoanalytical technique based on measuring the heat differences required to increase the temperature between a sample and a reference system as a function of the temperature. In the experiment the sample and reference systems are maintained at nearly the same temperature. Knowing the heat capacity of the reference system over the temperature range we can have access to the heat adsorbed by the sample.

This high resolution technique allows to detect phase transition temperatures and also often to characterize them [Stei69]. For example, one can distinguish between a collective phase transition (narrow peak) or a sequential one (broad peak). This technique has been essential for a critical comparison of the numerical results presented in this work to available experimental data.

CHAPTER 2

Molecular Dynamics

2.1 Background

In a classical context, the temporal evolution of a multibody system can be predicted if all positions and forces are known at a particular time. This was already proposed by Laplace in the 19^{th} century [T842]. The link between a given configuration and its future evolution is provided by Newtonian mechanics,

$$m_i \frac{d^2\mathbf{r_i}}{dt^2} = \mathbf{F_i} = -\nabla_{\mathbf{r_i}} U(\mathbf{r_1}, \mathbf{r_2}, \ldots, \mathbf{r_N}) \tag{2.1}$$

where N is the number of particles, $\mathbf{r_i}$ denotes the Cartesian coordinates of particle i, $\mathbf{F_i}$ is the force acting on it, and U is the potential energy of the system. Unfortunately, the analytical resolution of the coupled differential equations 2.1 can only be achieved when $N \leq 2$ [Qiu 90]. The only alternative for systems with more than two particles consists of the numerical integration of the coupled equations of motion. The constant improvement in CPU processing power has expanded the usage of numerical methods applied to multibody systems in many fields, e.g. astronomy, material science, chemistry, biology, etc.

The numerical technique used to study molecular systems using classical equations of motion is called Molecular Dynamics (MD). The first MD simulation dates back to 1957 when Alder and Wainwright simulated a system composed by hard spheres [Alde59]. Already in the 60's more realistic systems, such as Argon in the liquid phase [Rahm64], had been studied. In the 70's the first simulation of water was conducted [Rahm71]. Since then, classical MD has become one of the most widely used numerical techniques in modern science. Particularly, the complexity of the potential landscapes of biological systems makes ideal the usage of MD for their study. It provides reasonable structural and dynamical information in time and space averaged properties. In this Thesis, we use MD simulations to study the physical properties lipid bilayers.

2.2 Force Field

The interaction potential governing the interactions between particles is all the needed information to predict how the system will evolve in the classical context. The functional form of these potentials and their parameters are called the force field. As a general classification, the force field can be either atomistic or coarse-grained. The former describes the atomic motion of all atoms, whereas the latter lumps some of them into groups, while preserving the fundamental underlying physics [Marr07, Murt09]. The level of accuracy obtained by atomistic force fields is higher than for coarse-grained ones although the latter approaches require less computational resources. Therefore, when addressing properties that rely sensitively in molecular details, an atomistic force field is needed. In contrast, when the study of the problem is limited by the computational resources, a coarse-grained approach is then used [Marr09]. Solutions combining both approaches exist. For example, United Atom (UA) force fields which are extensively used in this work preserve the fully atomistic description for some parts of the molecule and incorporate atomic aggregates (pseudo-atoms) to describe others.

There is no unique force field for any given system, since both functional form and parameters might change. Several factors like target properties or the balance between computational resources and accuracy are taken into account while developing a force field. Several force fields related to biological systems exist, e.g. AMBER [Corn83, Wein84], CHARM [Broo83, MacK98], GROMOS [Guns87, Guns98], OPLS [Jorg84, Jorg88]. The choice of a force field is usually based on its accuracy to reproduce a given set of properties.

In general, force fields are normally assumed to consist of pairwise-additive potentials (more accurate descriptions may involve the use of three-body terms [Mack04] or non-additive potentials). A compromise between their accuracy and simplicity is essential. Most force fields can be described as:

$$U = U_{bond} + U_{ang} + U_{tors} + U_{vdw} + U_{coul} \tag{2.2}$$

The first three terms in Eq.2.2 correspond to the bond stretching, angle bending and torsional dihedral energy contributions for atoms separated by 1, 2 and 3 covalent bonds, respectively. They are usually extracted from quantum mechanical calculations, spectroscopy techniques, or X-ray crystallography [Schl02]. The last two terms correspond to the van der Waals and Coulomb interactions. These forces apply to all atom pairs except for those atoms within the same molecule separated by three or less covalent bonds. The parameterization of such terms is normally a hard task. In the case of the van der Waals interactions where no generalizable *ab initio* procedure is available, different approximations using X-ray diffraction data [Schl02] or by fitting simulations to experimental data (density, heat of vaporization...) have been used [Berg97]. Similarly, atom or atom group charge cannot be directly accessed by quantum mechanics. Several *ab initio* procedures have been developed to assign the partial charges to each atom or atom group, although their value may differ significantly depending on the used approach.

A widely spread and simple force field used in biological systems has the following functional form:

$$
\begin{aligned}
U = & \sum_{bonds} \frac{k_i^b}{2}\left(\mathbf{r_i} - \mathbf{r_i^{eq}}\right)^2 + \sum_{angles} \frac{k_i^\alpha}{2}\left(\theta_i - \theta_i^{eq}\right)^2 + \\
& + \sum_{torsions} \sum_{n} k_{\phi,n}\Big(1 + \cos\left(n\phi - \phi^{ref}\right)\Big) + \\
& + \sum_{pairs} \left(\left\{ \frac{C_{ij}^{(12)}}{r_{ij}^{12}} - \frac{C_{ij}^{(6)}}{r_{ij}^{6}} \right\}_{vdw} + \left\{ k_e \frac{q_i q_j}{r_{ij}} \right\}_{coul} \right)
\end{aligned}
\tag{2.3}
$$

Here, the bond and angle contributions are described as harmonic oscillator. This approximation is fast to use in a computer and provides an accurate description when being close around the equilibrium position. The torsional (dihedral) contribution is normally represented by a cosine series expansion. The complexity of the torsion profile will determine the number of terms used in the expansion. The behavior of long flexible molecules often relies in torsional motions and therefore an accurate description with a large number of terms is reasonable. Finally, the van der Waals terms are represented by *Lennard-Jones 12-6 functions* and the electrostatic contributions following the Coulomb's law. They constitute the real simulation time bottleneck since they expand over all possible particle (atoms or atom groups) pairs, whose number increases with the square of the total number of particles. In order to speed up the calculation several approaches have been proposed, see Sec. 2.3.3.

Different parameter values can be used for the same system and the same functional form (Eq. 2.3). These differences are due to the fact that the parameter optimization can be performed to fit different sets of system properties, and is also dependent on the fitting protocol. In any case, a consistent and correctly described implementation is necessary for the correct usage of a force field. Hence, mixing parameter values from different sources is often risky but sometimes a necessary practice.

2.3 Practical Implementation

Besides the choice of the force field, different algorithms are needed to efficiently integrate the equations of motion and to provide the correct ensemble. In this section, a general overview of these algorithms constituting the core of a MD program is provided.

2.3.1 Integrator

The integrator is the numerical tool that allows the numerical integration of the Newton's motion equations. Starting from a set the positions $\mathbf{r}_{i=1,N}$ and velocities $\mathbf{v}_{i=1,N}$ at a time t, the integrator generates a new configuration at time $t+\Delta t$, where Δt is the time step.

There are several numerical integration methods with different characteristics (stability, precision, symplecticness, simplicity...), and its choice is often problem-dependent [Leac01]. For MD, properties like time reversibility [Tuck92], preservation of the energy and momentum (symplectic) [Sanz94, Hair97], numerical stability for long time steps and low computational effort are critical.

The approximation as Taylor series expansions for positions and their temporal derivatives is a common assumption in any numerical integration method. One of the most widely

used family of integrators in MD derives from the Verlet algorithm [Verl67], that truncates the error for the coordinates at the fourth order, $O(\Delta t^4)$. The original formulation can be expressed as:

$$r(t+\Delta t) = 2r(t) - r(t-\Delta t) + \Delta t^2 a(t) + O(\Delta t^4), \tag{2.4}$$

where the propagation depends only on the positions and acceleration at time t and the position at $t-\Delta t$. Although this propagation scheme does not depend on the velocities, they can be estimated, for example, by:

$$v(t) = \frac{r(t+\Delta t) - r(t-\Delta t)}{2\Delta t}. \tag{2.5}$$

We used a variation of the Verlet method known as the leap-frog algorithm [Hock70]. It can be described as follows:

$$r(t+\Delta t) = r(t) + \Delta t\ v(t+\frac{1}{2}\Delta t) \tag{2.6}$$

$$v(t+\frac{1}{2}\Delta t) = v(t-\frac{1}{2}\Delta t) + \Delta t\ a(t). \tag{2.7}$$

This algorithm is rather robust and displays an excellent computer performance. It has, however, one important drawback: there is no temporal synchronization between positions and velocities. This does not allow an accurate calculation of the total energy of the system, as the kinetic and potential contributions are known at different times.

2.3.2 Time Step and Constraints

The choice of the time step Δt (the time difference between consecutive snapshots constituting the simulation trajectory) is far from being trivial, see Fig. 2.1. On the one hand, a short time step requires an exceedingly long number of iterations for a satisfactory sampling of the phase space. On the other hand, a long one may result in inaccurate or even erroneous trajectories. This is mostly due to the difficulty of capturing the high frequency motions. Furthermore, long time steps may also lead to numerical instabilities (unusual growth of energy, velocities and distances), especially due to the harmonic approximation in the high frequency modes simultaneously associated with short displacements (bonds and angles). As a compromise solution to both problems the time step is normally set to be $1/10^{th}$ of the period related to higher frequency motions of the system. In practice for biologically relevant systems the time step limit is $\sim$1 fs, see Table 2.1.

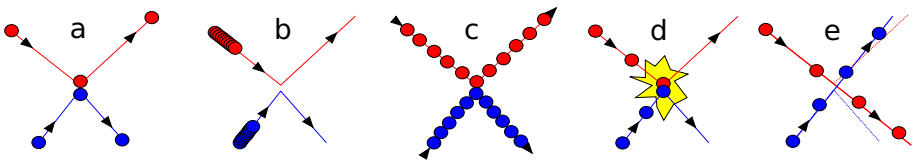

Figure 2.1: Collision simulation paths of two atoms obtained by a) analytical solution of the equation of motion (true path); MD simulations with b) very small, c) optimal and d, e) big time steps. Adapted from [Leac01].

Vibrational mode	Wave num. $(1/\lambda)$ [cm^{-1}]	Frequency ν=c/λ [s^{-1}]	Period $(1/\nu)$ [fs]	Ratio $h\nu/(k_BT)$
O-H stretch (st.)	3600	$1.1\cdot 10^{14}$	9.1	17
C-H stretch	3000	$9.0\cdot 10^{13}$	11.1	14
O-C-O asym. st.	2400	$7.2\cdot 10^{13}$	13.8	12
C=O st. (carbonyl)	1700	$5.1\cdot 10^{13}$	19.6	8
H-O-H bend	1600	$4.7\cdot 10^{13}$	21.2	7.3
H-C-H bend	1500	$4.5\cdot 10^{13}$	22.2	7
C-N st. (amines)	1250	$3.8\cdot 10^{13}$	26.3	6
C-C stretch	1000	$3.0\cdot 10^{13}$	33.3	4.7
O-C-O bend	700	$2.1\cdot 10^{13}$	47.6	3
C-C-C bend	300	$9.0\cdot 10^{12}$	111	1.4

Table 2.1: Ratios for some high-frequency vibrational modes relevant in biological systems at T=300 K. Adapted from [Schl02]

.

Processes in biological systems span over different time scales, see Table 2.2. Although they are coupled (fast fluctuations may induce a global rearrangement at large length and time scales), most biologically relevant processes are little influenced by high frequency motions [Bere98]. The time step is limited by these modes which are badly described in the classical context ($h\nu/k_bT>>1$) [Schl02]. To overcome this problem, the fastest motions are somehow forced to be constrained (see below), so that the time step can be increased without, in principle, significantly altering the correct temporal evolution. Additionally, the representation of bonds with constraints instead of harmonic potentials can be even seen as more realistic since at room temperature they are mostly in their ground state [Hess97].

There are several ways of fixing internal degrees of freedom in MD simulations. One extreme possibility is to consider the constituent molecules as rigid bodies. Doing so, the problem is reduced to the motion of the center of mass and the rotation of the molecules around it. The complexity of the implementation of this restriction and the complete loss of internal degrees of freedom often restrict its application. Another method consists of applying large enough forces to fix a given degree of freedom, for example a bond distance. This method is quite ineffective as it requires shorter time step.

The most common restriction method involves the usage of constraints. A constraint consists in a restriction in the value of a given degree of freedom that the simulation has to fulfill. Most constraint methods use holonomic constraints for fixing, for example, covalent bond lengths or bending angles. An example of a holonomic constraint of a bond length is given by

$$(\mathbf{r}_i - \mathbf{r}_j)^2 - d_{ij}^2 = 0, \tag{2.8}$$

where d_{ij} is the restricted distance between atoms or atom groups i and j. At best, an increase up to four times the time step is allowed [Hess97, Bere98]. The resolution of the non-linear equation set involved in length/angle restriction can be done by two different methods. One

Internal Motion	Timescale [Seconds]
Light-atom bond stretch	10^{-14}
Double bond stretch	$2 \cdot 10^{-14}$
Light-atom angle bend	$2 \cdot 10^{-14}$
Heavy-atom bond stretch	$3 \cdot 10^{-14}$
Heavy-atom angle bend	$5 \cdot 10^{-14}$
Global DNA twisting	10^{-12}
Sugar puckering (nucleic acids)	$10^{-12} - 10^{-9}$
Collective subgroup motion (e.g. hinge bending, allosteric transitions)	$10^{-11} - 10^{-7}$
Surface-sidechain rotation (proteins)	$10^{-11} - 10^{-10}$
Global DNA bending	$10^{-10} - 10^{-7}$
Site-juxtaposition (superhelical DNA)	$10^{-6} - 1$
Interior-sidechain rotation (proteins)	$10^{-4} - 1$
Protein folding	$10^{-5} - 10$

Table 2.2: Typical time scales of motions in biological systems. Adapted from [Schl02].

possibility is to sequentially solve each constraint in an iterative way, up to reaching a certain tolerance level. This is used by "SHAKE", one of the most common constraint methods [Ryck77]. An analytical solution of the "SHAKE" algorithm, named "SETTLE", is widely used for small molecules, for example water [Miya92]. The other option iteratively solves all constraints simultaneously by applying corrections on lengths and velocities up to the desired tolerance. In between them one finds "EEM" [Edbe86] and "LINCS" [Hess97], the latter widely used in this work. "LINCS" is about three to four times faster, it displays a better convergence behavior, and it can be more easily parallelized than "SHAKE" algorithm [Hess97].

2.3.3 Boundary Conditions and Long Range Interactions

The system size in MD simulations (simulation box size) is in the nanometer scale, far from the macroscopic scale. The simulated system size is mainly determined by the time scale of the studied process, the computer performance and the process itself. In any case, the size of the simulated system has to be finite, and therefore, special care has to be taken with those particles placed near the boundaries, particularly in small systems [Leac01].

In case of symmetric systems this problem can be handled by periodic boundary conditions (PBC) [Alle90]. These conditions avoid undesirable boundary effects that may be important in small systems. The idea is to replicate the simulation box in all directions, so that the coordinates of the atoms in the image boxes can be easily obtained by subtraction or addition of integral multiples of the box vectors.

Although PBC seem to solve the problem of boundary particles, some limitations remain. Some structural and dynamical properties of the system may be locally correlated. If the correlation distance is larger than the size of the box, the artificial periodic conditions can alter the studied property and, eventually, the behavior of the whole system (finite-size

effects) [Leac01]. In these cases an analysis of finite-size effects is mandatory. Long-range interactions may pose an additional problem. Contrary to the fast decay of the van der Waals interactions ($1/r^6$), the coulombic interaction between charges decays slowly ($1/r$) and extends over the simulation box.

The difficulties concerning the long range interactions in molecular dynamics are complex. As stated above, the number of long range interactions increase as N^2 and are very time consuming to compute. One possibility to reduce this problem is to use cutoffs, so that only the pairs inside a given cutoff are considered. This is supported by the fact that forces induced by a particle tend to zero with the distance. This approach requires the construction of a list of pairs of those particles closer than the cutoff distance, implying a substantial cost in CPU time. Algorithms based on the small changes in the surroundings of a given particle compared to the time step allow a substantial speed up of the method [Verl67]. The usage of cutoffs is only strictly accurate if the interaction with the particles outside the cutoff is zero. In practice this is only partially achieved in the case of van der Waals interactions. The $1/r$ dependence of the coulombic forces leads to an extremely slow decay, so that the number of artifacts reported due the usage of cutoffs to describe coulombic interactions is large [Patr03, Patr04, Baum05]. The intermolecular stress created by the abrupt truncation at the cutoff radio is the most evident [Leac01, Schl02]. This can be minimized by using smoothing terms or by the usage of charge groups, although it has proven not to be a definitive solution.

There are some alternative methods which avoid most of the artifacts coming from the cutoffs while providing an appropriate description of the atom or atom group environment even when using PBC. Most of the methods are derived from the so-called Ewald summation [Ewal21], where each particle interacts with those inside the central box and in their infinity image boxes. The Ewald summation was originally introduced because the electrostatic sum (for a salt crystal) is only conditionally convergent. Ewald's trick rewrites the interaction potential as the sum of two terms and makes the sum absolutely convergent as required by physics. In practice, we transform the harmonic series, $1/r$, which converge extremely slowly to a function with better convergence properties. This can be achieved by the following identity:

$$\frac{1}{r} = \frac{f(r)}{r} + \frac{1 - f(r)}{r} \tag{2.9}$$

where now each series converges more rapidly if $f(r)$ is chosen appropriately [Leeu80]. In practice, one term considers the short range interactions while the other describes long range charge distribution. Technically this is achieved by adding a Gaussian distributed charge around each point charge of opposite by same magnitude. The sum of the point charge and the shielding distribution is solved easily in the real space. In order to keep the original system unaltered, Gaussian distributed charges around each atom are added, but now with the same sign. This compensates the previous addition of charges and can be solved in the reciprocal space. This method scales in its original formulation with $O(N^2)$, but corrects many artifacts observed while using cutoffs. [Leac01]

Although Ewald summation can be optimized to scale as $O(N^{3/2})$ by choosing appropriately the width of the introduced Gaussian charge distributions, this is still a constraint when simulating large systems. Modifying the method allows the use of fast Fourier transforms to perform the charge summation and increases the performance to $O(N \log N)$. This

requires the transformation of the continuous distribution of charges to a grid-based charge distribution. One such a method is PME [Dard93] that is the one used in all the simulations in this Thesis. Several results confirm this method as one of the most reliable to simulate membranes [Patr03, Rog03].

2.3.4 Ensembles

The link between microscopic simulations and macroscopic world is provided by statistical mechanics. The definition of the working ensemble is crucial to define correctly the thermodynamic properties of the system. The natural ensemble of MD simulations is the microcanonical (constant particle number, volume and Energy (NVE)), although other ensembles like constant particle number, volume and temperature (NVT) or constant particle number, pressure and temperature (NPT) are more natural when comparisons with experiments are needed. Therefore, in order to set the appropriated simulations conditions, one needs to define T and P in the simulated system and provide a way to control them.

The macroscopic temperature of a system is the average of instantaneous temperatures over a long enough interval, $T=\langle T(t)\rangle_t$. For a microscopic system the instantaneous temperature is directly correlated with its kinetic energy and the number of degrees of freedom of the system, N_f, as follows

$$T(t) = \frac{1}{N_f k_B} \sum_{i=1}^{n} m_i \mathbf{v}_i(t) \mathbf{v}_i(t) \tag{2.10}$$

where k_B is Boltzmann's constant. Although the average temperature should remain constant during a simulation performed in the NVE ensemble, the presence of round-off errors in the integration algorithm and the truncation of the forces lead to small variations of the temperature. A straightforward way to modify the temperature, $T^{old} \Rightarrow T^{new}$, of a system is by scaling the velocities $V^{new} = c_T \cdot V^{old}$ at each time step. In the case the temperature is forced to be exactly fixed to a reference value, T_o, the scaling factor c_T is taken equal to $c_T = \sqrt{(T_o/T)}$. In this extreme case fast energy transfers and other artifacts like artificial pumping of energy to low-frequency modes appear [Harv98].

Other so-called weak coupling schemes consist of controlling the temperature by coupling the system to an external thermal bath. The Berendsen algorithm [Bere84] belongs to this category providing an effective exponential relaxation of the temperature towards the assigned reference value. In this case the scaling factor c_T can be obtained as

$$c_T = \sqrt{1 + \frac{\Delta t}{\tau_T}\left(\frac{T_0}{T(t)} - 1\right)} \tag{2.11}$$

where τ_T is the temperature coupling constant which stands for the coupling strength. The larger τ_T the weaker the coupling to the bath. In the limit that τ_T approaches Δt, the expression is equivalent as forcing the T to remain constant. Although this method is widely used, it does not, strictly speaking, reproduce the canonical ensemble. This can be partially overcome by the use of long enough τ_T, the removal of overall translation and rotation of the system, etc. Other schemes like Nosé-Hoover [Nose84, Hoov85] preserve the correct ensemble in a more natural way.

The macroscopic pressure is also the average of the instantaneous pressure of the system for a long enough time interval. The definition of the instantaneous pressure in simulated systems is less evident than for temperature. The usage of Clausius viral theorem provides a rather general method to access the instantaneous pressure in a condensed system. This theorem is based on the fact that the average of the temporal derivative of a bounded function is zero. If the particles are confined, $|\mathbf{r}(t1) - \mathbf{r}(t2)| < k$, one can state that:

$$m \cdot \left\langle \frac{\mathrm{d}(\mathbf{r} \cdot \dot{\mathbf{r}})}{\mathrm{d}t} \right\rangle = \left\langle \sum_{i=1}^{N} (\mathbf{r}_i \cdot \mathbf{F}_i) \right\rangle + 2 \cdot \langle K \rangle = 2 \cdot \langle K \rangle - \Xi = 0 \tag{2.12}$$

where $\mathbf{F}_i$ corresponds to the net force on the particle i, K is the kinetic energy of the system and Ξ is the virial contribution. The virial term can be separated into the terms corresponding the intra- and intermolecular forces.

$$\Xi_{int} = -\sum_{i=1}^{N} \mathbf{r}_i \cdot \mathbf{F}_i^{int} \tag{2.13}$$

which can be directly calculated from the simulation at each time step, and the external contribution originating from the pressure on the box surface

$$\Xi_{ext} = \int_S p_N \mathbf{r} \cdot \mathrm{d}\mathbf{S} \tag{2.14}$$

where p_N represents the component of the pressure normal to the surface element $\mathrm{d}\mathbf{S}$. Combining the expressions the scalar pressure is obtained to be

$$P = \frac{2K - \Xi_{int}}{3V}. \tag{2.15}$$

This expression allows the calculation of pressure in any simulated system from instantaneous positions, velocities and forces of the particles, and the box volume. Although the derivation of this equation is not strictly valid when periodic boundary conditions are applied, it can be proven that more general formulations lead to the same result [Hail92].

Using a weak coupling scheme, as it was shown for temperature, it is possible to maintain a constant pressure. This can be achieved by rescaling the positions of all particles and the box size, $\mathbf{r}_{new} = \mu \cdot \mathbf{r}_{old}$. The scaling factor can be expressed as

$$\mu = \sqrt[3]{1 + \frac{\Delta t}{\tau_P} \beta (P - P_0)} \tag{2.16}$$

where β is the compressibility of the system pressure. It is important to stress that the changes induced by the thermostat algorithm influence the calculation of the virial term and consequently the pressure, but not vice versa. Therefore, when both thermostat and barostat are applied, the thermal bath is applied first. An alternative pressure control reproducing a strictly correct ensemble is provided by the Parrinello-Rahman algorithm [Parr81].

2.4 Limitations

Although Molecular Dynamics is a well developed and successful technique for studding a vast number of systems, it has several limitations. Time and length scales, algorithms,

technical implementations are typical sources of restraints in the application of MD. The classical description of the system and the accuracy of such description result in additional limitations.

Molecular Dynamics largely relies on the available computer resources. They limit the simulated system in size and time. In contrast to other techniques where the computer memory plays a central role, current implementations of MD are basically constrained by processor time. Indeed, the size limitation of the system only reflects the need to sample properly the phase space, so a compromise between system size and simulation time is crucial. For this reason, the typical length and time scales involved in some biological processes often prevent them from being studied using MD.

Like all other computational methods, MD has its intrinsic limitations. The fundamental one arises from the act that it is based on a classical description. Although some quantum effects can be incorporated as average values into the model parameters, others can not be simply reproduced. In particular, processes including electronic rearrangements (e.g. chemical reactions) are not captured by this technique. Hybrid techniques combining Molecular Dynamics and Quantum Mechanics has be developed to address this issue [AAqv93, Bako96, Gao96]. Finally, MD displays exponentially diverging trajectories in relatively short time due to small differences in the initial configuration. This is caused mainly by integrators, the time step and the finite arithmetic used by the computer, but is also intrinsic to the chaotic nature of the equations [McCa94]. This limits the validity of singular events observed in the trajectories, placing the statistics over several runs or the calculation of averaged properties as the only relevant output [Elof93, Daur96].

In addition to the algorithm, the MD method requires a force field, i.e., a description of all interactions in the system. In principle, an atom is physically defined by its mass and number of electrons. However, the current MD functional forms do not allow a unique parameter set for each atom type, if we expect a real behavior. Different parameter sets have to be used for each specific atomic environment and protocol. The functional forms also restrict the portability of parameters between different force fields. Additionally, the usual pair-additive selection cannot incorporate some intrinsic multibody effects like polarization which is fundamental in many systems. In addition, as longer time scales are available, inaccuracies of the force fields are usually revealed [Oroz08]. Therefore, a constant revision of the available force fields is needed as the simulation times grow. Unfortunately, this is a non-rewarded hard task that requires an extensive collaboration.

Finally, it is important to understand that the simulations have, so to say, *their own physics*. Real systems have not periodic boundary conditions, neither they need shortcuts to account for the long range interactions nor approximations in the force field. In addition, these approximations require the introduction of complex algorithms and corrections to fill the gap between what it is simulated and what it is tried to be simulated: the real system. The progress observed in the last decades in this direction based on our deeper comprehension is perceptible. The increasing number of successfully studied systems clearly reflect it, moreover, the possibility to contrast the obtained results with experimental data has proven the accuracy of this technique, considered nowadays as the reference computational one in the molecular biology discipline and particularly in the membrane field.

CHAPTER 3

Motivation, Protocol and Analysis Tools

3.1 Motivation of the Thesis

The objective of this thesis is to study how the composition of a membrane effects its properties. The enormous number of molecular moieties present in cell membranes and their dissimilar distribution in a given organism provide a glimpse of this intricacy. The level of complexity contained within such small fractions of cell volume has created and inspired a large multidisciplinary membrane community.

Cell membranes act as a physical barrier but are also actively involved in countless cellular functions. Most of these functions require collective and specific combination of individual properties, functionalities and interactions of the different membrane constituents. The diversity of membrane components is responsible for its complex yet precise structure, dynamics and functionality.

Parallel to the experimental advances, theoretical modeling of multi-component membranes has also come a long way. The use of models and computer simulations has become an important and necessary tool to interpret the experimental observations and to understand cell membrane behavior. Molecular Dynamics is the most common numerical technique used for this purpose at the molecular scale. However, MD simulations do not simulate the actual complexity of real cell membranes. Simulations of lipid bilayers of two or three components do not display all of the behaviors observed in biological membranes. Due to their simplicity, simulations are often used to study the behavior of cell membranes in scenarios of reduced complexity. Understanding the behavior of such simplified systems yields further insight into their biological function. A simulation strategy based on systematic increase of the number of present moieties towards final natural composition may eventually open up new insights about more complex cell membrane behavior. Thus, for the purpose of this thesis, single compound pure systems are considered and studied first. Only after these simpler systems are understood can we introduce additional components to the membrane.

For this PhD thesis, the structure and dynamics of the plasmatic mammalian cell membrane in their molecular level have been researched. The outer leaflet of a plasmatic cell

membrane is mainly constituted of SLs, PhdChos and Cholesterol. Despite the important role of SLs, the area of concentration has been on PhdChos and Cholesterol moieties in bilayer systems. The study of the role of the unsaturated nature of PhdCho acyl chains and the effects of cholesterol in the membrane properties are the main concerns of the research presented in this Thesis.

In chapter 4 we deal with membranes composed of PhdChos that contain a double bond at different levels of their acyl chains. The role of the position of the double bond of the lipid moieties in the structure of the membrane is analyzed, in the absence and presence of cholesterol in the bilayers. The specific interaction between cholesterol molecules and the double bond of surrounding PhdChos leads to a non-monotonic behavior that maximizes the disorder of the membrane when the double bond is placed at the middle of a lipid acyl chain. This behavior is not as clear in the absence of cholesterol, thus suggesting a cholesterol-mediated lipid selection mechanism in mammalian outer plasmatic membranes.

In chapter 5 the intriguing problem of Monounsaturated membrane lipids is addressed. Monounsaturated membrane lipids have two possible acyl chain locations, *sn*–1 or *sn*–2, for the double bond. For all glycerol-based lipids present in mammalian cell membranes, the *sn*–1 chain is most commonly saturated. The reason for this is not known. We performed numerical simulations of positional isomers of PhdChos forming bilayers and small but systematic differences in all structural and dynamic membrane properties were found. More importantly, the presence of cholesterol was found to enhance these differences, suggesting again that lipid selectivity in nature is determined not only by the lipid properties but also by its differential interaction with cholesterol.

In chapter 6 the force field parameterization of double bond in unsaturated lipid acyl chains is examined. The standard parameters of the GROMOS87 force field and a corrected description by Bachar et al. are compared. Surprisingly, seemingly insignificant details in the force field can change even some of the qualitative trends presented in the previous chapters.

The interaction of cholesterol with PhdCho lipid components has been the main goal of study for our research. The detailed molecular analysis of the specific ordering and packing capabilities of cholesterol molecules is summarized in chapter 7. In this chapter we examine how the specific cholesterol's molecular structure is responsible for these capabilities, particularly, the presence of the two off-plane methyl groups from the sterol rigid which induce a specific symmetry for the location and orientation of other lipids in the membrane around a given cholesterol molecule.

Finally, chapter 8 contains the research on lipid membranes composed of cardiolipin molecules. In mammalian cells, such compounds are common constituents of mitochondria membranes, which seem to be more similar to bacterial than to eukaryotic plasmatic membranes. The unique features provided by their specific components attracted our attention and are studied in this chapter.

3.2 Protocol and Force Field

In this section a description of the simulation protocol and force fields used in this work will be provided. In order to obtain trustful simulation results two criteria were followed. First, only extensively tested combinations of force fields and protocols were considered. Only when

the initial combination did not provide an accurate description of the phenomena of interest alternative parameters were used. Second, in order to coherently compare results between simulations, we used common protocols and bilayer arrangements. This ensures a large number of similar characteristics between systems and will be discribed bellow. Afterwartds a description of the force field and peculiarities of the protocol used in the simulations discussed in chapters 4 to 7 is presented. Finally, the completely different force field used in chapter 8 will be studied.

All simulated systems had the same bilayer arrangement. Two inverted monolayers with the required lipid composition spread in the xy-plane are placed one over the other. Finally, two water slabs sandwich the bilayer in the z-direction. The simulation always uses periodic boundary conditions in the three directions with the usual minimum image convention. The periodicity in the xy-plane results in an extended simulated bilayer. In principle, the number of water molecules that separate the hydrophilic headgroups of opposite leaflets minimize the interaction between them.

All simulations were performed using the GROMACS software package [Lind01b, Spoe05a] in its 3.3.1 version and carried out in the NPT (constant particle number, pressure and temperature) ensemble. The temperature and pressure were controlled by using the weak coupling method [Bere84] with the relaxation times set to 0.6 and 1.0 ps, respectively [Bere84]. The temperatures of the solute and solvent were controlled independently to avoid the transfer of the kinetic energy from the bilayer to the solvent. We do so because the simulated energy exchange between different components is not perfect, resulting in an effective cooling of the membrane via the excessive transfer of energy towards the solvent [Spoe05b]. The pressure coupling was applied separately in the bilayer plane (xy-) and the perpendicular z-direction. The pressure was fixed to 1 bar for all simulations, whereas different temperatures were used. All bond lengths were systematically constrained which allowed a time step of 2 fs. The SETTLE algorithm [Miya92] was used to preserve the bond lengths in water molecules, whereas the lipid bond lengths were constrained with the LINCS algorithm [Hess97], see Sec. 2.3.2. The long range interactions were settled in the following way. A single 1.0 nm cutoff distance was used for the Lennard-Jones functions describing the Van der Waals interactions [Patr04]. Electrostatic interactions were described by the particle-mesh Ewald method (PME) [Essm95] with a real space cutoff of 1.0 nm, β-spline interpolation (of order 6), and direct sum tolerance of 10^{-5}. The simulation protocol applied here has been successfully applied in previous MD simulations [Rog01, Falc04, Aitt06, Niem06, Niem07].

The systems studied in chapters 4, 5, 6 and 7 are mostly constituted by phosphatidylcholines with acyl chains fixed to 18 carbons forming pure bilayers or mixed in different proportions with cholesterol. We used the standard united-atom force field parameters that have been extensively tested and verified for saturated dipalmitoylphosphatidylcholine (DPPC) molecules (see e.g., Refs. [Berg97, Patr04] and references therein). The partial charges used were taken from the underlying model description [Tiel96]. For the double bond in the unsaturated acyl chains, we used the description by Bachar et al. [Bach04], except in chapter 6 where we compared this choice to the standard double bond parameters of the GROMOS87 force field [Tiel99, Tiel02] which, in contrast to the Bachar's description, do not account for skew angles of saturated bonds next to a double bond [Niem06]. The Simple Point Charge (SPC) model [Bere81] was used for water. For cholesterol, we used the description of Holtje et al. [Holt01] as described in Ref. [Rog07a]. Although, most of

the simulations were performed at 338 K, different temperatures were used. The selected temperature is above the main phase transition temperature of DSPC (T_m= 328 K), the highest among the studied lipid species [Koyn98]. Any result which corresponds to a different temperature than 338 K will be indicated.

In chapter 8 the simulation of highly charged cardiolipin molecules in a lipid matrix resembling the natural ones will be described [Daum85]. In this case we used the all-atom OPLS (optimized parameters for liquid simulations) force field [Jorg96, Rizz99, Kami01, Pric01]. Partial charges on the PhdCho headgroup were taken from Takaoka et al. [Taka00], and those of PhdEtn were from Murzyn et al. [Murz99]. Both sets of charges were derived compatible with the OPLS methodology. The same partial charges were used for the phosphate and carbonyl groups of Card, and the standard OPLS charges were used for the hydroxyl group on the Card glycerol backbone and in the liking hydrocarbon chains. This parameterization has proven to reproduce the properties of lipid bilayers composed of PhdCho, PhdEtn and glycolipids [Rog07b]. For water, we employed the TIP3P model, which is compatible with the OPLS parameterization [Jorg83]. The temperature and pressure baths were implemented by using Nosé-Hoover [Nose84, Hoov85] and Parrinello-Rahman methods respectively [Parr81]. The working temperature was fixed at 310 K ensuring the fluid phase of all simulated bilayers.

In all simulations, equilibration of the system was monitored by following the time evolution of the area per lipid, potential energy, and temperature. In most cases 20 ns was enough to ensure a proper equilibration. The simulation length plays a crucial role in this work since most evaluated properties require large statistics. For pure systems, the simulation time always exceeded 100 ns. In the case of systems containing mixtures of lipids, the times were increased to at least 150 ns to allow a proper mixing. In cases where the diffusion rates were rather small due to the presence of high cholesterol concentration, 300 ns simulations were done, see chapter 7. To allow long time scales we limited the size of our systems. Even though their final size is always over the 64 lipids per layer. This has proven to be sufficient to minimize the finite-size effects due to the periodic boundary conditions [Tiel97]. The number of waters were chosen above the full hydration limit which is experimentally found to be about 0.36 [Inok78, Ruoc82] to 0.40 [Jani76] (in weight fraction of water) for DPPC in the L_α phase.

3.3 Membrane Properties: Analysis Tools

In this section we will discuss the general properties of the membrane that are evaluated from the simulation data. They include structural and dynamic properties which are systematically computed in all the systems. The error bars of all the properties computed in this Thesis were estimated using the block analysis method [Hess02], and are represented by twice the standard error.

3.3.1 Area per Molecule

The area per lipid molecule in a pure bilayer corresponds to the total average membrane area divided by the number of lipid molecules in a single leaflet. It is a basic variable that characterizes the bilayer structure, and its value depends significantly on the membrane

composition, hydration level of the membrane, ionic force of the medium, pH, temperature and pressure. The area per lipid value summarizes large amounts of structural and dynamic properties of the membrane, especially its ordering, so that it can be used to estimate several properties. The area per lipid is indicative of the membrane's phase. Phd membranes values below 0.46 nm^2 usually suggest a gel phase while those above 0.5 nm^2 suggest liquid disordered phase or in the case of cholesterol mixtures the liquid ordered one. Therefore, this property is critical to ensure the veracity of the simulated bilayers as we usually want to simulate them in the fluid phase, which constitutes the more biologically relevant phase.

Next, as membranes behave as incompressible fluid, the molecular volume can be considered well conserved at a given temperature [Pan06, Meye09]. Therefore, the area per lipid shows an inverse relation with the bilayer thickness. These two properties are well known to modulate membrane functionality, in particular of membrane proteins. Other properties related to the in-plane ordering as the acyl chain tilt and ordering are also closely related to the value of the area per molecule.

Finally, membrane permeability is directly correlated to the area per molecule, and not strictly to its thickness, as commonly thought [Nagl07, Math08]. Most in-plane dynamic properties are also modulated by the area per molecule of the bilayer. Higher values of the area per molecule generally increase the different motion modes (diffusion rates, chain and headgroup dynamics...).

The area per molecule provides an important additional feature. The observation of the evolution of the instantaneous area per lipid with time provides a good mechanism to determine the equilibration period of the simulated bilayer, see Sec. 3.2. When the equilibrium is reached, the area per molecule fluctuates around a mean value which is the one used to characterize the membrane. The presence of slow mixing processes compared to the simulation time scale can eventually invalidate the usage of the area per molecule to determine the simulation equilibration time.

While the area per lipid is trivial to compute in a single-component system, its definition is considerably more complicated in multi-component systems [Chiu02, Hofs03, Falc04, Edho05]. In multi-component membrane systems it is not obvious how the crosssectional area of a lipid should be defined and how the free area in the membrane plane should be distributed between the different molecule types. For the same reason, the volume per molecule is not well defined in many-component systems since there is no unique way to decompose the free volume to contributions occupied by individual molecule types. For a more detailed discussion of this matter, see Refs. [Chiu02, Hofs03, Falc04, Edho05].

The average area per Phd molecule, A_{PC}, in a single-component system is computed by dividing the total average area of the membrane, A, by the number of Phds molecules in a single leaflet ($N_{PC}/2$),

$$A_{PC} = \frac{A}{N_{PC}/2}. \tag{3.1}$$

For binary mixtures with cholesterol there are several definitions available for a comprehensive discussion see Ref. [Edho05]. We have used two variants. The first is analogous to the one used for the pure systems (Eq. 3.1). This method, which ignores the presence of cholesterol to compute the area per molecule, provides a good estimation of the spacing between lipids in the mixture systems when compared with the pure ones. The second

method provides a more accurate way to calculate the area per molecule by decomposing the area between the different moieties in membrane. This methodology complements the previous by providing a clear picture of the deviation presented by the molecular moieties from the ideal mixing where the areas shown in pure bilayers are preserved in the mixtures. The procedure developed by Hofsäßet al. defines the area per PC as [Hofs03]:

$$A^*_{PC} = \frac{2A}{N_{PC}}\left[1 - \frac{N_{chol}V_{chol}}{V - N_wV_w}\right] \tag{3.2}$$

where V is the volume of the simulation box, N_{PC} is the number of PC molecules, N_W is the number of water molecules, V_W corresponds to the volume occupied by a water molecule, N_{chol} stands for the number of cholesterols and V_{chol} is the volume of a cholesterol molecule. Essentially, this expression implies that the crosssectional area of a lipid divided by its volume equals the area of a membrane leaflet divided by its volume. APC can be computed provided that V_W and V_{chol} are known. V_W is obtained from an independent simulation of a slab of water molecules in the same simulation conditions (for SPC water molecules at 338K V_W =0.032 nm^3), and the cholesterol volume has been taken from its crystallized volume to be 0.541 nm^3 [Edho05]. The left over area that is not assigned to Phds corresponds to cholesterols and it can be calculated by [Hofs03]:

$$A^*_{chol} = \frac{2A\ V_{chol}}{V - N_wV_w} \tag{3.3}$$

The area per lipid is experimentally available for a large number of bilayer systems, so it is one of the most widely bilayer characteristics used to validate the simulation results. It can be extracted from several experimental techniques as diffraction (Sec. 1.6.2) and NMR (Sec. 1.6.1.3) experiments on bilayers. Calculation of the area per molecule always requires the interpretation of the experimental data by means of a modeling approach so that they depend on the used model approximations. Therefore, published experimental results often differ significantly. Direct comparison with other membrane properties that do not require model-based interpretation of the experimental data seems more appropriate. Membrane thickness or form factor (see Sec. 1.6.2) are two examples.

3.3.2 Membrane Thickness

The membrane thickness characterizes the transverse structure of the membrane. It constitutes an essential property of the bilayer that in turn modulates membrane functionality, like the hydrophobic mismatch [Mour84] responsible of some integral protein functionality. The membrane thickness strongly depends on the lipid composition. Changes in the headgroup, length or unsaturation level of the acyl chains are certainly reflected in its value.

Thickness provides direct information of the chain ordering. Highly ordered systems like those observed in the bilayer gel phases present mostly their lipid acyl chains in their extended conformation [Mars08]. This means that almost all dihedrals between the methyls groups are in *trans* orientation (180°). In this situation, assuming that the chains are perpendicular to the bilayer plane, the bilayer thickness achieves its maximum value. However, if lipids are tilted they show a thickness smaller than expected from the length of the acyl chain in the measured lipid moiety. More significantly it is the drastic reduction of the thickness observed in bilayers in their liquid phase as is seen over the main transition temperature (T_m). In this

situation, the acyl chains can access to a larger number of configurations, for example the gauche ones, and this implies an effective reduction of the acyl chain length in the direction perpendicular to the bilayer plane, and in turn of its thickness. Similarly, the incorporation of *cis* double bonds in an acyl chain, the ones used in this work, forces a bend in the chain conformation and therefore a reduction of the thickness is also observed.

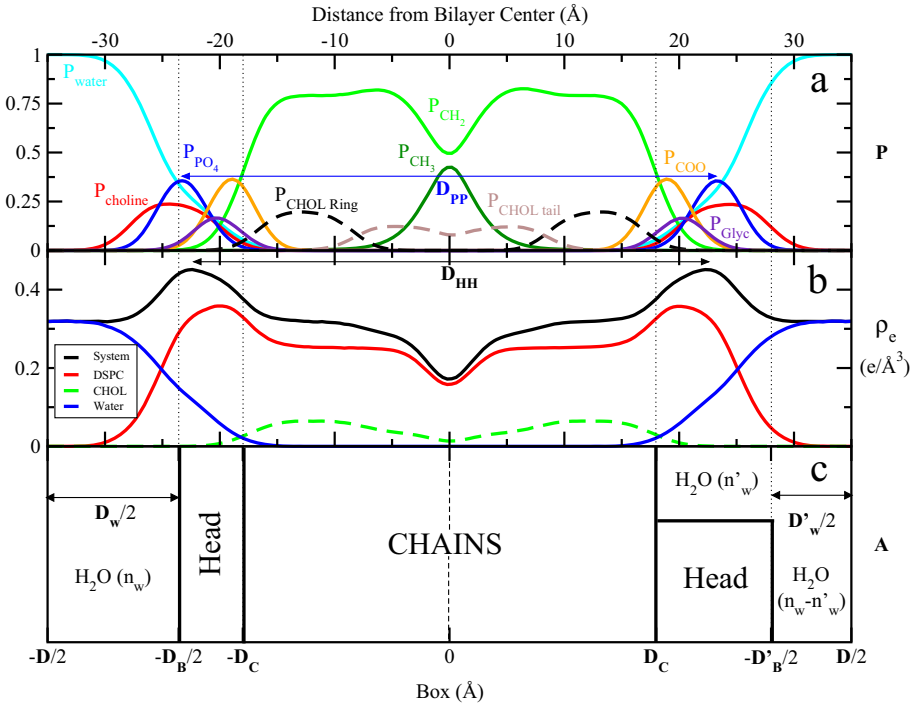

Figure 3.1: Three different representations of the transverse structure of the fully hydrated bilayer of DSPC mixed with 20 mol% of Cholesterol at 338 K in the L_α fluid phase. Panel (a) presents the probability distributions, P=(ρ_e^X/ρ_e), for different atomic sets in the system. Panel (b) shows the electron density profiles, ρ_e, for the whole system as well as for each different moiety in the system. Panel (c) contains a schematic representation of the membrane by usage of Gibbs dividing surfaces. The left side presents the simple three compartment region where no mixing of the headgroups and the water is assumed. In the right side is the more realistic representation of the headgroup region, where water shares space with the lipid headgroup. The x-axis is in Å along the bilayer normal with the same scale for (a), (b) and (c). In (c) the y-axis corresponds to the bilayer surface per lipid. The vertical lines crossing the graphs represent the approximated positioning of planes typically used by the experimentalists to define bilayer thickness. $2\mathbf{D_C}$ corresponds the thickness of the hydrophobic core. $\mathbf{D_B}$ and $\mathbf{D'_B}$ are the bilayer thickness where only the last explicitly considers the coexistence of lipid atoms and water molecules in the polar interfacial region. Additionally, $\mathbf{D_w}$ and $\mathbf{D'_w}$ are the respective water slab thickness. Finally, $\mathbf{D}$ corresponds to the repeat spacing between layers in multillamelar vesicles or stack bilayers. Adapted from [Nagl00] with own data [Mart07].

The extraction of the thickness from simulated membranes only requires the definition of the interface plane for each trajectory frame. There is no single correct definition, and in this work two different standard definitions were used. First, we used the temporal average distance between average position of phosphorus atoms in opposite leaflets, $\mathbf{D_{PP}}$ (see Fig. 3.1a) that is computed as

$$\mathbf{D_{PP}} = \langle \langle z_{P_i} \rangle_{n_1} - \langle z_{P_j} \rangle_{n_2} \rangle_t \tag{3.4}$$

where n_1 and n_2 correspond to the phosphorus atoms in each leaflet and z is the coordinate perpendicular to the bilayer plane. This distance allows an easy monitoring of the temporal variation of the bilayer thickness. This measure has a rather small associated error due to the large statistics available by measuring this distance at each time step, combined with the fact that the phosphorous atoms are placed in a rather fixed position in the membrane. This has been very important in our work when comparing the measures for different bilayers with similar thickness. The second used method requires the previous calculation of the system electron density profile, see Sec. 3.3.3. From the profile of the whole system, the bilayer thickness is taken as the distance, $\mathbf{D_{HH}}$, that is calculated as the distance between the two profile peaks, see Fig. 3.1b. This constitutes a common way to characterize the membrane as this value can be also obtained experimentally. However, this method has an important drawback since it does not account entirely for the hydrated region of the interface.

A large amount of experimental values for bilayer thickness can be found in the literature. Their comparison with simulation results is not straightforward as they are mainly based on non-physical volumetric models, see Fig. 3.1c. The only thickness measure that is available experimentally without any modeling is the repeat spacing, $\mathbf{D}$. It corresponds to the distance between two equivalent positions in adjacent bilayers for a stack of bilayers. Unfortunately, this distance is directly influenced by the level of hydration in the measured sample. Other reported thickness values rely on geometrical considerations of the positioning of different membrane groups and more importantly, they rely on the assumption that the molecular volume remains constant regardless of the environment and is only dependent on the temperature. These models are not directly reproducible by simulation data, and therefore the quantitative comparison is often difficult. For a good review on this issue see Ref. [Nagl00].

3.3.3 Density Profiles

Membrane density profiles correspond to the temporal average structure of some extensive properties as a function of the absolute position in an external reference system, see Fig. 3.1. Typical measured properties are mass, electronic density, charge, scattering length, occurrence, etc. For membranes, our interest is restricted to the z-direction, the one perpendicular to the bilayer plane. The in-plane fluid nature of bilayer ensures a constant value of any extensive property along the membrane plane. This value corresponds to average value of the considered property in the whole membrane.

Membrane density profiles can be obtained experimentally and can also be computed from Molecular Dynamics simulations. Although different experimental techniques provide access to different profiles, we will focus our attention on the electron density profiles, ρ_e, extensively used in this Thesis and accessible by small-angle X-ray scattering (SAXS). As shown in Sec. 1.6.2, SAXS provides direct access to the form factor, F(h) (Eq. 1.6), and as a result the density profile can be obtained via the following relation:

$$\rho_e(z) = \frac{F(0)}{D} + \frac{2}{D} \sum_{h=1}^{h_{max}} F(h) \cos\left(\frac{2\pi h z}{d}\right). \tag{3.5}$$

For Molecular Dynamics simulations, since the obtained trajectories contain the exact position of each particle, the calculation of electron density profiles, ρ_e, is a trivial process, see Fig. 3.1b. The method consists of binning the system and adding the number of electrons corresponding to each atom unit inside the corresponding bin. The obtained profiles are averaged along the simulation time. The described process assumes that the electrons corresponding to a given atom unit are placed in the center of the atom [Fell97, Chiu99]. Alternative methods not used in this work consist of placing a Gaussian distribution of electrons on each atom center [Tu95]. Eventually, this solution has been proven to be less accurate and too dependent on the choice of the Gaussian width [Benz05]. Due to the presence of periodic boundary conditions, the simulated systems may drift along the z-direction. This movement has to be removed before calculating ρ_e.

The shape of ρ_e of a lipid bilayer is presented in Fig. 3.1b. The minimum observed in the plot indicates the center of the bilayer and corresponds to the region where the terminal methyl groups reside. This region separates both leaflets and is usually taken as the origin of the z-axis. At both edges of the profile we find a constant value region that corresponds to the bulk water region. Another feature present in all systems is a clear maximum observed in each leaflet. They correspond to the headgroup regions where the heavy phosphate groups reside. Other features are not that general and are composition dependent.

In the whole bilayer profile, ρ_e, it is possible to compute subprofiles, ρ_e^X, of a given atomic set, X, see Fig. 3.1a. In this figure we have plotted the position of the choline, phosphate, glycerol, carbonyls, methylene and terminal methyls groups corresponding to a 1,2–stearoyl–*sn*–glycero–3–phosphatidylcholine (DSPC) lipid bilayer mixed with 20 mol% of Cholesterol at 338 K. The locations of the cholesterol ring and chain have been represented. These subprofiles may help to properly parameterize the simulated lipids as such details can be available experimentally combining X-ray and neutron diffraction methods [Wien92].

Electron density profiles can be also used for the calculation of the form factor, see Eq. 1.7. The benefit of using the form factor is that it can be computed from simulations and then compared with experimental model-free measurements; the form factor is essentially primary data measured from experiments.

3.3.4 Tilt

Tilt refers to the average angle between a studied vector, $A \mapsto B$, and the z-axis, which is perpendicular to the bilayer plane. The direction of the z-axis was chosen independently for each leaflet in a way that it always points from the headgroups towards the chains, so the analysis of each leaflet was be conducted independently. Several tilts are computed in this Thesis and unless otherwise stated, they are generically noted as $t_{A\mapsto B}$ where A corresponds to the initial atom name and B to the final atom name.

Some tilt measures can be correlated to membrane ordering. For example, the tilt of the lipid chains, cholesterol ring and cholesterol chains are the most frequently used to study membrane ordering. As a general rule, the larger tilt the weaker the ordering. This correlation between tilt and ordering is only strictly valid in fluid phases (as those simulated in this Thesis). Gel phases may display a tilted packing which should not be confused with a disordered state. The tilt of the lipid chains is calculated by using the vector between the methyl placed next to the carbonyl group and the terminal methyl group, t_{sn-1} and t_{sn-2}

for each chain. The cholesterol (sterol) ring is defined using the ring carbon attached to the hydroxyl group and the ring carbon attached to the cholesterol (sterol) chain, t_{CHOL}. The tilt of the flexible cholesterol (sterol) chain is defined using the vector between the chain methyl which links to the chain to the cholesterol ring and the one before the last methyl group, t^t_{CHOL}.

Other tilt measures account for the behavior of the headgroups at the lipid/water interface. The usual choice is the tilt of the vector connecting the phosphorus atom and the nitrogen atom of the amine group, $t_{P\mapsto N}$. The vectors used in this Thesis to calculate molecular tilt angles are schematically presented in Fig. 3.2.

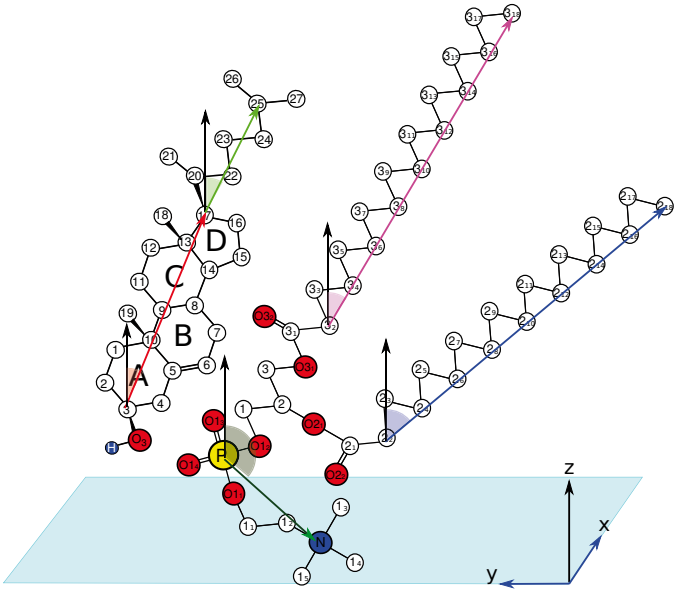

Figure 3.2: Graphical representation of the most common tilts used in this Thesis. The definition segments and the correspondent angles for PhdCho and cholesterol are depicted: t_{sn-1} (purple), t_{sn-2} (blue), $t_{P\mapsto N}$ (dark green), t_{CHOL} (red) and t^t_{CHOL} (green).

3.3.5 Pair Correlation Functions

The fluid nature of the membrane, due to the balance between the attractive intermolecular interaction and the disordering thermal motion, is shown by the inexistence of a sharply defined (solid-like) positional ordering. This can be easily proven by scattering experiments where no diffraction peaks are observed in the bilayer plane. Despite this, membranes in their fluid phase indeed display certain levels of spatial ordering. The analysis of this ordering allows the identification and description of the fundamental interactions between membrane components that are responsible of the final membrane structure. This analysis is usually performed using pair correlation functions. In general, a pair correlation function describes the probability of finding a particle (defined as a the center of mass of a molecules or a part of it) at a given position, $\mathbf{r}$, respect another one. This can be expressed as [Alle90]:

$$g(\mathbf{r}) = \frac{V}{N_1 N_2} \left\langle \sum_{i=1}^{N_1} \sum_{j=1}^{N_2} \delta(\mathbf{r} - \mathbf{r}_{ij}) \right\rangle \tag{3.6}$$

where N_1 and N_2 correspond to the number of reference and surrounding particles respectively, placed in the analyzed volume V, and the brackets reflect temporal averaging. The correlation functions are normalized so that they are equal to 1 if the density of surrounding particles at a position $\mathbf{r}$ is equal to their system's average density.

Although $g(\mathbf{r})$ is originally defined in three dimensions, sometimes it is not possible to define an internal coordinate axis equivalent for all reference particles that remains invariant in time. The alternative to use a laboratory reference axis in a fluid system results in the averaging of all three coordinates due to the molecular motion. In some special cases, coordinates can be clearly defined in fluid systems corresponding to directions where the fluidity is restricted, like the perpendicular direction to the membrane plane. Pair correlation functions are often simplified to a single coordinate function corresponding to the distance between particles, which is always well defined and independent of the chosen reference axis. In this case pair correlation functions are called radial distributions. In membranes, due to the anisotropy in the z-direction, we can also define a radial distribution in the bilayer plane, by using only the xy-coordinates of the considered particles. Both types of radial distributions have been used depending on the particular needs.

The analysis in terms of pair correlation functions provides the following information. First, the presence of peaks reflects the preferred distances between the analyzed particles, see Figs. 3.3a and 3.3b. Second, the area under the peaks directly correlates to the probability of such positioning. Third, the presence of repeating peaks with the distance reflects long-range ordering. The smaller the drops of the height of the peaks with the distance, the larger the ordering between the two considered particles (compare Figs. 3.3a and 3.3b).Fourth, the presence of high peaks at characteristic covalent bonding distances (even when no covalent bond is explicitly present) usually reflects closely interacting particles, see Fig. 3.3c. Finally, when the correlation between atom groups is analyzed, the smallest distance that makes $g(r) = 0$ corresponds to the minimum approach distance between the analyzed atoms, see Fig. 3.3c.

3.3.6 Order Parameter

Although lipid diffusive motions are basically restricted to the bilayer plane, part of this mobility also influences the transverse structure. Differential behavior observed in tilt and molecular tumbling on lipid segments located at different depths of the membrane is a direct consequence. To estimate such behavior an order parameter, S_{mol}, is introduced for each considered lipid segment. This variable quantifies the environmental fluidity felt by the selected lipid segment by evaluating its order. The concept of ordering refers to the deviation of the segment geometry with respect to the one expected in an ideal ordered chains which is completely perpendicular to the bilayer plane, with all bonds permanently in *trans* conformation. In order to do so, this variable considers both the tilt of the segment respect the bilayer normal and the dispersion around the mean tilt value. S_{mol} evaluates the angle, θ, between the chosen segment (usually connecting two alternating methyl groups of an acyl chain) and the bilayer normal with the following relation:

$$S_{mol} = \frac{1}{2} \left\langle 3\cos^2\theta - 1 \right\rangle_{t,mol} \tag{3.7}$$

brackets refer to the temporal and molecular average. The most common lipid segments

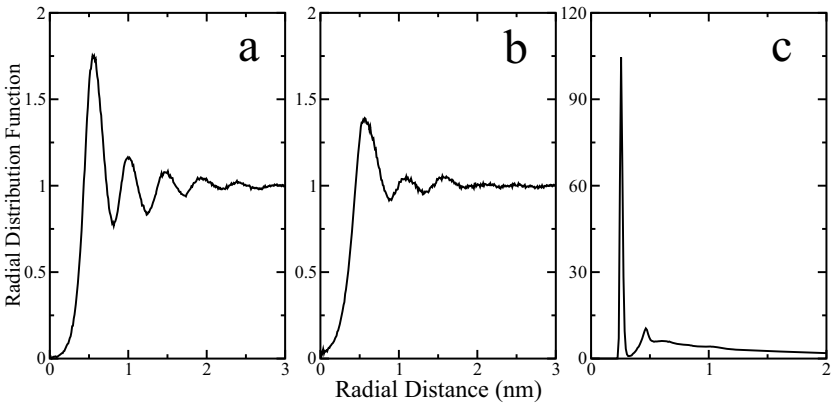

Figure 3.3: Typical outputs from radial distribution functions (RDF) in fluid environments like our simulated membranes. Panel (a) shows a rather ordered pattern corresponding to the positional correlation between the center of mass of cholesterol ring fragments and the center of mass of the *sn*–1 chains in the mixture of DSPC with 20 mol% of cholesterol. Panel (b), instead, shows a significantly decreased ordering pattern corresponding to the same fragment pairs, although this time for a mixture of DOPC with 20 mol% of cholesterol. Panel (c) shows the output of the positional atomic based correlation between the oxygens in the cholesterol hydroxyl group and the DSPC carbonyl oxygens in the esters linking the acyl chains with the glycerol group for the same system as in panel (a). In the latter example, despite cholesterol and DSPC molecules are not covalently bonded, these two groups act as closely interacting pairs. A range of distances with $g(r) = 0$ can be observed, corresponding to the exclusion distance between the two interacting atoms due to short-range repulsive electronic forces. Data extracted from [Mart08b].

segments studied with these functions is the one between two methylene carbon atoms spanned by two bonds in the acyl chains. The obtained S_{mol} between the atoms C_{n+1} and C_{n-1} is assigned to the C_n atom placed in between. Saturated acyl chains perpendicular to the bilayer plane with all bonds in *trans* configuration (that corresponds to the minimum energy configuration) S_{mol} equals 1. This value corresponds to perfect ordered chains only partially found in non-tilted gel phases. In fluid phases acyl chains are tilted and do not remain in their *trans* configurations, so the associated S_{mol} values are significantly smaller.

Other typical studied segments are the C-H in the acyl chains. The order parameter of these segments, S_{CD}, can be obtained experimentally as introduced in Eq. 1.2. In completely perpendicular saturated acyl chains (all bonds in *trans* conformations) the angle between the *C–H* bonds and the bilayer normal is close to 90° resulting in $S_{CD} \sim -1/2$. In fluid bilayers this value increases as a signature of the higher disorder, see Fig. 3.4. As a general rule the higher disorder the higher the value obtained for S_{CD}.

Since the united atom model does not account for hydrogen atoms, the calculation of S_{CD} is not straightforward. Two equivalent solutions can be used to overcome this difficulty. The first method consists of virtual addition of the hydrogen atoms using ideal geometry criteria for location in the simulation trajectory data. The second method uses second order tensor [Aitt07] to describe the order parameter, S_{ij}, defined as:

$$S_{ij} = \frac{1}{2} \left\langle 3 \cos\theta_i \cos\theta_j - \delta_{ij} \right\rangle_{t,mol} \tag{3.8}$$

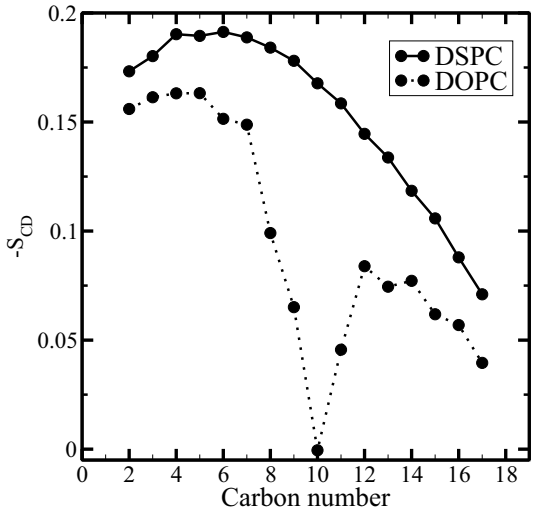

Figure 3.4: The S_{CD} order parameter profiles for the *sn*–2 chain of DSPC (d18:0) and DOPC (18:1c9) at 338 K are shown. Carbon numbers correspond to the numbering of the methyl groups along the acyl chain, see Fig. 3.2. These two profiles contain the typical features displayed by S_{CD} for a saturated Phd (DSPC) and an unsaturated Phd (DOPC) in the fluid phase. They display the typical maximum (notice that normally we represent $-S_{CD}$) around the 6^{th} carbon which correspond to the most ordered region of the layer. We can see that moving from the maximum towards the bilayer center (i.e. larger carbon numbers), the segments become more disordered finding the highest disordering section in the bilayer center. The comparison between DOPC and DSPC profiles shows that DSPC bilayer is substantially more ordered than DOPC bilayer. In the DOPC curve the presence of a double bond is visualized by the presence of a deep constituted not only by the atoms attached to the sp2 carbons (atoms 9 and 10) but also to the methyls nearby the double bond (especially atoms 8 and 11).

where θ_i is the angle between the i^{th} molecular axis and the bilayer normal. At any non-terminal sp3 carbon, C_n, placed along the acyl chain, the molecular axis is defined using the two neighboring carbon atoms. The z-axis corresponds to the vector linking C_{n-1} and C_{n+1} atoms. The x-axis is chosen perpendicular to C_{n-1}, C_n and C_{n+1} atoms, whereas the y-axis is chosen to be perpendicular to the previous two vectors. All vectors are chosen unitary. According to this reference axis system, for sp3 hydrogen atoms with their ideal tetrahedral geometry the S_{CD} is reduced to:

$$S_{CD} = \frac{2}{3}S_{xx} + \frac{1}{3}S_{yy}. \tag{3.9}$$

For segments containing double bonds the geometry corresponding to the sp2 hybridization is different than for the saturated sp3 methyl groups. So, for lipid segments involving a double bond, Eq. 3.9 does not reproduce the position of the hydrogen atoms anymore. Instead, for *cis* double bonds, the hydrogens share the same plane with the C_{n-1}, C_n and C_{n+1} atoms and have an ideal angle of 120°, so that one can obtain the S_{CD} from the following expression:

$$S_{CD} = \frac{1}{4}S_{zz} + \frac{3}{4}S_{yy} - \frac{\sqrt{3}}{2}S_{yz} \tag{3.10}$$

where in this case the z-axis is taken parallel to the double bond. It is important to notice that the higher values of S_{CD} reported at the double bond position do not reflect lower

ordering, but a completely different geometry, see Fig. 3.4. Therefore, direct comparison of the disorder between saturated and unsaturated segments is not possible from the S_{CD} calculation. The comparison of saturated carbons provides information about which acyl chain segment is more disordered.

Often, in order to compare different moieties we compute the average of the order parameters,$\langle -S_{CD} \rangle$, belonging to all carbon groups of an acyl chain. This provides a unique measure that reflects the whole chain ordering. To optimize the comparison between saturated and unsaturated species these averages exclude the carbon atoms of the double bonds, since as stated before, they display drastically different S_{CD} values due to their different geometry and not to their ordering differences with the saturated homologues.

3.3.7 Interface Interactions

In membranes we can distinguish three topologically different groups of interactions with rather distinctive nature: the interactions in the hydrophobic region, the interactions between the lipids heads, and finally the interactions between the headgoups and the solvent. These last two interactions take place at the water-lipid interface, and are mainly originated by polar interactions and hydrogen bonds (contrary to the hydrophobic region interactions that have mainly a van der Waals nature). The calculation of the number of hydrogen bonds, water bridges and charge pairs provides a reasonable description of the membrane interface as they constitute the major intermolecular terms. Their calculation from a MD trajectory depends largely on the used definition because the simulated system does not implicitly considers such terms as hydrogen bonds, which clearly requires electronic rearrangements, not considered in MD. To define a hydrogen bond we have first to identify the possible donor and acceptor atoms capable of promoting hydrogen bond formation. In this Thesis the only atoms considered capable to act as donors are in the hydroxyl functional group found in water, cholesterol and cardiolipin lipid molecules. The number of acceptors is substantially larger, since, besides the former hydroxyl groups, the phosphate oxygens in the choline group and carbonyl groups in the ester linkages have to be considered. Next, we need to define some geometrical constrains between the involved atoms that corresponds to a hydrogen bond. The geometrical definition of a hydrogen bond used is quite restrictive. Not only restricts the distance between the donor and acceptor oxygens to be smaller than 3.25 Å, but also the angle between the $\overrightarrow{O_{donor} - O_{acceptor}}$ vector and $\overrightarrow{O_{donor} - H}$ vector to be smaller than 35°. The selected distance 3.25 Å corresponds to the first minimum in the radial distribution function (RDF) between water oxygens and Phd oxygens [Murz01]. A water bridge corresponds to a water molecule simultaneously hydrogen bonded to two different lipid oxygen atoms. This kind of structure seems to substantially stabilize the system. The charge pairs are completely different entities. They are formed when a negative charged carbonyl or non-ester phosphate oxygen interacts closely with a positively charged choline methyl group. Only radial distance between the two groups is taken into account and is restricted to be smaller than 4 Å. The obtained results for the three mentioned interface interactions can be given as total numbers, but also in some occasions we are interested in the particular contribution of an atom to these interactions. This can provide, for example, an idea of how exposed the different oxygen groups are from the lipid components to the water molecules.

3.3.8 Basic Dynamic Properties: Diffusion Coefficient and Autocorrelation Functions

The fluid nature displayed by biological membranes is probably one of their most interesting characteristics. Fluidity refers to all motion modes of the membrane. These modes range from collective membrane deformations that involve millions of molecules to the localized rotational motions present in each fragment belonging to a flexible lipid acyl chain. Such motional diversity complicates its systematic characterization.

The limited size of the bilayer systems used in this Thesis and the applied periodic boundary conditions prevent from any significant undulation in the simulated membranes, and therefore, any dynamic contribution from undulation modes is considered. Our limited time simulation restricts also dynamical processes to the nanoseconds time scale, so that slower motions are not accessible by our simulations. We do not observe the flipping of lipids between leaflets since this process occurs at characteristic times of the order of seconds for the considered moieties [Stec02, Angl07, Papa07]. Molecular in-plane diffusion and self-rotation are the fastest motions that can be analyzed using our simulations, therefore they constitute our slowest modes.

Lateral diffusion in the bilayer plane is an important dynamic property. It can be measured by both experiments (Sec. 1.6.1.1) and simulations. It measures the capacity of the moiety to move along the leaflet. The lipid lateral diffusion is characterized from simulation by measuring the diffusion coefficient

$$D_i = \lim_{\tau\to\infty}\left[\frac{1}{4t}\langle|\mathbf{r}(t+\tau)-\mathbf{r}(t)|^2\rangle_{i,t}\right] \tag{3.11}$$

where $\langle|\mathbf{r}(t+\tau)-\mathbf{r}(t)|^2\rangle$ is the mean-square displacement (MSD) of the center of mass of a lipid in the xy-plane averaged over all molecules of type i in the membrane. A linear (diffusive) regime of the MSD is identified in the simulations after some equilibration time, allowing the calculation of the diffusion coefficient. Each monolayer in the membrane can drift during the simulation. Therefore, the motion of the center of mass of individual leaflets has to be removed before computation of the lipid MSD. When controlling the pressure of the system by rescaling the box, the diffusion coefficient can also be altered, the parameters chosen for the controlling bath are therefore critical. The coupling pressure constant has to be taken long enough to minimize the influence of the pressure bath on the obtained diffusion coefficients.

Other useful motion modes describing the dynamical nature of the membrane correspond to the rotational modes of the different lipid species or parts of them. These modes can be obtained by analyzing the so-called autocorrelation functions (ACF) of specific intramolecular vectors. The idea is to choose a functional form so that when the system evolves far from the original configuration its value decreases. These functions measure the temporal memory of the system to retain a particular configuration. Therefore, the longer time the configuration is retained, the slower the analyzed mode. A simple definition of the time-dependent ACF is provided by a temporal correlation following the first associated Legendre function of an intramolecular vector $\mathbf{f}(t)$ of the analyzed molecule,

$$C_1(\tau) = \langle\mathbf{f}(t)\cdot\mathbf{f}(t+\tau)\rangle_{t,mol}. \tag{3.12}$$

In this Thesis different vectors $\mathbf{f}(t)$ have been analyzed for both PhdChos and cholesterol moieties. In the case of PhdChos, to study different rotational motions, several vectors at different depths and molecular parts of the lipid molecule were chosen. The lipid flexibility combined with changing membrane characteristics along the z-direction result in independent internal rotational modes for each lipid segment. The study of the headgroup was performed by the examination of the temporal correlation of the vector connecting the phosphorous and the nitrogen atoms in the choline group (PN vector). This vector provides an idea of the dynamics of the lipid headgroup at the lipid/water interface. The vector connecting the first and third carbons of the glycerol group was also studied, accounting for the rotational motion of the lipid glycerol backbone. The analysis of the temporal correlation of the vector connecting the first and last methylene groups of an acyl chain provided information about the overall rotation of lipid chains. These vectors allowed us to explore the complex rotational motions observed in a PhdCho as a membrane constituent.

In the case of the cholesterol molecule, its rigid ring forces its rotation as a rigid body, so any intramolecular vector in the ring can be in principle chosen to study its molecular rotation. We choose the vector joining atoms C6 and C11, see Fig. 3.2. The motion of the cholesterol flexible acyl chain can be also analyzed. In all cases, the ACFs measure how fast a molecule or part of a molecule rearranges its orientation.

The Legendre polynomials are a useful set of functions to describe the temporal correlation of a dynamic system by its relation with experimental measures. In particular to compare simulation results and experimental data from NMR or EPR, one should focus on the second associated Legendre polynomial that is formally expressed as:

$$C_2(\tau) = \frac{1}{2}\left\langle 3[\mathbf{f}(t)\cdot\mathbf{f}(t+\tau)]^2 - 1\right\rangle_{t,mol} \tag{3.13}$$

where $\mathbf{f}(t)$ is the studied vector (in this case in its unitary version). As advanced in Sec. 1.6.1.3, NMR experiments provide data to directly compare with the latter correlation function when applied to the CH vector, see Eq. 1.5. As introduced in Sec. 3.3.6, the absence of hydrogen atoms in the used united atom approach was overcome by the reconstruction of the CH vectors assuming a perfect geometry according to the carbon hybridization.

The proposed correlation functions are equal to 1 at $\tau = 0$. The nature of the studied motions result in a stretched exponential decay with τ before reaching a plateau. The features of the correlation curves summarize the characteristics of all the internal motion mechanisms of the analyzed vector and their effective time scales. The plateau observed at long times is a direct consequence of the restricted motion in the z-direction, due to the lack of fluidity in the direction perpendicular to the bilayer plane. This means that the studied vectors were restricted to a particular angular cone around the z-axis. In fact, the characteristics of the specific angular cone for the studied segment determine the position of the plateau, although the relation varies with the used Legendre polynomial. The ACF for any vector without rotation restrictions decreases to zero for long enough times when using Legendre polynomials.

The analysis of the correlation decay is more complicated since the information of the possible internal motion modes is convoluted in the correlation decay. The simplest way to address this problem is to use the definition of a decay half-time, $t_{1/2}$. This quantity allows us to compare rotational speeds between different vectors. Unfortunately, this property has

several drawbacks. First, it only takes into account the fastest of all the possible internal modes, ignoring the slower ones. Second, and related to the latter, it has accuracy problems. Finally, there is no an analogous experimental data that can be used to compare and validate the computed decay half-times. Another alternative is to calculate the area under the correlation decay and over the plateau. This provides a time constant, τ_i, which is a weighted average of the characteristic times of the internal modes of the analyzed vector. The main drawback in this case is the presence of noise in the correlation curve and particularly in the plateau region since it decreases significantly the accuracy of the measure.

Although the previous two measures are used in this Thesis, special attention was paid to an alternative one. The proposed method provides a more detailed view covering more possible time scales, and simultaneously improving the accuracy. It relies on fitting the correlation curves to a particular function and extracting the different relaxation times from those fitted curves. Correlation functions reveal stretched exponential decays that can be fitted by a sum of exponentials, each one with a different decay time scale [Lind01a]. Normally, three exponentials were used,

$$C(\tau) = k + Ae^{-\tau/a} + Be^{-\tau/b} + Ce^{-\tau/c} \tag{3.14}$$

where the constant, k, is needed to capture the restrained motion in the z-axis. In principle, each exponential can be identified as a particular motion mode or as a group of modes with similar time decay. The number of exponentials is chosen so all used exponentials have significantly large non-negative amplitudes. Adding more exponential terms could lead to very small or even negative amplitudes that would be physically unreasonable.

The exact nature of each mode depends on the chosen vector. Typically, in membrane lipids the fast modes correspond to local reorientations (e.g. *trans-gauge* isomerization [∼ps]) and the slower ones to molecular (e.g. rigid-body-like rotation of the whole molecule [∼ns]) or even collective motions (limited impact on our systems due to our simulation time scales). The obtained values can be compared with NMR data if available [Brow83]. By fitting the correlation data to Eq. 3.14 the amplitude coefficients and characteristic relaxation times can be calculated. An average relaxation time, hereafter referred to as the average time constant(ATC), can be computed by weighting the characteristic relaxation times of each exponential decay type by their amplitudes ($ATC = (A \times a + B \times b + C \times c)/(A + B + C)$). This measure is inversely proportional to the rotational velocity of the studied vector and approaches to the characteristic time calculated by the integration of the ACF curve.

Finally, in chapter 8, we were interested in the study of the dynamic behavior of the interactions between different molecules at the membrane interface. The considered interactions include hydrogen bonds between different molecular pairs and charge pairs, whose definitions are provided in Sec. 3.3.7. To do so, differently defined autocorrelation functions (ACF) were used. These functions describe the interacting segments dynamics and were defined as follows:

$$C_{hw}(\tau) = \frac{\langle hw(t+\tau)hw(t)\rangle}{\langle hw(t)\rangle} \tag{3.15}$$

where the function $hw(t)$ is equal to 1 if the interaction exists and zero otherwise. Starting at unity, the decay of these correlation curves provides the characteristic time of the dynamics

of the studied interaction. The faster the decay, the weaker is the interaction. They also display a plateau, due to the finite size of the simulated system.

CHAPTER 4

Structural Effect in Membranes of the Double Bond Position in PhdCho Acyl Chains: The Selective Role of Cholesterol

4.1 Objective and Summary

PhdChos are the most abundant lipids in animal cell membranes [Olss97]. As described in Sec. 1.3.1.1, they can differ in length, degree of unsaturation and location of the double bonds in each acyl chain. Their acyl chains are typically monounsaturated with a *cis* double bond located approximately in the middle [Seel77]. There is currently no explanation for the preferred double bond position. Although many experimental and theoretical studies have addressed the effect of the length [Avel87, Cevc88, Wang95, Koyn98, Petr00, Rawi00, Huan01, Kuuc08b] and the degree of unsaturation [Di95, Koyn98, Rawi00, Bach04, Olli07a] of the acyl chains, there are only few studies dealing with changes induced by varying the location of the double bond within the acyl chain, and its preference to be located around the middle of the acyl chain [Seel77, Wang95, Kane98, Mars99, Rawi00]. Moreover, from the latter most address the experimental determination T_m instead of the analysis of the general membrane properties.

To understand this better we have simulated eleven pure membranes (only one PhdCho moiety) in the fluid phase. All simulated PhdChos had the same acyl chain length of l8 carbons. We used lipids with equal to eliminate possible effects emerging from mismatches in chain lengths. These simulations were used to check whether there is a connection between the double bond location and the physical properties of the membrane that justifies the observed natural preference for the double bond placed near the center of the acyl chain. One of the bilayers consisted of PhdCho molecules with two fully saturated 18:0 stearyl chains (Distearoylphosphatidylcholine, DSPC: d18:0). The other remaining ten systems had at least one *cis*-monounsaturated acyl chain, 18:1cX (where X shows the position of the double blond, see Fig. 4.1). Seven of those systems had two monounsaturated chains (d18:1cX) and the remaining three systems only one chain, the *sn*–2, was monounsaturated (18:0;18:1cX or m18:1cX). The position of the double bond was varied systematically and symmetrically along the chain as described in Sec. 4.2.

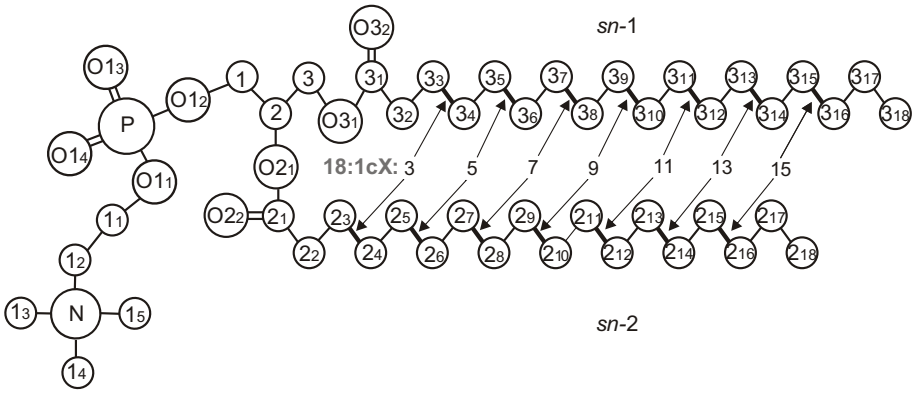

Figure 4.1: Molecular structures of the PhdCho studied molecules including the numbering of atoms. Unsaturated bonds have been marked and numbered in both chains. The chemical symbol for carbon atoms, C, has been omitted for clarity

Our results show that disorder reaches its maximum when the double bond is located in the middle of the acyl chain (DOPC: *d*18:1c9; SOPC: *m*18:1c9). On the contrary, the absence of double bonds in the acyl chain (DSPC: *d*18:0) leads to the highest order. We also observe a decay in membrane order when the double bond is shifted either to the headgroup or to the end of the chain respect the middle point. Such non-monotonic behavior (when it is characterized as a function of the double bond position) is however, non-symmetric. The displacement towards the headgroup causes a very small, although statistically significant, decay. The displacement towards the end of the chain results in a clear ordering approaching the behavior of the saturated species (DSPC). In any case, unsaturated PhdChos display the largest differential behavior with respect to their saturated analogues when double bonds are placed in the middle of their acyl chains. Although this observation is clear when comparing to PhdChos with the double bond near the chain end, it becomes weaker when considering the double bond closer to the headgroup.

Although the above finding is important in understanding of the relevance of the double bond position, it has to be tested in multicomponent biomembranes. As one of the major components in mammalian cells, cholesterol is an excellent candidate to perform this study. In contrast with the large number of different PhdChos moieties in cell membranes [Olss97], cholesterol is unique. Our conjecture is that the specific requirements of the double bond position and lipid selection in natural membranes are at least in part related to the interactions between PhdCho and cholesterol.

To test our hypothesis, we conducted the same simulations as described above but here adding 20 mol% of cholesterol. This corresponds to a typical physiological concentration [Olss96]. The addition of cholesterol induces lipid ordering, the so-called condensing effect. Our simulations show that the condensing is strongly influenced by the lipid moieties, and in particular by the double bond position. The previously reported differences for pure systems are much more enhanced when cholesterol is present in the membrane. The presence of cholesterol emphasizes the differences between DOPC and DSPC as the most disordered and ordered moieties respectively, from all studied lipids. Therefore, it can be conjectured that the incorporation of unsaturated PhdCho moieties constitutes a simple mechanism to promote the fluidity in membranes, especially if the double bond is close to the middle of the

acyl chain. Cholesterol is found to enhance the non-monotonic behavior observed for pure bilayers: moving the double bonds to the chain end or to the headgroup strongly increases lipid ordering respect to DOPC. This indicates that cholesterol contributes to the natural unsaturation heterogeneity in PhdCho acyl chains.

We have also identified the restriction induced by the rigid cholesterol ring to the flexible acyl chains of the PhdCho as the underlying molecular mechanism responsible of the observed ordering effect. For unsaturated lipids, the interaction of the double bond and the off-plane cholesterol methyl groups (see Fig. 1.4b) acts against condensing effect. It is observed that the maximal interaction is produced when the double bond is placed in the middle of the acyl chain explaining the enhanced non-monotonic behavior observed in our simulated cholesterol-containing bilayers. The absence of interaction with double bonds provides the saturated lipids with the highest condensing effect when mixed with cholesterol. Our conjecture is therefore, that natural lipid selection displays a preference for those lipids that yield a distinctive behavior of the formed membrane, so justifying the natural preference for either saturated or unsaturated lipids with the double bond in the middle of their acyl chains.

The research described in this chapter resulted in the publications [Mart07] and [Mart08b] included in this Thesis.

4.2 Descriptions of Simulated Systems

This chapter comprises the results of a total of 22 membrane simulations: eleven pure membranes composed of different PhdCho moieties and another eleven with the same moieties but now containing 20 % molar of cholesterol. The pure membranes were constituted by 128 lipids, divided in 64 lipids per layer. In the case of mixed systems 32 molecules of cholesterol were added, equally distributed in each layer. The number of water molecules was ∼3900, representing ∼25–30 water molecules per lipid ensuring a proper hydration [Petr04].

All lipids used in simulations had acyl chains of 18 carbons. The selected length was based on the natural occurrence of oleyl chains (18:1c9) in the PhdChos in biomembranes [Olss97], e.g. POPC and DOPC. The imposed equal length of the two chains tried to isolate the effect of the presence and position of the double bond from those originating from the asymmetry of the acyl chains. This choice was made since there is a significant amount of experimental data concerning some of the selected systems thus allowing a validation of the obtained results (DSPC, DOPC, DVPC, SOPC).

Our first bilayer consisted of saturated 18:0 stearyl chains (DSPC: *d*18:0). In the next seven systems both *sn*–1 and *sn*–2 chains were *cis* monounsaturated. The position of the double bond was varied systematically and symmetrically as follows: for the *sn*–1 acyl chain between atoms $C3_3$–$C3_4$ (*d*18:1c3), $C3_5$–$C3_6$ (*d*18:1c5), $C3_7$–$C3_8$ (*d*18:1c7), $C3_9$–$C3_{10}$ (DOPC: *d*18:1c9,), $C3_{11}$–$C3_{12}$ (divacenylphosphatidylcholine, DVPC: *d*18:1c11,), $C3_{13}$–$C3_{14}$ (*d*18:1c13), and $C3_{15}$–$C3_{16}$ (*d*18:1c15); and for the *sn*–2 chain between atoms $C2_3$–$C2_4$ (*d*18:1c3), $C2_5$–$C2_6$ (*d*18:1c5), $C2_7$–$C2_8$ (*d*18:1c7), $C2_9$–$C2_{10}$ (DOPC: *d*18:1c9), $C2_{11}$–$C2_{12}$ (DVPC: *d*18:1c11), $C2_{13}$–$C2_{14}$ (*d*18:1c13), and $C2_{15}$–$C2_{16}$ (*d*18:1c15). The remaining three systems had the *sn*–1 chain saturated (18:0) and only the *sn*–2 chain unsaturated as follows: between atoms $C3_5$–$C3_6$ (*m*18:1c5), $C3_9$–$C3_{10}$ (SOPC: *m*18:1c9,), and $C3_{13}$–$C3_{14}$ (*m*18:1c13). From here over, we refer to these bilayers by the index corresponding to the position of the double bond

(the first carbon atom index in Fig. 4.1), and we assign the index 17 to the fully saturated DSPC bilayer. Figure 4.1 shows the structure and the numbering of atoms in the DSPC molecule as well as the positions of the double bonds in the unsaturated species. Numbering of atoms in the cholesterol molecule is displayed in Fig. 1.4b.

The initial configurations of our pure systems were taken from a previously equilibrated lipid bilayer with 128 dioleoylphosphatidylcholine (DOPC) [Olli07b]. The other ten membrane systems were constructed by changing the position of the double bond or removing them for the saturated moieties. Minimization was required to relax the new position of the double bond. Afterwards, all systems were simulated for 100 ns with the original GROMACS description of a Carbon-Carbon double bond, see Sec. 6.2. Finally, the parameters of the double bond were corrected using the description provided by Bachar et al [Bach04] and the simulation extended for at least 100 additional nanoseconds. This protocol was repeated again with the mixed systems containing 20 mol% of cholesterol by replacing the initial configuration by the final structure of a simulation of 128 DOPC molecules and 32 molecules of cholesterol [Olli07b]. The slower dynamics presented by the systems containing cholesterol required the simulations to be extended up to at least 150 ns to ensure proper mixing of components. The simulation details are described in Sec. 3.2.

4.3 Structural Membrane Properties

Assuming that the natural preference for the double bond to be placed around carbons 9 and 10 in the lipid acyl chain (see Fig. 4.1) is not governed by some unknown specific interaction with some membrane protein. One would expect to find some particularity in the physical properties conferred by those lipids to the membrane. For this reason, the main purpose of this section is to study the effect of lipid unsaturation and the double bond location on membrane properties. This is performed for both pure and 20 mol% of cholesterol bilayers. The numerical values of many of the analyzed properties can be found in Table 4.1 and Table 4.2. In all the presented results, error bars were estimated using the block analysis method [Hess02] and are given as twice the standard error.

4.3.1 Area per Molecule and Condensing Effect

The area per molecule is one of the most direct measures obtained from membrane MD simulations. Besides its importance to monitor the equilibration of the system, it also estimates the ordering of the system, which is a fundamental concept to determine the membrane state, see Sec. 3.3.1. Furthermore, as the area per molecule is typically characterized in experimental works, it often constitutes the unique way to quantitatively validate the simulation results.

The calculated areas per lipid, A_{PC}, from all simulated system are shown in Fig. 4.2, and their numerical values are listed in Tables 4.1 and 4.2. Overall values are larger than 0.5 nm^2, indicating that all studied bilayers were in a fluid phase. At this stage we are going to focus on the results concerning single-component bilayers presenting both lipid acyl chains monounsaturated [Mart07]. As can be seen in figure 4.2a when the double bond is displaced from position 9 (corresponding to DOPC) towards the end of the chain, the limiting case being the saturated DSPC lipid, we find a significant reduction in the average area per PhdCho, about 0.062 nm^2. When the double bond position is displaced from the middle

Bilayer *d*18:1cX	3	5	7	9	11	13	15	*d*18:0
length (ns)	150	165	155	150	150	150	150	150
	105	**110**	**100**	**110**	**102**	**100**	**112**	**100**
A_{box} (nm^2)	44.354	45.441	46.519	46.694	45.773	44.438	42.382	39.763
	46.314	**46.442**	**46.662**	**46.669**	**46.046**	**45.162**	**43.887**	**42.845**
V_{box} (nm^3)	309.43	309.84	310.15	310.07	309.94	309.79	309.53	309.33
	298.27	**298.23**	**298.36**	**298.40**	**298.49**	**298.64**	**298.83**	**299.05**
A_{PC} (nm^2)	0.693	0.710	0.727	0.730	0.715	0.694	0.662	0.621
$\pm$0.003 nm^2	**0.724**	**0.727**	**0.729**	**0.731**	**0.719**	**0.706**	**0.686**	**0.669**
η_{DB} (Å^2)	3.580	4.413	5.279	5.4144	4.695	3.652	2.046	0
	2.710	**2.810**	**2.953**	**3.065**	**2.501**	**1.810**	**0.814**	**0**
A^*_{PC} (nm^2)	0.629	0.644	0.660	0.663	0.649	0.630	0.602	0.564
A^*_{CHOL} (nm^2)	0.255	0.261	0.267	0.268	0.263	0.256	0.2443	0.229
$\mathbf{D_{PP}}$ (nm)	4.119	4.116	4.042	4.028	4.099	4.209	4.382	4.630
$\pm$0.01 nm	**3.714**	**3.711**	**3.707**	**3.709**	**3.760**	**3.825**	**3.922**	**4.012**
$\mathbf{D_{OO}}$ (nm)	3.044	3.182	3.129	3.126	3.181	3.271	3.435	3.623
$\mathbf{D_{PO}}$ (nm)	0.538	0.467	0.456	0.451	0.459	0.469	0.473	0.504
$\mathbf{D_{HH}}$ (nm)	4.001	4.042	3.842	3.833	3.919	3.980	4.4322	4.486
$\pm$0.03 nm	**3.524**	**3.547**	**3.535**	**3.441**	**3.663**	**3.648**	**3.782**	**3.882**
V_{PC} (nm^3)	1.331	1.334	1.336	1.336	1.335	1.333	1.331	1.330
	1.345	**1.345**	**1.346**	**1.346**	**1.347**	**1.348**	**1.349**	**1.351**
$\langle -S_{CD} \rangle$								
sn–1	0.184	0.165	0.152	0.150	0.165	0.184	0.223	0.261
	0.106	**0.103**	**0.102**	**0.107**	**0.115**	**0.125**	**0.143**	**0.151**
sn–2	0.192	0.168	0.153	0.152	0.164	0.185	0.219	0.262
	0.111	**0.108**	**0.105**	**0.106**	**0.116**	**0.129**	**0.144**	**0.151**
CHOL	0.185	0.170	0.154	0.158	0.171	0.184	0.211	0.251
No. of gauche								
sn–1	2.82	3.06	3.09	3.06	2.95	2.83	2.54	2.92
	3.10	**3.20**	**3.20**	**3.17**	**3.13**	**3.08**	**2.91**	**3.51**
sn–2	2.57	3.02	3.10	3.07	2.99	2.85	2.57	2.92
	2.90	**3.19**	**3.18**	**3.17**	**3.13**	**3.08**	**2.90**	**3.50**
Tilt (deg)								
t_{sn-1}	28.7	28.4	30.2	31.6	30.7	28.9	25.5	21.7
	37.6	**37.2**	**37.6**	**37.7**	**38.2**	**36.9**	**35.4**	**34.2**
t_{sn-2}	27.5	27.6	29.4	30.6	30.4	28.3	25.5	21.1
	36.4	**36.3**	**36.8**	**36.6**	**37.5**	**36.0**	**34.7**	**33.5**
$t_{P\mapsto N}$	100.1	100.2	100.4	100.5	100.1	99.6	98.9	98.1
	101.8	**101.4**	**101.4**	**101.5**	**101.2**	**100.9**	**100.5**	**100.2**
t_{CHOL}	30.3	27.7	28.9	28.1	26.5	24.7	22.6	19.6
t^t_{CHOL}	39.9	38.0	40.0	39.5	37.9	36.4	33.5	28.7
Hydrogen Bonds	6.03	6.08	6.19	6.19	6.12	6.05	5.89	5.67
	6.40	**6.40**	**6.42**	**6.44**	**6.41**	**6.36**	**6.26**	**6.21**
Water bridges	0.90	0.90	0.89	0.89	0.89	0.91	0.94	0.97
	0.92	**0.93**	**0.92**	**0.93**	**0.93**	**0.95**	**0.97**	**0.98**
Charge pairs	4.67	4.62	4.50	4.47	4.59	4.72	4.94	5.23
	4.41	**4.47**	**4.45**	**4.41**	**4.49**	**4.56**	**4.69**	**4.74**

Table 4.1: Average results characterizing bi-monounsaturated lipid bilayer systems. Bold letters are used to mark pure systems, light-face letters those containing 20 mol% CHOL.

Bilayer m18:1cX	5	9	13	d18:0
length (ns)	150	155	150	150
	105	**100**	**100**	**100**
A_{box} (nm^2)	43.018	44.134	42.778	39.763
	44.921	**45.232**	**44,254**	**42.845**
V_{box} (nm^3)	309.932	310.302	309.872	309.33
	298.654	**298,787**	**299.061**	**299.05**
A_{PC} (nm^2)	0.672	0.690	0.668	0.621
$\pm$0.003 nm^2	**0.702**	**0.707**	**0.691**	**0.669**
η_{DB} (Å^2)	5.079	6.827	4.710	0
	3.244	**3.729**	**2.201**	**0**
A^*_{PC} (nm^2)	0.6103	0.6263	0.607	0.564
A^*_{CHOL} (nm^2)	0.247	0.253	0.246	0.229
$\mathbf{D_{PP}}$ (nm)	4.328	4.242	4.354	4.630
$\pm$0.01 nm	**3.837**	**3.823**	**3.905**	**4.012**
$\mathbf{D_{OO}}$ (nm)	3.380	3.331	3.370	3.623
$\mathbf{D_{PO}}$ (nm)	0.474	0.456	0.492	0.504
$\mathbf{D_{HH}}$ (nm)	4.281	4.121	4.483	4.486
$\pm$0.03 nm	**3.634**	**3.651**	**3.658**	**3.822**
V_{PC} (nm^3)	1.335	1.337	1.334	1.330
	1.348	**1.349**	**1.351**	**1.351**
$\langle -S_{CD} \rangle$				
sn–1	0.221	0.207	0.220	0.261
	0.139	**0.136**	**0.141**	**0.151**
sn–2	0.188	0.172	0.198	0.262
	0.113	**0.113**	**0.131**	**0.151**
No. of gauche				
sn–1	3.19	3.26	3.19	2.92
	3.56	**3.57**	**3.64**	**3.51**
sn–2	2.95	3.03	2.79	2.92
	3.17	**3.16**	**3.02**	**3.50**
Tilt angle(deg)				
t_{sn-1}	25.4	26.7	25.6	21.7
	35.4	**35.8**	**35.1**	**34.2**
t_{sn-2}	25.7	28.6	26.7	21.1
	36.1	**37.1**	**35.9**	**33.5**
$t_{P\mapsto N}$	99.3	99.5	98.9	98.1
	101.0	**100.8**	**100.4**	**100.2**
t_{CHOL}	24.5	25.9	23.6	19.6
t^t_{CHOL}	34.9	37.2	34.6	28.7
Hydrogen Bonds	5.93	6.02	5.93	5.67
	6.33	**6.35**	**6.30**	**6.21**
Water bridges	0.93	0.92	0.93	0.97
	0.95	**0.95**	**0.96**	**0.98**
Charge pairs	4.88	4.75	4.88	5.23
	4.58	**4.56**	**4.64**	**4.74**

Table 4.2: Average results characterizing monounsaturated lipid bilayer systems. Bold letters are used to mark pure systems, light-face letters those containing 20 mol% CHOL.

of the chain towards the lipid headgroup, the average area per PhdCho is reduced as well, but now the reduction is substantially smaller, about 0.007 nm^2, that is close to the order of the error bar ($\pm$0.003 nm^2). Nonetheless, A_{PC} has a maximum when the double bond resides in the middle of an acyl chain, in accordance to experiments [Mars99] which indicates the main transition temperature to be the smallest when the double bond is located in the middle of the chain. Comparison with experimental values shows good agreement: Petrache et al. [Petr00] obtained an average area per lipid of 0.66 nm^2 at 338 K for a DSPC bilayer (0.670 nm^2 in our simulations), and X-ray data for fully hydrated DOPC bilayer provided the range 0.721–0.740 nm^2 for the area per lipid [Nagl00, Liu04, Kuuc05b, Math08, Pan09] (0.731 nm^2 $\pm$0.003 nm^2 in our simulations).

Changing our focus to PhdCho species with double bond only present at the *sn*–2 acyl chain, we observe clear similarities with the results reported above. The area per molecule again displays a maximum when the double bound is placed in the middle of the acyl chain (SOPC). We again observe that the drop showed when the double bond is moved from position 9 to the end of the acyl chain is significantly larger than when the displacement is performed to the headgroup. In this case, comparison to experimentally measured areas per molecule is limited to pure SOPC bilayers. Experiments gave $\sim$0.66 nm^2 at 303 K for fully hydrated SOPC bilayers [Rand88, Pan09]. In our simulations we obtain a larger value (0.707 nm^2) but at a temperature that is 35 K higher. A typical increase of 0.01 nm^2 per 5–7 K [Pan08] leads to good agreement with our simulated value.

Comparing the areas per molecule between the two simulation sets leads to the expected result that moieties with two unsaturated acyl chains are more disordered than their analogous with just one unsaturated acyl chain. This is a consequence of the extra kink due to the double monounsaturated moieties in the hydrophobic region that implied a more difficult lateral packing. Despite this is valid when comparing absolute values of the area per molecule, the behavior is surprisingly reversed when evaluating the disordering efficiency, η_{DB}, provided by each double bond present in the considered lipid moiety, see Fig. 4.2c. The disordering efficiency was evaluated using DSPC as a reference system as follows:

$$\eta_{DB} = \frac{A_i - A_{DSPC}}{n_{DB}} \tag{4.1}$$

where A_i and A_{DSPC} are the areas per molecule of the analyzed and DSPC bilayers, and n_{DB} corresponds to the number of double bonds present in the chains of the analyzed lipid moiety. The numerical values are listed in Table 4.1 and Table 4.2. These values show that the addition of a single double bond in the middle of the *sn*–2 chain is able to disorder the system up to 3.73 Å^2 that is the most effective way to maximize the disorder in pure bilayers. It is also showed that the addition of a double bond to the other (saturated) acyl chain does not promote as much disorder as the first double bond, see Fig. 4.2c. Interestingly, SOPC with a single double bond form more disordered membranes than *d*18:1c13 and *d*18:1c15 moieties that contain an extra double bond. This indicates that double bond position can be a more important factor in determining membrane ordering than the number of double bonds itself.

We have pointed out above the agreement between our results and the experiments reported in Refs. [Wang95] and [Mars99]. Being more specific, the experiments show that the main phase transition temperature for lipids with monounsaturated acyl chains is the

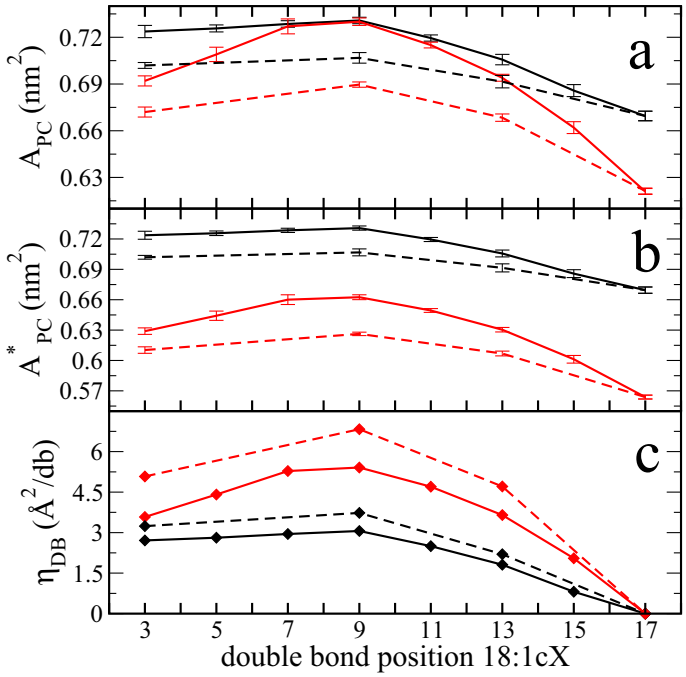

Figure 4.2: Area per molecule in PhdCho membranes. Panel (a) presents the area per molecule, A_{PC}, calculated by dividing the box xy area for the number of PhdChos, Eq. 3.1. Panel (b) presents the area per molecule, A^*_{PC}, calculated by the procedure developed by Hofsäßet al., Eq. 3.2. Panel (c) presents the increase of area per molecule and per double bond respect to the saturated system, η_{DB}, derived from results in panel (a). All results are shown as a function of the double bond position. Solid lines correspond to di-monounsaturated lipids (d18:1cX), whereas dashed ones correspond to single chain monounsaturated lipids (m18:1cX). In both cases, position 17 corresponds to (saturated) DSPC. Black curves correspond to pure systems, while red curves to mixtures with 20 mol% of cholesterol.

lowest when the double bond resides at the middle of a chain. We in turn find that the area per lipid is the largest when the double bond is located in the chain's center. To confirm the correlation between the two properties, Table 4.3 summarizes experimental data for a number of one-component lipid systems. This data displays an inverse correlation between the average area per lipid and the main phase transition temperature. Clearly, the lower is the T_m, the larger is the average area per lipid.

For PhdCho/CHOL bilayers, the values for A_{PC} are significantly smaller than for their single-component counterparts, as a signature of the condensing effect produced by cholesterol, see Fig. 4.2b. The effect due to the double bond position is qualitatively similar to the presented above for pure membranes. When cholesterol is present, the non-monotonic behavior is much more pronounced. A clear maximum is observed in the area per PhdCho when the double bond is placed in the middle of an acyl chain (DOPC) for the di-monounsaturated moieties. When the double bond approaches either the headgroup or the end of the chain, the area per PhdCho was substantially reduced. Such reduction is particularly large when the unsaturation is moved deeper into the bilayer, the largest difference being 0.099 nm2 when DOPC is replaced with DSPC.

Equivalent behavior is observed for the monounsaturated moieties that display smaller areas in comparison to their di-monounsaturated counterparts. Following the same trends as

LIPID	Temperature (K)	Area/Lipid (Å^2)	T$_m$ (K)	Reference
DLPC	338	71.2	272	[Petr00]
DMPC	338	68.5	296	[Petr00]
DPPC	338	67.1	314	[Petr00]
DSPC	338	66.0	328	[Petr00]
DLPC	323	67.1	272	[Petr00]
DMPC	323	65.4	296	[Petr00]
DPPC	323	63.3	314	[Petr00]
DPPC	323	64.4	314	[Kuuc06]
DOPC	303	72.4	253	[Kuuc05b]
DOPC	303	72.4	253	[Pan08]
POPC	303	68.3	271	[Kuuc05b]
DLPC	303	62.6	272	[Petr00]
DLPC	303	63.2	272	[Kuuc05a]
DMPC	303	60.0	296	[Petr00]
DMPC	303	60.6	296	[Kuuc05a]

Table 4.3: The inverse relation between the main phase transition temperatures T$_m$ (from Ref. [Silv82]) and the average area per lipid for a number of different lipid species and temperatures.

bilayers formed by di-monounsaturated PhdChos, we find the larger area per molecule in the bilayer constituted by SOPC (m18:1c9) molecules, which shows the highest disordering efficiency among the studied moieties, η_{DB} =6.83 Å^2. Interestingly again, cholesterol-containing membranes of SOPC (m18:1c9) are more disordered than d18:1c13 and d18:1c15 moieties as reported for pure bilayers, but also in this case d18:1c3 moiety.

Focusing our attention on Fig. 4.2a, it can be seen that the addition of 20 mol% of cholesterol to the pure systems does not increase the total area of the systems and even displays a substantial drop. This is particularly evident for the saturated DSPC molecule where the simulation system shrinks $\sim$ 7 %, and it is also important in the remaining systems except DOPC (d18:1c9), d18:1c7 and DVPC (d18:1c11) where the area remains rather unchanged. This implies that the systems have a negative spacing effect; namely that the distance between the PhdCho headgroups is reduced when cholesterol is added. Although this effect was described by means of ^{31}P NMR experiments in PhdCho bilayers at moderated cholesterol concentrations [Yeag75], our MD model is known to slightly overestimate such effect. The negative spacing effect can be also understood as a consequence of negative values for the cholesterol partial molar area resulting from the non-ideal mixing properties showed by membrane components [Edho05].

Comparison with experimental values also shows a good agreement: DOPC bilayers with 20 mol% of cholesterol lead to A_{DOPC}=0.673–0.675 nm^2 [Hung07, Math08], whereas we obtain A^*_{DOPC}=0.663 nm^2±0.003 nm^2 (calculated by the procedure developed by Hofsäß et al., Eq. 3.2). Recent results by Pan et al. increased these values setting a new range between 0.710 and 0.730 nm^2 [Pan09]. The same authors have evaluated SOPC with 20 mol% of cholesterol reporting values between 0.64 and 0.68 nm^2 [Pan09], while we obtain A^*_{SOPC}=0.626. At this stage it is important to remark the difficulties of comparing our

reported areas to those obtained from experiments. The straightforward calculation of A_PC from our simulation contrasts with the substantial number of assumptions and simplifications needed by experimentalists. In this particular case both ranges seem to be in very good agreement with our reported A_{PC}, despite Pan et al. suggested that they should be compared with A^*_{PC}. However, our model is able to capture differences induced by minor changes in the molecular structure and the main trends when displacing double bonds in the lipid acyl chains. These behaviors are in qualitative agreement with all available experimental results, although the comparison based on absolute values certainly requires special care.

4.3.2 Membrane Thickness and Phd volume

In this section we will focus on the changes experimented by the system in the transversal structure when the double bond is shifted along the chain. We will first study the membrane thickness and then introduce the concept of molecular volume which links this property to the already presented area per molecule.

To characterize the thickness of the membrane the $\mathbf{D_{PP}}$ distance was used, see Sec. 3.3.2. Its dependence with the double bond position is plotted in Fig. 4.3a (also given in Tables 4.1 and 4.2). As expected, a decrease in the average area per molecule was accompanied by an increase in thickness, see Fig. 4.2, as these two properties usually hold an inverse relation due to the rather well conserved lipid volume (V_{PC}), see below. Therefore, the thickness presented its maximum in the saturated DSPC bilayer, and its minimum in DOPC and SOPC for the di-mono- and monounsaturated bilayers, respectively. This is only strictly correct for the bilayers containing cholesterol, because as before the presence of cholesterol enhances the asymmetry of the thickness curve. As can be seen in Fig. 4.2a, pure systems have a rather invariant value of the thickness when the double bond is shifted from the middle of the acyl chain (position 9) to underneath of the lipid headgroup, as it was observed for the area per molecule. It is also seen that values of $\mathbf{D_{PP}}$ in the bilayers with cholesterol (4.630–4.028 nm) are systematically larger than those showed by pure systems (4.012–3.707 nm) which are fully in agreement with the drops in the area per molecule experienced by the addition of cholesterol to the bilayer. Therefore, the addition of 20 mol% of cholesterol has a double effect on the thickness. Firstly, it increases by 0.3–0.6 nm the thickness of the membrane. Secondly, the thickness amplification is asymmetric being stronger when the double bond is far from the middle of the acyl chain, and as a consequence arising a clear minimum in the thickness at position 9.

For sake of completeness, the average z-distance between cholesterol oxygens in opposite layers ($\mathbf{D_{OO}}$) is plotted in Fig. 4.2b as a function of the double bond position. These curves display almost the same pattern as the $\mathbf{D_{PP}}$ ones. As a consequence, the average distance between cholesterol oxygen atoms and phosphorous atoms in the same leaflet ($\mathbf{D_{PO}} = (\mathbf{D_{PP}} - \mathbf{D_{OO}})/2$) is shown to be rather uniform in all simulated bilayers, suggesting that cholesterols are equally inserted in all the membranes, at $\sim$5 Å deeper from the phosphorus position, see Fig. 4.2c. Later we will show that this is a consequence of the preference of the cholesterol hydroxyl to be attached to the carbonyl groups of the lipid acyl chains, which can be also seen experimentally [Yeag75, Huan77].

Despite the accurate measures provided by $\mathbf{D_{PP}}$, direct comparison with experiments is rather complicated, and not straightforward. Instead, experiments provide another thickness

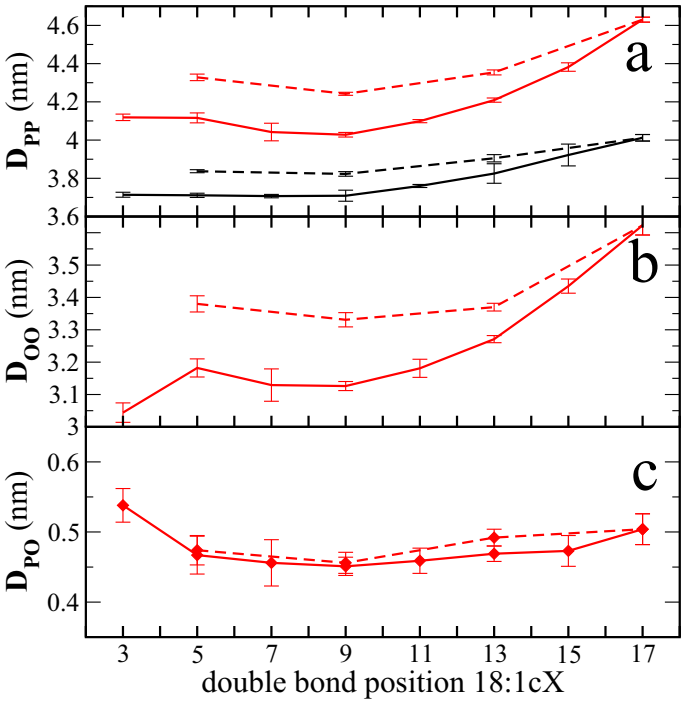

Figure 4.3: Thickness in PhdCho membranes as a function of the double bond position. Panel (a) presents the bilayer thickness, $\mathbf{D_{PP}}$, as defined in Eq. 3.4. Panel (b) presents the distance between the oxygens of cholesterols in different layers, $\mathbf{D_{OO}}$. Panel (c) shows how deep the cholesterol is inserted in the membrane $\mathbf{D_{PO}} = (\mathbf{D_{PP}} - \mathbf{D_{OO}})/\mathbf{2}$. All results are shown as a function of the double bond position. Solid lines correspond to di-monounsaturated lipids (d18:1cX), whereas dashed ones correspond to single chain monounsaturated lipids (m18:1cX). Black curves correspond to pure systems, while red curves mixtures with 20 mol% of cholesterol.

measure which can be easily compared with our simulation results: the distance between the two peaks in the electron density profiles from diffraction experiments, $\mathbf{D_{HH}}$, see Sec. 3.3.2. The numerical values of $\mathbf{D_{HH}}$ for our simulations can be found in Tables 4.1 and 4.2. $\mathbf{D_{HH}}$ can be also estimated from other techniques as NMR. In this latter case, $\mathbf{D_C}$ is measured, and can be used to estimate $\mathbf{D_{HH}}$ by assuming a constant value between the phosphate and the Gibbs dividing surface of the hydrocarbon region ($\mathbf{D_g}$) by

$$\mathbf{D_{HH}} = 2 \cdot [\mathbf{D_C} + \mathbf{D_g}] \tag{4.2}$$

where $\mathbf{D_g}$ value is typically taken as 4.95 Å [Kuuc05b, Pan09] and considered constant for all PhdCho bilayers. Recent experimental results have reduced its value to ∼3.9 Å for DOPC membranes [Kuuc08a] which improves the comparison with our experimental results and puts under objection the previous assumption. Pure DSPC bilayer was characterized at 338 K by Petrache et al. They found a value for the hydrocarbon thickness $\mathbf{D_C}$ of 1.56 nm that results in an estimated value of $\mathbf{D_{HH}}$ of 3.90 nm [Petr00] in a perfect agreement with our value 3.88 ±0.03 nm.

Our comparison with experiments has another difficulty: the temperature. As we wanted to study membranes in their fluid phase at the same temperature, the chosen temperature (338 K, that is slightly above the transition temperature for DSPC) was unusually high. Most of the experimental values for unsaturated moieties are obtained at smaller temperatures.

Therefore, in order to provide a proper comparison of the data, we have to take into account the deviations in the measures coming from the temperature difference between the experiments and our simulations. This can be done by the usage of the "head-to-head contractivity" defined by Pan et al. [Pan08] as:

$$\alpha_{HH} = \left(\frac{1}{\mathbf{D_{HH}}}\right) \cdot \left(\frac{\partial \mathbf{D_{HH}}}{\partial T}\right)_{\Pi} \tag{4.3}$$

For pure DOPC bilayers at 303 K, α_{HH} is equal to 0.0014 K^{-1}. Different experimental values of $\mathbf{D_{HH}}$ at 303 K for pure DOPC bilayers reported a range from 3.67 to 3.71 nm [Nagl00, Liu04, Kuuc05b, Hung07, Math08, Pan08, Pan09]. Based on this range and extrapolating by using α_{HH} for DOPC at 303 K, the thickness at 338 K is expected to be between 3.49 and 3.53 nm. Our simulation value is 3.44 $\pm$0.03 nm, providing a very good agreement with the experimental results. Since values for α_{HH} are not available for the other lipids and mixtures, we assume that α_{HH} is the same for the other simulated bilayers. As a result, we can also validate our simulations by comparing our results with the available experimental data for pure SOPC bilayers and 20 mol% of cholesterol mixtures of DOPC and SOPC, all of them at 303 K. The thicknesses reported for pure SOPC bilayers are in a range between 3.90 to 3.92 nm at 303 K [Hung07, Pan09]. Correcting these values to represent our working temperature we obtain an estimated range from 3.70 to 3.72 nm, that compares nicely with our obtained value 3.65$\pm$0.03 nm. Finally for cholesterol mixtures we find experimental ranges of 3.92–3.89 nm for DOPC [Hung07, Math08, Pan09] and 4.25–4.20 nm for SOPC [Hung07, Pan09], that once they are corrected to our working temperature they correspond to 3.69–3.72 nm and 4.04–3.99 nm, respectively. These ranges compare properly with the ones obtained in our simulated systems, 3.83 nm for DOPC and 4.12 nm for SOPC with a deviation of only 1 Å. The bigger deviation of our cholesterol mixtures can be understood in terms of a possible overestimation of the α_{HH} for the systems with cholesterol, which are expected to be less sensible to the variation of temperatures than the pure ones.

To conclude this section we would like to address the lipid volume (V_{PC}). This property is considered to be rather constant in all bilayer systems and basically dependent on the lipid structure and temperature [Pan06]. Most models used by experimentalists to extract structural information from their measures are based on this assumption as it allows to connect the transverse and the lateral structures of lipid bilayers [Nagl00]. It is usually assumed that the molecular fragments constituting the lipids (e.g. glycerol, choline, etc.) have a temperature dependent specific volume. Therefore, one can estimate the molecular volume of a lipid by just knowing its structure [Nagl00] and summing the volume of their different pieces. According to this, all PhdChos used in our simulations are supposed to have the same lipid volume if they have the same number of double bonds. The calculation of the lipid volume from our data confirmed that the latter assumption is reasonable, see Tables 4.1 and 4.2. In our simulation we computed V_{PC} by subtracting the volume of water and cholesterol molecules from the total simulation box volume. The water volume was obtained by simulating a box of water with the same simulation conditions as in the bilayer simulations, resulting in 0.0320 nm^3/water. The cholesterol volume instead was taken from experiments as 0.541 nm^3/cholesterol [Edho05]. Both were considered constant in all simulated systems.

Our simulations clearly show that PhdChos having the same number of double bonds

report V_{PC} values inside the experimental error ($\sim$2 parts in 1000), which is in agreement with experimental observations. The volumes for pure di-mono- and monounsaturated bilayers are 1.347$\pm$2 and 1.349$\pm$2 nm^3/PhdCho, respectively. These values agree with the available experimental data for DOPC [Nagl00, Kuuc05b], after the appropriated thermal corrections are applied [Pan08]. Considering that the saturated DSPC moiety displays a volume of 1.351 nm^3/PhdCho, we observe that the presence of each double bond reduces the volume of the PhdCho as it is suggested by experiments [Nagl00]. Even though a finer comparison taking into consideration the error range shows, for example, that all the monounsaturated lipids and the di-monousaturated lipids with the double bonds close to the end of the chain present the same V_{PC} as the saturated DSPC. Therefore, the V_{PC} not only depends on the particular molecular structure but also on the ordering level of the membrane. This equals to say that variations in area per molecule are not fully compensated by variations in membrane thickness. This phenomenon is more relevant when analyzing the systems containing cholesterol. In this case the ordering effect is even able to reverse the expected behavior of V_{PC} as the saturated moiety presented the smaller V_{PC}. This clearly indicates that despite the common assumption of constant V_{PC} is adequate for pure membranes, it is not strictly correct when dealing with mixed systems.

Another fact supporting the latter conclusion is observed when comparing the membrane volume between pure and mixed systems. The membrane volume was defined as the volume of the simulation box minus the volume occupied by water. In this comparison if all moieties really conserve their volume, the membrane volume in the mixed systems would be the same as in pure ones but adding a constant value that stands for the volume of cholesterol molecules. Although this could be partially achieved by supposing a value of 0.501 nm^3/cholesterol instead of the used 0.541 nm^3/cholesterol, it is clear that there are some deviations, especially in the most ordered systems. The most clear example is found in DSPC where in order to have a constant V_{PC} between pure and mixed system a V_{chol} of $\pm$0.46 is needed. Therefore, we conclude that the common assumption of the conservation of the molecular volume is just an approximation to the real behavior, although acceptable in many situations.

4.3.3 Transversal Structure of the Membrane

A more detailed insight into the transverse structure of a lipid bilayer was achieved by computing the electron density profiles, which provide an average distribution of the atoms along the z-axis (see Sec. 3.3.3). The obtained profiles are plotted in Fig. 4.4 and, in general, they show a good agreement with the experimental ones measured by Hung et al [Hung07]. The profiles show the typical features obtained from diffraction experiments; namely, two pronounced peaks at the phosphate group positions and a minimum in the middle of the bilayer [Nagl00], see Fig. 4.4. The distances between the peaks are different and comparable to the experimental ones as already stated in the previous section. Additionally, at distances after $\pm$3 nm one can observe the bulk water region with a constant value of $\sim$313 e/(nm^3) that is equivalent to a water density of 9.36 g/cm^3, typical of the SPC model. The convergence of all curves to the same numerical value is a signature that the level of hydration of all the systems was appropriated.

The profiles report an interesting, well defined behavior when cholesterol is incorporated. First, the inclusion of cholesterol manifests a reduction in system density in the middle

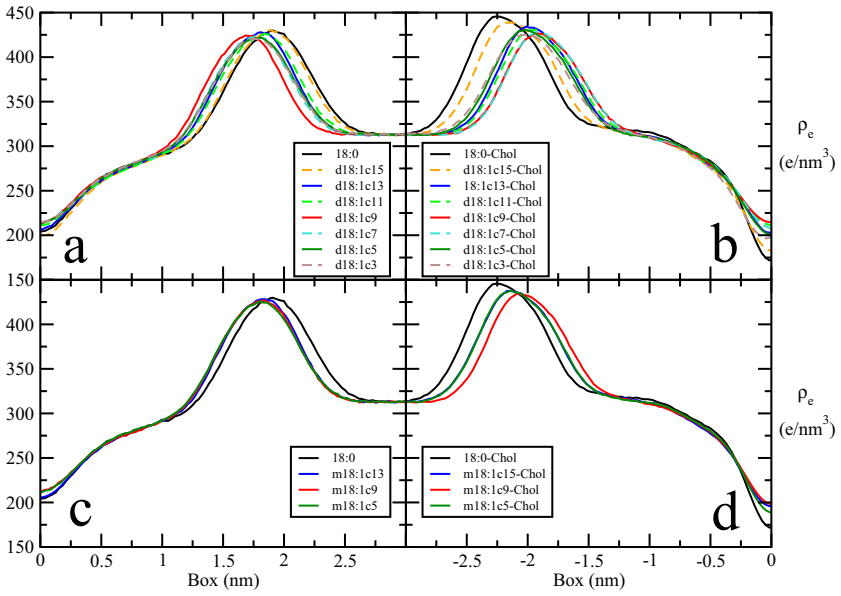

Figure 4.4: Comparison of the electron density profiles for PhdCho bilayers presenting different number and location of double bonds in their acyl chains. Panels (a) and (c) show single component bilayer. Panels (b) and (d) bilayers contain 20 mol% of cholesterol. Panel (a) and (b) cover the di-monounsaturated lipids while panels (c) and (d) monounsaturated ones. Solid and dashed curves in panels (a) and (b) are used just for better contrast between curves.

of the bilayer that has been also observed experimentally [Subc94] (compare panels (a)-(b) and (c)-(d)). Second, the presence of cholesterol pushes the lipids from the center of each layer resulting in a pronounced constant density region on it. This is a signature of cholesterol-induced lipid ordering that results in reducing area and increasing thickness.

4.3.4 Order of Acyl Chains

Another typical parameter computed in membrane MD simulations is the order parameter. As introduced in Sec. 3.3.6, it quantifies the ordering of chains, although most of its importance relies on the fact that it can be directly compared to NMR experimental data, see Sec. 1.6.1.3. Figure 4.5 displays the S_{CD} profile for each simulated system.

The analysis of panels (a), (b) and (c) of Fig. 4.5 clearly shows that all simulated systems had their less ordered region in the middle of the bilayer. They provide two examples of clear evidence of the structural changes suffered in a pure system upon addition of 20 mol% of cholesterol. First, pure systems show to be less ordered than their correspondent mixtures with cholesterol. This is seen by the significantly lower values displayed in the profiles (notice that we plot -S_{CD}) in the pure systems as compared to the mixtures ones. Second, the general shape of the profiles is altered. While pure systems show increasing -S_{CD} values from carbons 17 to 6 and only a very small decay afterwards, the mixed systems show a clear maximum around C8. The presence of these maxima can be attributed to the presence of the rigid tetracyclic cholesterol ring in the middle of the layer that significantly orders its surroundings (carbon numbers 5 to 10). Panel (c) also shows that in monounsaturated lipids the saturated chain is significantly more ordered that the saturated one.

The double bond position has a clear impact on the profiles. Its location influences

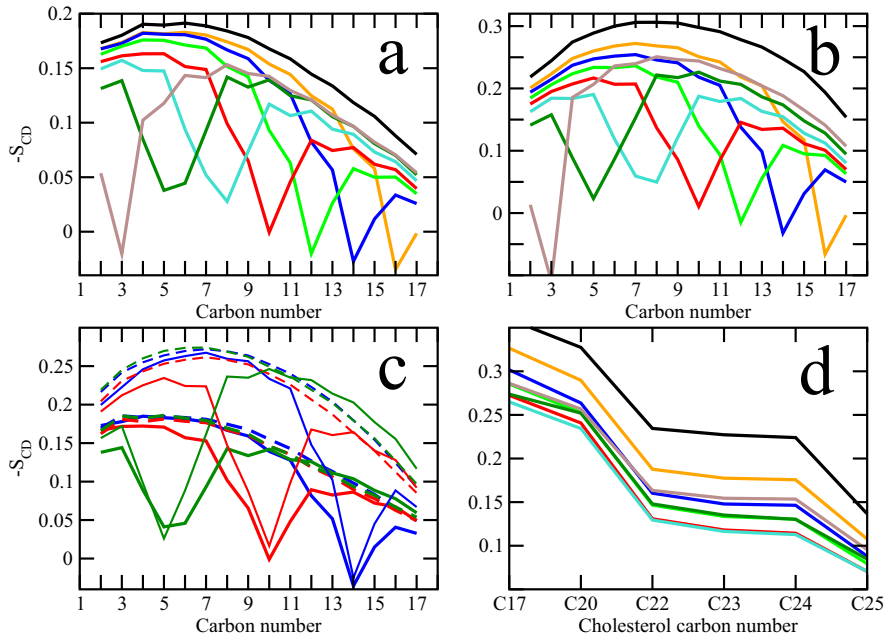

Figure 4.5: Deuterium order parameter (S_{CD}) profiles for (a) *sn*–2 chains for pure di-monounsaturated PhdCho bilayers, (b) *sn*–2 chains for di-monounsaturated PhdCho bilayers with 20 mol% of cholesterol, (c) *sn*–1 (dashed) and *sn*–2 (solid) chains for pure (thick) and mixed with 20 mol% of cholesterol (thin) monounsaturated PhdCho bilayers, and (d) cholesterol chain in di-monounsaturated lipid bilayers. The following color scheme is used to identify the position of the double bond in each system: 18:0 (black), 18:1c15 (orange), 18:1c13 (blue), 18:1c11 (light-green), 18:1c9 (red), 18:1c7 (turquoise), 18:1c5 (dark-green) and 18:1c3 (brown)

the ordering of the whole acyl chain, but is particularly prominent in the vicinity of the double bond. A more detailed observation of the profiles shows that those systems presenting more ordered profiles (systematic higher $-S_{CD}$ values over the profile) correspond to the systems with smaller areas per lipid. This behavior is easier to observe by averaging the $-S_{CD}$ profiles. The mean values of $-S_{CD}$ (averaged over all segments with the exception of the segments involved in the double bond) for the *sn*–1 and *sn*–2 chains are plotted as a function of the double bond position in Figs. 4.6a and 4.6b, and are also given in Tables 4.1 and 4.2. They show a global decrease in chain order when the double bond is moved from the membrane-water interface to the middle of the chain. Beyond this point, an increase in chain order is observed when the double bond is moved from position 9 (that corresponding to DOPC) towards the end of the chain (membrane center). The presence of cholesterol in the systems results in an amplification of the described effect in comparison to the pure systems. No statistical differences were found between the ordering of the *sn*–1 and *sn*–2 chains for the di-monounsaturated systems.

In a similar way, we calculated the S_{CD} values of the methylene groups of the cholesterol chains, Fig. 4.5d. The profiles show a very similar shape in all systems, although they present different values reflecting the different ordering environments. The calculation of their average value leads to the same conclusions presented for the PhdCho acyl chains (not shown). This shows that besides the evident local disorder that the double bonds create around its position, their disordering effect usually propagates to the whole system. This for example justifies the different ordering observed in all saturated chains in the monounsaturated membranes, see

Fig. 4.5c. Although all of them are stearyl chains, they present different ordering patterns due to the different environment caused by the unsaturation in the *sn*–2 chain.

Our results for S_{CD} in the case of DSPC were consistent with the experimental data by Petrache et al. [Petr00]. The dips due to double bonds in the order parameter profiles have been observed in a number of experimental studies, see e.g. Ref. [Olli07a]. DOPC profiles could partially be compared with experimental data by Warschawski and Devaux [Wars05] where the ordering of the carbon segments surrounding the double bond show a good agreement with our data.

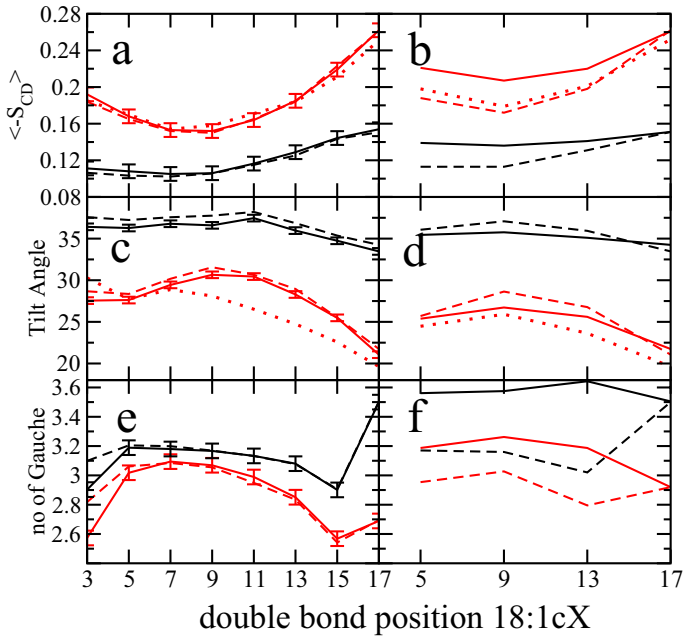

Figure 4.6: Average values of the S_{CD} order parameter as a function of the double bond position for (a) di-monounsaturated PhdCho bilayers and (b) monounsaturated PhdCho bilayers. Average tilt angle as a function of the position of the double bond for (c) di-monounsaturated PhdCho bilayers and (d) monounsaturated PhdCho bilayers. *Gauge* number as a function of the position of the double bond for (e) di-monounsaturated PhdCho bilayers and (f) monounsaturated PhdCho bilayers. Black curves correspond to pure systems, while red curves to mixtures with 20 mol% of cholesterol. The line style represents *sn*–1 chain (solid), *sn*–2 chain (dashed) and Cholesterol (dotted). In panels (a) and (b) cholesterol refers to the chain while panels (c) and (d) to the ring.

4.3.5 Orientation and Conformation

The ordering of the membrane is related to the arrangement of the different molecular fragments. In this analysis several fragments have shown to be good indicators of such ordering. The most relevant fragments to be studied are the acyl chains and the cholesterol ring (when present).

Ordering of an acyl chain is basically determined by two factors: its tilt angle with respect to the bilayer normal, and its structural conformation. Considering first the tilt, the angle between the bilayer normal and the vector connecting the first and the last atom in an acyl chain is studied, see Sec. 3.3.4. Figures 4.6c and 4.6d show its average value as a

function of the double bond for both *sn*–1 and *sn*–2 chains (see also Tables 4.1 and 4.2). In cholesterol-free membranes, the tilt remains rather constant when the double bond is placed in a position close to the interfacial membrane-water region, and only a slight increase is observed when the double bond is moved towards the middle part of the acyl chain. Moving the double bond beyond the middle part and towards the acyl chain end leads to an observable decrease of the tilt angle. For mixed bilayers, these effects are strongly amplified, and the tilt angle shows a pronounced maximum for DOPC/CHOL. In di-monounsaturated systems *sn*–1 chain report around 1° higher values than *sn*–2 chain which can be easily justified by the tendency of the membrane to minimize the mismatch of the chains ends, which is known to be energetically costly.

Considering next the acyl chain's structural conformation, they can be described as the average values of *gauche* configurations per chain (no. of Gauche). A high value is indicative of a more disordered chain. All torsion angles between aliphatic carbons in each chain are considered except the one between atoms O1, C1, C2 and C3 (Fig. 4.1) as it does not present well defined *trans–gauche* equilibrium states. Angles with values 60°± 30°, and 300°± 30° are assigned to $gauche^+$ and $gauche^-$, respectively [Rog01]. Such averages are plotted as a function of the double bond position in Figs. 4.6e and 4.6f for both pure and mixed systems. The values are also provided in Tables 4.1 and 4.2. The presence of cholesterol decreases the number of *gauche* conformations, a clear signature of chain ordering. In general, the qualitative behavior for di-monounsaturated systems is similar in pure and mixed systems. We should note that the number of *gauge* torsions is smaller for unsaturated lipids than for saturated ones, since the double bond never adopts a *gauche* conformation. Using the same argument we can explain the differences observed between *sn*–1 and *sn*–2 chains in the monounsaturated systems where one of the chains is always unsaturated while the other remains saturated. As for the differences between the *sn*–1 and *sn*–2 chains, we find their properties essentially similar.

A more detailed analysis of the probability distribution of *gauche* configurations, this time along the chain, shows an increasing fraction of *gauche* conformations towards the end of the chain. Analyzing the pure systems we also observe that one of the most striking effects of a double bond is its influence on acyl chain conformations. First of all, a double bond influences the torsion angle next to it by decreasing its *gauche* probability (see Fig. 8 in Ref. [Mart07]). Secondly, there is an increase of oscillations of the *gauche* probability along the chain: the probability of odd torsions increases, whereas that of even torsions decreases. The effects found are larger for the lipid species where a double bond was localized closer to the middle and beginning of the chain. A previous study showed that a redistribution of the *gauche* probabilities can modulate the order of the chains [Rog01].

For the mixed systems we can also study the cholesterol tilt as a measure of the ordering of the system. We define the sterol ring tilt as the angle between the vector across the steroid nucleus (from C3 to C17 in Fig. 1.4b) and the bilayer normal, t_{CHOL} [Aitt06, Vain06]. The tilt values as a function of the double bond position are presented in Figs. 4.6c and 4.6d, or alternatively in Tables 4.1 and 4.2. From those plots one can conclude that cholesterol tilt remains almost constant when the double bond is close to the headgroup, whereas a significant decrease is found when the double bond crosses the middle and is moved towards the end of the acyl chains. Finally, comparing panels (a) and (b) with (c) and (d) in Fig. 4.6, a well established result is confirmed: the smaller the sterol tilt is, the stronger is the ordering

ability of the sterol molecule [Aitt06, Rog07a, Rog08a].

4.3.6 Ordering in the Membrane Plane

To quantify the main characteristics of lipid-lipid and lipid-cholesterol interactions, we computed the intermolecular two-dimensional radial distribution functions (RDFs, see Sec. 3.3.5) for the center of mass of PhdCho and cholesterol molecules. The RDF's for PhdCho/PhdCho pairs and for PhdCho/CHOL pairs do not display any defined structure. However, structural properties might be frequently unnoticed when utilizing the RDF's for large and flexible molecules, so that correlations between specific and smaller atom groups generally reveal more information.

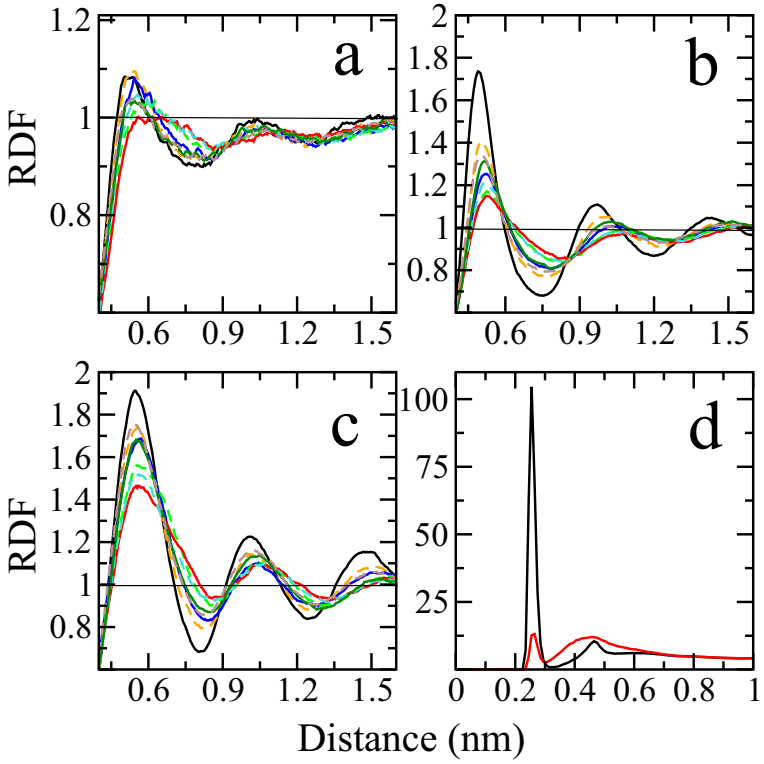

Figure 4.7: Radial distribution functions (RDF) of *sn*–2 chains around themselves in (a) pure di-monounsaturated bilayers, and (b) mixed di-monounsaturated ones. Panel (c) shows the RDF's of the *sn*–2 chains around cholesterol rings. All fragments are described by their center-of-mass positions. The following color scheme is used to identify the position of the double bond in each system: 18:0 (black), 18:1c15 (orange), 18:1c13 (blue), 18:1c11 (light-green), 18:1c9 (red), 18:1c7 (turquoise), 18:1c5 (dark-green) and 18:1c3 (brown). Solid and dashed curves are used for a better contrast between curves. Panel (d) shows the RDF's between cholesterol's oxygen and carbonyl oxygens in *sn*–1 (red) and *sn*–2 (black) chains in the DSPC/CHOL system. The other membranes (*d*18:1cX and *m*18:1cX) showed the similar profiles as the ones presented in panel (d).

RDF's for the center of mass of the *sn*–2 acyl chains of the di-monounsaturated mixed systems shown in Fig. 4.7b exhibit a clearly ordered structure with a first peak at 0.50 nm and almost two more resolved maxima. The smallest correlation is found for the DOPC/CHOL membrane. When the unsaturation is moved either towards the end of the chains or the lipid

headgroups, the correlation is increased. We find the highest correlation in the saturated DSPC/CHOL system. No relevant differences are found for the correlations between *sn*–2/*sn*–2 *sn*–1/*sn*–1, and *sn*–1/*sn*–2 pairs. Similar behavior is found in pure systems, Fig. 4.7a, although they display considerably lower order, reflecting the L_α phase of the pure systems instead of the L_o phase in mixtures. Despite the significant drop in order, a peak around 0.56 nm and a second weaker peak at a larger distance are still observed especially in the DSPC system. RDF's between the center of mass of the *sn*–2 acyl chains and cholesterol ring molecules in Fig. 4.7c also present a well defined structure with a first peak at 0.55 nm and at least two still well resolved maxima at larger distances. Again, the smaller correlation was observed for the DOPC/CHOL system. No preference for a specific chain is found for cholesterol.

The RDF's are also useful when applied to atoms or rather small groups of atoms to search for the relevant interactions in the system. For example, to explain why the position of cholesterol is independent of double bond location (see Sec. 4.3.2) we performed three-dimensional RDF's between cholesterol hydroxyl group and different parts of PhdCho molecules. The different behavior between the carbonyls of the *sn*–1 and *sn*–2 chains can be observed as an example in Fig. 4.7d. In all systems a strong interaction with *sn*–2 carbonyl oxygens is noticed, as well as a smaller one with choline methyl groups. This indicates that CHOL–PhdCho interaction is mainly mediated by the affinity between the cholesterol hydroxyl and PhdCho carbonyl and choline methyl groups. This justifies that cholesterol is equally inserted in all the simulated bilayers. Such result is confirmed below when studying hydrogen bonding and charge pairing between PhdCho and cholesterol molecules, and was also found in previous numerical studies for DPPC/CHOL bilayers [Chiu02].

4.3.7 Surface Structure and Intermolecular Interactions

In this section we will study three possible intermolecular binding modes: hydrogen bonds, water bridges and charge pairs, see Sec. 3.3.7. All of these interaction modes are critical for membrane stability. The average number of hydrogen bonds between PhdCho molecules and water characterizes lipid hydration. Such a variable is plotted in Fig. 4.8a as a function of the double bond position for both mixed and pure di-monounsaturated systems (the values are provided in Tables 4.1 and 4.2). We find that systems with cholesterol present a more pronounced response with respect to the double bond position, whereas it remains rather constant in the pure systems. The effect of the double bond position follows the behavior of the area per lipid; namely, the DOPC system has the largest number of hydrogen bonds. In both pure and mixed systems, the phosphate oxygens form the largest fraction of hydrogen bonds with water (an average of 1.62(pure)/1.55(mixture) for each oxygen atom) since they are more exposed to the aqueous phase. The two carbonyl oxygen atoms show a rather distinct interaction with water: the one on the *sn*–2 chain (O22) forms an average of 1.58(pure)/1.47(mixture) hydrogen bonds per oxygen, whereas the other (O32) only forms an average of 0.64(pure)/0.56(mixture) hydrogen bonds per oxygen. This is a consequence of the fact that the *sn*–1 chains are more deeply inserted in the membrane. The presented preferential hydrogen bonding locations are not strongly altered by the PhdCho used in the simulation. The decrease in the total number of hydrogen bonds observed for the membranes with a smaller area is mainly due to the decrease of hydrogen bonds between water and the

carbonyl oxygen atoms.

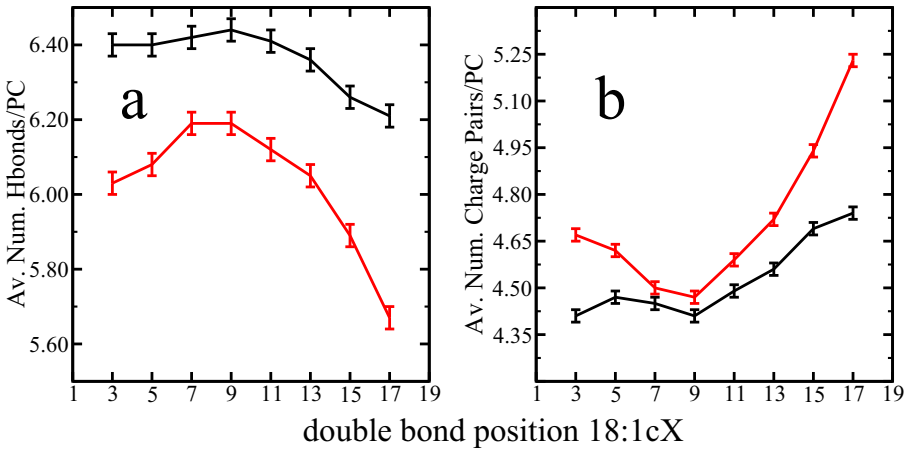

Figure 4.8: (a) Average number of hydrogen bonds with water per PhdCho as a function of the double bond position. (b) Average number of charge pairs involving two PhdCho molecules (PhdCho/PhdCho) as a function of the double bond location. In both panels the black line stands for pure PhdCho bilayers and the red line for mixed PhdCho/CHOL bilayers.

The average number of hydrogen bonds between the cholesterol hydroxyl group and the different oxygens of the PhdCho molecules do not show any particular trend when the position of the double bond is varied. They do, however, display a selective behavior. A clear preference of hydrogen bonding between the hydroxyl group and the *sn*–2 carbonyl is observed (an average of 0.36 hydrogen bonds per cholesterol molecule). This preference is due to the fact that the carbonyl in the *sn*–2 acyl chain is located closer to the surface than the carbonyl in the *sn*–1 chain, thus providing a more polar and hydrated environment to the cholesterol hydroxyl. The average number of hydrogen bonds per cholesterol molecule is reduced to 0.08 for the *sn*–1 carbonyl. No interactions with phosphate group oxygens are observed. Such interactions would imply an exposure of the cholesterol ring nucleus to water. Finally, preferential hydrogen bonding modes between cholesterols and PhdCho oxygens are not substantially influenced by the location of the double bond indicating that cholesterol is equally inserted in all of the studied systems, see Sec. 4.3.2 and 4.3.6.

The other interaction that proved to be relevant for the membrane stability corresponds to the water bridges. We observe how the occurrence of this binding mode remains rather constant in all our systems 0.90–0.98±0.05, see Tables 4.1 and 4.2. This property concerns the stability of the membrane as it reflects the linkage of two lipid molecules by a water molecule that simultaneously forms one hydrogen bond with each lipid. This obviously restrains the molecular movement, and seems to be a characteristic feature of the headgroup, as it is not affected much by the change of the acyl chains.

To conclude, charge pairing describes the electrostatic interactions between positively (i.e. a methyl group in PhdCho choline) and negatively charged (i.e. phosphate oxygens in PhdCho or the cholesterol hydroxyl group) molecular moieties. In agreement with previous studies [Murz01, Murz06], a decrease in the surface area leads to an increase in the number of the charge pairs involving two PhdCho molecules. This is shown in Fig. 4.8b for both pure and mixed systems as a function of the double bond position for di-monounsaturated moieties (see also Tables 4.1 and 4.2).

4.3.8 Cholesterol Methyl Groups Analysis

So far, all the structural information we have gathered show a clear change in the structural properties of the mixed systems when compared with the pure ones. Such changes result in a clear maximum/minimum of the considered properties around DOPC system (non-monotonic behavior). The representation of those properties with respect to the double bond position, showed an interesting effect: the displacement of the double bond from the center (DOPC) towards the head or the chain is not equivalent. We found that changing the position of the double bond closer to the end of the chain produced a significantly higher variation of the properties than the equivalent displacement towards the headgroup. At this stage, despite we have extensively described the nature of such changes, the ultimate molecular mechanism responsible for such behavior has remained hidden.

Some studies by Róg et al. [Rog07a, Poyr08] have stressed the importance of the cholesterol off-plane C18 and C19 methyl groups in the ordering and condensing capability of cholesterol. These groups create an asymmetry in the cholesterol structure by defining its smooth (α) and rough (β) sides, and are believed to be responsible for the tilt of the sterol ring in the bilayer. Figure 4.9 depicts the three-dimensional radial distribution functions (RDF's) between the centers of mass of the double bonds and the off-plane cholesterol methyl groups C18 and C19. The RDF curves display two clear maxima. The first peak at the distance of 0.45–0.5 nm is due to the direct interaction between the double bond and the off-plane methyl groups, whereas a second peak is found at 0.7–0.8 nm. In our analysis we only consider the first peak as it reflects the only real interaction.

These profiles reveal how the double bonds in different monounsaturated acyl chains are distributed with respect to the C18 and C19 groups. Since the modeled interactions between the cholesterol methyl groups and the double bond are governed by van der Waals forces, Fig. 4.9 in part describe the strength of the attractive interaction between them. To characterize these interactions in a more detailed manner, Figs. 4.10a and 4.10b show the values of the RDFs at the approximate position of the first maximum, 0.48 nm ($I_{0.48}$), as a function of the location of the double bond. It is observed how the interaction with C18 (Fig. 4.10a) displays a maximum for DOPC. In the case of C19 (Fig. 4.10b), the behavior is different and shows the highest interaction with the double bond close to the water interface.

In the case of DOPC, for which the condensation effect is minimized, the double bond is at the same z-level as the C18 group, thus impeding an optimal area condensation. Therefore, the stronger is the interaction between a double bond and the C18 group, the weaker is the ordering and condensation effects of cholesterol. When the double bond is located deeper in the membrane, the interaction with C18 is strongly reduced (double bond and C18 are placed at different z-levels), and the condensation effect becomes amplified. However, when the double bond is placed closer to the lipid headgroup, the condensation effect is amplified mostly due to the reduction of the impediment caused by the C18 group, although the steric influence of C19 increases. The balance of these two effects determines the observed asymmetry in the general behavior: area condensation is increased when the double bond is moved towards the headgroup, but to a smaller extent than when moving it towards the end of the acyl chain due to the presence of C19. It seems evident, therefore, that C18 is considerably more important than C19 in respect to the interplay with the double bond. Such differential interaction may be explained by the fact that C18 affects a more ordered

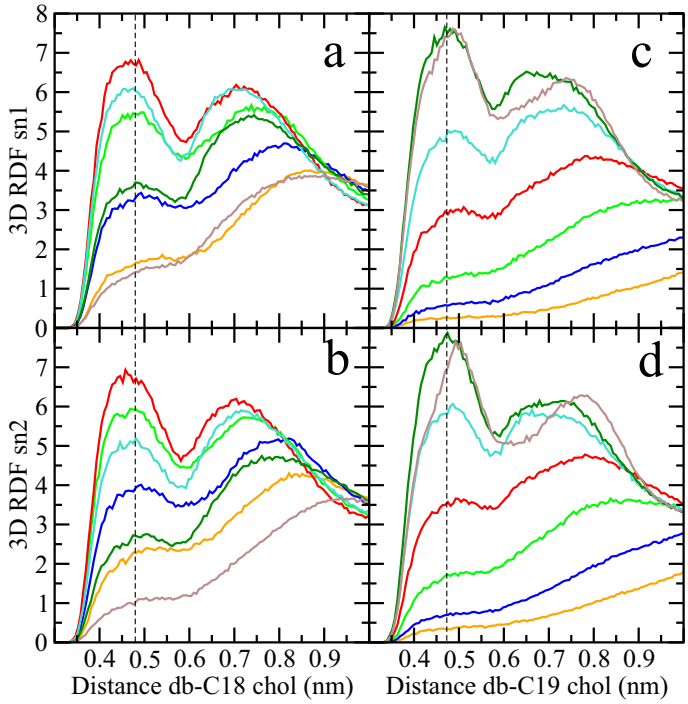

Figure 4.9: The three-dimensional RDF of the double bond center of mass around cholesterol C18 (a, c) and C19 (b, d) methyl groups in the *sn*–1 (a, b) or *sn*–2 (c, d) chains. The following color scheme is used to identify the position of the double bond in each system: 18:1c15 (orange), 18:1c13 (blue), 18:1c11 (light-green), 18:1c9 (red), 18:1c7 (turquoise), 18:1c5 (dark-green) and 18:1c3 (brown). The vertical dashed horizontal line at 0.48 nm shows the approximate location of the maximum of each curve that was used to calculate $I_{0.48}$

region of the acyl chains (see Fig. 4.5) than C19 methyl group.

To establish more or something besides out of completeness, we analyzed the relative height along z-axis between the double bond and the C18 and C19 methyl groups, see Figs. 4.10c and 4.10d. Our analysis shows that the strength of the interaction observed in Figs. 4.9 is inversely related to their different level of insertion in the membrane. Although such result might seem obvious, the three-dimensional nature of the RDF requires this confirmation. As a result we can conclude that double bonds interact with the C18 and C19 cholesterol methyl groups more strongly when both shared the same level of insertion in the membrane. This is noticed also when comparing panels (a) and (b) with (c) and (d) of Fig. 4.10, respectively.

4.4 Discussion and Conclusions

PhdChos are among the most common Phds in natural membranes. A major fraction of the lipid acyl chains in PhdChos are monounsaturated, the double bond residing typically at the center of an acyl chain. The reason for such preference was completely unknown and we have tried to shed some light to this issue.

The only available experimental studies concerning the position of the double bond have shown that the position of the double bond influences the temperature of the main phase transition T_m [Seel77, Seel78, Stub84, Wang95, Koyn98, Huan01] such that lipid species with

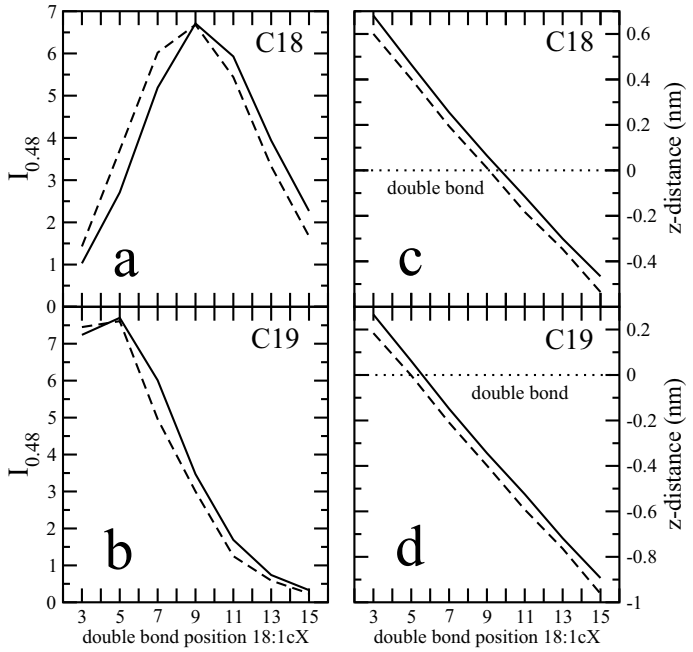

Figure 4.10: Values at 0.48 nm ($I_{0.48}$) of the three-dimensional RDF's of the double bond center of mass around (a) cholesterol C18 and (b) C19 methyl groups as a function of the double bond position. Relative height along z-axis between the double bond and the (c) C18 and (d) C19 methyl groups as a function of the double bond position. Dashed lines correspond to *sn*–1 chains and solid lines to *sn*–2 chains.

the double bond located close to the center of the chain were characterized by the lowest phase transition temperatures. However, a direct connection between the phase transition temperature and membrane properties above is not straightforward. The main difficulty is that T_m is related to the packing and the van der Waals interactions in the gel phase, while at physiological temperatures, or above them, natural membranes are in the fluid phase. Comparing experimental areas per molecule at a given temperature with the T_m of the lipid we discover a general inverse relation between both properties. In our case, we find that membranes composed of lipids with a double bond in the middle of their chains are characterized by the largest disorder. Moreover, when the double bond is moved from the center of an acyl chain the disorder decreases. These findings are therefore absolutely consistent with experiments for the dependence of T_m on the double bond position and also suggest the faculty of promoting disorder as a probable reason for the preference of the double bond in the middle of the acyl chain.

Indeed, the results of our simulations concerning pure systems show that the position of the double bond affects the membrane structural properties. The stronger disordering effect is observed when the double bond is located in the middle of the chain. The overall effect can be observed, for example, in the membrane area: the area per lipid of the DOPC was 0.045 nm^2 larger than that of *d*18:1c15, and 0.062 nm^2 larger than that of a fully saturated DSPC. Consistently with the increase of the surface area per lipid when the double bond is placed in the middle of the acyl chain, we observe that membranes became thinner and the acyl chains become more disordered. An increase in the surface area also leads to a decrease in direct headgroup interactions and to an increase in interactions between headgroups and

water, in agreement with previous studies [Murz06]. The observed differences are in general rather small, especially when moving the double bond from the center towards the headgroup. Therefore, to justify the natural preference for lipids with the double bond in the center of their acyl chains due to the reported higher disordering capabilities in pure membranes seems possible but not probable.

Natural membranes are constituted by many moieties. From those cholesterol has shown experimentally to be tightly related to the PhdCho composition [Slot83, Shir94]. Due to this, we conjectured about the possibility that the specific requirements of the double bond position and lipid selection in natural membranes are at least in part related to the interactions between PhdChos and cholesterol. We also know that such interaction can also play a crucial role in the formation of functional platforms of ordered lipids and cholesterol called rafts.

Comparison between our simulation results in Pure PhdCho membranes and PhdCho/CHOL systems clearly shows pronounced effects of cholesterol. Firstly, the inclusion of cholesterol in lipid bilayers leads to the well known condensation effect. Secondly, as compared to the single-component bilayers, the area per PhdCho is strongly reduced, and consistently, the membranes become thicker. All these effects are accompanied by an increase in chain ordering and a reduction of the chain tilt and number of *gauche* conformations. Further, cholesterol reduces the number of H-bonds between PhdCho molecules and water. What is more, our analysis shows an enhanced non-monotonic and asymmetric behavior in a number of membrane properties when the double bond position is varied. Smallest cholesterol-induced effects are found for the DOPC/CHOL bilayer. This system displays the largest values for the membrane area and volume, acyl chain tilt, number of *gauche* conformations and lipid hydration, and consequently, the smallest membrane thickness, chain ordering, and number of charge pairs. Displacing the double bonds towards the lipid headgroup or the end of the acyl chain leads to a reduction of the area per PhdCho. Additionally, the lipid chains are found to become less tilted, more ordered and packed, and the membranes, in turn, become thicker, denser and less hydrated. All these changes are much more pronounced when the double bond is close to the end of the lipid acyl chains compared to being in the vicinity of the lipid headgroup. For comparison, in pure PhdCho bilayers the effects due to varying the double bond position have been found to be significantly smaller or even marginal when double bond is moved from the acyl chain center to the headgroup.

The non-monotonic and asymmetric behavior observed for the structural membrane properties can be rationalized by looking at PhdCho/CHOL interactions at atomic level. Firstly, our results indicate that the position of cholesterol in a membrane is only weakly dependent on the location of a double bond in a lipid acyl chain, as it is mainly determined by the interaction between the cholesterol hydroxyl group and the *sn*–2 carbonyls through hydrogen bonding. Secondly, the systems presenting the higher disorder show a closest distance between their double bonds and the C18 cholesterol methyl group. In a minor extent, the interaction of the double bond with the C19 methyl group also showed to promote disorder. The combination of these two factors (constant depth of the off-plane methyl groups in all membranes and the finding of the direct interaction of those methyl groups with the double bonds as an enhanced disordering mechanism) is sufficient to explain the differences of the membrane properties when the double bond position is varied. The position of the double bond in the acyl chain fixes its depth in the membrane to a certain region. Our data shows that the double bond region of the PhdCho acyl chains interacts with the C18

cholesterol methyl group stronger when the double bond was located in the middle of an acyl chain (DOPC). When the double bond is translated towards the end of the chain, its interaction with C18 is reduced, the mutual packing of CHOL and PhdCho is then promoted, and the area per PhdCho is decreased. Instead, when the double bond position is shifted to the vicinity of the lipid headgroup, the interplay between the double bond and C18 is also reduced but the influence of C19 then leads to a smaller modification of membrane properties. Our finding suggests that the interaction between C18 and the semi-rigid double bond fragment of the PhdCho affects the tilt of cholesterol and surrounding acyl chains, and discriminates the effect of cholesterol depending on the location of the PhdCho double bond, explaining the observed non-monotonic behavior. The presence of C19, instead, is responsible of the asymmetry in of the behavior of the reported membrane properties.

Summarizing, we have demonstrated that the presence of cholesterol clearly amplifies the non-monotonic behavior observed in a number of structural properties of membranes with respect to the double bond position, indicating that cholesterol contributes to explain the natural unsaturation heterogeneity in PhdCho acyl chains. Even more importantly, most obvious signs of disorder in membrane properties are found when the double bond is located close to the middle of an acyl chain, proposing that to be a simple mechanism for promoting highly fluid membrane domains in biological membranes. We conjecture that this could be a reason behind the biological preference for monounsaturated acyl chains with the double bond between carbons C9 and C10. What remains to be considered if cholesterol plays any role in the biological membrane preference for PhdCho moieties with saturated *sn*–1 chains and monounsaturated *sn*–2 ones. This issue will be addressed in the next chapter 5.

CHAPTER 5

Study of the Biological Preference for *sn*–1 Saturated and *sn*–2 Unsaturated PhdChos as a Membrane Constituents: Differences Between Positional Isomers SOPC and OSPC in Membranes With and Without Cholesterol

5.1 Objective and Summary

In this chapter we will continue unrevealing the reasons behind the natural preference for specific lipid moieties. In particular we shift our attention to a rather unexplored topic concerning also the PhdCho acyl chains. Phds with two different acyl chains may have positional isomers as each chain has two non-equivalent possible locations, *sn*–1 or *sn*–2 (the *sn*–1 chain attached at carbon/position 3 and the *sn*–2 chain attached at carbon/position 2 of the glycerol moiety, see Fig. 1.3). For all glycerol-based lipids present in cell membranes, the *sn*–1 chain is most commonly the saturated one whereas the *sn*–2 chain is usually mono- or polyunsaturated; namely, double bonds are preferably located in the *sn*–2 chain [Van 65, Romi72, Cron75, Sait77]. This preference has been observed in both eukaryotic [Bare99, Rams02, Meer05] and prokaryotic [Rott79b, Iske98] membranes. For example, measurements for mycoplasma show 8:1 preference for the double bond(s) to be located in the *sn*–2 position for lipids containing 18:1 chains [Silv77]. This preference appears to be very systematic but the cause for this finding is unknown.

To our knowledge, there are only relatively few articles which have addressed this issue [Davi81, Davi83b, Davi84, Simi88, Ichi99, Inou99]. Calorimetric studies have shown that the main transition temperature, T_m, depends slightly on the particular chain on which the double bond is located; if the *sn*–1 is the unsaturated chain, T_m is about 2–4 K higher for a lipid with two 18-carbon chains as compared to the double bond being in the *sn*–2 chain [Davi81, Davi83b, Ichi99, Inou99]. In addition, calorimetric measures and other methods have shown that a mixture of cholesterol with positional isomers indicates cholesterol interactions with PhdCho in the gel phase to be influenced by the position of the unsaturated chain [Huan77, Davi83b, Davi84]. Unfortunately, biological data focusing on the relevance of

positional isomers of saturated and unsaturated chains is also rather limited [Cron74, Cron75]. For example, it was shown that in hepatoma cells, there is a loss of positional preference of the unsaturated chain associated with elevated concentration of cholesterol [Dyat74]. Similarly in mycoplasmas with high levels of cholesterol, large amount of lipids with *sn*–1 unsaturated and *sn*–2 saturated have been observed [Rott79a, Davi81].

In this work, we employ atomistic simulations to consider positional *sn*–1/*sn*–2 isomers in a pure bilayer and in a binary mixture with 20 mol% of cholesterol. The PhdChos used in this work are monounsaturated, having only an individual double bond either in the *sn*–1 or in the *sn*–2 chain. We found that differences between isomers are small but perceptible, and they increase when mixed with cholesterol. The molecular mechanism leading to these differences seems to be related to the chains' length mismatch in the bilayer, and it is enhanced in the cholesterol-containing membranes by the interaction of the double bond in the PhdCho acyl chain with the C18 cholesterol methyl group, as happened in the study of the double bond position. Our main finding is that membranes composed by positional isomers have unequal physical properties. The nature of these differences is rather small but clearly detectable.

The research described in this chapter resulted in the publication [Mart09] included in this Thesis.

5.2 Descriptions of Simulated Systems

To explore the effect of positional *sn*–1/*sn*–2 isomers a total of 8 membranes were compared. Four of those membranes were constituted by a single lipid, while the other four were binary mixtures of the same PhdCho moieties with 20 mol% of cholesterol. Two different monounsaturated PhdCho lipids, which are positional isomers, were used in this study: 1–stearoyl–2–oleoyl–*sn*–glycero–3–phosphatidylcholine (SOPC: *m*18:0/1) and 1–oleoyl–2–stearoyl–*sn*–glycero–3–phosphatidylcholine (OSPC: *m*18:1/0). The structures are shown in Fig. 5.1. These isomers were chosen since they are the only ones with some available experimental data to validate our simulations. The remaining two PhdCho moieties were used as a reference system. In particular, we used the fully saturated 1,2–distearoyl–*sn*–glycero–3–phosphatidylcholine (DSPC: *d*18:0) and di-monounsaturated 1,2–dioleoyl–*sn*–glycero–3–phosphatidylcholine (DOPC: *d*18:1) bilayers, see Fig. 5.1. As a result, all studied PhdCho had chains with exactly 18 methyl groups. This choice is critical on the analysis of the obtained results as will be discussed below.

Atomic-scale Molecular Dynamics simulations of the eight membrane systems were carried out. The first four (pure) bilayers were composed of a total of 128 PhdCho molecules, and the remaining four (mixed) systems had 32 cholesterol molecules in addition to the 128 PhdChos. All of the bilayers were hydrated with around 3,900 water molecules. Six out of eight membranes used here were already analyzed in the previous chapter 4. Only the OSPC membranes, pure and mixed, were specifically run to complete the problem addressed in this chapter. The protocol was the same as discussed for the other 6 simulations, and the construction was identical to the SOPC membranes although this time the *sn*–1 chain was the only one remaining monounsaturated (OSPC), see Sec. 4.2. All compared systems were simulated at 338 K, and the simulation times are above 100 ns for pure systems and 150 ns for mixtures.

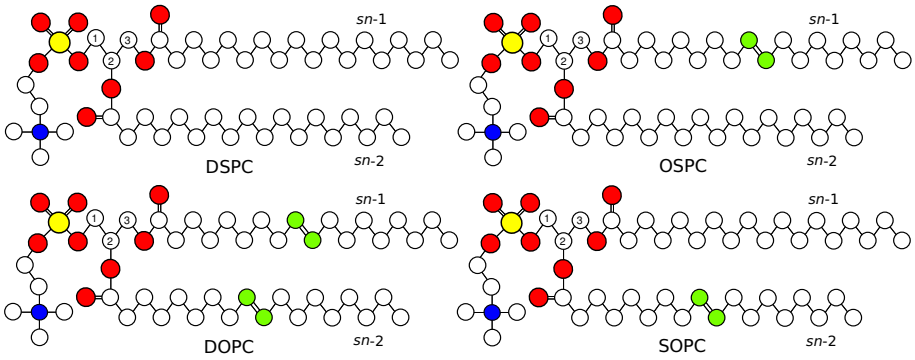

Figure 5.1: Molecular structure of the monounsaturated positional isomers SOPC and OSPC. Additionally, the reference systems used are also depicted DOPC (di-monounsaturated) and DSPC (saturated). The following color scheme is used to identify the different atom types: Oxygen (red), nitrogen (blue), phosphorus (yellow), carbon (white) and double bond position (green). No hydrogens are plotted as we have used an united atom forcefield.

5.3 Structural and Dynamical Membrane Properties

In order to provide a complete picture of the behavior of the membranes regarding the two studied positional isomers, we calculated several physical properties covering both structure and dynamics of the membrane. The summary of the structural information is given in Table 5.1. In all the presented results, error bars were estimated using the block analysis method [Hess02] and are given as twice the standard error.

5.3.1 Area per Molecule and Thickness

As a fundamental property of membranes we calculated the area per molecule following the procedure by Hofsäßet al. [Hofs03], see Table 5.1. It can be observed that SOPC bilayers has a larger A^*_{PC} than their OSPC counterparts. The difference between SOPC and OSPC is small but statistically significant for both single component (0.46 Å^2) and cholesterol-containing (0.75 Å^2) systems. Therefore, the addition of cholesterol enhances the differences between the positional isomers. This result indicates that the lipid with the double bond in its *sn*–2 chain (SOPC) induces more disorder.

Contrary to SOPC and the two reference systems, DOPC and DSPC, there is no available data of the area per molecule for OSPC neither pure or with cholesterol. Even though as all those systems show good agreement with experiments, Sec. 4.3.1, due to the minor differences between OSPC and SOPC we do not expect deviations now for the OSPC ones. Moreover, it is important to notice the agreement between calorimetric experiments and the observed differences in area per molecule. Table 5.1 provides the main transition temperatures, T_m, for the single component systems studied here. Interestingly, they are inversely correlated with the areas per molecule, as has also been observed for many PhdChos [Mart08a]. The nature of such correlation is not unequivocal (a given T_m do not mean a specific area per molecule), but it has been shown to be significant enough to compare lipids with small structural differences [Mart08a]. For our monounsaturated species, a difference of 2–4 K has been found between SOPC and OSPC [Davi80b, Davi81, Ichi99, Inou99]. In this case, such difference is associated with a small difference in the area per molecule, 0.46 Å^2, and captures

	DSPC	OSPC	SOPC	DOPC
T_m ($L_\beta \mapsto L_\alpha$) (K)	328.80	281.90	279.90	232.90
A^*_{PC} (Å^2)	66.95±0.31	70.21±0.19	70.67±0.34	73.08±0.21
	56.39±0.19	**61.88±0.31**	**62.63±0.17**	**66.25±0.24**
η_{DB} (Å^2)	NA	5.49	6.24	4.93
	NA	**3.27**	**3.73**	**3.06**
$\mathbf{D_{PP}}$ (nm)	4.63	4.28	4.25	4.04
±0.01 nm	**4.01**	**3.84**	**3.82**	**3.71**
$\langle -S_{CD} \rangle$ (±0.003)				
sn–1	0.261	0.177	0.208	0.150
	0.151	**0.114**	**0.136**	**0.106**
sn–2	0.262	0.217	0.172	0.152
	0.154	**0.140**	**0.113**	**0.106**
Tilt angle (deg)				
t_{sn-1}	21.74	28.53	26.72	31.56
	34.25	**37.36**	**35.76**	**37.75**
t_{sn-2}	21.06	25.34	28.64	30.65
	33.46	**34.73**	**37.08**	**36.59**
$t_{P \mapsto N}$	98.90	99.30	99.51	100.49
	100.24	**100.81**	**100.80**	**101.50**
t_{CHOL}	19.63	24.29	25.91	26.52
t^t_{CHOL}	28.70	34.93	37.17	37.89
$\langle d_{bilayer\ center} \rangle$ (Å± 0.1)				
sn–1	2.06	2.75	1.72	2.33
	2.17	**2.72**	**1.72**	**2.24**
sn–2	2.62	2.16	3.11	2.66
	2.57	**2.16**	**3.04**	**2.52**
chain mismatch	0.56	-0.59	1.39	0.33
	0.40	**-0.56**	**1.32**	**0.28**
$\langle d_{C18} \rangle$ (Å± 0.1)				
sn–1 ($C3_9$-$C3_{10}$)	0.07	<u>0.36</u>	0.70	<u>-0.06</u>
sn–2 ($C2_9$-$C2_{10}$)	-0.70	-0.37	<u>-0.02</u>	<u>-0.65</u>

Table 5.1: Average results characterizing DSPC, OSPC, SOPC and DOPC membrane properties. Bold letters are used to mark pure systems, whereas light-face letters those containing 20 mol% CHOL. NA stand for not applicable. Underlined values show the double bond position. T_m values were extracted from Ref. [Ichi99].

the predicted correlation between T_m and area per lipid. In the systems where cholesterol is included, the comparison is not as straightforward. Calorimetric profiles show minor differences in shape between SOPC and OSPC with 17–23 mol% of cholesterol [Davi83b], as well as the differences in area observed in our systems with 20 mol% of cholesterol.

At this point, a simple evaluation of the efficiency (η_{DB}) of the double bond to induce disorder seems adequate, see Eq. 4.1. This analysis shows that placing the double bond in the *sn*–2 chain increases the disordering effect considerably, see Table 5.1. It is also important to notice that the addition of a second double bond (DOPC), having a lipid with two monounsaturated chains, does not double its effect. Instead, a drop in the ratio for the area increase per double bond is found. These features are significantly enhanced in the presence of cholesterol.

Additionally, as a complementary parameter of the area per molecule we have computed the membrane thickness. The observed differences between SOPC and OSPC, although statistically different, were small: 0.2 Å for the pure and 0.4 Å for the mixed systems (see Table 5.1). Despite its smallness, the observed trend is consistent with the area per molecule: the larger area per molecule, the thinner membrane.

5.3.2 Molecular Ordering

The molecular ordering is again evaluated by computing the S_{CD} profiles of the acyl chains, see Sec. 3.3.6. Analysis of the S_{CD} profiles revealed that the saturated chains in OSPC and SOPC lipids display different behavior, see Fig. 5.2. If we consider the saturated chains (*sn*–1 in SOPC and *sn*–2 in OSPC), we find essentially identical order close to glycerol, while for carbons 7–18 are considerably less ordered in SOPC. If we next focus our attention to the unsaturated chains (*sn*–2 in SOPC and *sn*–1 in OSPC), SOPC is less ordered close to the glycerol group than OSPC (carbons 1–7), but slightly more ordered in the membrane center beyond the double bond position (carbons 12–18).

In order to clarify which acyl chains are globally more ordered, we calculates the $\langle -S_{CD} \rangle$ mean values excluding the unsaturated carbons, see Table 5.1. Averages for DOPC and DSPC membranes are also given as reference values. We conclude that both saturated and unsaturated chains display a higher ordering in OSPC systems than in SOPC bilayers, though the differences are small. Both chains contributed to the higher ordering of OSPC systems, but most of this effect is due to the saturated acyl chain. In mixed bilayers with cholesterol, a similar outcome is obtained, the only difference being that cholesterol increases the difference between SOPC and OSPC.

Although the observed differences are small in our simulations, it has to be noticed that NMR is a particularly sensitive technique. In particular, NMR was successfully used in similar systems where the differences were even smaller than those shown here [Repa05, Bung09]. Therefore one should expect that the data provided here can be tested in the near future.

Complementary to the previous information, we have calculated the average tilt angles with respect to the z-axis for the *sn*–1 and *sn*–2 chains, for the cholesterol ring, and for the cholesterol chain, see Table 5.1. The measurements and definitions of the axes are identical to those provided in Sec. 3.3.4. This data shows differential behavior in the saturated chain between positional isomers. That is, while the tilt of an unsaturated chain remains nearly unaltered between isomers (difference of about 0.28° for pure bilayers and 0.11° for mixed

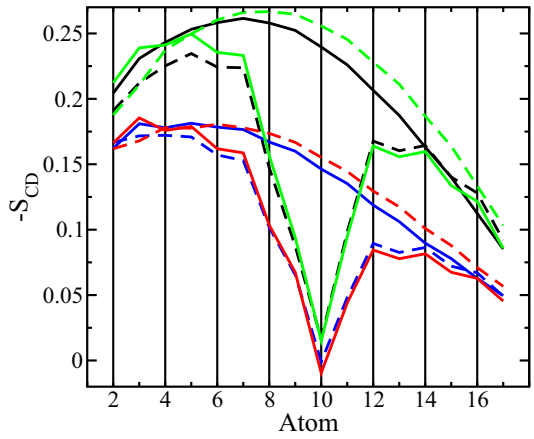

Figure 5.2: S_{CD} order parameter profile for both chains, *sn*–1 (solid) and *sn*–2 (dashed), in the pure systems (SOPC in blue, OSPC in red) and in mixtures including 20 mol% of cholesterol (SOPC in black, OSPC in green) al 338 K. The error bars are smaller than ±0.005.

systems), the differences are much larger for saturated chains (1.03° and 1.38° for pure and mixed membranes, respectively). Interestingly, in mixed systems a difference of 1.62° in the cholesterol tilt between OSPC and SOPC membranes is also observed (see Table 5.1). The tilt of cholesterol has been recently recognized to be a relevant measure of a sterol's ability to condense/order a bilayer. Therefore, the observed differences in cholesterol tilt explain why the differential behavior between positional isomers is amplified by cholesterol [Aitt06, Vain06, Rog08a]. OSPC membrane displays a smaller cholesterol tilt in agreement with the higher average order of lipid acyl chains and the smaller area per lipid compared to the SOPC system.

5.3.3 Acyl Chain Mismatch

Previous studies about the asymmetry between the two lipid acyl chain lengths have concluded that phospholipid chain length mismatch can induce disorder, see for example Refs. [Cevc91, Ali98]. Such mismatch can be understood as the difference in depth reached by the two chains of a given Phd, thus it can be rationalized by computing the distance between the terminal methyl groups at each chain of the lipid. To do so, we have calculated the mass density profiles in the direction perpendicular to the bilayer plane for the end methyl groups ($C3_{18}$ for the *sn*–1 chain and $C2_{18}$ for the *sn*–2 chain, see Fig. 5.1) of each leaflet independently. We have then computed the barycenter (center of gravity) of the obtained four mass density profiles ($C3_{18}$ in upper and lower layer; $C2_{18}$ in upper and lower layer). For a given terminal methyl group ($C3_{18}$ or $C2_{18}$), the distance between the two barycenters correspond to twice the distance from the terminal methyl group to the bilayer center (see data for $\langle d_{bilayer\ center} \rangle$ given in Table 5.1). Subtracting this distance for $C3_{18}$ (that in principle is less deeply inserted) from the value for $C2_{18}$ we obtain the mismatch between the chains (see "chain mismatch" data in Table 5.1).

For symmetric lipids (e.g. lipids with the same number of double bonds and chain length), such as the DSPC, DSPC/CHOL, DOPC, DOPC/CHOL membranes, the chain mismatch is positive. This means that the *sn*–1 end methyl group ($C3_{18}$) is inserted deeper than the *sn*–2

one ($C2_{18}$), as a result of a deeper inserted ester-linkage with the glycerol in the *sn*–1 chain compared to the *sn*–2 chain (see Fig. 3.2). A similar positive but much larger chain mismatch is found in SOPC and SOPC/CHOL membranes, indicating that the saturated *sn*–1 chain of SOPC extends deep to the membrane like a semi-rigid rod, while the unsaturated *sn*–2 chain adopts a more disordered (tilted) conformation. In the case of the OSPC and OSPC/CHOL systems, the situation is the opposite. We find a negative value for chain mismatch: the ester-linkage of the unsaturated *sn*–1 chain is placed deeper in the membrane than the ester-linkage of the saturated *sn*–2 chain, but the *sn*–1 chain adopts a more disordered (tilted) conformation because of the double bond, and this latter effect dominates.

The *absolute* value of the mismatch is in fact the relevant quantity in terms of disordering. The larger the value, the more disorder is induced by the mismatch effect explained above. Symmetric lipids (DSPC, DOPC) are a good reference for small mismatch effects (0.28–0.56 Å, see Table 5.1). We observed similar values for OSPC (0.56 and 0.59 Å), but at least twice as large values for SOPC (1.32 and 1.39 Å). This justifies why the SOPC moiety (having a larger chain length mismatch) displays a larger area per molecule than OSPC (having a smaller mismatch effect). In membranes with cholesterol a systematic increase of the mismatch within the range 0.04–0.16 Å in absolute value is observed. No major changes are expected from such small increments between pure and mixed bilayers, so the mechanism responsible of the amplification of the differences when cholesterol is present has to be different.

5.3.4 Interaction between Double Bond and Off-Plane Cholesterol Methyl Group C18

So far we have justified the differences in area per molecule observed between SOPC and OSPC bilayers. However, we have not explained the mechanism that causes these differences to increase when cholesterol is added. In the previous chapter, it was shown that the proximity of the double bond to the off-plane methyl group of cholesterol, C18 (see Fig. 1.4b), induces disorder in the system. In order to elucidate the role of this feature in our mixed bilayers, we have tracked the relative position in the z-direction (normal to the bilayer plane) of both groups in the system. Following a similar procedure as described in the former section, we compute the distance in the z-axis between the center of mass of the double bond and the C18 group in cholesterol.

The relative z-positions of the center of mass of the lipid chain segments $C3_9$–$C3_{10}$ and $C2_9$–$C2_{10}$ with respect to C18 of cholesterol, $\langle d_{C18} \rangle$, are given in Table 5.1. A clear correlation between the interaction ($\langle d_{C18} \rangle$) and disorder promotion is observed. We observe that in the case of SOPC, their z-positions are almost the same (0.02 Å), while the vertical positions in the case of OSPC are considerably different (0.36 Å). This explained why the SOPC membrane is more disordered upon addition of cholesterol than OSPC, or from another perspective, why the ability of cholesterol to order the surrounding lipids was smaller for SOPC than for OSPC.

5.3.5 Form Factor: A Way to Test the Results

Considering the difficulties to rigorously compare computer simulation data with experiments, let us introduce the scattering form factor, $F(q)$. The asset of using the form factor is that

it can be computed from simulations and then compared with experimental 'model-free' measurements; the form factor is essentially primary data measured from experiments.

From our simulations we calculated the form factors as follow. First, the relative electron density profile $\rho_e(z)$ was computed by subtracting the electron density of bulk water from that of the simulated system, where z is the direction perpendicular to the bilayer. The scattering form factors were then calculated using Eq. 1.7. The form factors are plotted in Fig. 5.3 for the simulated pure and cholesterol-containing systems for both SOPC and OSPC membranes. Currently, no experimental data is available for such systems, but the obtained results could be validated in future experiments. However, form factor curves for simulated DOPC bilayers have been successfully compared to experimental data, sec Sec. 6.3.1. In Fig. 5.3 we can clearly see that the positions of the minima of $F(q)$ are correlated with the area per molecule: minima at smaller wave numbers q imply a smaller area per molecule [Pan08].

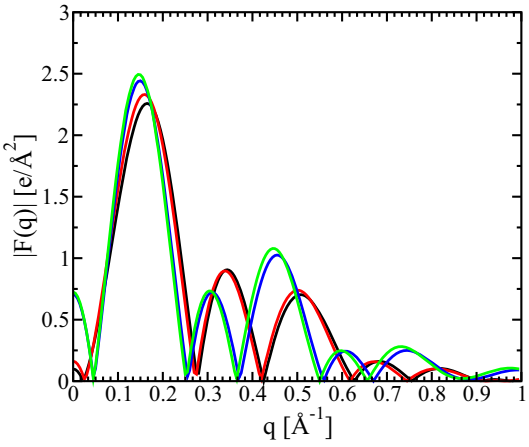

Figure 5.3: Form factors, $|F(q)|$, as a function of the wave number q for the simulated pure SOPC (black), pure OSPC (red), SOPC/CHOL (blue), and OSPC/CHOL (green) bilayers at 338 K.

5.3.6 Lipid and Cholesterol Rotational Motion

In this Thesis most of the attention has been focused on the structural properties of the membrane. However, dynamic properties are in membranes at least as important as the structural ones. Unfortunately, a reliable description of many dynamic properties is still severely restricted by the simulation time. As a result only a few fast modes can be correctly described from the present membrane simulation times, and from those very few can be validated to experimental data.

The rotational motions of the different lipid species can be studied by computing time-dependent autocorrelation functions (ACFs), see Sec. 3.3.8. Physically, ACFs measure how fast a molecule, or part of a molecule, rearranges its orientation as a response to changes in its surroundings. By means of the first Legendre polynomial ($C_1(\tau)$; Eq. 3.12) four different molecular fragments are examined: the headgroup, the two acyl chains, and the cholesterol plane.

For the PhdCho headgroup, we study the PN vector, see Sec. 3.3.8. This choice isolates the behavior of the interface from the complex intramolecular motion of the flexible PhdCho chains. Figure 5.4a shows the ACF for the PN vector in SOPC and OSPC membranes with and without cholesterol. Data for the reference systems, e.g. DSPC and DOPC, is also provided. The relaxation times are found to follow the same order with and without cholesterol. The saturated DSPC system has the longest relaxation time, whereas the di-monounsaturated DOPC system shows the fastest relaxation time. Systems containing OSPC and SOPC display very similar temporal correlation decays in between the two systems mentioned above. These results follow the same trends as found for the area per molecule. In all cases, the presence of cholesterol dramatically slows down the vector motion. Importantly, the ACF curves decay but reach a non-zero plateau value as $\tau \to \infty$, this reflects that the studied vector does not rotate freely in all directions. Although PN vector rotation in the xy-plane is basically unrestricted, the motion in the z-direction is restricted by its tilt angle $t_{P\mapsto N}$; namely, the vector is wobbling in a vertical cone with the average angle $t_{P\mapsto N}$. Values of angle, $t_{P\mapsto N}$, for different systems are close to 100°, and it is easy to prove that $C_1(\tau \to \infty) = \langle \cos^2(t_{P\mapsto N}) \rangle$. No qualitative differences are found for $t_{P\mapsto N}$ between the studied lipid species (see Table 5.1).

Similar behavior for the PN vector is also found for the glycerol vector, corresponding to the vectors joining atoms C1 and C3 (see Fig. 1.4a). The relaxation times are about twice larger than those for the PN vector, and the vector itself is much less tilted ($C_1(\tau \to \infty)$ ∼0.3, data not shown).

To study acyl chain rotation, we have focused on the vectors connecting $C3_2$ and $C3_{18}$, and $C2_2$ and $C2_{18}$ carbon groups for *sn*–1 and *sn*–2 chains, respectively. The correlation curves are shown in Figs. 5.4b and 5.4c. Plateau values for the acyl chains were directly related to their tilt angle provided in Table 5.1. Inspection of the correlation curves allowed us to make some clear conclusions. First, acyl chain vector rotation is restricted to a smaller tilt angle compared with PN vectors. In addition, the relaxation time is much shorter than for the PN vector. Second, the area per molecule is an important factor: the larger the area, the faster the decay. Third, double bond enhances rotational motion (see OSPC and SOPC in Figs. 5.4b and 5.4c), and increases the tilt angle. Fourth, for a given symmetric lipid (e.g. DSPC, DOPC), the correlation of *sn*–1 chain rotation is lost slightly faster than the *sn*–2 one. That is a consequence of the fact that *sn*–1 chains are inserted deeper into the bilayer. For the monounsaturated PhdChos study in this paper, the combination of the previous effects results in a large difference between the behaviors of the two chains in OSPC, whereas the decay for the two chains in SOPC are only moderately different (consequences of double bond presence are compensated by the *sn*–2 effect in SOPC). When mixed with cholesterol, the previous features are typically enhanced and, as general trends, rotational motion is slowed down and the plateau values are reduced due to the increase in chain ordering and the reduction in area per molecule.

Finally, in order to study the rotational modes of cholesterol molecules, we have chosen the vector between the cholesterol atom groups C6 and C11 (Fig. 5.4d). This choice accounts for the rotation of the rigid ring-system of the sterol molecule, see Sec. 3.3.8. For this mode, the ACF curves show the same correlation with the area per molecule as is observed for the PN rotation: when mixed with DSPC, cholesterol motion is slower than for DOPC. Motion of cholesterol in SOPC and OSPC present an intermediate behavior between DOPC and

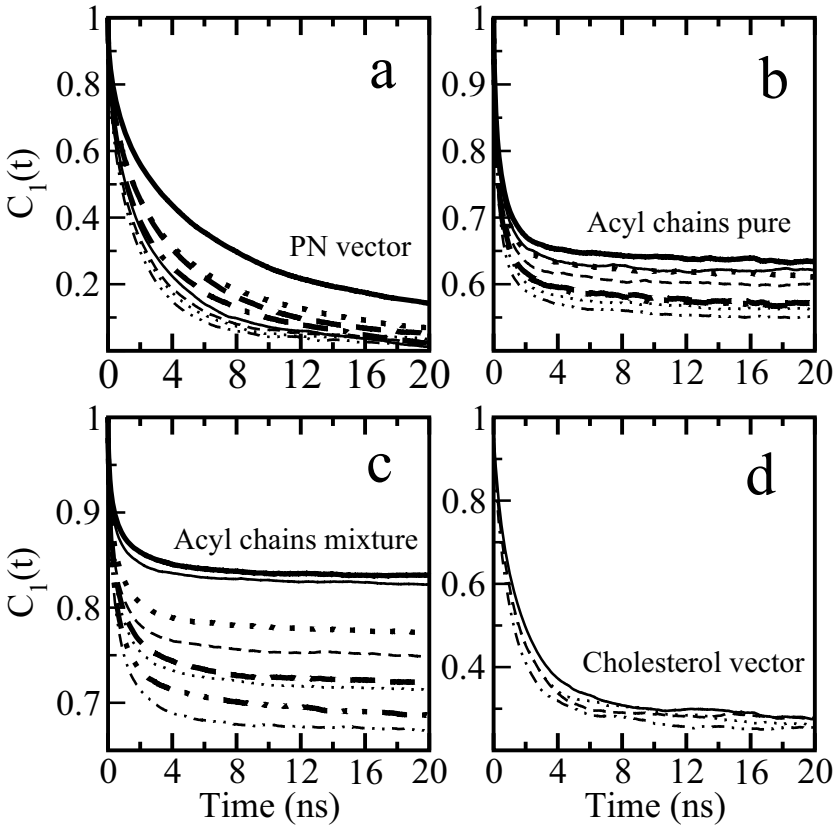

Figure 5.4: Auto correlation functions, $C_1(\tau)$, of the (a) PN vector; (b) $C_2 \rightarrow C_{18}$ vector of the two lipid chains in the pure systems; (c) $C_2 \rightarrow C_{18}$ vector of the two lipid chains in the cholesterol mixtures; and (d) C6→C11 cholesterol vector for the moieties DSPC (solid), OSPC (dotted), SOPC (dashed), and DOPC (dot-dashed). In panel (a) pure systems are represented by thin lines and binary systems by thick ones. In panels (b) and (c) thin lines correspond to *sn*–1 chains and thick ones to *sn*–2.

DSPC, and practically indistinguishable.

5.3.7 Chain Dynamics

To characterize the dynamics along the acyl chain, we computed the autocorrelation functions, $C_2(\tau)$, corresponding to the second associated Legendre function for each CH vector (not shown), see Eq. 3.13. This choice allows a straightforward comparison with NMR experiments [Lind01a, Murz01, Past02], although no data is still available for any of our systems. The information contained in the decay curves has been condensed by the extraction of the *ATC* parameter. The calculation procedure and additional details can be found in Sec. 3.3.8.

This property is inversely proportional to the rotational velocity of the studied carbon segment. We have plotted the obtained values for the chains of the positional isomers in pure systems in Fig. 5.5a, and for bilayers with cholesterol in Fig. 5.5b. Qualitatively, the curves display decays in a roughly exponential fashion in the carbon segments approaching the bilayer center (notice the logarithmic scale in Fig. 5.5). The slowest rotations (up to ∼1 ns) are found for the carbons close to the membrane/water interface, whereas the inner carbon groups in the bilayer center rotate much faster (10–20 ps). The latter is a

signature of the disordered nature of the hydrophobic region. Moreover, in systems with cholesterol we find larger correlation times as a signature of area reduction and increase of chain ordering. Although our aim is on comparing the two monounsaturated lipids with each other, it is noteworthy that the experimental values by NMR for DPPC [Brow83] show good agreement with the general behavior and the order of magnitude of the computed correlation times. Similar agreement is found with effective characteristic times computed from autocorrelation functions in simulations of polyunsaturated PhdChos [Olli07a]. In this last work they computed the effective characteristic times by integrating the ACF curve as is detailed in Sec. 3.3.8. We have also used this method in this work and the results were identical to those obtained by *ATC*.

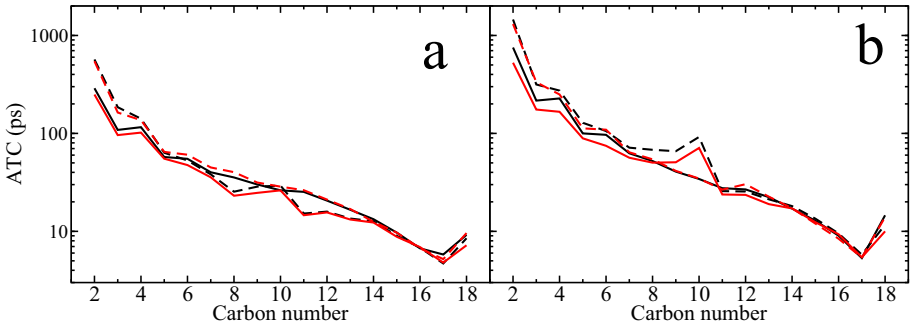

Figure 5.5: Average time constant (*ATC*) for the CH vectors in the *sn*–1 (solid) and *sn*–2 (dashed) acyl chains of SOPC (black) and OSPC (red). (a) Pure systems; (b) bilayers with cholesterol.

Looking at the curves in Fig. 5.5a (pure systems) we observe that the effect of a double bond consists of an enhancement of rotation of the neighboring methyl groups along the same chain (carbon numbers 8, 11, 12 and 13). The carbons involved in the double bond (9 and 10), however, are slower than their neighbors, but have similar relaxation times than the same carbon numbers in the saturated chain. On the other hand, in cholesterol-containing systems the effect is different, as can be seen from Fig. 5.5b. In that case, the methyl groups neighboring double bond carbons do not show enhancement in their rotational motion, and carbons involved in the double bond are significantly slowed down. For example, carbon 10 in the *sn*–2 chain of SOPC had ATC=91.98 ps whereas the corresponding carbon in the *sn*–1 chain has ATC=34 ps. This effect is more pronounced in the case of the unsaturated SOPC acyl chain, than in the case of corresponding OSPC chain: carbon 10 in the *sn*–1 chain of OSPC has ATC=71.0 ps whereas carbon 10 in *sn*–2 has ATC=34.0 ps. Therefore, cholesterol increases rigidity of the double bond region. It is interesting that this effect is stronger when the double bond is in the *sn*–2 chain (SOPC) than when placed in the *sn*–1 chain (OSPC), so that even though the area per molecule for SOPC/CHOL bilayers is larger than for OSPC/CHOL mixtures, the atoms involved in the double bond rotate much slower in SOPC/CHOL bilayers than in OSPC/CHOL systems. As a result, it seems plausible that the origin of the greater area per molecule for SOPC has its origin in the increased rigidity of the double bond region, which interacts weakly with the cholesterol ring.

	DSPC	OSPC	SOPC	DOPC
Pure bilayer	11.7	17.2	18.7	18.8
Mixed bilayer	3.21	7.95	7.08	11.1
Cholesterol	3.77	9.14	8.15	15.8

Table 5.2: Lateral diffusion coefficients ($\mu m^2/s$) for lipids in pure and mixed systems. Errors associated with diffusivities are ±14% in pure systems and ±10% in the mixed bilayers

5.3.8 Lateral Diffusion

As our final topic, we examine the lateral diffusion of lipid molecules in the bilayer plane by measuring the diffusion coefficient of their center of mass in the xy-plane, Eq. 3.11. For technical details see Sec. 3.3.8. The mean-squared displacements (MSD) for the PhdCho moieties are presented in Fig. 5.6. A linear regime is identified at long times for both pure and mixed systems. Slopes in the 20–30 ns period are computed to determine the lateral diffusion coefficients provided in Table 5.2. For mixed systems the diffusion coefficients of cholesterol molecules are also provided.

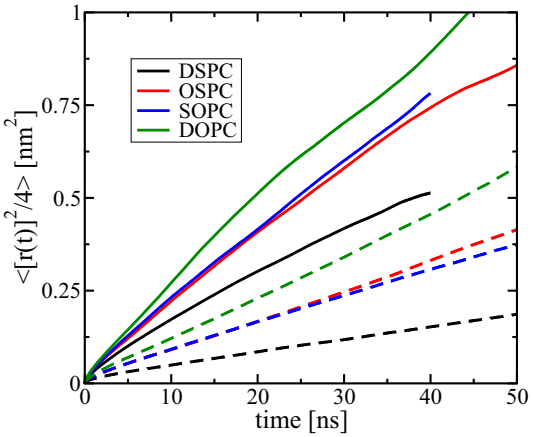

Figure 5.6: Temporal evolution of the mean-squared displacements in the xy-plane for the PhdCho moieties in the pure bilayers (solid lines) and in the mixed systems (dashed lines).

System specific comparison with experimental values is not possible since there is no experimental data for any of the studied lipids in the simulated conditions; in particular, no diffusion coefficients have been reported for OSPC and SOPC at any temperature. For DOPC, diffusion coefficients were measured by Filippov et al. [Fili03] at T=303 K (D=10 $\mu m^2/s$) and T=333 K (D=26 $\mu m^2/s$) using pulsed-field gradient NMR technique. In comparison, we find D=18.8 $\mu m^2/s$ for pure DOPC at 338 K. We run an additional simulation of DOPC at 303 K for 140 ns that yields D=6.8 $\mu m^2/s$. Both of our measured values are therefore in a good agreement with the available experimental data, although larger systems and longer times would be appropriate for better comparison. Considering diffusion to express Arrhenius type behavior, we estimated the activation energy for pure DOPC bilayers to be 25 kJ/mol. From their experiments, Filippov et al. [Fili03] estimated the barrier to be 27 kJ/mol.

On the basis of our experience, the reported error estimates for lateral diffusion coefficients determined from atomistic simulations are commonly too optimistic. This is largely due

to the practice to determine the diffusion coefficient from the early-time data in the MSD, where fluctuations are the smallest. As the definition for D indicates, the diffusion coefficient is well defined only at the long-time limit where the MSD is proportional to time. At short times, the exponent is less than one, and only above some characteristic time scale that is about 20 ns in the fluid phase, one finds the true diffusive behavior with an exponent of one. In practice this implies that one should find the regime where the MSD is proportional to t^1, and since this occurs at longer times, the fluctuations in the MSD data are also quite pronounced, increasing error bars for diffusion. Using our simulation data, we estimated the errors associated with lateral diffusion coefficients to be at least ± 10 %. Recent studies by Bockmann et al. are consistent with this view [Bock03]. When reasonable error estimations are taken into account, see Table 5.2, the diffusion coefficients of SOPC and OSPC are indistinguishable. Nonetheless, what we could conclude reliably was the trend of diffusion rate for increasing disorder: as the PhdCho moieties contain more double bonds, their lateral diffusion increases. The same feature is found in mixed systems with cholesterol. In the latter systems it was additionally found that cholesterols diffuse slightly faster that the surrounding lipids. Due to limited statistics of the above results, we stress the importance of considering lateral dynamics more carefully in future studies when long-time scale simulations will be more feasible.

5.4 Discussion and Conclusions

We have described and discussed atomistic simulation results for two glycerol-based phospholipids, SOPC and OSPC, which differ in a seemingly minor manner: the only difference is the position of an individual double bond. In SOPC the double bond is located in the *sn*–2 chain, like in many abundant lipid types [Van 65, Romi72, Cron75, Sait77], while in OSPC it is instead placed in the *sn*–1 chain. Despite this subtle difference, nature prefers double bond(s) to be placed in the *sn*–2 chain for reasons that have remained largely unknown.

Our simulations show small but consistent differences between the properties of the membranes characterized by the two positional isomers, in agreement with the available experimental data. SOPC, having the double bond in the *sn*–2 chain, is more disordered than OSPC, and the results of all the physical properties we explore —both structural and dynamical— are consistent with this finding. Further, in mixed systems with cholesterol, the differences between the SOPC and OSPC systems become even larger, suggesting that the location of the double bond in monounsaturated glycerol-based phospholipids really makes a difference. Although the differences between SOPC- and OSPC-based systems are essentially small, differences of similar order of magnitude were discussed and successfully interpreted in the experimental literature. For example, the results for S_{CD} profiles show that the differences between SOPC/CHOL and OSPC/CHOL systems can be as large as 10 %, or even more.

The origin of the differences in membrane properties between the two positional isomers is obviously of particular interest. Results of our simulations suggest that acyl chain length mismatch is the relevant factor to take into account. We show that the average positions along the z-axis of the terminal *sn*–1 and *sn*–2 carbon atoms differ even in lipids with symmetric chains. In DSPC and DOPC bilayers we find a chain mismatch of 0.40 and 0.28 Å, respectively. The chain mismatch changed substantially in lipids with different acyl chains:

OSPC shows a chain mismatch of 0.56 Å while for SOPC this value is 1.32 Å; that is, we find a difference of almost 2 Å between the two monounsaturated species that are identical except for the position of the double bond. For comparison, the carbon-carbon distance in hydrocarbon chains is about 1.5 Å. Experimental studies on monolayers built of highly asymmetric lipids such as 18:0–8:0 PhdCho, and their comparison to symmetric ones such as 18:0–18:0 PhdCho, have also shown that chain asymmetry is a strong disordering factor [Ali98].

One of the most interesting questions arising from this work is why the presence of cholesterol increases the observed differences between SOPC and OSPC bilayers. In the previous chapter we have proven that the effects of a double bond depend on its position in the acyl chain, particularly when cholesterol is present. We showed that the ordering and condensing effects of cholesterol were the lowest when the double bond was located in the middle of a chain, close to the cholesterol off-plane methyl group C18. Thus, interference of the double bond with the methyl group C18 seemed to be responsible for the decrease of cholesterol condensation and ordering effect in the bilayer, see Sec. 4.3.8. Since, on average, the double bond in SOPC is placed closer to the cholesterol methyl group than the one in OSPC, the more disordered nature of the SOPC bilayer with respect to the OSPC bilayer is evident when cholesterol is around.

In conclusion, the simulations outcome suggests that the natural selectivity for the Phds positional isomers —*sn*–1 saturated and *sn*–2 unsaturated— is the result of the evolutionary preference by the cell for those positional isomers which enhance the membrane disorder. Furthermore, this preference is based not only by the properties of the lipid itself, but also by its differential interaction with other membrane components, in particular cholesterol.

CHAPTER 6

Influence of *Cis* Double Bond Parameterization on Lipid Membrane Properties

6.1 Objective and Summary

Membrane simulations by MD have become popular during the last two decades and several membranes composed of different lipid moieties and proportions have been studied. However, the number of studies focused on ensuring the quality of the used molecular description (force filed) has been far more limited. In general, most of the MD community working on biomembranes relies on a few excellent works on parameterization, normally optimized for very specific molecules. For example, the force field used in this work for the PhdChos was originally optimized only for the saturated DPPC lipid [Tiel96]. As a result, before conducting a simulation containing different lipids from those already parameterized, one must parameterize them first. The parameterization process from scratch is normally discarded in practice since it is very time consuming. Instead, most of the authors, including ourselves, assume some portability in the parameters allowing the study of lipids with minor molecular structural changes from those already parameterized. Unfortunately, the consequences of such assumptions are not always predictable.

As the reliability of MD simulations crucially depends on the interaction potential (force field), which determines the final system properties, one has to consider the possible model limitations [Tiel97]. The quality of the force field is the decisive factor, since seemingly tiny details can cause rather drastic changes in membrane properties. Therefore, as the previous two chapters explore the changes in membrane properties induced by the double bonds in unsaturated lipids, special effort was put to contrast the accuracy of the used parameters to describe the double bond and its surroundings.

In this chapter we show that the description of a double bond in a lipid hydrocarbon chain is a subtle matter. At the time where the simulations in chapters 4 and 5 were performed, some of the available force fields for lipids parameterized the *cis* double bond as a simple improper torsion (which dictates the planarity of the double bond region) together with non-clear small corrections for the adjacent dihedrals (see, for example the "GROMOS87",

Ref. [Tiel02]). Also at that time, by means of *ab initio* calculations of small molecules like *cis*–2–hexen, Bachar et al. [Bach04] developed another set of force field parameters to describe the double bond region (the one used in our simulations), accounting for *skew* states in the vicinity of the double bond for polyunsaturated Phds. Though it is likely that different descriptions of the double bond give rise to quantitatively somewhat different membrane properties, in particular in the hydrophobic region of a membrane [Niem06, Olli07a], the actual relevance of this issue has remained unclear.

In this chapter we study the importance of double bond parameterization. We employed atomistic MD simulations to determine the effect of the double bond description in di-monounsaturated PhdCho membranes. Both single lipid and binary mixtures with 20 mol% of cholesterol were considered. We compared different schemes for the double bond by varying systematically its position along the lipid hydrocarbon chains, see Sec. 4.2. The results give rise for concern: they indicate that the double bond description changed not only the quantitative but also the qualitative trend of membrane behavior. We find that the description which accounts for *skew* states shows a maximum in the area per lipid when the double bond resides at the middle of an acyl chain in agreement with experimental data on the main transition temperature T_m [Wang95, Mars99]. The description that does not accommodate *skew* states, however, predicts a monotonically decreasing area per lipid as the double bond is shifted from the glycerol backbone to the end of an acyl chain. Further data for other structural properties is consistent with this finding.

The results highlight the importance of describing double bonds in a realistic manner, as we did in our simulations. If the double bond description is too simplistic, artifacts may arise if the role of double bonds is important for the property that is being analyzed. In our case, we find that the force field that does not account for *skew* states in the vicinity of a double bond yields results that are not only quantitatively but also qualitatively incorrect with respect to experimental findings reported in the previous chapters.

The research described in this chapter resulted in the publication [Mart08a] included in this Thesis.

6.2 Descriptions of Simulated Systems

To test the two different double bond parameterizations (GROMOS87 [Tiel02] and Bachar [Bach04]), side-by-side, we apply both parameterizations in 14 different bilayers, corresponding to the di-monounstaurated systems where the double bond position is systematically moved along the chain (see Sec. 4.2 and Fig. 6.1), totaling 28 simulations. For each pair, we used identical initial configurations such that the only difference was in the description of the double bond. This allowed us to monitor how the systems behaved due to different parameterizations, and how the differences are reflected in the physical observables of the pure (7 systems) and mixed 20 mol% of cholesterol (7 systems) bilayers.

In the first set of simulations, we used the double bond description by Bachar et al. [Bach04] which explicitly describes the *skew* states of saturated bonds next to a double bond. Given that an accurate description is of particular importance in the case of polyunsaturated lipids [Gros06, Niem06, Olli07a], Bachar et al. derived their parameters from *ab initio* calculations. The other set of simulations was performed by using the standard double bond parameters of

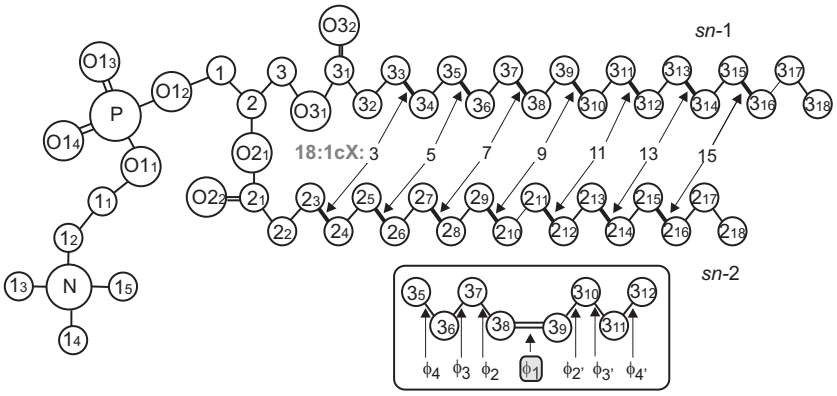

Figure 6.1: Molecular structure and numbering of atoms of the PhdCho molecules used in our simulations. The unsaturated bonds are marked and numbered in both chains. In the inset, the dihedral angles (ϕ_i) affected by the double bond parameterization are shown for the *sn*–1 chain of *d*18:1c9 (DOPC) moiety. The chemical symbol for carbon atoms, C, is omitted.

the GROMOS87 force field [Tiel99, Tiel02], that does not account for the *skew* states.

To analyze the differences between the two parameterizations, we considered the dihedral angles ϕ_1, ϕ_2, ϕ_3, and ϕ_4 close to the double bond (in Fig. 6.1, these dihedrals are marked for DOPC). Figure 6.2 depicts the normalized probability distributions of dihedral angles for both force fields for the case of a pure DOPC bilayer (other moieties in pure and mixed bilayers yield similar behavior). When the two double bond descriptions are compared each other, the dihedral next to the double bond (ϕ_2) is significantly modified. ϕ_3 displays only a rather small change, whereas ϕ_1 and ϕ_4 are mostly unaltered. The GROMOS87 force field [Tiel99, Tiel02] keeps the ϕ_2 dihedral in a rather fixed *trans* configuration (180°), whereas the parameters of Bachar et al. allow for a more flexible and dynamic configuration between the two maxima at -120° and 120°. Therefore, Phds whose parameterization accounts for the *skew* states give rise to a less packed configuration and more extended torsions.

Other parameters are also available like those provided by OPLS (Optimized Parameters for Liquid Simulations) united atom force field [Jorg88] which uses an alternative description of double bonds. This parameterization leads to a broad distribution of ϕ_2 angles between 60° and -60° (range of angles equivalent to *skew* states) but with a maximum at 180° [Murz01, Rog06]. In this study we did not test this parameterization due to the rather limited usage of this force field in current membrane simulations.

Finally, let us briefly discuss a technical matter related to the double bond parameterization by Bachar et al. The force field for the double bond region in Ref. [Bach04] was developed for a diunsaturated hydrocarbon region where two double bonds were separated by an individual single bond. In our study, however, the acyl chains are monounsaturated. To confirm that the description of Ref. [Bach04] can be exploited in our model, we performed *ab initio* calculations using Gaussian03 with two basis sets (B3LYP/6–31G(d) and B3LYP/6–31G**) for *cis*–4–octene, which included a single double bond. For this molecule, we focused on the dihedral potential next to the double bond since that potential is the most sensitive one. Both basis sets yield similar potentials [1] whose qualitative nature is in line with the

[1] In the original paper by Bachar et al. [Bach04] there is a typographical error in the potential of ϕ_2. The correct one is $V(\phi_2) = -5.685 + 7.470[1 + \cos(\phi_2)] + 3.900[1 + \cos(2\phi_2)] + 1.100[1 + \cos(3\phi_2 - 180)])$

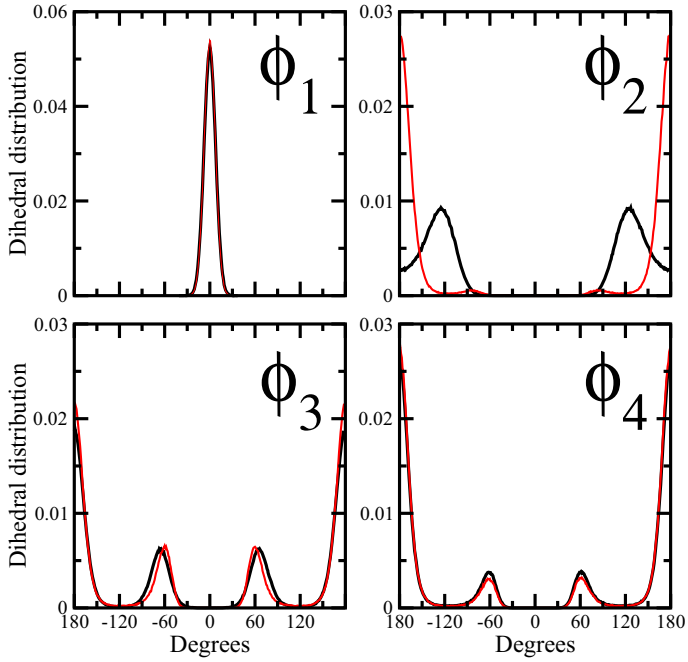

Figure 6.2: Dihedral angle distributions for the dihedrals ϕ_1 (double bond), ϕ_2, ϕ_3, and ϕ_4 shown for the *d*18:1c9 moiety (DOPC). The black lines correspond to the force field by Bachar et al. [Bach04] that accommodates *skew* states, whereas the red curves result from the force field parameterization [Hess97, Tiel02] that does not account for such states.

results reported in Ref. [Bach04]. The minor quantitative difference in the barrier height results from the different test molecules used in Ref. [Bach04] and our study. Nonetheless they indeed yield identical angle distribution profiles.

6.3 Structural Changes Due to the Parameterization

In order to compare the performance of both parameterizations we have computed some relevant membrane properties. From all membrane properties, the average area per lipid in the membrane plane is the most commonly used to characterize packing as well as structure of lipid bilayers. We calculate the average area per PhdCho by dividing the total area of the simulation box by 64, the number of PhdCho molecules in a single leaflet, A_{PC}. Figure 6.3a shows that the area per molecule is significantly higher for the systems where the parameterization accounted for *skew* states. This finding is in agreement with the behavior of the dihedral angle ϕ_2.

It is worthwhile to note two important features from Fig. 6.3a. First, the change in the area per molecule extends up to 0.06 nm^2 which is surprisingly large considering that this change can be attributed to a single dihedral angle. Such a strong effect was also observed by the developers of the force field [Bach04], although in their case only one lipid type was explored. Second, changes are not systematic but rather system dependent resulting in a different qualitative behavior with respect to the location of the double bond. The force field by Bachar et al. yields a maximum in the area per molecule for the *d*18:1c9 PhdCho bilayer [Mart07] in agreement with experiments (see below). The presence of cholesterol in

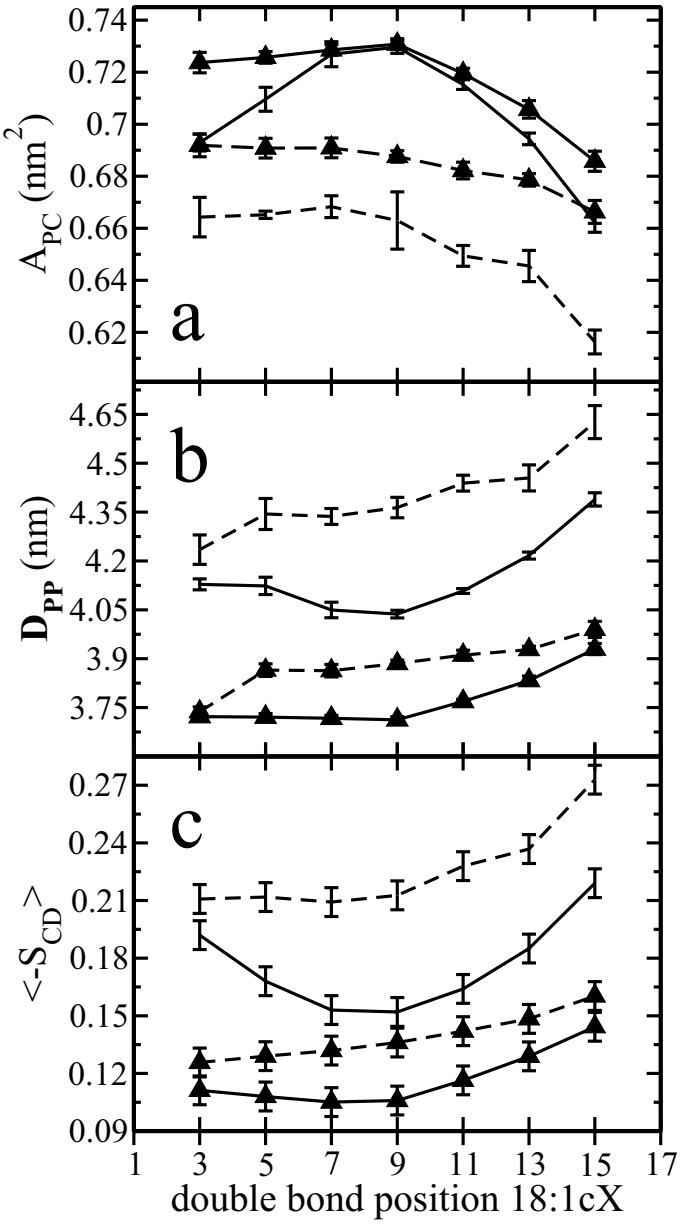

Figure 6.3: (a) The area per PhdCho, (b) the membrane thickness, and (c) the average values of the $\langle -S_{CD} \rangle$ order parameter shown as a function of double bond position. The solid lines correspond to the force field parameterization by Bachar et al. whereas the dashed curves stand for the parameterization that does not account for *skew* states. Results are shown for both pure PhdCho bilayers (triangles) and PhdCho/CHOL mixtures (lines without symbols).

the PhdCho/CHOL system increases this maximum even further [Mart08b].

The force field that does not account for *skew* states produces an area per molecule that increases monotonically as the double bond position is translated from the end of an acyl chain towards the headgroup. This behavior is found in both pure PhdCho and mixed PhdCho/CHOL bilayers. The largest differences between the two force field descriptions are found for PhdCho/CHOL systems when the acyl chains of PhdChos have a double bond at the central part of the chain. This is due to the fact that the ϕ_2 dihedral is in these cases interacting with the most rigid part of the cholesterol ring system and also with one of the off-plane methyl groups [Mart08b]. Above, we pointed out the agreement between our results and the experiments reported in Refs. [Wang95] and [Mars99]. Being more specific, these calorimetric experiments showed that the main phase transition temperature for lipids with monounsaturated acyl chains is the lowest when the double bond resided at the middle of a chain. We find that the area per lipid is the largest when the double bond is located in the chain's center. As suggested in Sec. 4.3.1 both properties usually present an inverse correlation.

To gain more insight into the transverse structure we also calculated the thickness of the bilayers by considering $\mathbf{D_{PP}}$, see Sec. 3.3.2. Figure 6.3b shows the resulting membrane thicknesses as a function of the double bond position. We find that the results express similar features as the area per lipid discussed above. The force field by Bachar et al. yielded a non-monotonic behavior with a minimum in the *d*18:1c9 bilayers. This behavior is enhanced in the presence of cholesterol. The other force field that does not accommodate *skew* states, on the other hand, predicts membrane thickness to increase monotonically as the double bond is shifted from the glycerol group region to the end of an acyl chain. Changes in membrane thickness due to the *skew* states are also rather pronounced. In particular in the PhdCho/CHOL systems the changes are as large as 0.4 nm. Thickness changes of this size have been shown to alter the functioning of some membrane proteins [Kill98].

To conclude the comparison, we analyze the deuterium order parameter S_{CD} along the acyl chain that accounts more directly for the membrane molecular ordering in the hydrophobic region. Additionally, this property can be also measured accurately from NMR experiments [Davi83a], so we expect future experimental validation of the present results. The $\langle -S_{CD} \rangle$ mean values (averages over the saturated segments) for the *sn*–2 PhdCho acyl chains are plotted as a function of the double bond position in Fig. 6.3c. For the force field by Bachar et al., we find a minimum in the $\langle -S_{CD} \rangle$ curves when the double bond resided at the middle of an acyl chain. This is in agreement with the above discussed behavior for the area per lipid. The minimum is particularly evident in the PhdCho/CHOL systems where the interplay between the double bond and the rigid steroid structure enhances the effect. The force field that does not account for the *skew* states is again qualitatively different from the above. Instead of showing a minimum, $\langle -S_{CD} \rangle$ increases monotonically as the double bond is translated towards the end of the acyl chain.

6.3.1 DOPC is Better Described by New Parameterization

In the previous section we have clearly seen that both parameterizations lead to not only quantitative but also qualitatively different results. However, the statement of which force field describes better the real properties of the membranes was not totally clarified. The comparison

with experiments is less straightforward to conduct, since Refs. [Wang95] and [Mars99] are the only ones dealing with effects due to varying location of a double bond in monounsaturated acyl chains. Consequently, the comparisons between simulations and experiments are mainly focused on pure DOPC membranes due to the available experimental data.

Already in Sec. 4.3, we have shown that DOPC simulations using Bachar's parameterization are in very good agreement with the available experimental data. Hereafter, however, we will focus on comparing with more detail the results obtained from both parameterizations. We start describing the area per lipid as one of the basic parameters defining membrane properties. Experimental data based on X-ray diffraction techniques for fully hydrated DOPC bilayers have resulted in values of 0.721– 0.725 nm^2 for the area per lipid [Nagl00, Liu04, Petr04] while the force field in Ref. [Bach04] yields 0.731 nm^2. Meanwhile, the force field that does not account for *skew* states leads to an area of 0.688 nm^2 per DOPC molecule. Additionally, the membrane thickness determined from electron density profiles [Nagl00, Liu04, Petr04, Hung07] varies between 3.67 and 3.71 nm, while the force field with *skew* states results in a value of 3.71 nm and the other one yielding a thickness of 3.89 nm. The comparison here is in favor of Bachar's parameterization. This conclusion requires more supporting evidences.

As an additional criterion to judge the merits of the two force field descriptions, consider Fig. 6.4. It shows the S_{CD} order parameter profile along the *sn*–2 acyl chain for DOPC (*d*18:1c9), where the double bond resides at the middle of the acyl chains. The fact that the two double bond parameterizations yield different quantitative results is not a surprise, since the average areas are also different. What is more striking is the different qualitative behavior close to the double bond (carbons 10–12). For comparison, Warschawski and Devaux [Wars05] have reported NMR data for lipid chain ordering in fluid DOPC membranes at 310 K. They found that the chain order parameter has an absolute minimum at the carbon position 10 followed by a minor increase for the carbon 11. This behavior is consistent with the simulations where *skew* states are taken into account. For the other force field without *skew* states, however, the S_{CD} profile for carbons 10–12 is substantially different. A full comparison with experiments is difficult to make due to the different temperatures used in experiments (310 K) and our simulations (338 K). The comparison is even more difficult due to the fact that the order parameter values reported in Ref. [Wars05] are based on ^1H–^{13}C dipolar couplings which provides systematically smaller values compared to ^2H methods like ours (see discussion in Ref. [Wars05]). Despite this difficulty, the qualitative nature of the order parameter data for carbons 10–12 is in favor of the force field that accounts for the *skew* state.

Finally, considering the difficulties to rigorously compare simulation data with experiments, we used the scattering form factor, $F(q)$, to confirm that the *skew* state makes the difference in the DOPC force field. The goodness of the form factor is that it is essentially primary data measured from experiments and can be easily computed from simulations, see Sec. 1.6.2. Unfortunately, experimental data for the form factors was only available at 303 K. In order to avoid the problem of comparing data corresponding to membranes at different temperatures, additional shorter simulations were conducted for DOPC (*d*18:1c9) at 303 K. They were simulated over a period of 60 ns using the same protocol as described in Sec. 3.2. Only the last 40 ns were used for analysis. In Figure 6.5, the form factors are plotted for the simulated pure DOPC membranes using the two force fields at 303 K. The data extracted from the experimental form factor in Ref. [Pan08] is also plotted for comparison. The results indicate a

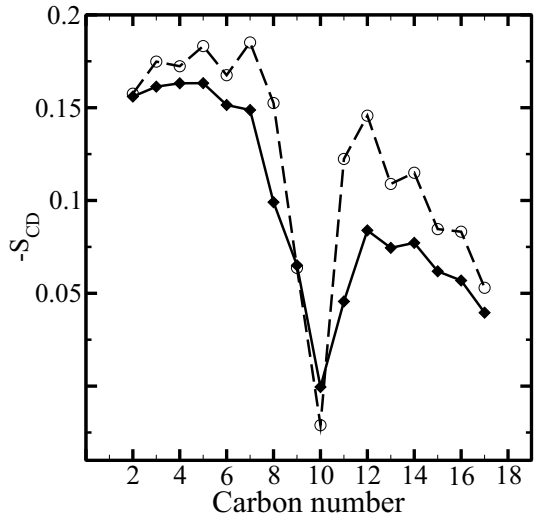

Figure 6.4: The S_{CD} order parameter profile for the *sn*–2 chain of DOPC (*d*18:1c9) with the two different double bond parameterizations. Carbon numbers follow the notation in Fig. 6.1. The solid lines correspond to the force field by Bachar et al. that accommodates *skew* states, whereas the dashed curves result from the force field parameterization that does not account for *skew* states.

better agreement between the experimental scattering form factor [Pan08] and the simulation using a force field that accounts for the *skew* state. The performance of the DOPC force field where the *skew* state is not included is substantially weaker.

Summarizing, comparison of DOPC simulations with experiments allows us to conclude that the force field including the *skew* states describes the double bond substantially better than the force field that does not take them into account.

6.4 Discussion and Conclusions

Force field parameterization is a complex issue since there is no a unique force field for any given system. It has been found that certain interactions are particularly important in the sense that seemingly minor changes in their parameterization may have a pronounced influence on system properties. In soft and biological matter, these are typically electrostatic interactions and hydrogen bonds, since they are the strongest interactions with respect to thermal energy. A number of lipid membrane studies have shown that these concerns are justified [Patr03, Patr04, Sonn07].

As van der Waals interactions in the hydrophobic core of a membrane are considerably weaker than electrostatic interactions, one usually assumes that the parameterization of hydrocarbon chains is a matter of less concern. In this chapter, however, we have questioned this point of view by considering the treatment of double bonds in atomistic MD simulations of unsaturated lipid membranes. We have found that changes in the double bond parameterization lead to quantitative differences in membrane properties. What is considerably more surprising is the fact that the different double bond descriptions lead to results that are also qualitatively different.

The studied membrane systems were comprised of PhdCho lipids with di-monounsaturated

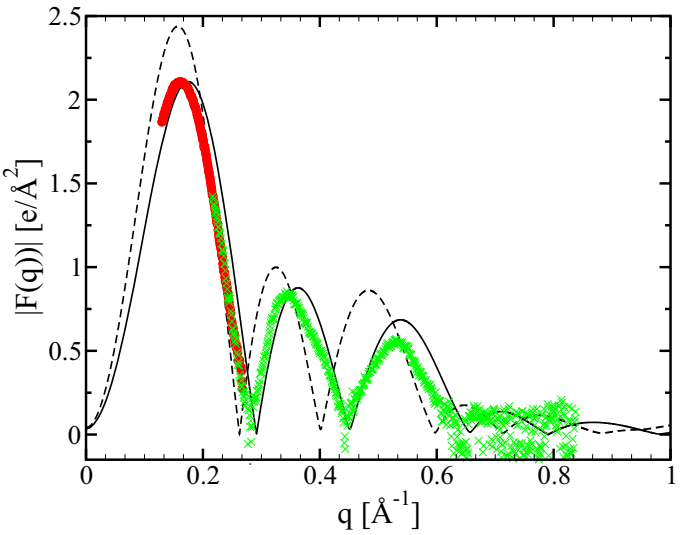

Figure 6.5: Absolute form factors as a function of the wave number q for the simulated pure DOPC bilayers at 303 K. The two cases shown by the solid and dashed lines correspond to the force field parameterization by Bachar et al. and the parameterization that does not account for the *skew* states, respectively. Solid red circles and green crosses correspond, respectively, to the experimental ULV and ORI experimental data for DOPC at also 303 K (for more details, see Ref. [Pan08]).

acyl chains. As it was done in Sec. 4.2, the location of the double bond is displaced along the acyl chains and different membrane properties were analyzed. This study has been performed using two different parameterization descriptions for the double bond in the unsaturated lipid chains, the old GROMOS87 [Tiel02] and the new by Bachar et al. [Bach04]). The force field that accounts for *skew* states predicts that the membrane is most disordered when the double bond resides in the center of the acyl chain. This is manifested as a maximum in the area per lipid and a minimum in the thickness and the S_{CD} order parameter profile for DOPC membranes. This behavior is consistent with experimental findings [Wang95, Mars99], which show the main phase transition temperature of single-component lipid bilayers to have a minimum under similar conditions. Meanwhile, if the force field does not accommodate *skew* states next to the double bond, similar non-monotonic behavior (and a minimum or maximum) in area per lipid and S_{CD} is not observed.

When cholesterol is added to the system, the trends discussed above become even more pronounced suggesting that the proper description of double bonds becomes increasingly important in many-component membranes, where the interplay of different molecule types becomes relevant. The non-monotonic behavior in the area per lipid observed mainly in mixed PhdCho/CHOL bilayers has been proposed in this Thesis to explain the natural preference for lipids with double bonds located in the middle of the stearyl acyl chains [Mart08b]. As far as molecular models are concerned, this effect is only obtained when the force field accommodates *skew* states.

CHAPTER 7

Cholesterol Induces Specific Spatial and Orientational Order in Cholesterol/PhdCho Membranes

7.1 Objective and Summary

Cholesterol is the most common lipid component in animal cell membranes [Ohvo02]. Experimental and theoretical studies have shown that cholesterol has the tendency to form regularly distributed lateral structures [Ali07, Chon09] in membranes. On the macroscopic level they are related to the L_o phase (see Sec. 1.4), but the actual atomic-level lipid organization and the associated physical mechanisms responsible for this organization have remained unclear. Conceptual models like the **Condensed Complex** model [Radh05] (based on low-energy Phd-CHOL complexes), the **Superlattice** model [Chon94a] (based on the existence of extended ordered distributions) and **Umbrella** model [Huan99] (based on the fact that cholesterol have a small hydrophilic headgroup which cannot shield from water its big hydrophobic ring) have been proposed for describing the formation of these structures (see Sec. 1.5), but they are not able to differentiate cholesterol from other sterols. There is, however, an increasing amount of evidence that the organizing mechanisms are specific to the structure of cholesterol. This view is supported, for example, by the fact that cholesterol and the structurally very similar ergosterol [Czub06] are known to enable formation of rafts, while many other sterols lack this capability [Li03, Wang04, Aitt06, Vain06, Rog08b].

Despite numerous experimental and simulation studies detailing cholesterol's unique ability to induce order in membrane while preserving significant in-plane motion. Very few studies have focused in the in-plane membrane structure emerging from the interactions of cholesterol with other lipids in the cholesterol-rich domain, which has remained unresolved [Rog08b, Berk09, Pand09]. Therefore, here we focus on the nanoscale lateral organization of cholesterol-containing membranes.

In this chapter we show how the specific molecular structure of cholesterol determines the lateral lipid organization. In particular, we observe that the presence of a smooth (α-face) and rough (β-face) face in the cholesterol ring (see Fig. 7.1) is critical to induce such ordering. To do this we performed atomistic Molecular Dynamics simulations of different membranes

composed of various cholesterol concentrations and either saturated (DSPC) or unsaturated (DOPC) phospholipids. Additional simulations with a cholesterol-like sterol lacking the methyl groups on the β-face (DCHOL, see Fig. 7.1b) were also carried out to determine the particular effects of the off-plane methyl groups. The main results of this work were to observe that the cholesterol molecules preferentially locate in the second coordination shell ($\sim$1 nm), thus avoiding direct CHOL-CHOL contacts, and that the cholesterol off-plane methyl groups induce a three-fold symmetrical arrangement of proximal cholesterol molecules. The distribution of relative orientations between two cholesterol molecules separated by a single lipid molecule displays a clear non-random pattern that is revealed by the existence of preferred relative CHOL-CHOL orientations. In all these findings, the role of the cholesterol off-plane methyl groups is observed to be fundamental. The biological significance of our findings is discussed in this chapter especially in the concluding section 7.9.

7.2 Descriptions of Simulated Systems

In order to precisely describe the environment surrounding the cholesterol molecule and to analyze how this environment depends on the concentration of cholesterol, we performed a total of 13 atomistic Molecular Dynamics simulations of membrane systems containing either the fully saturated DSPC or di-unsaturated DOPC mixed with 10, 20, 30, 40 and 50 mol% of cholesterol in the fluid phase (338 K). For comparison, additional simulations were performed with 20 and 40 mol% *flat cholesterol* (DCHOL) [Rog07a, Poyr08], whose structure corresponds to that of cholesterol with the C18 and C19 methyl groups removed. Figure 7.1b shows the structural differences between cholesterol and DCHOL. Each membrane contained 128 PhdChos and the corresponding number of sterol molecules (14, 32, 56, 86 and 122), see Table 7.1 for the exact composition of each system.

First, we constructed a DOPC membrane containing 50 mol% of cholesterol starting from a membrane containing four lipids and four cholesterols in each leaflet. To minimize artificial ordering, cholesterol molecules were randomly rotated in the DOPC matrix. This patch was replicated 4x4 in the membrane xy-plane. Next, 6186 water molecules were added to the system. The final configuration of a 10 ns simulation was used as a starting configuration for the DSPC system with 50 mol% of cholesterol. The same configuration was used for DOPC with 40 mol% of cholesterol after randomly removing the appropriate number of cholesterol molecules. To construct the other bilayers this procedure, of removing cholesterol molecules until the desired concentration is reached, was repeated. The simulation times of each system totaled 200–300 ns including 20 ns of equilibration. The total simulated time exceeded 3 μs. Simulation details are fully described in Sec. 3.2.

7.3 Structural Membrane Properties

In this section we will provide a general overview of the properties of the simulated membranes. As many of the findings were already discussed in chapter 4, here we mainly focus in the changes of the membrane properties as a function of the cholesterol concentration. The values of the analyzed properties are summarized in Table 7.1.

To begin with, we focus our attention in the area per molecule, see Fig. 7.2. The differences

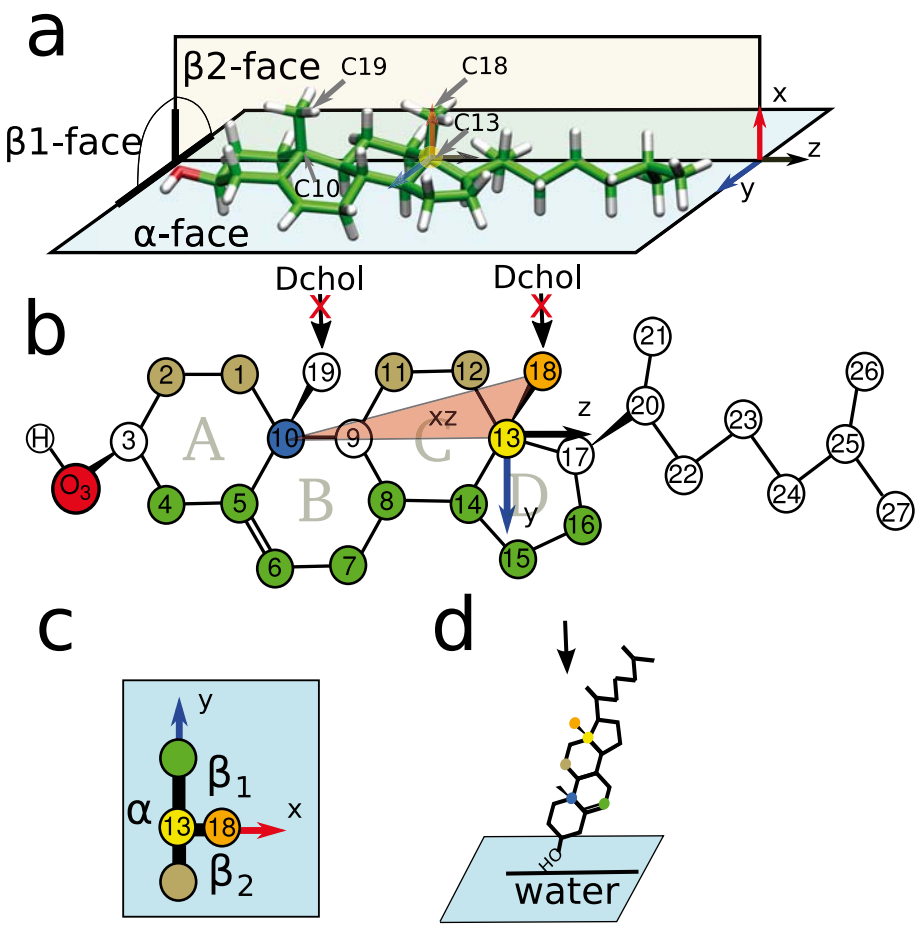

Figure 7.1: Panel (a) shows the three-dimensional structure of cholesterol. The positions of cholesterol's flat α-face and the rough β1- and β2-subfaces due to the two off-plane methyl groups C18 and C19 are shown. Panel (b) provides the numbering of the carbon atoms. Panels (a) and (b) show the reference axes used in Sec. 7.5. The origin of the axis is C13 colored in yellow. The vector between C13 (yellow) and C18 (orange) points along the x-axis. The triangle between C18 (orange), C13 (yellow) and C10 (blue) is in the xz-plane and is depicted in red. This plane divides the molecule between the β1-face $y >0$ and β2-face $y <0$. The atoms of cholesterol which belong to the β1-face are shown in brown, while those in the β2-face are colored in green. Panel (c) shows a schematic view of cholesterol as a projection in the reference xy-plane from the terminal acyl chain towards the head as shown in Panel (d) by the arrow. This schematic view is used in sections 7.5, 7.7 and 7.8. The other sterol analyzed in this chapter, DCHOL, is obtained by the removal of the off-plane methyl groups C18 and C19 as shown in Panel (b).

		CHOL					DCHOL	
Bilayer	Pure	10	20	30	40	50	20	40
num. PhdCho	128	128	128	128	128	128	128	128
num. sterol	0	14	32	56	86	122	32	86
χ_c (mol%)[a]	0.0	9.9	20.0	30.4	40.2	48.8	20.0	40.2
num. water	3941	6186	6186	6186	6186	6186	3806	6186
length (ns)	100	240	322	352	326	327	280	232
	110	**232**	**330**	**310**	**348**	**300**		**192**
A_{box} (nm^2)	42.844	41.479	39.901	39.233	42.488	48.277	40.757	39.964
	46.70	**46.67**	**46.63**	**47.06**	**49.21**	**53.39**		**50.25**
A_{PC} (nm^2)	0.669	0.648	0.623	0.613	0.664	0.754	0.637	0.624
$\pm$0.003 nm^2	**0.731**	**0.729**	**0.729**	**0.735**	**0.769**	**0.834**		**0.785**
A^*_{PC} (nm^2)	0.669	0.622	0.566	0.514	0.500	0.489	0.590	0.501
	0.730	**0.700**	**0.662**	**0.617**	**0.579**	**0.541**		**0.629**
A^*_{CHOL} (nm^2)		0.250	0.230	0.215	0.215	0.223	0.181	0.166
		0.282	**0.268**	**0.254**	**0.246**	**0.244**		**0.204**
$\mathbf{D_{PP}}$ (nm)	4.01	4.27	4.60	4.94	4.97	4.87	4.51	5.05
$\pm$0.01 nm	**3.71**	**3.85**	**4.03**	**4.24**	**4.40**	**4.45**		**4.25**
$\mathbf{D_{OO}}$ (nm)		3.33	3.60	3.90	3.96	3.95	3.50	4.03
$\pm$0.01 nm		**2.92**	**3.14**	**3.39**	**3.58**	**3.70**		**3.39**
$\mathbf{D_{PO}}$ (nm)		0.47	0.50	0.52	0.50	0.46	0.51	0.506
$\pm$0.01 nm		**0.46**	**0.44**	**0.43**	**0.41**	**0.38**		**0.43**
$\mathbf{D_{HH}}$ (nm)	3.82	4.12	4.53	4.85	4.89	4.77	4.34	5.02
$\pm$0.03 nm	**3.44**	**3.74**	**3.83**	**4.11**	**4.22**	**4.28**		**4.24**
V_{PC} (nm^3)[b]	1.351	1.344	1.330	1.309	1.3043	1.3166	1.351	1.3350
	1.346	**1.341**	**1.336**	**1.331**	**1.330**	**1.336**		**1.374**
$\langle -S_{CD} \rangle$								
sn–1	0.151	0.193	0.256	0.339	0.363	0.358		0.3788
	0.106	**0.124**	**0.152**	**0.191**	**0.227**	**0.252**		**0.201**
sn–2	0.154	0.194	0.259	0.340	0.363	0.359		0.379
	0.106	**0.126**	**0.152**	**0.190**	**0.224**	**0.246**		**0.196**
Tilt (deg)								
t_{sn-1}	34.3	29.2	22.4	14.2	11.7	11.8	23.9	11.0
	37.8	**35.4**	**31.2**	**26.2**	**21.6**	**19.0**		**25.1**
t_{sn-2}	33.5	28.6	21.5	13.6	11.0	11.0	23.5	10.9
	36.6	**34.9**	**30.9**	**25.8**	**21.2**	**19.0**		**25.5**
$t_{P\mapsto N}$	100.2	99.4	98.3	97.1	96.9	97.3	98.5	96.9
	101.5	**101.0**	**100.5**	**99.9**	**99.3**	**98.5**		**99.8**
t_{CHOL}		25.7	20.9	13.3	10.1	9.2	23.9	10.8
		29.7	**28.6**	**23.7**	**18.9**	**14.7**		**25.2**
t^t_{CHOL}		35.8	30.5	20.1	16.9	17.7	51.4	18.5
		40.6	**39.2**	**34.7**	**30.0**	**26.6**		**48.1**

Table 7.1: Average results characterizing DSPC (light-face) and DOPC (bold) membranes with different cholesterol concentrations. [a]χ_c stands for the molar fraction of sterol. [b]For V_{PC} we have assumed V_{CHOL}=0.541 nm^3 [Edho05] and V_{CHOL}=0.4332 nm^3 estimated from V_{CHOL} by subtracting the theoretical volume of two methyl groups (2 x 0.0539 nm^3/CH_3 [Nagl00]).

between A_{PC} (Area box/128 PhdCho) and A^*_{PC} (Hofsäßmethod, Eq. 3.2) profiles deserve a few comments. First we concentrate on Fig. 7.2a. It shows decreasing (DSPC) and constant (DOPC) A_{PC} values while increasing the cholesterol concentration up to 30 mol%. At this point the trend of each curve changes to show increasing values. In particular, DSPC displays a minimum at this molar fraction. The explanation for this behavior is rather simple. The expected increase of area in the system due to the addition of cholesterols is compensated for DOPC or even more than compensated for DSPC by a decrease in the area of the PhdChol molecules, due to the ordering effect of cholesterol on their acyl chains. This is valid up to concentrations around 30 mol%. Above this cholesterol fraction the ordering of PhdCho chains can no longer compensate for the extra area occupied by the added cholesterols, thus we observe a net increase in the area of the system. Focusing now on Fig. 7.2b, which provides an estimation of the real area occupied by a PhdCho at a given χ_c, we observe that the behavior of A^*_{PC} indeed supports our previous description as it shows decreasing profiles in both cases. Additionally, we observe different behaviors between DSPC and DOPC profiles above 30 mol%. This reflects different underlying mechanisms responsible of the change in the trend (see Fig. 7.2a) at 30 mol% for saturated (DSPC) and unsaturated (DOPC) membranes. In the case of DSPC, lipid molecules reach a level of condensation that cannot be exceeded, $\sim$0.5 nm^2. Therefore, the addition of cholesterol molecules leads to a net increment in the simulation box as they have constant A^*_{CHOL} for concentrations over 30 mol% (see Table 7.1). DOPC, however, shows a permanent decreasing profile suggesting that it can be further compressed if the cholesterol concentration is increased even further. Taking into account that A^*_{CHOL} displays substantially higher values in the case of DOPC membranes than for DSPC membranes, it is understandable that the area associated with the added cholesterol molecules is not compensated for by the decrease in DOPC area once A^*_{CHOL} remains constant at high cholesterol concentrations. This higher value for A^*_{CHOL} in DOPC membranes reflects the more unfavorable interaction of cholesterol with unsaturated lipids. The higher values of A^*_{CHOL} are also responsible of the flat profile observed for A_{DOPC} below 30 mol% of cholesterol.

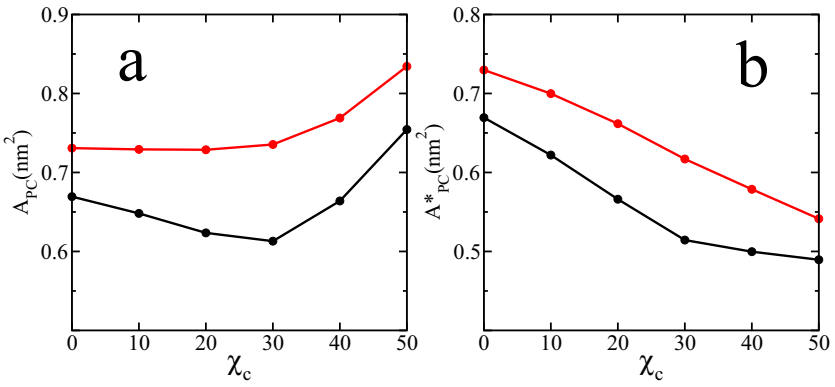

Figure 7.2: Area per molecule of DSPC (black) and DOPC (red) membranes as a function of χ_c. Panel (a) presents the area per molecule, A_{PC}, calculated by dividing the box xy area by the number of PhdChos, Eq. 3.1. Panel (b) presents the area per molecule, A^*_{PC}, calculated by the procedure developed by Hofsäßet al., Eq. 3.2.

The dependence of membrane thickness on the cholesterol fraction also displays interesting

behavior. In Fig. 7.3 we have plotted $\mathbf{D_{PP}}$ and $\mathbf{D_{OO}}$ for DOPC and DSPC as a function of χ_c. As in the area per lipid we observe two different behaviors, especially for the saturated moieties. The thickness of the membrane increases monotonously with the addition of cholesterol up to 30 mol%. The growth is significantly higher for DSPC than for DOPC. Above 30 mol% this increasing behavior is attenuated and even reversed for DSPC at 50 mol% of cholesterol, which might suggest some interdigitation between layers. The observed behavior is similar to that observed for a lipid monolayer isotherm experiment. In this case, the compression of a lipid monolayer in the liquid ordered phase results in a change in the chain tilt so that it becomes more perpendicular to the layer. This happens until the solid phase is reached and further compression cannot be accommodated by a change of the tilt but instead compression of the heads, which is substantially harder. The only difference with our system is that the effect of the compression is induced by the cholesterol addition. This view is totally consistent with the average lipid tilt values computed in our simulations, see Fig. 7.4a. Finally, subtracting $\mathbf{D_{PP}}$ and $\mathbf{D_{OO}}$ profiles we notice again that cholesterol is virtually equally inserted in all membranes as its depth respect the phosphorous position differs in less than 1 Å along z-axis.

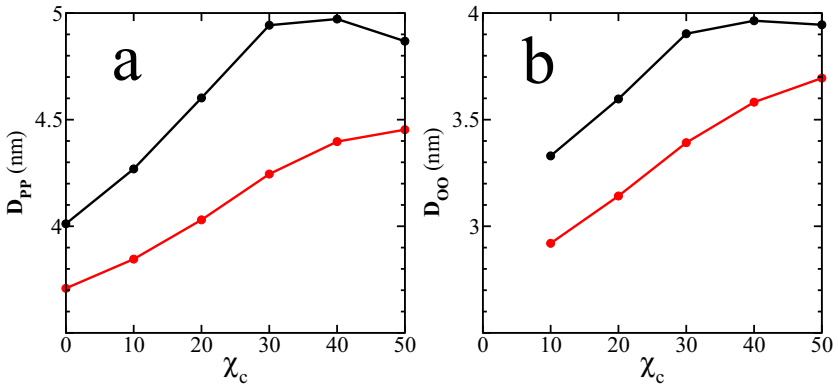

Figure 7.3: Thickness of DSPC (black) and DOPC (red) membranes as a function of the cholesterol molar fraction. Panel (a) presents the bilayer thickness, $\mathbf{D_{PP}}$, as defined in Eq. 3.4. Panel (b) presents the distance between the oxygen atoms on the cholesterol molecules in different layers, $\mathbf{D_{OO}}$.

Another property that needs some special attention is the order parameter S_{CD}. As expected increasing cholesterol concentration leads to higher ordering in the PhdCho acyl chains, see Fig. 7.4b. In the case of saturated lipid (DPSC) the ordering due to cholesterol addition increases quicker than that for the unsaturated ones (DOPC). In general, the observed profiles are in full agreement with the previously reported properties, showing a more pronounced increase for DSPC compared to DOPC membranes, and the correspondent plateau at high cholesterol concentration. If now we focus our attention on the S_{CD} profiles along the acyl chain, we confirm that the cholesterol ordering ability is especially prominent in the middle of the acyl chain and negligible in the center of the membrane, see Fig. 7.5. Interestingly, DSPC profiles at 40 and 50 mol% are almost equal suggesting that this is the highest ordering that the DSPC chains allow in the presence of cholesterol. The values for the order parameter for DSPC at large cholesterol fractions, however, indicate that acyl chains are more disordered than in the gel phase. We also notice that although PhdCho

chain behavior is very similar when mixed either with cholesterol or DCHOL, this is not true for DOPC membranes. As a result, we can conclude that the cholesterol structure is very specific and any change to it may lead to variations in its interaction with other lipids in the membrane.

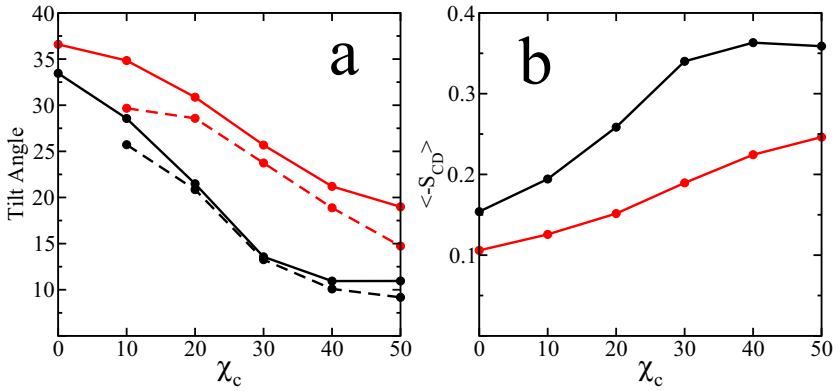

Figure 7.4: (a) Tilt and (b) the average values of the $\langle -S_{CD} \rangle$ in DSPC (black) and DOPC (red) membranes as a function of the cholesterol molar fraction. In panel (a) solid lines correspond to t_{sn-2} whereas dashed curves stand for t_{CHOL}.

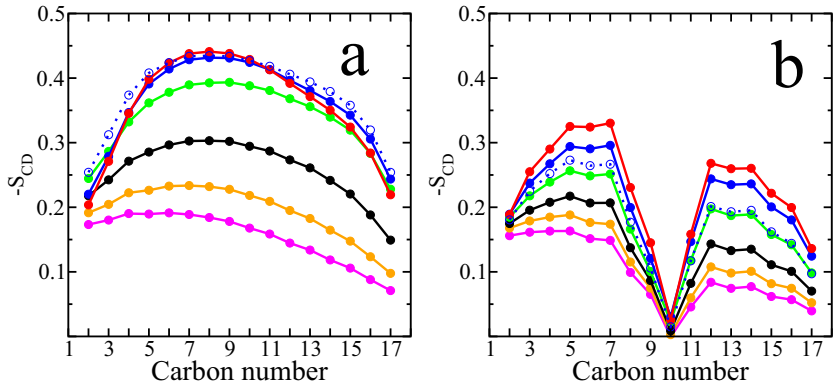

Figure 7.5: Deuterium order parameter (S_{CD}) profiles for (a) DSPC, and (b) DOPC membranes. The following color scheme is used to identify the cholesterol concentration in each system: 0 mol% (magenta), 10 mol% (orange), 20 mol% (black), 30 mol% (green), 40 mol% (blue) and 50 mol% (red). Results for the simulation containing 40 mol% DCHOL is presented with dotted lines.

Finally, although our model was extensively validated in Sec. 4.3, we want now to ensure that the observed behavior as a function of the cholesterol concentration is realistic. A^*_{PC} can be compared qualitatively and in the case of DOPC also quantitatively with the experimental results by Pan et al. [Pan09]. They observe, as we do, decreasing profiles over the whole χ_c range and similar numerical values for DOPC area per lipid, at least for low cholesterol fractions. At high cholesterol concentrations, we realize that our model leads to membranes slightly more condensed than they should be. For more saturated moieties like DMPC or even SOPC (only 1 unsaturated chain) Pan et al. also observe the presence of a plateau for concentrations over 30 mol% as we do for DSPC membranes. The same comparison is

applicable to the thickness values provided by Pan et al. [Pan09], which display the same trends as in our simulations. However, our simulated membranes are thicker, especially at high cholesterol concentrations, despite the reported experimental values being measured at lower temperatures than in our simulations. Despite this differences, we can conclude that our simulations indeed demonstrate realistic behavior and can be used for the study of cholesterol-containing membranes.

7.4 Absence of Direct CHOL-CHOL contacts

To begin the analysis of the cholesterol surroundings, we computed pair correlation functions (RDF) around the center of mass of cholesterol molecules for each simulated system, see Sec. 3.3.5. The results for DSPC systems are shown in Fig. 7.6. For the CHOL-PhdCho pair (data is provided only for DSPC/20 mol% CHOL), the RDF has its main peak at a distance of ∼0.5 nm. As this is also the first peak, it corresponds to the first coordination shell. In contrast, the main peak for CHOL-CHOL pair correlations is located at ∼1.0 nm. It corresponds to the second peak and hence it accounts for the second coordination shell. The physical interpretation of this observation is that cholesterol molecules prefer to be placed in the second cholesterol coordination shell instead of being located in adjacent positions [Niem07, Riss08]. This behavior is common in all systems with moderate cholesterol concentrations. Only at high cholesterol concentrations (>30 mol%) does the occurrence of close contacts (<0.8 nm) become relevant (see Table 7.2) since the membrane is then crowded with cholesterol molecules.

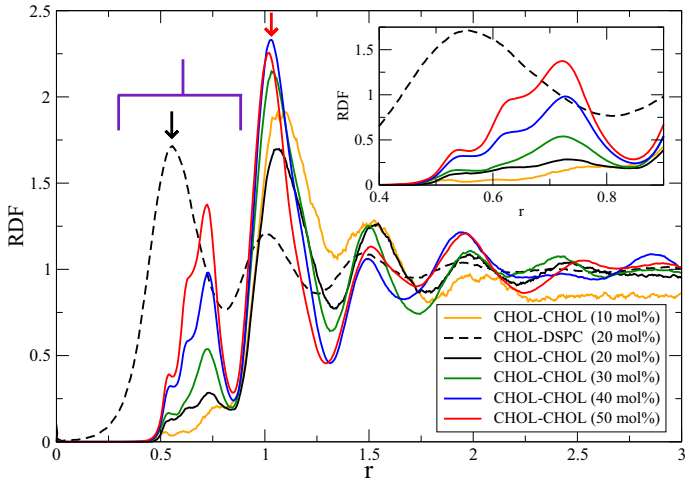

Figure 7.6: Pair correlation functions, RDF, for CHOL-CHOL (solid) and CHOL-DSPC (dashed) pairs in the simulated DSPC/CHOL membranes at different cholesterol concentrations. The color code indicates the cholesterol content: 10 mol% (orange), 20 mol% (black), 30 mol% (green), 40 mol% (blue) and 50 mol% (red). Data for CHOL-DSPC pairs is only provided for the system with 20 mol% of cholesterol. The radial distance from the center of mass of a cholesterol molecule is denoted by r. The inset shows a magnification of the first coordination shell. For CHOL-CHOL, the peak increases with increasing cholesterol concentration. The shapes of CHOL-CHOL peaks at high concentrations clearly show that they are composed of three overlapping peaks with maxima at approximately 0.45, 0.65 and 0.73 nm.

Segment	10%	20%	30%	40%	50%
0.4-0.8 nm	0.253	0.228	0.277	0.480	0.670
	0.300	**0.368**	**0.364**	**0.516**	**0.700**
0.8-1.1 nm	1.49	1.24	1.40	1.46	1.44
	1.51	**1.39**	**1.46**	**1.47**	**1.41**

Table 7.2: Ratio of cholesterol density averaged inside the first (0.4–0.8 nm) and the second (0.8–1.1 nm) coordination shells with respect to the total mean density. We have used 1.1 nm to define the range of the second coordination shell around cholesterol. In the next section we will show that the coordination shells around cholesterols are slightly elliptical instead of spherical due to the cholesterol molecular shape. To avoid any contribution from the third coordination shell, all measures of the second coordination shell were conducted between 0.8–1.1 nm. Although using 1.1 nm instead of 1.3 nm corresponding to the minimum in the 1D profiles presented in Fig. 7.6 has negligible influence on the conclusions described in this table, it is important in section 7.6.

The inset in Fig. 7.6 shows that the peaks observed in the first CHOL-CHOL coordination shell (0.4–0.8 nm) at high cholesterol concentrations are due to a superposition of three closely spaced individual peaks. This is a clear signature of the existence of three distinct preferential CHOL-CHOL pairs within the first coordination shell and warrants a more detailed analysis using angular information in addition to the radial distance. This analysis will be provided in Sec. 7.8.

Figure 7.6 also shows that the second coordination shell does not have any indications of possible superposition of multiple maxima even at high cholesterol concentrations. However, in the angular analysis presented in the next section preferential directions are also clearly observed, so it seems that in this case the related effects have been averaged in the angular summation.

In addition, Table 7.2 shows that the number of CHOL-CHOL contacts increases systematically in the first shell upon increasing cholesterol concentration. Such behavior is not observed for the second coordination shell in which the ratio of densities (density of the shell/total average density) is fairly constant for all cholesterol fractions. Similar behavior is found for DOPC but with a slightly higher occurrence of direct CHOL-CHOL contacts (see Table 7.2). This is expected since cholesterol has a higher affinity for saturated than for unsaturated lipids.

The absence of direct CHOL-CHOL contacts at low cholesterol concentrations may be due to the small hydrophilic headgroup of cholesterol; a close contact between two sterol molecules is not energetically favorable since such a contact would prefer high curvature of the membrane in order to shield the hydrophobic cholesterol ring system. In a planar bilayer, this would lead to the exposure of the hydrophobic membrane core to water and thus be energetically very costly. The entropic cost of having two rigid cholesterol molecules in direct contact is also high. It is thus favorable to have a Phd molecule with a flexible chain next to a cholesterol molecule. Such an arrangement is one of the key ingredients of the Umbrella model of Huang and Feigenson [Huan99]. In agreement with the findings above, in the Umbrella model the free-energy cost of covering a CHOL-CHOL dimer is much

higher than that of covering a single cholesterol molecule. As in the case of the cholesterol containing bilayers, direct DCHOL-DCHOL contacts are also very unfavorable.

Finally, due to crowding at large sterol fractions, direct CHOL-CHOL contacts are unavoidable and can lead to jumps in the cholesterol chemical potential at certain concentrations in PhdCho/CHOL bilayers [Ali07]. The above differences in free-energy may explain the jumps in the cholesterol chemical potential observed experimentally in PhdCho membranes containing large amount of cholesterol (>30 mol%) [Ali07].

7.5 Three-Fold Lateral Order

Next we analyze lateral ordering of lipid molecules by computing the in-plane two-dimensional average density. Here, we computed the total densities instead of probability densities as in the case of RDF above. Since we are computing two-dimensional density distributions, we obtain angular information in contrast to the angularly averaged one-dimensional RDF.

The analysis was performed in the following way: for each cholesterol molecule the origin was centered at the C13 group (see Fig. 7.1a). Then, the x-axis was defined by the C13-C18 direction and the xz-plane was chosen to include the C13-C10 vector (see Fig. 7.1b). Using this frame of reference for each cholesterol molecule, we computed the averaged two-dimensional density distributions for methyl groups in PhdCho acyl chains (see Fig. 7.7a) and for the atom groups in the cholesterol ring (see Fig. 7.7b) projected in the reference xy-plane in both cases.

Figure 7.7 shows the distributions for a DSPC membrane with 20 mol% of cholesterol. The first shell located at ∼0.5 nm (see also Fig. 7.6) is occupied almost exclusively by PhdCho molecules, while the second one at ∼1 nm (see also Fig. 7.6) is where cholesterol molecules reside. In both cases ordering is strongly suppressed in the positive x-direction. This results from the steric effects of the C18 and C19 off-plane groups on the rough β-face of cholesterol.

In all cases we observed at least three coordination shells for PhdCho acyl chains. The lower value is the one typically found in DOPC membranes, see Fig 7.8. For the saturated DSPC moiety the number of shells increases to four or even five (data not shown). For example, Fig. 7.7a shows four clear coordination shells in the DSPC 20 mol% of cholesterol system, which is a consequence of cholesterol's strong ordering ability and its affinity for saturated moieties [Mart08b].

Interestingly, the distance between each coordination shell is about ∼0.5 nm. A closer inspection of the first coordination shell reveals that PhdCho acyl chain ordering is anisotropic in the bilayer plane and five clearly defined maxima appear (see Fig. 7.7a). Although this is true for all the analyzed systems, some of these maxima merge in the DOPC systems leaving only three preferred locations, see Fig 7.8. This behavior can be understood in terms of the more fluid nature shown by membranes consisting of unsaturated lipids, possibly denoting a less restricted environment. Similar analysis of DOPC-CHOL and SM-CHOL interactions by Pandit et al. in a ternary mixture (DOPC-SM-CHOL) did not show the same ordering symmetry found here [Pand04]. The main reason for this discrepancy is the presence of an additional lipid (SM) in the cholesterol surroundings that compete with DOPC to be close to the cholesterol. Moreover, the behavior of a ternary mixture usually cannot be directly derived from that of binary ones. Finally, the actual time-scales accessible for MD simulations

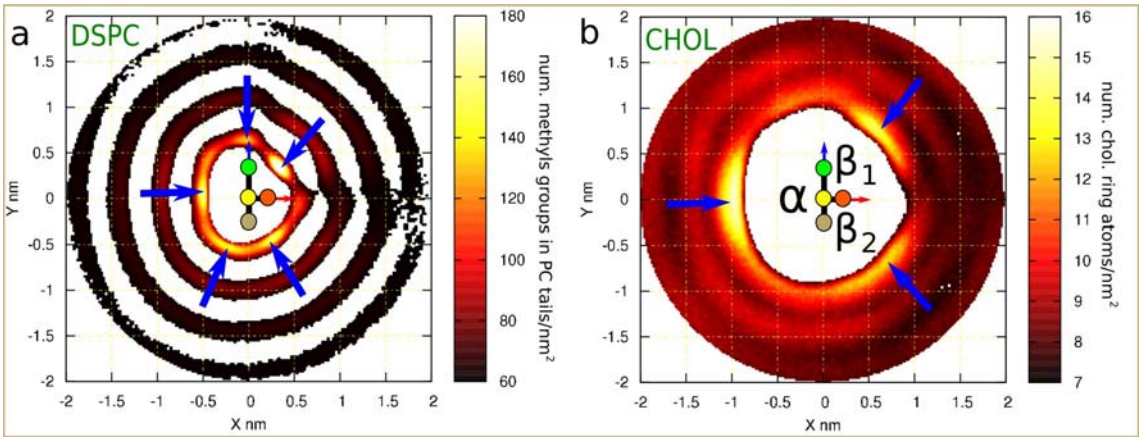

Figure 7.7: Two-dimensional density distributions for (a) DSPC acyl chains and (b) cholesterol molecules around a tagged cholesterol. Data shown is for the DSPC bilayer with 20 mol% of cholesterol. Each plot shows a schematic representation of the tagged cholesterol as described in Fig. 7.1. The different faces of cholesterol can be distinguished in both panels: the smooth α-face corresponds to the region x <0 and the rough β-face to x >0. The β-face is divided into two sub-faces: $\beta 1$ for y >0 and $\beta 2$ for y <0. Panel (a) shows the density distribution of methyl groups of both acyl chains per nm^2. The first coordination shell is located around 0.5 nm from the center of the tagged molecule. The five preferred locations for PhdCho chains are marked by the blue arrows. Cholesterol's ability to induce order is demonstrated by three additional less structured coordination shells. Panel (b) shows the density distribution of atoms in the ring of the cholesterol molecule (17 atoms per cholesterol molecule). Panel (b) also shows that cholesterol molecules avoid the first coordination shell covered by the PhdCho acyl chains. Instead a clear and structured second coordination shell appears. The three emerging peaks are marked with blue arrows. Each peak is on a different face (α, $\beta 1$ and $\beta 2$) displaying a three-fold symmetry.

do not allow complete equilibrium to be achieved for ternary mixtures, which require longer relaxation times than two-component systems. The last two points will be discussed in detail in the next chapter where we will present some MD simulations of ternary systems.

The arrangements of cholesterol molecules with respect to each other are even more interesting. Clear anisotropy and well-defined triangular symmetry with a clear peak at the α-face and two maxima at the β-face are observed. The β-face maxima split further into the two sub-faces $\beta 1$ and $\beta 2$ (see Figs. 7.1c and 7.7b). The two-dimensional density plots for DOPC bilayers display similar trends to those seen for DSPC but with slightly less well-defined peaks and coordination shells, see Fig 7.8. This concurs with the established fact that cholesterol orders saturated chains more than unsaturated ones [Mart08b].

The presence of this three-fold symmetry was previously shown by a visualization of isosurfaces of lipids and cholesterol molecules around a given cholesterol molecule by Pitman et al. [Pitm04] They found, however, that cholesterol was often located in the first coordination shell. This is probably due to the use of polyunsaturated lipids. They have less ability to pack laterally with cholesterol molecules compared to the monounsaturated lipids used in this work. Our simulations at high cholesterol concentrations also display density peaks in the first coordination shell although at different positions in the two-dimensional averaged density profiles (at angle ranges [-10°–10°], [80°–100°] and [240°–270°]; see Sec. 7.8).

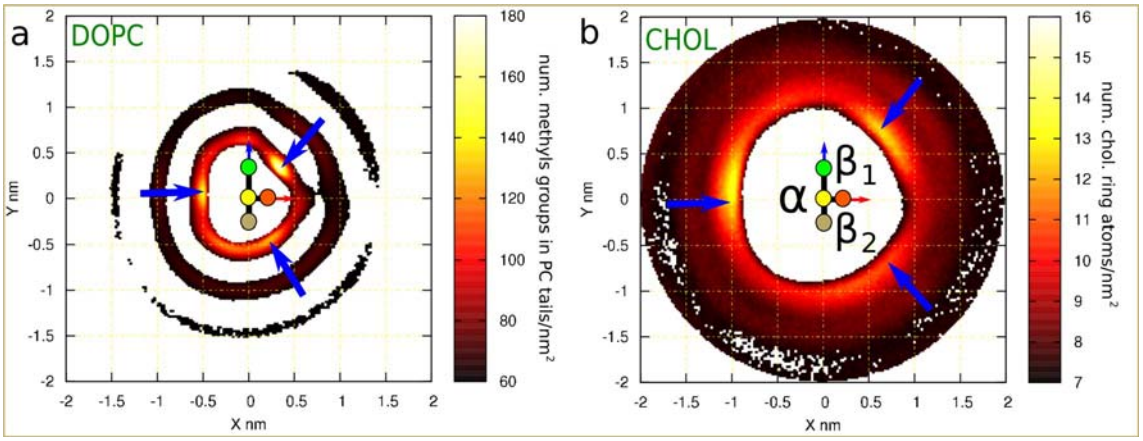

Figure 7.8: Two-dimensional density distributions for (a) DOPC acyl chains and (b) cholesterol molecules around a tagged cholesterol. Data shown is for the DOPC bilayer with 20 mol% of cholesterol. Additional details can be found in Fig 7.7.

The importance of off-plane cholesterol methyl groups to lateral ordering anisotropy was confirmed by computing the two-dimensional density functions for membranes containing DCHOL instead of CHOL. The purpose of simulating this *flat sterol* stems from the biosynthetic pathway of cholesterol [Bloc91]. The first sterol on this pathway is lanosterol, which has a structure similar to that of cholesterol except for three additional methyl groups located at both faces of lanosterol. The additional methyl groups are gradually removed in the biosynthetic process. Since the cholesterol biosynthetic pathway is thought to reflect evolutionary changes that finally result in the optimized cholesterol structure, one may think that further optimization could be achieved by removing the two remaining methyl groups from cholesterol. It leads to the (non-natural) DCHOL sterol molecule used in some of our simulations to determine the role of the off-plane methyl groups.

To define the axes in an equivalent manner to that of cholesterol, the positions of missing methyl groups in DCHOL molecule were reconstructed assuming tetrahedral geometry. As a consequence α- and β- faces can be recognized although both faces are smooth for DCHOL. For both PhdChol acyl chain and sterol distributions, a two-fold symmetry is observed with one broad peak on each side of the sterol plane, see Fig. 7.9. Cholesterol distribution shows a clear preference for forming triangular arrangements (see Fig. 7.10a) as can be seen from the two-dimensional density probability functions in Fig. 7.7b. DCHOL, instead, displays linear-like patterns (Fig. 7.10b) as a result of the two-fold symmetry displayed in the two-dimensional density distribution functions in Fig. 7.9. In Fig. 7.10, we present snapshots of one leaflet of the DSPC/CHOL and DSPC/DCHOL membranes. Triangular ordering of cholesterol and a linear array of DCHOL are clearly identified. Although lanosterol is not considered in our simulations, we predict that it would not show three-fold symmetry due to the off-plane methyl groups present on the α-face. Since the C18 cholesterol methyl group has been shown to disturb membrane structure more than C19, which is closest to the headgroup [Mart08b], we expect that the methyl group attached to C14 in lanosterol would disturb the membrane more than the methyl groups attached to the C4 position closer to the headgroup. Hence, we predict some sort of four-fold symmetry for lanosterol-containing membranes.

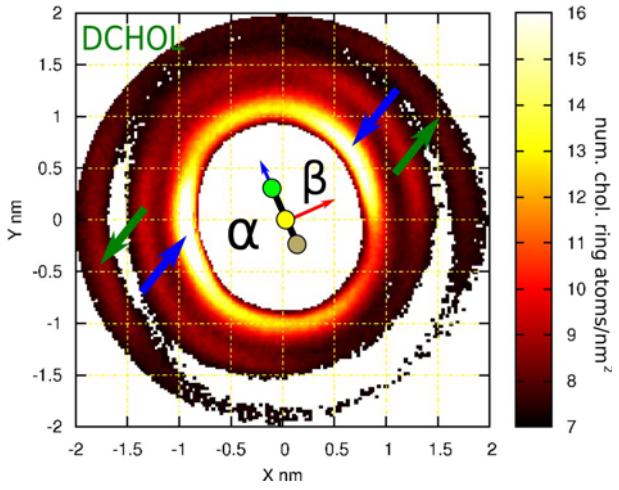

Figure 7.9: The two-dimensional average density distribution for DCHOL molecules around a tagged DCHOL. This corresponds to the density distribution of atoms in the ring of the DCHOL molecules (15 atoms per DCHOL molecule). The data presented corresponds to a DSPC bilayer with 20 mol% DCHOL. A schematic representation of the tagged DCHOL is shown at the center. As DCHOL does not possess off-plane methyl groups it is represented by a simple rod. As the presence of C18 is required to define the axes (see Fig. 7.1), the missing methyl groups in DCHOL molecule were reconstructed assuming tetrahedral geometry and thus α- and β- faces can be recognized. A comparison between the two sides of DCHOL shows that their behavior is similar to behavior of the smooth cholesterol face. Similar to the behavior of cholesterol, no DCHOL is seen in the first coordination sphere. On each side of the second coordination shell a peak facing the rod is observed (marked with blue arrows). Some structure is still present in the outer coordination shell (∼1.8 nm) displaying peaks collinear with the previous ones (green arrows). This reflects a strong preference to form linear DCHOL-DCHOL structures.

7.6 Orientational Order of Lipids Around Cholesterols

In this section we show that phospholipids prefer specific positions and orientations in the first cholesterol coordination shell. This is an important finding as it also influences ordering in the second shell as will be discussed in detail below.

Initially, we calculated the center of mass of each acyl chain for a given PhdCho molecule with at least one acyl chain in the first coordination shell. The chains were found to have an average separation between their *sn*–1 and *sn*–2 acyl chains of (0.55–0.85±0.2) nm, which depends on the considered moiety and membrane system. Next, we analyzed the orientation of PhdCho molecules in the first coordination shell with respect to their neighboring cholesterol molecules. Our analysis was performed as follows: 1) we selected PhdCho molecules with the center of mass of at least one of their acyl chains in the first coordination shell (up to 0.75 nm from center of mass) of a given cholesterol. 2) For these lipids we computed (a) the vector joining the centers of mass of the two acyl chains and (b) the vector between the center of mass of the cholesterol molecule and the mid-point of the above-calculated vector. This angle is denoted by θ. To better capture the symmetry properties, we used a 90 degree representation where both acyl chains are considered equivalent. Using this symmetry, the independent angles, labeled θ_{90}, run up to 90 degrees and the remaining θ values are covered by symmetry. We call θ_{90} the *co-localization angle*. Its relation to θ is shown on the right

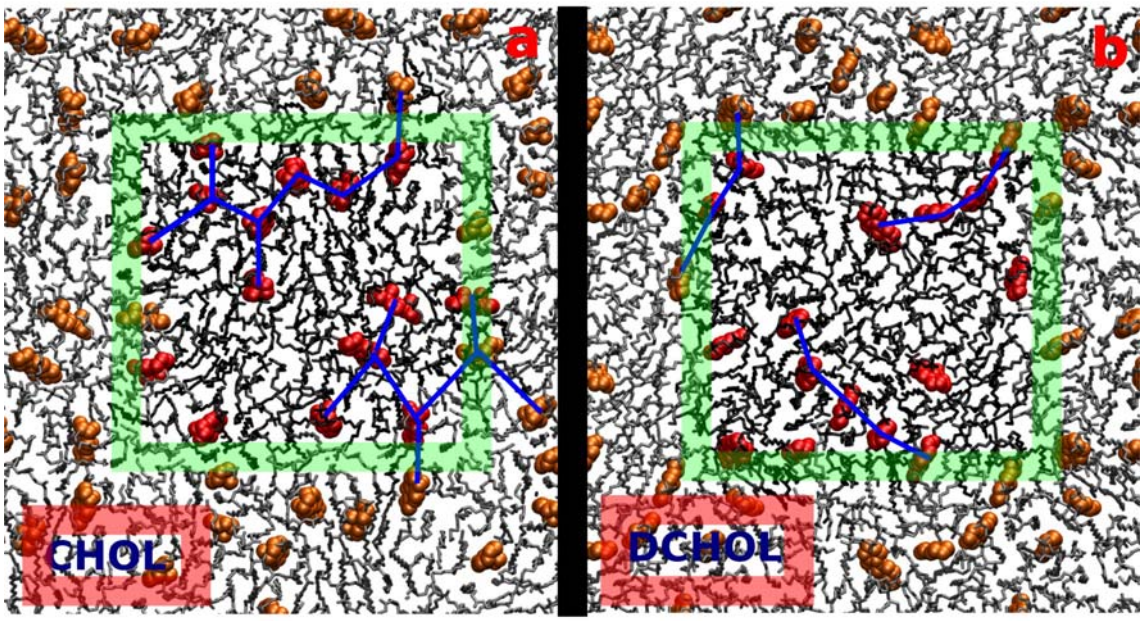

Figure 7.10: Top view of an equilibrated configuration of (a) the DSPC/CHOL bilayer and (b) the DSPC/DCHOL system at 20 mol% of sterol in both cases. Only one leaflet is presented for clarity. PhdCho molecules are shown as black sticks and sterols using space-filling representation in red color. The simulation box is shown by the green square with periodic images plotted around it. Sterols in periodic images are show in orange (instead of red as in the simulation box) and lipids in gray. Panel (a) shows triangular connections between neighboring cholesterol molecules. The blue lines between cholesterols form triangular patterns. Panel (b) displays the linear connections between DCHOL molecules. This fundamental difference is due to the missing off-plane methyl groups in the DCHOL molecule.

hand side of Fig. 7.11. θ_{90}=0° corresponds to the situation in which all of the centers of masses are lined up (PhdCho collinear to cholesterol). The angle θ_{90}=90° corresponds to the situation in which the centers of masses corresponding to the lipid acyl chains are at equal distances from the cholesterol center of mass (*facing* orientation). Distributions of the *co-localization angle* are shown in Fig. 7.11.

Figure 7.11 shows that the orientation of lipids around cholesterol molecules depends strongly on cholesterol concentration and on the type of PhdCho lipids. DOPC promotes profiles with less structure (less selectivity) than DSPC. This is particularly clear at high cholesterol concentrations. The profiles show gradual changes upon varying cholesterol concentrations. At 10 mol% of cholesterol, the profiles for both DOPC and DSPC are qualitatively similar, favoring angles between 0–45 degrees. At larger cholesterol fractions, and particularly for DSPC membranes, the orientation profile displays preferential peaks at 0, 45 and 90 degrees. This is clearly observed for DSPC membranes (>20 mol% of cholesterol) and to a lesser extent in DOPC systems (>30 mol% of cholesterol). It seems plausible that there is a class of PhdCho molecules that can be categorized by the preference for a 90° *co-localization* angle, especially at high cholesterol concentrations. Such lipids are likely to be sandwiched between two cholesterol molecules. We conjecture that this collective interaction involving two cholesterol molecules sandwiching a lipid is a fundamental mechanism responsible of cholesterol ordering ability. This justifies why membranes with

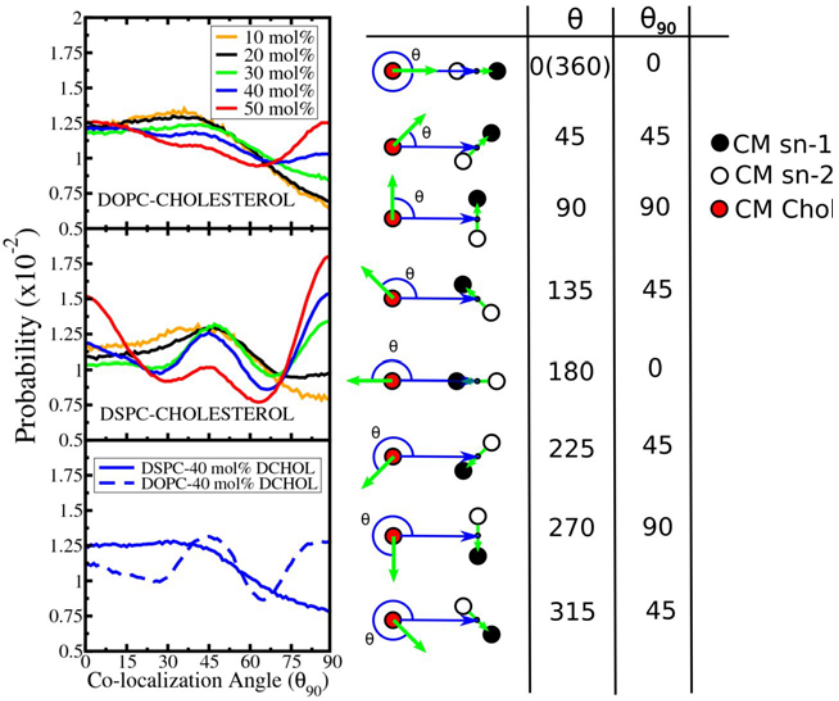

Figure 7.11: Distribution profiles of the *co-localization* angles for all simulated systems for lipids inside the first coordination shell of cholesterol. Color code indicates sterol content. The graphical representation of the *co-localization* angle is provided next to the graphs. Green arrows denote the vector joining the centers of mass of the two acyl chains and the blues ones the vector between the center of mass of the cholesterol molecule and the mid-point of the previous vector. The red, white and black dots are the centers of mass of the *sn*–1 acyl chain, the *sn*–2 acyl chain and the cholesterol ring, respectively. The θ_{90} representation is used to represent the *co-localization* angle in all graphs (θ_{90}=0° corresponds to collinear, θ_{90}=45° to diagonal and θ_{90}=90° to *facing* orientations).

small cholesterol concentrations (<5 mol%) form disordered L_α phases (see Sec. 1.4). At such low fractions, cholesterol molecules are dispersed and act totally independently from each other. Conversely, at higher cholesterol concentrations, the formation of domains rich in cholesterol is observed as well as a substantial increase of lipid order. By locally increasing the concentration of cholesterol, these domains actually allow significant cooperation between the cholesterol molecules, ordering the lipids confined between them.

Finally, the results for DCHOL reveal that despite the small differences between the cholesterol and DCHOL profiles (compare PhdCho/CHOL and PC/DCHOL at 40 mol%), the off-plane methyl groups on cholesterol have little influence on lipid orientations which are determined mainly by the lipid moieties themselves.

A more detailed analysis shows that the orientations of PhdCho molecules depend also on the side of the cholesterol molecule that is neighboring the analyzed chain. This is observed only for high cholesterol concentrations (>30 mol%) in DSPC bilayer and for 50 mol% in DOPC bilayer (not shown).

7.7 Orientational Order of CHOL in the Second Coordination Shell

In our last analysis concerning the cholesterol second coordination shell, we focus on its the orientational order. We have already seen that neighboring sterol molecules (corresponding to the 1 nm coordination shell) interact in such a way that a particular triangular symmetry appears in their relative spatial distribution. This occurs despite the fact that at least one PhdCho molecule is intercalated between every two proximal cholesterol molecules. The planar structure of cholesterol and the off-plane methyl groups are fundamental for this organization. Moreover, our analysis shows that the relative orientation between two neighboring cholesterols display preferential angles.

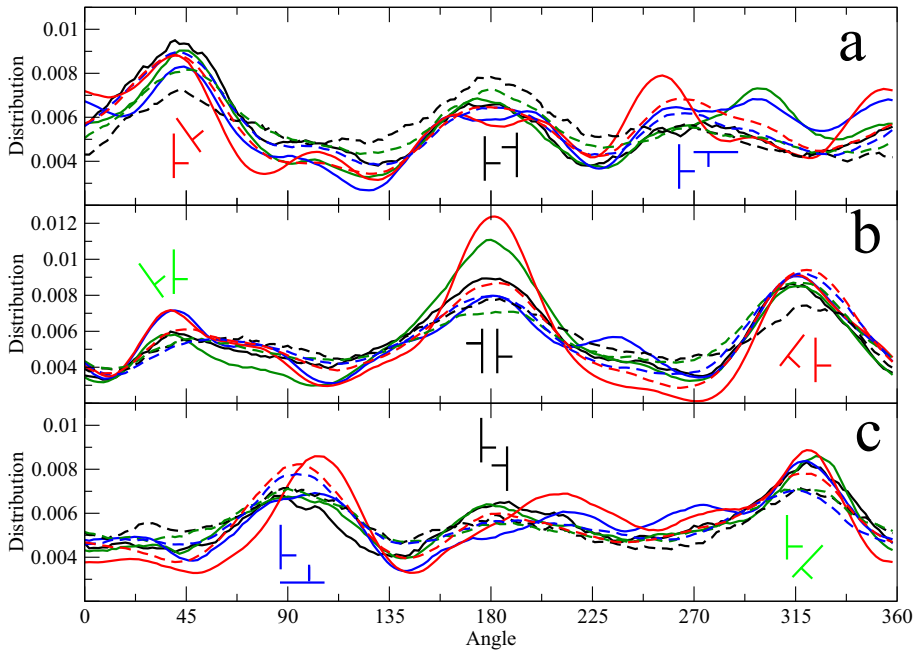

Figure 7.12: Angle distribution for cholesterol pairs corresponding to the three preferred locations displayed in the CHOL-CHOL two-dimensional density functions. The angle in the x-axis is the one formed by the C6-C11 vectors of each cholesterol molecule in the pair. All the curves in a given panel display the same qualitative behavior and here we are interested only in characterizing the common trends. Panel (a) refers to the $\beta 1$ peak. Panel (b) contains the data for the α peak. Panel (c) corresponds to the $\beta 2$ peak. Solid lines correspond to DSPC systems whereas the dashed curves correspond to DOPC membranes. The color code indicates cholesterol content: 20 mol% (black), 30 mol% (green), 40 mol% (blue), and 50 mol% (red). Simulations with 10 mol% cholesterol are not provided due to poor statistics. Preferred configurations are plotted schematically at each distribution maximum. Equivalent configurations are displayed in green, blue, and red, whereas those plotted in black are not equivalent.

We computed the occurrence distribution for the angle formed between the C6-C11 vectors (see Fig. 7.1) of two proximal cholesterol molecules in different sectors of the second Chol-Chol coordination shell. These sectors are defined as follows: NE [22.5°–67.5°], N [67.5°–122.5°], NW [122.5°–157.5°], W [157.5°–202.5°], SW [202.5°–247.5°], S [247.5°–292.5°], SE [292.5°–337.5°], E [337.5°–22.5°], where 0° is in the x-direction and angles increase anti-clockwise.

This was done by computing separately the relative angle of cholesterol pairs at a radial distance range of 0.8–1.1 nm in the different angular sectors defined above. The relative angle distributions are plotted in Fig. 7.12 for the three preferred locations in the CHOL-CHOL two-dimensional density function ($\beta 1$ (NE[22.5°–67.5°]), α (W[157.5°–202.5°]), and $\beta 2$ (SE[292.5°–337.5°])) for DSPC and DOPC species and different cholesterol concentrations. In all cases, we observed three maxima corresponding to the preferential relative orientations. These nine preferred configurations are schematically depicted in Fig. 7.12, but it is important to notice that some of them are equivalent: the first peak for the α location is equivalent to the third peak in the $\beta 2$ sector. Next, the third peak in α is equivalent to the first peak in $\beta 1$ and, finally, the third peak in $\beta 1$ is equivalent to the first peak in $\beta 2$. Essentially, only six different independent configurations are present.

7.8 Cholesterol in the First Coordination Shell

Finally, we will briefly address direct CHOL-CHOL contacts. As already seen in Sec. 7.4, at large cholesterol fractions, the occurrence of direct CHOL-CHOL contacts increases as a consequence of cholesterol crowding. The particular configuration of such CHOL-CHOL structures reveals interesting features. Figure 7.13 shows the two-dimensional density distribution for DSPC system with 50 mol% of cholesterol. Comparing this figure to the same distribution for the 20 mol% of cholesterol case in Fig. 7.7b, a substantial increase in the occurrence of cholesterol in the first coordination shell is observed. Moreover, Fig. 7.13 reveals the existence of three preferred approaching directions for direct CHOL-CHOL contacts at the following angles: [-10°–10°], [80°–100°] and [240°–270°]. These configurations lead to the three peaks observed at short distances in the CHOL-CHOL radial one-dimensional distributions plotted in Fig. 7.6. The occurrence of these preferred configurations dramatically decays at lower cholesterol concentrations. In fact, they are imperceptible for cholesterol fractions below 30 mol% for the DSPC system and 40 mol% for the DOPC systems.

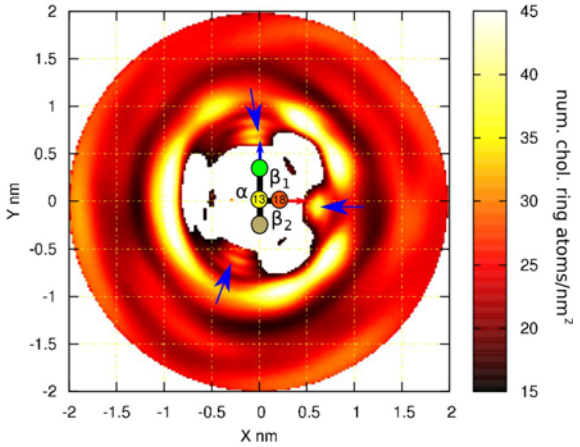

Figure 7.13: Two-dimensional density distributions for cholesterol molecules around a tagged cholesterol for a DSPC bilayer with 50 mol% of cholesterol. The axis system is the same as defined in Sec. 7.5. The blue arrows show the position of the preferred directions for direct CHOL-CHOL contacts.

Not only positional ordering, but also orientational ordering, is found between cholesterols

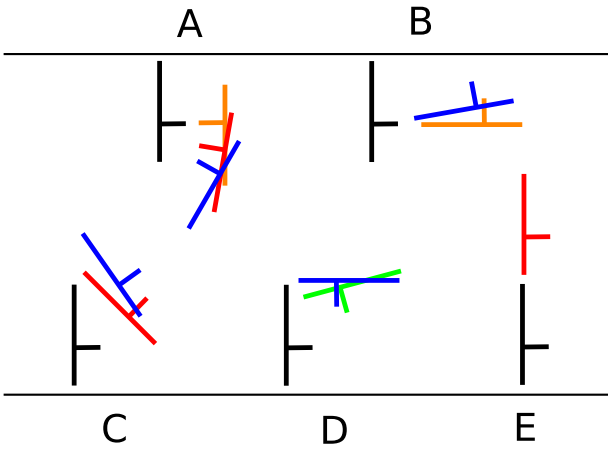

Figure 7.14: Representation of the five major cholesterol conformations observed in the first cholesterol coordination shell. In black the central cholesterol is shown (oriented as in the two-dimensional density distributions), and around it, the position and orientation of the surrounding cholesterol molecules in the observed configuration are presented. Since some configurations can be easily exchanged in the simulation trajectories, they have been plotted together and considered as the same conformation. The color of the cholesterols indicates an estimation of the probability of each conformation, ordered from the higher to the lower: orange, red, blue, and finally green. The exchange of roles between the central and the surrounding cholesterols lead to identical configurations as they are the same molecule.

in direct contact. Here, we have conducted the same analysis as described in the previous section (7.7) for this first coordination shell. It is important to notice that compared with the structures in the second coordination shell, these are significantly better resolved. The orientational peaks are higher and narrow than those for the second coordination shell (see Fig. 7.12). This can be interpreted as arising from the presence of more restricted configurations. The obtained preferential configurations are summarized and detailed in Fig. 7.14. Some configurations resemble the ones observed in the second coordination shell (for instance those labeled as A, C and D), but others are different. Instead no resemblance is found with the cholesterol crystals packing structures [Shie81, Hsu02], which is not surprising due to their three-dimensional nature. It is also interesting to notice that the preferred orientational configurations correspond to the most populated sectors [-10°–10°], [80°–100°], whereas the sector [240°–270°] is more flexible and does not contribute with any defined CHOL-CHOL relative orientation.

In order to shed light on the possible permanent or long term nature of the interaction between two cholesterols in direct contact we have also computed the life-time of the CHOL-CHOL structures in the first coordination shell. To do so, temporal autocorrelation functions of direct CHOL-CHOL contact occurrence (defined within the distance of the first coordination shell) are computed, and the time needed to lose the correlation is extracted. For the case in Fig. 7.13, which is likely to present the longest interaction duration due to its reduced mobility (see Sec. 7.3), the mean life-time of CHOL-CHOL structures is found to be of the order of a few nanoseconds, implying that they cannot be considered to be stable (crystal nucleation sites), but rather transient, structures.

7.9 Discussion and Conclusion

Our findings suggest that the structural characteristics of cholesterol are largely responsible for its ordering abilities. Its small headgroup and rigid ring structure prevent direct sterol-sterol contacts to a large degree in order to avoid the exposure of hydrophobic membrane regions to water. Therefore, a PhdCho lipid is often located between two sterol molecules. Off-plane cholesterol methyl groups determine the positional and orientational ordering of PhdChos around cholesterol molecules, which, in turn, induce a triangular symmetry for the location of cholesterol in the second coordination shell with well-defined relative orientations. Splitting the β-face into two sub-faces is fundamental for this ordering mechanism and its effect is remarkable considering the (lateral) fluid nature of the system.

The cholesterol biosynthetic pathway shows a systematic removal of methyl groups from the steroid ring. Each removal step optimizes sterol properties in terms of ordering and condensing effects [Aitt06]. This observation could lead to the erroneous conclusion that the remaining methyl groups are just evolutionary fossils. However, recent studies have shown that their presence regulates the sterol ring tilt angle in the bilayer [Rog07a, Poyr08], and the interaction with double bonds of neighboring lipid acyl chains, see chapter 4. Both factors are important in determining a sterol's condensation ability in mammalian cell membranes.

In this study, we again provided direct evidence of the importance of these methyl groups for inducing collective arrangements of cholesterol and lipid acyl chains. Our results provide compelling evidence for the tendency of cholesterol to self-assemble with PhdChos in specific configurations that are relevant in lipid organization and ordering at larger length and longer time scales. In particular, the condensation effect is more pronounced for (saturated) DSPC molecules because they are more easily oriented by cholesterol in comparison to DOPC molecules (where both acyl chains are monounsaturated). The ability of cholesterol to promote *facing* (θ_{90}=90°) configurations, especially in saturated lipids, represents a key mechanism for cholesterol to induce order in the membrane. In this *facing* conformation a lipid can be sandwiched by two cholesterol molecules decreasing its sectional area and therefore producing the well known condensation effect.

Furthermore, the sterols' abilities to form ordered structures at longer ranges were revealed by comparing cholesterol with our control simulations using DCHOL. As a direct outcome of the sterol-sterol 2D-density plots, cholesterol can clearly be seen as promoting the formation of (dynamic) triangular networks, whereas DCHOL is organized in linear arrays (see Fig. 7.10). Triangular configurations are able to, eventually, expand into two-dimensional sterol-rich regions. Moreover, comparison of the membrane areas between DSPC/CHOL and DSPC/DCHOL membranes reveals a counterintuitive finding: although DCHOL allows a closer lateral approach (due to the absence of C18 and C19), the membrane area at moderate sterol concentrations (for the same sterol content) is larger in DSPC/DCHOL than in DSPC/CHOL. Again, a three-fold symmetry in the lipid arrangement (Cholesterol) is able to condense the membrane more in a two-dimensional system than a two-fold configuration (DCHOL). At high cholesterol concentrations (i.e. 40 mol%) this situation is inverted for DSPC due to the increase of sterol-sterol contacts: DCHOL dimers are easier to pack laterally than cholesterol ones due to the absence of off-plane methyl groups.

Next, we discuss experimental observations of membranes with lanosterol. As previously commented, lanosterol is the first sterol in the 19-step biosynthetic pathway to cholesterol

[Bloc91] whose membrane properties are well characterized experimentally [Miao02]. In lanosterol, the three-fold symmetry is broken by additional two methyl groups located on the α-face of the steroid ring. The physical properties of lanosterol have important differences compared to those of cholesterol. First, lanosterol's condensing and ordering effects are significantly reduced compared to those of cholesterol. Most importantly, however, unlike cholesterol, lanosterol is unable to promote the formation of the liquid ordered phase over a wide range of temperatures and concentrations [Miao02, Beat05]. Cholesterol is able to do this even at physiological concentrations (>20 mol%). Another sterol is coprostanol, a product of cholesterol biodegradation, obtained by the reduction of the double bond. Coprostanol differs from other sterols by a *cis* connection between rings A and B. Consequently, the steroid ring in coprostanol is not planar, and both coprostanol and lanosterol therefore lack a flat ring face. In membranes coprostanol has a characteristic phase behavior that differs from other sterols: instead of liquid-liquid coexistence, a liquid-solid coexistence region is observed [Beat05, Stot06]. Whether both observations are related to the lack of three-fold symmetry remains to be established, but in the light of the results presented here this is the most likely hypothesis.

CHAPTER 8

Role of Cardiolipins in the Inner Mitochondrial Membrane

8.1 Objective and Summary

In nature, some membranes contain specific lipids that are rarely found elsewhere. This is the case for the inner bacterial membrane or closely related ones such as mitochondrial membranes, which contain cardiolipins (Cards) with molar concentrations ranging from 5 to 20 mol% [Daum85, Hovi90, Hoch92, Gome99].

Cardiolipins constitute a class of lipids that is in many ways exceptional. Unlike most other lipid types, cardiolipins are divalent anionic lipids with four acyl chains. This unusual structure results from their dimeric nature where two phosphatidyl moieties are linked together through a central glycerol group [Pang42, LeCo64]. Consequently, Cards typically have four acyl chains that are usually unsaturated, though the specific fatty acids found in Cards vary depending on the organisms. For example, in mammalian heart cell membranes the fatty acids of Cards are mostly linoleic acid, whereas in some marine organisms the most abundant type is docosahexaenoic acid [Kraf02]. The structure of Cards is characterized by a large hydrophobic region and a strongly charged and relatively small headgroup, which together mean that Cards favor negative curvature and in aqueous solution form different types of aggregates ranging from cylinders to inverted micelles and hexagonal structures [Powe85, Ales07, Dahl07]. Furthermore, there is another reason to emphasize that the strongly charged nature of Cards makes them quite different from other lipids: since direct electrostatic interactions between charged species are strong, they can act as both stabilizers and destabilizers of membranes [Shoe02, Nich05, Zhao07b]. In particular, although there are a number of different anionic lipids in typical eukaryotic cell membranes, Cards are virtually the only charged lipid species in mitochondria [Hovi90].

Cardiolipins are involved in an exceptionally broad variety of functions, including stabilization of membrane proteins and respiratory complexes [Krau04, Lena07] as well as electron and proton transfer [Hoch92, Gome99, Lena07]. Due to their charged nature, Cards are also involved in maintaining the electrochemical proton gradient across membranes, which enables ATP synthesis and ADP-ATP translocation [Lena07]. Cards also play an important

role in programmed cell death [Gonz07], aging and oxidative stress [Sast00, Sanz06], and in numerous metabolic illnesses such as Barth syndrome or thyroid dysfunction [Schl06]. The diverse roles of cardiolipins have been extensively discussed by Schlame et al. [Schl00].

The main purpose of this chapter is to investigate the molecular mechanisms of how the presence of Card molecules modifies membrane properties and influences membrane structure. This is essential for the understanding of stability and transport and signaling processes in mitochondria, and it is also required to extend the current models to include new features such as charge transport involving Cards. The systems we study here are constructed to reflect the natural lipid composition in the inner membrane of mitochondria (50 mol% PhdCho, 40 mol% PhdEtn and 10 mol% Card; see Ref. [Daum85]). All the lipids used contain the same acyl chains: linoleic acid. Unfortunately, the amount of experimental data available to compare with our selected membrane is rather limited. This combined with the fact that our work constitutes one of the first attempts to simulate such ternary system [Dahl07, Dahl08] has forced us to focus on its comparison with several reference systems of reduced complexity. These reference systems, also simulated in the present study, are pure and a two-to-two combinations of the constituents of the ternary mixture

From the performed simulations we find that the influence of Cards on membrane properties is basically at the membrane-water interface and it depends strongly on membrane composition. On the one hand, Cards significantly alter the properties of PhdChos leading them to form a substantially more ordered state. This effect is a consequence of the formation of stable charge pairs in the interface between the moieties. On the other hand, Cards barely change the PhdEtns properties. In addition, we observe that the influence of Cards in the ternary membrane is significantly different from its influence in binary mixtures with PhdCho and PhdEtn. As a consequence, for example, the ternary mixtures present a larger number of interlipid hydrogen bonds and lower number of charge pairs among the simulated systems. Finally, we do not find any spontaneous tendency for Cards to aggregate. Moreover, Card aggregates are shown to be rather unstable when introduced in the initial configuration of the simulation. This latter evidence reflects the importance of other membrane mechanisms, beyond the direct interaction between Card molecules, for the formation of the Card rich domains observed in the membranes [Mile00, Mats06, Mile09].

Beyond the limited application of the results in this chapter to the bacterial/mitochondrial membrane, a more general conclusion in the context of this Thesis can be extracted. Here we have learnt that the properties of multicomponent bilayers (and cell membranes are indeed multicomponent) cannot be exclusively deduced from the combination of the behavior of binary or pure ones. Therefore, the applicability of all the cholesterol effects reported in the former chapters to the cell membranes must be considered with caution as they might be modified or altered when other components are present.

The research described in this chapter resulted in the publication [Rog09a] included in this Thesis.

8.2 Descriptions of Simulated Systems

In order to study the inner mitochondrial membrane, we have simulated six different membrane compositions. From these compositions only the PC-PE-CL (see Table 8.1) mimics the

mitochondrial composition [Daum85] (50 mol% PhdCho, 40 mol% PhdEtn and 10 mol% Card). The other compositions correspond to reference membranes with a reduced level of complexity, namely binary mixtures (PC-CL, PC-PE, PE-CL; see Table 8.1) and pure membranes (PC, PE; see Table 8.1). All the lipids used have the same diunsaturated linoleic acid (18:2c9,12) as acyl chains. This means that they resemble the real inner mitochondrial membrane lipids [Kraf02]. Figure 8.1 shows the structures and the numbering of the atoms in all lipid molecules used in this study. The exact composition of each membrane is described in the following table.

Membrane	PhdCho (PC)	PhdEtn (PE)	Card (CL)	water	Na^+
PC	128			3614	
PC-CL*	100		14	3586	28
PC-PE	70	58		3614	
PC-PE-CL*	54	46	14	3586	28
PE		128		3614	
PE-CL*		100	14	3586	28

Table 8.1: Number of molecules of each kind in each simulated membrane. The names PC, PC-CL, PC-PE, PC-PE-CL, PE and PE-CL will be used in this section to refer to the particular membranes described above where PC, PE and CL are used as acronyms for the presence of PhdCho, PhdEtn and Card in the membranes, respectively. *Two simulations with different initial configurations correspond to each composition. In the first simulation Cards were randomly distributed in the membrane, whereas in the second Cards were initially aggregated.

At this stage it is important to highlight that the simulations proposed here present some important differences to those in the previous chapters. Firstly, they are entirely based on the OPLS all atom (OPLSaa) force field and, therefore, all hydrogens are explicitly considered. Secondly, water is described by the TIP3 model as it is the only one compatible with the OPLSaa parameters. Thirdly, as Cards are charged species (-2 e), Na^+ cations are incorporated to ensure the electro-neutrality of the system, see Table 8.1.

As a matter of fact, the charge of cardiolipins has remained somewhat uncertain, and a consensus on this matter remains to be found [Nich05, Mile09]. Some experimental evidences seem to indicate, though, that Cards are either singly (-1 e) or doubly charged (–2 e), depending not only on pH but also on environmental factors such as the concentration of Cards [Nich05, Mile09]. Here, we consider cardiolipins as molecules with two negative charges, assuming both acidic sites to be ionized. Considering the time scale of the simulations, about 100 ns, our choice (-2 e) is as justified as the other (-1 e) since we inevitably model a transient state of the membrane.

The initial structures of all bilayers were obtained by arranging the lipid molecules in a regular array in the bilayer xy-plane with an initial surface area of 0.32 nm^2 per lipid chain. All the moieties were placed randomly. An additional simulation of the systems containing Cards was performed where the initial structure corresponded to the aggregates of Cards. All the simulations were performed at 310 K (fluid phase), over a time scale of 130 ns. The first 40 ns were considered to be an equilibration period and, therefore, the remaining period

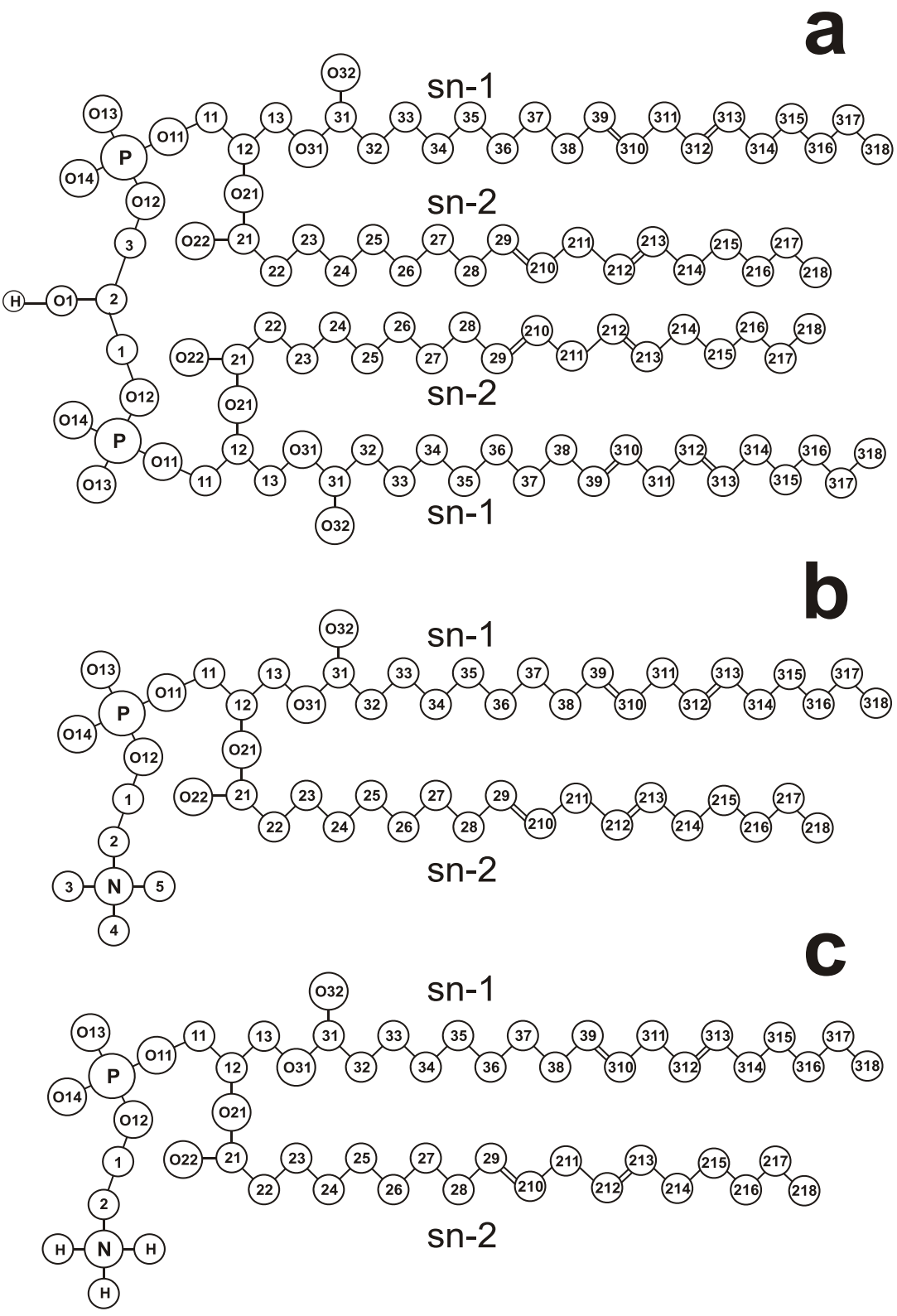

Figure 8.1: The molecular structures of (a) Card, (b) PhdCho, and (c) PhdEtn molecules including the numbering of atoms.

of 90 ns of each trajectory was analyzed. Equilibration was monitored by following the time development of area per lipid, temperature and potential energy, which settled to their equilibrium values after 34–36 ns (data not shown). For details about the used protocol and force field see Sec. 3.2.

8.3 Do Cardiolipins Aggregate?

One of the interesting features of Cards that has attracted a significant amount of attention is their capacity to promote membrane domains in bacteria and mitochondria [Dowh08, Schl08, Mile09]. These Card-enriched domains seem to be especially critical when the membrane experience high-curvature processes that require large membrane deformations as in bacterial division [Mile05] or in the cristae of mitochondrial membranes [Dowh08]. Despite the mechanism underlying the formation of these Card-enriched domains is not clear, a recent model proposing a curvature-mediated mechanism for such aggregation seems rather plausible [Huan06]; however, we cannot totally rule out the possibility that Card aggregation is also partly driven by short-range interactions between Card molecules.

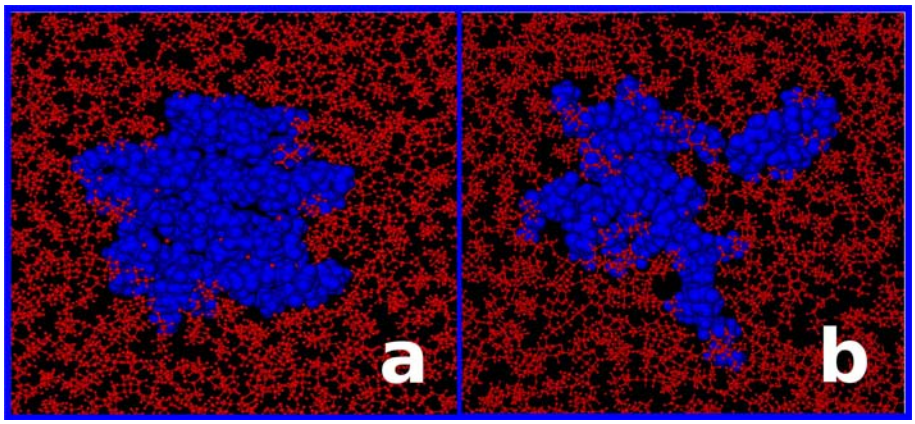

Figure 8.2: Panel (a) show the initial state of the PC-PE-CL simulation while panel (b) show the last configuration (130 ns) of the same system. PhdCho and PhdEtn are shown as red sticks and Cards are shown in blue using space-filling representation. The comparison of both panels suggests that the aggregate state does not represent the optimal state of the system. The other membranes PC-CL and PE-CL showed similar behaviors.

This latter possibility presented us with some trouble when choosing the initial state for our Card-containing membrane simulations. Since our membranes are small and constrained by the periodic boundary conditions, the simulated membranes cannot curve significantly. Therefore, if the unique mechanism for aggregation is related with curvature fluctuations, the most probable equilibrium configuration for the Card molecules is in a non-aggregated state. Instead, if Cards really tend to aggregate though lipid interaction, then some aggregates will be present at equilibrium. These two options constitute a problem because of the slow diffusion motions of the lipids compared to simulation time scale. In fact, if the initial state is non-aggregated, we could not expect any aggregation after 130 ns of simulation although it would represent a real equilibrium state of the system. Similarly, if we start with a totally aggregated system again it is not possible to reach a final non-aggregate configuration with

this short simulation time. In order to minimize this limitation, all simulations with Cards were doubled. The first set of simulations considers a random initial location of Cards, while in the second set all Cards are inserted as a single initial aggregate.

As clearly stated above, using this strategy we cannot expect to reach absolute equilibrium states in all the simulations, but we expect to observe the evolution of the systems, which helps us to determine the most probable final equilibrium configuration. Using this method, we observed that all systems that initially had Card aggregates showed a clear tendency for these aggregates to break-up, see Fig. 8.2. In contrast, no single aggregate formation was observed in the initially random systems. Although these two findings are not completely conclusive, they seem to indicate that the non-aggregated configuration is the closest to the equilibrium state. The simulations that started from the random initial configurations are the ones analyzed in the following sections.

8.4 Structural and Dynamical Membrane Properties

To understand the changes induced by the Cards in the membranes we have analyzed several structural and dynamic properties in the simulated systems. We have especially concentrated our attention on the water-membrane interface, where the highly charge nature of Cards is likely to have the greatest affect. Errors were calculated by using the block analysis method [Hess02] and are given as twice the standard error.

8.4.1 General Properties

As usual, we are interested in the area per lipid. Here, however, the area was calculated per acyl chain by dividing the total surface area by the number of acyl chains in one leaflet (the number of chains per leaflet is constant in all systems). This approach was chosen because a Card molecule has 4 hydrocarbon chains whereas PhdCho and PhdEtn molecules have only 2. The values obtained for the surface areas per chain are given in Table 8.2. As the data shows, the addition of Card in a PC membrane condenses the system by 0.02 nm^2 per acyl chain, while in the PC-PE matrix the effect is smaller, about 0.01 nm^2 per acyl chain, and in the PE bilayer cardiolipins do not show any observable effect.

Membrane	area[nm^2]	thickness [nm]
PC	0.340±0.001	4.1
PC-CL	0.318±0.001	4.1
PC-PE	0.318±0.001	4.2
PC-PE-CL	0.308±0.001	4.2
PE	0.299±0.003	4.4
PE-CL	0.296±0.001	4.3

Table 8.2: Average area per hydrocarbon chain and membrane thickness.

The observed differences in the surface area imply that the values of membrane thickness are also slightly different. To illustrate this, Fig. 8.3a shows the membrane density of the

lipids along the bilayer normal in pure PC and PE bilayers; these two bilayers represent the systems with the largest and the smallest area, respectively. Membrane thickness is not a uniquely defined parameter. In fact, although $\mathbf{D_{PP}}$ distance is appropriate to characterize the thickness of pure systems, it displays different values when applied to multicomponent systems depending on the chosen moiety. For example, in the mixed PC-PE-CL system the distances are 4.30±0.01, 4.10±0.01, and 4.06±0.02 nm for PhdCho, PhdEtn, and Card respectively. This indicates that Card molecules are located further away from the water-membrane interface region than PhdChos and PhdEtns. Figure 8.3b shows the density profiles of PhdCho, PhdEtn and Card molecules in the mixed PC-PE-CL bilayer. It can be observed that PhdEtns and Cards are positioned deeper in the membrane than PhdChos. Similar trends are observed in all systems and are likely related to the sizes of the polar headgroups; larger headgroups (PhdCho) tend to protrude more toward the water phase than small ones (Card). Similarly PhdEtns, with headgroups smaller than those of PhdChos, are located deeper in the membrane than PhdChos, and more in the aqueous phase than Cards. Due to these discrepancies, we use the distance between points at which the water and membrane densities match as a measure for membrane thickness for all the systems. The computed values are given in Table 8.2. The values obtained are in agreement with the area per chain given; namely they show an inverse relation, as expected.

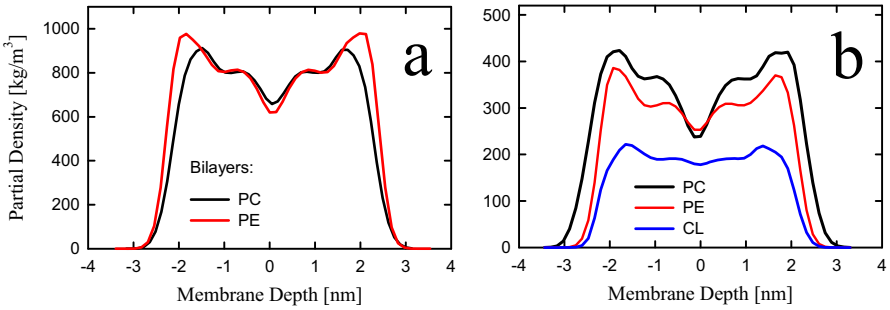

Figure 8.3: Partial density profiles along the bilayer normal. (a) PC and PE bilayers; (b) PC-PE-CL bilayer. The coordinate z = 0 corresponds to the membrane center.

To characterize the order of the acyl chains, profiles of the molecular order parameter S_{mol} are shown in Fig. 8.4. The order parameter for the nth segment of an acyl chain, S_{mol}, was calculated using Eq. 3.7. As Fig. 8.4 shows, the presence of Card molecules increases the order of the PhdCho chains but it has practically no influence on the PhdEtn acyl chains. This is in agreement with the changes in the surface area. In the PC-PE-CL mixture (Fig. 8.4d), the chain ordering of all lipid species is close to each other, though PhdChos are slightly more ordered than PhdEtns and Cards, and PhdEtns are somewhat more ordered than Cards. These small differences are in agreement with the slightly different positions of these lipids along the bilayer normal (Fig. 8.3b).

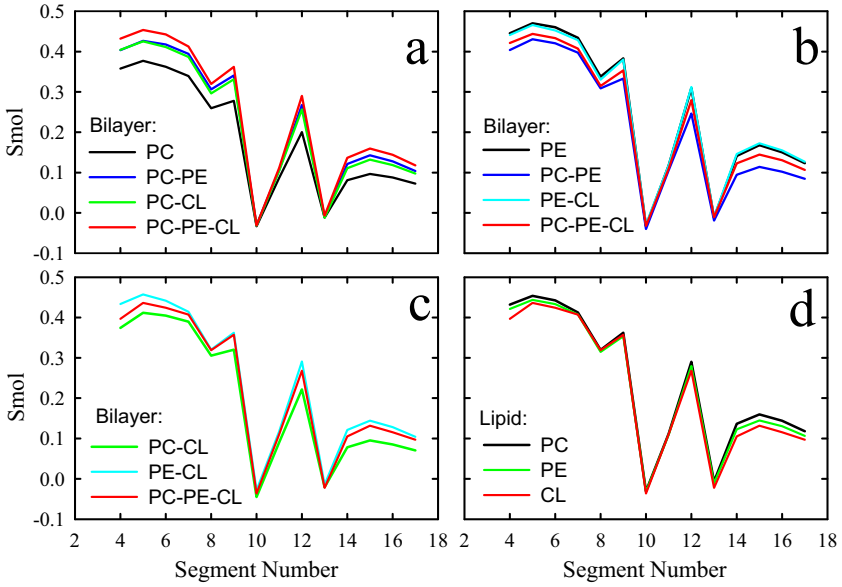

Figure 8.4: Profiles of the molecular order parameter (S_{mol}) calculated for *sn*–1 chains of (a) PhdCho, (b) PhdEtn, and (c) Card molecules, comparison in different bilayers. (d) PhdCho, PhdEtn, Card molecules in the PC-PE-CL bilayer. Results for segments 2–3 are not included due to the carbonyl group; the description in that case is not well defined.

8.4.2 Membrane-Water Interface

The rotational autocorrelation functions (see Eq. 3.12) of the PN vectors of PhdChos and PhdEtns are shown in Fig. 8.5. The effect of Cards on the headgroup dynamics is clear from Fig. 8.5: Cards restrict the rotation of both the PhdCho and PhdEtn headgroups. The effect is, however, much stronger for PhdChos. It is interesting that there is no strong correlation between the rotation of the PN vector and the surface area accessible for the PhdCho and PhdEth headgroups. Although it can be found that rotation rates follow the trends observed for surface area in the considered bilayers, a similar change of area can lead to very large or to merely moderate effects. The lack of simple correlation is likely to result from the intermolecular interactions, whose number and strength depend on the particular composition. This issue is discussed in more detail in the following sections.

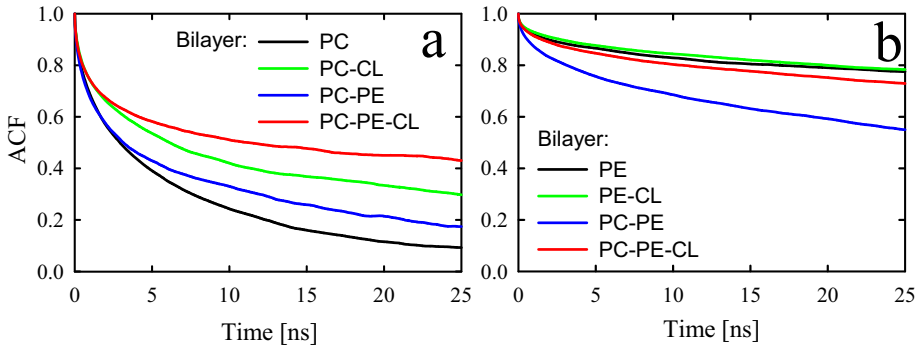

Figure 8.5: Rotational autocorrelation function of the PN vector of (a) PhdCho and (b) PhdEtn molecules in the different analyzed bilayers.

	lipid		
Membrane	PhdChol	PhdEtn	Card
PC	7.54		
PC-CL	7.56		13.99 (6.99)
PC-PE	7.58	9.63	
PC-PE-CL	7.40	9.85	13.34 (6.67)
PE		9.66	
PE-CL		9.56	13.63 (6.81)

Table 8.3: Number of hydrogen bonds between any oxygen in lipids and water. The number of hydrogen bonds assuming that one Card molecule is equivalent to two PhdCho molecules is provided in parenthesis. Errors are less than 0.05.

	pairs					
Membrane	A-A per A	A-B per A(B)	A-C per A(C)	B-B Per B	B-C per B(C)	C-C Per C
PC	1.02					
PC-CL	1.15		0.00(0.01)		13.99(6.99)	0.24
PC-PE	0.58	0.74(0.89)		1.96		
PC-PE-CL	0.48	0.35(0.42	0.02(0.06)	1.57	0.51(1.67)	0.08
PE				4.46		
PE-CL				3.81	0.02(0.16)	0.27

Table 8.4: Number of intermolecular water bridges between lipid molecules. A, B and C correspond to PhdCho, PhdEtn and Card molecules, respectively. Errors are about 5%.

The number of hydrogen bonds between water and any hydrogen bond acceptor or donor atom of lipid molecules and the number of water bridges between lipid headgroups are given in Tables 8.3 and 8.4. The number of hydrogen bonds between the water molecules and lipids is similar in all bilayers; the observed differences are in the range of 2–5%. The differences between the lipid species are likely to be related to the headgroup positions along the bilayer normal (Cards are located deeper in the membrane and are, thus, less hydrated) and to the differences between the surface areas of the membrane systems (larger areas correlate with higher hydration). On average, a PhdCho binds to about 7.5 water molecules, a PhdEtn binds to about 9.5 water molecules (including hydrogen bonds with the amino group), and finally a Card binds to about 13.5 water molecules. The number of water molecules hydrating the choline groups is similar in each of the bilayers, about 11 water molecules per PhdCho (not shown). Water bridges are most common linking two PhdEtn molecules. The presence of Cards, and especially of PhdChos, decreases the number of water bridges (Table 8.4).

Finally, to describe the dynamics of hydration, we calculated the autocorrelation function for hydrogen bonded water with any lipid molecule, as described in Eq. 3.15. This analysis follows the approach of Rapaport [Rapa83], Chandra [Chan00] and Balasubramanian et al. [Bala02] for the dynamics of hydrogen bonding. The computed autocorrelation functions

shown in Fig. 8.6 indicate that the presence of Cards stabilizes water bonding. PhdEtns are found to bond the water molecules more strongly than PhdChos.

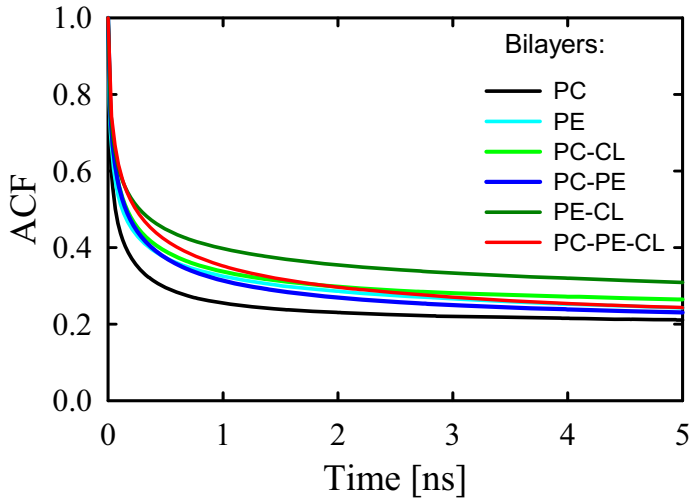

Figure 8.6: Autocorrelation function of water bonding with membrane surface in PC, PE, PC-PE, PC-CL, PE-CL, and PC-PE-CL bilayers.

8.4.3 Intermolecular Hydrogen Bonding

Unlike PhdChos, both PhdEtns and Cards are capable of participating in hydrogen bonding as hydrogen donors due to the presence of an ammonium group in PhdEtn and a hydroxyl group in Card. The numbers of hydrogen bonds between PhdEtns and other lipids are given in Table 8.5. The highest number of intermolecular hydrogen bonds is observed in the ternary PC-PE-CL bilayer. This is surprising since the comparison of the pure PhdEtn membrane with PC-PE and PE-CL do not reveal any increment of the hydrogen bond occurrence. This observation emphasizes the fact that the properties of ternary mixtures cannot be simply deduced from less complex binary systems. PhdEtn molecules also form a significant number of intramolecular hydrogen bonds and their number follows the values of the corresponding surface areas (when the area is larger, the headgroups are more extended and the number of intramolecular hydrogen bonds is lower). At this point it is important to specify that in contrast to previous models of PhdEtns, in our model these intramolecular hydrogen bonds appear to be more dynamic, in agreement with experimental data. We also analyzed the role of each of the oxygen atoms from the lipid species in the establishment of hydrogen bonds with PhdEtn molecules. We observe that the phosphate oxygens O13 and O14 are the predominant hydrogen bond acceptors (80–90% of hydrogen bonds). Instead, hydrogen bonds between ammonium groups and carbonyl oxygens (O22 and O32) are rare. This pattern is practically the same for all membrane and lipid types. In contrast, the Card hydroxyl group does not participate in intermolecular hydrogen bonding. This group is mainly involved in interactions with water and rarely in intra-molecular bonding.

To better describe the dynamics of hydrogen bonds between lipid pairs, we checked their stability in different membranes by means of Eq. 3.15. We observed that the same pair of lipids (PhdEtn-PhdEtn, PhdCho-PhdEtn, PhdEtn-Card) present different behavior depending on the system (not shown); however, as a general trend, the PhdEtn-PhdEtn

Membrane	B-B *intra*	B-B *inter*	A-B	B-C	Total *inter*
PE	1.78	2.97			2.97
PE-CL	1.63	2.67		0.36(2.59)	3.03
PC-PE	1.61	1.80	0.89(0.74)		2.69
PC-PE-CL	1.39	1.37	1.56(1.33)	0.51(1.67)	3.44

Table 8.5: Average number of hydrogen bonds between the PhdEtn ammonium group and other lipids per PhdEtn (PhdCho or Card in parenthesis). A, B and C correspond to PhdCho, PhdEtn and Card molecules, respectively. Errors are less than 0.05.

Membrane	A-A *intra*	A-A *inter*	A-B	A-C	Total
PC	0.34	3.01			3.01
PC-CL	0.32	2.04		0.79(5.67)	2.83
PC-PE	0.32	1.56	0.69(0.84)		2.25
PC-PE-CL	0.25	0.64	0.46(0.54)	0.91(3.51)	2.01

Table 8.6: Average number of inter- and intramolecular charge pairs per PhdCho (PhdEtn or Card in parenthesis). A, B and C correspond to PhdCho, PhdEtn and Card molecules, respectively. Errors are less than 0.04.

bonds are found to be the most stable ones, the PhdEtn-Card bonds being somewhat stable but less than the previous ones, while the PhdEtn-PhdCho bonds are the least stable.

8.4.4 Charge Pairing

While PhdCho molecules do not participate in hydrogen bonds as hydrogen donors, they can be connected via charge pairs due to electrostatic interactions between the positively charged choline groups and the negatively charged oxygen atoms [Pase00]. The number of inter- and intra-molecular charge pairs given in Table 8.6 show that the number of charge pairs per PhdCho molecule is reduced in mixed bilayers compared to the pure PC bilayer. The strongest reduction is observed in the three-component bilayer, and is not compensated for by new charge pairs with other lipids. The trend for the total number of inter-molecular charge pairs can be rationalized by its inverse relation with $t_{P\mapsto N}$. The $t_{P\mapsto N}$ for PhdCho is 99.7° for PC, 102.5° for PC-CL, 105.9° for PC-PE, and 108.9° for the PC-PE-CL system. That is, the deeper the $-N(CH_3)_3$ group penetrates to the water phase, the less accessible are the negatively charged oxygens to form charge pairs. In the case of bilayers including PhdEtns, another contribution arises from the competition for acceptors with stronger hydrogen bonds. Strong preference for charge pairs between PhdChos and Cards is observed, especially in the three-component bilayer. Interestingly, charge pairs are shown to be less selective than hydrogen bonds, presenting significant number of charge pairs with the carbonyl oxygen atoms O22 and O32 in addition to the accessible phosphate oxygen atoms O13 and O14.

Additionally, we have analyzed the stability of the charge pairs. We observe that charge

Membrane	PhdCho	PhdEtn	Card
PC-CL	0.28		0.97
PC-PE-CL	0.39	0.56	0.64
PE-CL		0.28	0.70

Table 8.7: Number of bonded ions per lipid molecules. Errors are less than 0.03.

Membrane	A-A per A	A-B per A(B)	A-C per A(C)	B-B per B	B-C per B(C)	C-C per C
PC-CL	0.21		0(0)			0.16
PC-PE-CL	0.12	0.35(0.41)	0(0)	0.30	0.19(0.62)	0
PE-CL				0.23	0.10(0.70)	0.14

Table 8.8: Number of ion bridges per lipid molecule. A, B and C correspond to PhdCho, PhdEtn and Card molecules, respectively. Errors are less than 0.02.

pairs are more stable in mixed bilayers and, in particular, the presence of Card increases the stability of charge pairs considerably. The most stable charge pairs are those between PhdChos and Cards, while the stability of PhdCho-PhdCho and PhdCho-PhdEtn charge pairs is quite similar.

8.4.5 Na^+-Lipid Interactions

In this section, we shift our attention to the ions that are included in the system to preserve the overall charge neutrality when the negative charged Cards are present. In agreement with experimental results [Alle84, Macd87], the unique nature of each ion, Na^+ in this work, does not allow the generalization of the following results to other cations, especially to divalent ones.

In agreement with previous simulations of charged lipids [Zhao07b], the sodium counterions were strongly bonded to the lipid headgroups. In our analysis, we considered the ions bonded with lipid oxygens if the distance between them was less than 0.3 nm, which correspond to the position of the first minimum in the radial distribution functions of sodium ions with respect to the lipid oxygen atoms (data not shown). Additionally we have computed the number of ion bridges. An ion is considered to be bridging two lipids if it is simultaneously bonded with their oxygen atoms. The numbers of ions bonded with lipids are given in Table 8.7, and the number of ion bridges in Table 8.8. Both tables lead us to believe the sodium ions are preferably bonded with Cards due to their net charge, and hence create numerous bridges between Cards and PhdEtns.

8.5 Discussion and Conclusions

In this chapter, we have built a detailed atomistic model for inner mitochondrial membranes containing cardiolipin (10 mol%), PhdCho (50 mol%) and PhdEtn (40mol%) molecules

(PC-PE-CL), and their properties have been characterized by large-scale atomistic Molecular Dynamics simulations. Additionally, pure and binary membranes (PC, PE, PC-PE, PC-CL and PE-CL) were used as reference systems. The number of reference systems is justified since we wanted (a) to characterize the interactions of Cards in typical two-component systems, and (b) to study a corresponding ternary system to investigate which if any, of its properties can be deduced from those of the two-component systems. Also, since this is the first atom-scale simulation study of membranes including cardiolipins, and the limited number of comparable experimental data available of the simulated systems, we preferred to focus on trends that result from the presence of Card molecules in between these membranes.

To begin with, our model shows that Cards do not tend to be aggregated when approaching equilibrium. This finding reduces the possibility of the existence of short-range attractive interactions between Cards. This observation supports the curvature-mediated mechanism [Huan06] as the only driving force for the formation of rich Card domains usually found *in vivo* [Mile09]. We also found that the effect of Card on each of the three matrices (PC-CL, PE-CL and mixed PE-PC-CL) is different. As a result, the effect of Cards in PE-PC-CL bilayer cannot be derived from the effect of Card on either of PC-CL or PE-CL systems alone. The structure of a Card molecule is unusual and its effect on the interactions seems to be non-additive.

Effect of Cards seems to be particularly strong in the case of PhdChos. The addition of Card molecules into a PhdCho bilayer leads to a small condensation in surface area and a related increase in the order of acyl chains. This result agrees with other computational and experimental data, which show a decrease in membrane permeability and increased stability when Card is present in PhdCho bilayers [Macd87]. At the interfacial region, we observed PhdChos to form charge pairs preferentially with Cards rather than with other lipids. These pairs are also considerably more stable than PhdCho-PhdCho pairs and are likely to be responsible for the observed slowing down of the rotational motion of the PhdCho headgroups. The total number of charge pairs is, nevertheless, lower in a mixed than in a pure bilayer, though it is compensated for by bonding via counterions.

In the case of PhdEtn based bilayers, Card molecules have, surprisingly, virtually no influence on membrane condensation or hydrocarbon chain order. Hydrogen bonds between PhdEtns and Cards were observed to be less frequent and less stable than those between PhdEtn molecules. The total number of hydrogen bonds is similar in pure and mixed bilayers, and headgroup rotation is almost unaffected, suggesting that intramolecular hydrogen bonding dominates over intermolecular bonding. The only additional interactions at the water-membrane interface are ion bridges.

The behavior of mixed PC-PE bilayers is very interesting as PhdCho and PhdEtn molecules influence each other's properties. This can be observed from the fact that the observed surface area of 0.635 ± 0.001 nm^2 is lower than the simple average of 0.643 nm^2 for a mixture of 70 PhdCho and 58 PhdEtn molecules. The number of PhdEtn-PhdEtn hydrogen bonds (1.80) is substantially higher than the number of PhdEtn-PhdCho hydrogen bonds (0.89), despite PhdCho molecules being in larger proportion. This contrasts with the fact that the number PhdCho-PhdCho charge pairs is larger than PhdCho-PhdEtn pairs. When Cards are added to a mixed PC-PE bilayer membrane, the surface area remains unaffected while the interface region becomes less dynamic; rotations of both PhdCho and PhdEtn headgroups slow down. Rotation of the PhdCho headgroups in PC-PE-CL bilayer is the slowest among all three

bilayer systems while the rotational motions of the PhdEtn headgroups are similar to those found in pure PE and PE-CL bilayers. In agreement with experiments [Pinh94], we find that the tilt of the PN vector of PhdChos in the ternary systems increases by 9° compared to a pure PhdCho bilayer. In the experiments of Pinheiro et al., the change in the PN dipole orientation was ∼6° and increased for increasing Card concentration [Pinh94]. In general, the effect of Cards in a PE-PC-CL bilayer leads to a complex behavior that cannot be deduced from the binary (PE-CL, PC-CL) systems.

At the molecular interaction level, we observed that the PhdEtn-PhdEtn hydrogen bonds are more common and stable than the PhdEtn-PhdCho and PhdEtn-Card ones, and that the PhdCho-Card charge pairs are the most frequent and stable. It should be stressed that in the ternary systems, the total number of hydrogen bonds is the highest among all membranes while the number of charge pairs is the lowest. This indicates stronger interlipid interactions in the PC-PE-CL bilayer than in any of the other bilayers.

In conclusion, we observed that the effects of Cards in ternary membrane systems are complex and cannot be easily deduced from its behavior in binary mixtures. Interestingly, Cards had virtually no effect on PhdEtn in a binary mixture contrary to the PhdCho one. This last point is likely to be important for the role of Cards in mitochondria as the stabilization-destabilization of the inner membrane is one of the most important factors in mitochondrial apoptosis.

Bibliography

[AAqv93] J. Åqvist and A. Warshel. "Simulation of enzyme reactions using valence bond force fields and other hybrid quantum/classical approaches". *Chem. Rev.*, Vol. 93, No. 7, pp. 2523–2544, 1993.

[Aitt06] J. Aittoniemi, T. Róg, P. Niemela, M. Pasenkiewicz-Gierula, M. Karttunen, and I. Vattulainen. "Tilt: Major Factor in Sterols' Ordering Capability in Membranes". *J. Phys. Chem. B*, Vol. 110, No. 51, pp. 25562–25564, 2006.

[Aitt07] J. Aittoniemi, P. S. Niemelä, M. T. Hyvönen, M. Karttunen, and I. Vattulainen. "Insight into the Putative Specific Interactions between Cholesterol, Sphingomyelin, and Palmitoyl-Oleoyl Phosphatidylcholine". *Biophys. J.*, Vol. 92, No. 4, pp. 1125–1137, Feb. 2007.

[Alde59] B. J. Alder and T. E. Wainwright. "Studies in Molecular Dynamics. I. General Method". *J. Chem. Phys.*, Vol. 31, No. 2, pp. 459–466, 1959.

[Alec82] M. R. Alecio, D. E. Golan, W. R. Veatch, and R. R. Rando. "Use of a fluorescent cholesterol derivative to measure lateral mobility of cholesterol in membranes". *Proc. Natl. Acad. Sci. U. S. A.*, Vol. 79, No. 17, pp. 5171–5174, Sep. 1982.

[Ales07] A. Alessandrini, G. Valdrè, U. Valdrè, and U. Muscatello. "Defects in ordered aggregates of cardiolipin visualized by atomic force microscopy.". *Chem. Phys. Lipids*, Vol. 146, No. 2, pp. 111–124, Apr 2007.

[Ali07] M. R. Ali, K. H. Cheng, and J. Huang. "Assess the nature of cholesterol–lipid interactions through the chemical potential of cholesterol in phosphatidylcholine bilayers". *Proc. Natl. Acad. Sci. U. S. A.*, Vol. 104, No. 13, pp. 5372–5377, March 2007.

[Ali98] S. Ali, J. M. Smaby, M. M. Momsen, H. L. Brockman, and R. E. Brown. "Acyl chain-length asymmetry alters the interfacial elastic interactions of phosphatidylcholines.". *Biophys. J.*, Vol. 74, No. 1, pp. 338–348, Jan 1998.

[Alle06] D. Allender and M. Schick. "Phase Separation in Bilayer Lipid Membranes: Effects on the Inner Leaf Due to Coupling to the Outer Leaf". *Biophys. J.*, Vol. 91, No. 8, pp. 2928–2935, Oct. 2006.

[Alle84] P. R. Allegrini, G. Pluschke, and J. Seelig. "Cardiolipin conformation and dynamics in bilayer membranes as seen by deuterium magnetic resonance". *Biochemistry*, Vol. 23, No. 26, pp. 6452–6458, 1984.

[Alle90] M. P. Allen and D. J. Tildesley. *Computer Suimulation of Liquids.* Oxford University Press, New York, 1990.

[Alme95] P. F. F. Almeida and V. W. L. C. "Lateral diffusion in membranes". In: *Structure and Dynamics of Membranes: From Cells to Vesicles*, pp. 305–357, Elsevier, Amsterdam, The Netherlands, 1995.

[Ande02] R. G. W. Anderson and K. Jacobson. "A Role for Lipid Shells in Targeting Proteins to Caveolae, Rafts, and Other Lipid Domains". *Science*, Vol. 296, No. 5574, pp. 1821–1825, June 2002.

[Angl07] T. C. Anglin, J. Liu, and J. C. Conboy. "Facile Lipid Flip-Flop in a Phospholipid Bilayer Induced by Gramicidin A Measured by Sum-Frequency Vibrational Spectroscopy". *Biophys. J.*, Vol. 92, No. 1, pp. L01–L03, Jan. 2007.

[Avel87] M. Aveldano and H. Sprecher. "Very long chain (C24 to C36) polyenoic fatty acids of the n-3 and n-6 series in dipolyunsaturated phosphatidylcholines from bovine retina". *J. Biol. Chem.*, Vol. 262, No. 3, pp. 1180–1186, Jan. 1987.

[Bach04] M. Bachar, P. Brunelle, D. P. Tieleman, and A. Rauk. "Molecular Dynamics Simulation of a Polyunsaturated Lipid Bilayer Susceptible to Lipid Peroxidation". *J. Phys. Chem. B*, Vol. 108, No. 22, pp. 7170–7179, 2004.

[Bako96] D. Bakowies and W. Thiel. "Hybrid Models for Combined Quantum Mechanical and Molecular Mechanical Approaches". *J. Phys. Chem.*, Vol. 100, No. 25, pp. 10580–10594, 1996.

[Bala02] S. Balasubramanian, S. Pal, and B. Bagchi. "Hydrogen-bond dynamics near a micellar surface: origin of the universal slow relaxation at complex aqueous interfaces.". *Phys. Rev. Lett.*, Vol. 89, No. 11, p. 115505, Sep 2002.

[Bare99] Y. Barenholz and T. E. Thompson. "Sphingomyelin: biophysical aspects". *Chem. Phys. Lipids*, Vol. 102, pp. 29–34, 1999.

[Baum05] A. Baumketner and J.-E. Shea. "The Influence of Different Treatments of Electrostatic Interactions on the Thermodynamics of Folding of Peptides?". *J. Phys. Chem. B*, Vol. 109, No. 45, pp. 21322–21328, Nov. 2005.

[Beat05] M. E. Beattie, S. L. Veatch, B. L. Stottrup, and S. L. Keller. "Sterol structure determines miscibility versus melting transitions in lipid vesicles.". *Biophys. J.*, Vol. 89, No. 3, pp. 1760–1768, Sep 2005.

[Benz05] R. W. Benz, F. Castro-Roman, D. J. Tobias, and S. H. White. "Experimental Validation of Molecular Dynamics Simulations of Lipid Bilayers: A New Approach". *Biophys. J.*, Vol. 88, No. 2, pp. 805–817, Feb. 2005.

[Berc81] T. Berclaz and H. M. McConnell. "Phase equilibriums in binary mixtures of dimyristoylphosphatidylcholine and cardiolipin". *Biochemistry*, Vol. 20, No. 23, pp. 6635–6640, 1981.

[Berc84] T. Berclaz and M. Geoffroy. "Spin-labeling study of phosphatidylcholine-cardiolipin binary mixtures". *Biochemistry*, Vol. 23, No. 18, pp. 4033–4037, 1984.

[Bere81] H. J. C. Berendsen, J. P. M. Postma, W. F. van Gunsteren, and J. Hermans. *Intermolecular Forces*, Chap. Interaction models for water in relation to protein hydration, pp. 331–342. Reidel, Dordrecht, The Netherlands, 1981.

[Bere84] H. J. C. Berendsen, J. P. M. Postma, W. F. van Gunsteren, A. DiNola, and J. R. Haak. "Molecular dynamics with coupling to an external bath". *J. Chem. Phys.*, Vol. 81, No. 8, pp. 3684–3690, 1984.

[Bere98] H. J. C. Berendsen. *Computational Molecular Dynamics: Challenges, Methods, Ideas*, Chap. Molecular Dynamics Simulations: The Limits and Beyond, pp. 3–36. Vol. 4 of *Lecture Notes in Computational Science and Engineering*, Springer Verlag, 1998.

[Berg97] O. Berger, O. Edholm, and F. Jähnig. "Molecular dynamics simulations of a fluid bilayer of dipalmitoylphosphatidylcholine at full hydration, constant pressure, and constant temperature". *Biophys. J.*, Vol. 72, No. 5, pp. 2002–2013, May 1997.

[Berk09] M. L. Berkowitz. "Detailed molecular dynamics simulations of model biological membranes containing cholesterol". *Biochim. Biophys. Acta, Biomembr.*, Vol. 1788, No. 1, pp. 86–96, Jan. 2009.

[Bloc91] K. Bloch. *Biochemistry of Lipids, Lipoproteins and Membranes*, Chap. Cholesterol: evolution of structure and function, pp. 363–381. Elsevier, Amsterdam, 1991.

[Bloo88] M. Bloom and O. G. Mouritsen. "The evolution of membranes". *Can. J. Chem.*, Vol. 66, pp. 706–712, 1988.

[Bloo91] M. Bloom, E. Evans, and O. G. Mouritsen. "Physical properties of the fluid lipid-bilayer component of cell membranes: a perspective.". *Q. Rev. Biophys.*, Vol. 24, pp. 293–397, 1991.

[Blum82] A. Blume, D. M. Rice, R. J. Wittebort, and R. G. Griffin. "Molecular dynamics and conformation in the gel and liquid-crystalline phases of phosphatidylethanolamine bilayers". *Biochemistry*, Vol. 21, No. 24, pp. 6220–6230, 1982.

[Boci78] D. F. Bocian and S. I. Chan. "NMR Studies of Membrane Structure and Dynamics". *Annu. Rev. Phys. Chem.*, Vol. 29, No. 1, pp. 307–335, 1978.

[Bock03] R. A. Böckmann, A. Hac, T. Heimburg, and H. Grubmüller. "Effect of Sodium Chloride on a Lipid Bilayer". *Biophys. J.*, Vol. 85, No. 3, pp. 1647–1655, 2003.

[Broo83] B. R. Brooks, R. E. Bruccoleri, B. D. Olafson, D. J. States, S. Swaminathan, and M. Karplus. "CHARMM: A program for macromolecular energy, minimization, and dynamics calculations". *J. Comput. Chem.*, Vol. 4, No. 2, pp. 187–217, 1983.

[Brow00] D. A. Brown and E. London. "Structure and Function of Sphingolipid- and Cholesterol-rich Membrane Rafts". *J. Biol. Chem.*, Vol. 275, No. 23, pp. 17221–17224, June 2000.

[Brow83] M. F. Brown, A. A. Ribeiro, and G. D. Williams. "New view of lipid bilayer dynamics from 2H and 13C NMR relaxation time measurements". *Proc. Natl. Acad. Sci. U. S. A.*, Vol. 80, No. 14, pp. 4325–4329, July 1983.

[Brow92] D. A. Brown and J. K. Rose. "Sorting of GPI-anchored proteins to glycolipid-enriched membrane subdomains during transport to the apical cell surface". *Cell*, Vol. 68, No. 3, pp. 533–544, Feb. 1992.

[Brow97] D. A. Brown and E. London. "Structure of Detergent-Resistant Membrane Domains: Does Phase Separation Occur in Biological Membranes?". *Biochem. Biophys. Res. Commun.*, Vol. 240, No. 1, pp. 1–7, 1997.

[Brow98] D. A. Brown and E. London. "Functions of lipid rafts in biological membranes". *Annu. Rev. Cell Dev. Biol.*, Vol. 14, No. 1, pp. 111–136, 1998.

[Bung09] A. Bunge, A.-K. Windeck, T. Pomorski, J. Schiller, A. Herrmann, D. Huster, and P. Müller. "Biophysical characterization of a new phospholipid analogue with a spin-labeled unsaturated fatty acyl chain.". *Biophys. J.*, Vol. 96, No. 3, pp. 1008–1015, Feb 2009.

[Cevc88] G. Cevc, J. M. Seddon, R. Hartung, and W. Eggert. "Phosphatidylcholine-fatty acid membranes. I. Effects of protonation, salt concentration, temperature and chain-length on the col loidal and phase properties of mixed vesicles, bilayers and nonlamellar structures". *Biochim. Biophys. Acta, Biomembr.*, Vol. 940, No. 2, pp. 219–240, 1988.

[Cevc91] G. Cevc. "How membrane chain-melting phase-transition temperature is affected by the lipid chain asymmetry and degree of unsaturation: an effective chain-length model.". *Biochemistry*, Vol. 30, No. 29, pp. 7186–7193, Jul 1991.

[Chan00] Chandra. "Effects of ion atmosphere on hydrogen-bond dynamics in aqueous electrolyte solutions". *Phys. Rev. Lett.*, Vol. 85, No. 4, pp. 768–771, Jul 2000.

[Chen97] K. Cheng, M. Ruonala, J. Virtanen, and P. Somerharju. "Evidence for superlattice arrangements in fluid phosphatidylcholine/phosphatidylethanolamine bilayers". *Biophys. J.*, Vol. 73, No. 4, pp. 1967–1976, Oct. 1997.

[Chiu02] S. Chiu, E. Jakobsson, R. J. Mashl, and H. L. Scott. "Cholesterol-Induced Modifications in Lipid Bilayers: A Simulation Study". *Biophys. J.*, Vol. 83, No. 4, pp. 1842–1853, Oct. 2002.

[Chiu99] S. Chiu, E. Jakobsson, S. Subramaniam, and H. Scott. "Combined Monte Carlo and Molecular Dynamics Simulation of Fully Hydrated Dioleyl and Palmitoyl-oleyl Phosphatidylcholine Lipid Bilayers". *Biophys. J.*, Vol. 77, No. 5, pp. 2462–2469, Nov. 1999.

[Chon09] P. L.-G. Chong, W. Zhua, and B. Venegas. "On the lateral structure of model membranes containing cholesterol". *Biochim. Biophys. Acta, Biomembr.*, Vol. 1788(1), pp. 2–11, 2009.

[Chon94a] P. L. Chong. "Evidence for regular distribution of sterols in liquid crystalline phosphatidylcholine bilayers.". *Proc. Natl. Acad. Sci. U. S. A.*, Vol. 91, No. 21, pp. 10069–10073, Oct 1994.

[Chon94b] P. L. Chong, D. Tang, and I. P. Sugar. "Exploration of physical principles underlying lipid regular distribution: effects of pressure, temperature, and radius of curvature on E/M dips in pyrene-labeled PC/DMPC binary mixtures". *Biophys. J.*, Vol. 66, No. 6, pp. 2029–2038, June 1994.

[Cook06] I. R. Cooke and M. Deserno. "Coupling between Lipid Shape and Membrane Curvature". *Biophys. J.*, Vol. 91, No. 2, pp. 487–495, July 2006.

[Corn83] B. Cornell and M. Keniry. "The effect of cholesterol and gramicidin A' on the carbonyl groups of dimyristoylphosphatidylcholine dispersions". *Biochim. Biophys. Acta, Biomembr.*, Vol. 732, No. 3, pp. 705–710, 1983.

[Cott04] K. Cottingham. "Do You Believe in Lipid Rafts?". *Anal. Chem.*, Vol. 76, No. 21, pp. 403A–406A, 2004.

[Crai78] I. F. Craig, G. S. Boyd, and K. E. Suckling. "Optimum interaction of sterol side chains with phosphatidylcholine". *Biochim. Biophys. Acta, Biomembr.*, Vol. 508, No. 2, pp. 418–421, 1978.

[Cron74] J. E. Cronan. "Regulation of the fatty acid composition of the membrane phospholipids of Escherichia coli.". *Proc. Natl. Acad. Sci. U. S. A.*, Vol. 71, No. 9, pp. 3758–3762, Sep 1974.

[Cron75] J. Cronan, J. E. and E. P. Gelmann. "Physical properties of membrane lipids: biological relevance and regulation.". *Bacteriol. Rev.*, Vol. 39, pp. 232–256, 1975.

[Czub06] J. Czub and M. Baginski. "Comparative Molecular Dynamics Study of Lipid Membranes Containing Cholesterol and Ergosterol". *Biophys. J.*, Vol. 90, No. 7, pp. 2368–2382, Apr. 2006.

[Dahl07] M. Dahlberg. "Polymorphic Phase Behavior of Cardiolipin Derivatives Studied by Coarse-Grained Molecular Dynamics". *J. Phys. Chem. B*, Vol. 111, No. 25, pp. 7194–7200, 2007.

[Dahl08] M. Dahlberg and A. Maliniak. "Molecular dynamics simulations of cardiolipin bilayers.". *J. Phys. Chem. B*, Vol. 112, No. 37, pp. 11655–11663, Sep 2008.

[Dale07] D. L. Daleke. "Phospholipid Flippases". *J. Biol. Chem.*, Vol. 282, No. 2, pp. 821–825, Jan. 2007.

[Damj95] S. Damjanovich, G. Vereb, A. Schaper, A. Jenei, J. Mató, J. P. Starink, G. Q. Fox, D. J. Arndt-Jovin, and T. M. Jovin. "Structural hierarchy in the clustering of HLA class I molecules in the plasma membrane of human lymphoblastoid cells". *Proc. Natl. Acad. Sci. U. S. A.*, Vol. 92, No. 4, pp. 1122–1126, Feb. 1995.

[Dani34] J. F. Danielli and H. Davson. "A contribution to the theory of permeability of thin films". *J. Cell. Compar. Physl.*, Vol. 5(4), pp. 495–508, 1934.

[Dard93] T. Darden, D. York, and L. Pedersen. "Particle mesh Ewald: An N [center-dot] log(N) method for Ewald sums in large systems". *J. Chem. Phys.*, Vol. 98, No. 12, pp. 10089–10092, 1993.

[Daum85] G. Daum. "Lipids of mitochondria". *Biochim. Biophys. Acta, Rev. Biomembr.*, Vol. 822, No. 1, pp. 1–42, 1985.

[Daur96] X. Daura, B. Oliva, E. Querol, F. X. Avilés, and O. Tapia. "On the sensitivity of MD trajectories to changes in water-protein interaction parameters: The potato carboxypeptidase inhibitor in water as a test case for the GROMOS force field". *Proteins*, Vol. 25, No. 1, pp. 89–103, 1996.

[Davi03] U. David Metzler, Iowa State University. *Biochemistry (2 volume set), 1 & 2The Chemical Reactions of Living Cells.* ACADEMIC PRESS, second Ed., april 2003.

[Davi79] J. Davis, B. Maraviglia, G. Weeks, and D. Godin. "Bilayer rigidity of the erythrocyte membrane 2H-NMR of a perdeuterated palmitic acid probe". *Biochim. Biophys. Acta, Biomembr.*, Vol. 550, No. 2, pp. 362–366, 1979.

[Davi80a] J. H. Davis, M. Bloom, K. W. Butler, and I. C. Smith. "The temperature dependence of molecular order and the influence of cholesterol in Acholeplasma laidlawii membranes". *Biochim. Biophys. Acta, Biomembr.*, Vol. 597, No. 3, pp. 477–491, 1980.

[Davi80b] P. J. Davis, K. P. Coolbear, and K. M. Keough. "Differential scanning calorimetric studies of the thermotropic phase behavior of membranes composed of dipalmitoyllecithin and mixed-acid unsaturated lecithins.". *Can. J. Biochem*, Vol. 58, No. 10, pp. 851–858, Oct 1980.

[Davi81] P. J. Davis, B. D. Fleming, K. P. Coolbear, and K. M. W. Keough. "Gel to liquid-crystalline transition temperatures of water dispersions of two pairs of positional isomers of unsaturated mixed-acid phosphatidylcholines". *Biochemistry*, Vol. 20, No. 12, pp. 3633–3636, 1981.

[Davi83a] J. H. Davis. "The description of membrane lipid conformation, order and dynamics by 2H-NMR". *Biochim. Biophys. Acta, Rev. Biomembr.*, Vol. 737, pp. 117–171, 1983.

[Davi83b] P. J. Davis and K. M. W. Keough. "Differential scanning calorimetric studies of aqueous dispersions of mixtures of cholesterol with some mixed-acid and single-acid phosphatidylcholines". *Biochemistry*, Vol. 22, No. 26, pp. 6334–6340, 1983.

[Davi84] P. Davis and K. Keough. "Scanning calorimetric studies of aqueous dispersions of bilayers made with cholesterol and a pair of positional isomers of 3-sn-phosphatidylcholine". *Biochim. Biophys. Acta, Biomembr.*, Vol. 778, No. 2, pp. 305–310, 1984.

[Deme72] R. Demel, K. Bruckdorfer, and L. V. Deenen. "The effect of sterol structure on the permeability of lipomes to glucose, glycerol and Rb^+". *Biochim. Biophys. Acta, Biomembr.*, Vol. 255, No. 1, pp. 321–330, 1972.

[Deva04] P. F. Devaux and R. Morris. "Transmembrane Asymmetry and Lateral Domains in Biological Membranes". *Traffic*, Vol. 5, No. 4, pp. 241–246, 2004.

[Dewe71] M. M. Dewey and L. Barr. "Some Considerations About the Structure of Cellular Membranes". In: F. Bronner and A. Kleinzeller, Eds., *Current Topics in Membranes and Transport*, pp. 1 – 33, Academic Press, 1971.

[Di95] L. Di and D. M. Small. "Physical Behavior of the Hydrophobic Core of Membranes: Properties of 1-Stearoyl-2-linoleoyl-sn-glycerol". *Biochemistry*, Vol. 34, No. 51, pp. 16672–16677, 1995.

[Diet01] C. Dietrich, L. A. Bagatolli, Z. N. Volovyk, N. L. Thompson, M. Levi, K. Jacobson, and E. Gratton. "Lipid Rafts Reconstituted in Model Membranes". *Biophys. J.*, Vol. 80, No. 3, pp. 1417–1428, March 2001.

[Dimo00] R. Dimova, B. Pouligny, and C. Dietrich. "Pretransitional Effects in Dimyristoylphosphatidylcholine Vesicle Membranes: Optical Dynamometry Study". *Biophys. J.*, Vol. 79, No. 1, pp. 340–356, July 2000.

[Doug05] A. D. Douglass and R. D. Vale. "Single-Molecule Microscopy Reveals Plasma Membrane Microdomains Created by Protein-Protein Networks that Exclude or Trap Signaling Molecules in T Cells". *Cell*, Vol. 121, No. 6, pp. 937–950, June 2005.

[Dowh08] W. Dowhan, M. Bogdanov, and E. Mileykovskaya. *Biochemistry of lipids. Lipoproteins and Membranes*, Chap. Functional roles of lipids in membranes, pp. 1–37. Elsevier Press, 2008.

[Dyat74] E. V. Dyatlovitskaya, G. V. Yanchevskaya, and L. D. Bergelson. "Molecular species and membrane forming properties of lecithins in normal liver and hepatoma.". *Chem. Phys. Lipids*, Vol. 12, No. 2, pp. 132–149, Apr 1974.

[Edbe86] R. Edberg, D. J. Evans, and G. P. Morriss. "Constrained molecular dynamics: Simulations of liquid alkanes with a new algorithm". *J. Chem. Phys.*, Vol. 84, No. 12, pp. 6933–6939, 1986.

[Edho05] O. Edholm and J. F. Nagle. "Areas of Molecules in Membranes Consisting of Mixtures". *Biophys. J.*, Vol. 89, No. 3, pp. 1827–1832, Sep. 2005.

[Edid03] M. Edidin. "The state of lipid rafts: From Model Membranes to Cells". *Annu. Rev. Biophys. Biomol. Struct.*, Vol. 32, No. 1, pp. 257–283, 2003.

[Edid94] M. Edidin, M. C. Zúñiga, and M. P. Sheetz. "Truncation mutants define and locate cytoplasmic barriers to lateral mobility of membrane glycoproteins". *Proc. Natl. Acad. Sci. U. S. A.*, Vol. 91, No. 8, pp. 3378–3382, Apr. 1994.

[Eige94] M. Eigen and R. Rigler. "Sorting single molecules: application to diagnostics and evolutionary biotechnology". *Proc. Natl. Acad. Sci. U. S. A.*, Vol. 91, No. 13, pp. 5740–5747, June 1994.

[Elof93] A. Elofsson and L. Nilsson. "How Consistent are Molecular Dynamics Simulations? : Comparing Structure and Dynamics in Reduced and Oxidized Escherichia coli Thioredoxin". *J. Mol. Biol.*, Vol. 233, No. 4, pp. 766–780, 1993.

[Elso01] E. L. Elson. "Fluorescence Correlation Spectroscopy Measures Molecular Transport in Cells". *Traffic*, Vol. 2, No. 11, pp. 789–796, 2001.

[Essm95] U. Essmann, L. Perera, M. L. Berkowitz, T. Darden, H. Lee, and L. G. Pedersen. "A smooth particle mesh Ewald method". *J. Chem. Phys.*, Vol. 103, No. 19, pp. 8577–8593, 1995.

[Ewal21] P. P. Ewald. "Die berechnung optischer und elektrostatischer gitterpotentiale". *Ann. Phys.*, Vol. 64, pp. 253–287, 1921.

[Falc04] E. Falck, M. Patra, M. Karttunen, M. T. Hyvnen, and I. Vattulainen. "Lessons of Slicing Membranes: Interplay of Packing, Free Area, and Lateral Diffusion in Phospholipid/Cholesterol Bilayers". *Biophys. J.*, Vol. 87, No. 2, pp. 1076–1091, Aug. 2004.

[Feig06] G. W. Feigenson. "Phase behavior of lipid mixtures". *Nature Chem. Biol.*, Vol. 2, pp. 560–563, 2006.

[Feig09] G. W. Feigenson. "Phase diagrams and lipid domains in multicomponent lipid bilayer mixtures". *Biochim. Biophys. Acta, Biomembr.*, Vol. 1788(1), pp. 47–52, 2009.

[Fell97] S. Feller, D. Yin, R. Pastor, and A. MacKerell. "Molecular dynamics simulation of unsaturated lipid bilayers at low hydration: parameterization and comparison with diffraction studies". *Biophys. J.*, Vol. 73, No. 5, pp. 2269–2279, Nov. 1997.

[Fili03] A. Filippov, G. Oradd, and G. Lindblom. "The Effect of Cholesterol on the Lateral Diffusion of Phospholipids in Oriented Bilayers". *Biophys. J.*, Vol. 84, No. 5, pp. 3079–3086, 2003.

[Fost71] J. F. Foster and W. D. Wilson. "Conformation-dependent limited proteolysis of bovine plasma albumin by an enzyme present in commercial albumin preparations". *Biochemistry*, Vol. 10, No. 10, pp. 1772–1780, 1971.

[Frye70] L. D. Frye and M. Edidin. "The Rapid Intermixing of Cell Surface Antigens After Formation of Mouse-Human Heterokaryons". *J. Cell Sci.*, Vol. 7, No. 2, pp. 319–335, Sep. 1970.

[Full04] J. Füllerkrug and K. Simons. "Lipid Rafts and Apical Membrane Traffic". *Annals of the New York Academy of Sciences*, Vol. 1014, No. Gastroenteropancreatic Neuroendocrine Tumor Disease Molecular and Cell Biological Aspects, pp. 164–169, 2004.

[Gao96] J. Gao. *Reviews in Computational Chemistry*, Chap. Methods and applications of combined quantum mechanical and molecular mechanical potentials, pp. 119–185. Vol. 7, VCH Publishers, New York, 1996.

[Garb95] S. Garbay, N. Rozes, and A. Lonvaud-Funel. "Fatty acid composition of Leuconostoc oenos, incidence of growth conditions and relationship with malolactic efficiency". *Food Microbiology*, Vol. 12, pp. 387–395, 1995.

[Gaus03] K. Gaus, E. Gratton, E. P. W. Kable, A. S. Jones, I. Gelissen, L. Kritharides, and W. Jessup. "Visualizing lipid structure and raft domains in living cells with two-photon microscopy". *Proc. Natl. Acad. Sci. U. S. A.*, Vol. 100, No. 26, pp. 15554–15559, 2003.

[Ge98] M. Ge and J. H. Freed. "Polarity Profiles in Oriented and Dispersed Phosphatidylcholine Bilayers Are Different: An Electron Spin Resonance Study". *Biophys. J.*, Vol. 74, No. 2, pp. 910–917, Feb. 1998.

[Genn89] R. B. Gennis. *Biomembranes-Molecular Structure and Function.* Springer-Verlag, New York, 1989.

[Gers78] N. L. Gershfeld. "Equilibrium Studies of Lecithin-Cholesterol Interactions: I. Stoichiometry of Lecithin-Cholesterol Complexes in Bulk Systems". *Biophys. J.*, Vol. 22, No. 3, pp. 469–488, June 1978.

[Gold69] L. V. Golde, G. Scherphof, and L. V. Deenen. "Biosynthetic pathways in the formation of individual molecular species of rat liver phospholipids". *Biochim. Biophys. Acta, Lipids Lipid Metab.*, Vol. 176, No. 3, pp. 635–637, 1969.

[Gome99] B. Gomez and N. C. Robinson. "Quantitative determination of cardiolipin in mitochondrial electron transferring complexes by silicic acid high-performance liquid chromatography.". *Anal Biochem*, Vol. 267, No. 1, pp. 212–216, Feb 1999.

[Gonz07] F. Gonzalvez and E. Gottlieb. "Cardiolipin: setting the beat of apoptosis.". *Apoptosis*, Vol. 12, No. 5, pp. 877–885, May 2007.

[Gort25] E. Gorter and F. Grendel. "On bimolecular layers of lipoids on the chromocytes of the blood". *J. Exp. Med.*, Vol. 41, pp. 439–443, 1925.

[Grah04] T. R. Graham. "Flippases and vesicle-mediated protein transport". *Trends Cell Biol.*, Vol. 14, No. 12, pp. 670–677, 2004.

[Gros06] A. Grossfield, S. E. Feller, and M. C. Pitman. "Contribution of omega-3 fatty acids to the thermodynamics of membrane protein solvation.". *J. Phys. Chem. B*, Vol. 110, No. 18, pp. 8907–8909, May 2006.

[Grov06] J. T. Groves. "CHEMISTRY: Unveiling the Membrane Domains". *Science*, Vol. 313, No. 5795, pp. 1901–1902, Sep. 2006.

[Guns87] W. F. van Gunsteren and H. J. C. Berendsen. *Gromos-87 manual*. Biomos BV, Nijenborgh 4, 9747 AG Groningen, The Netherlands, 1987.

[Guns98] W. F. van Gunsteren, X. Daura, and A. E. Mark. *Encyclopedia of Computational Chemistry*, Chap. Gromos force field, pp. 1211–1216. Wiley, 1998.

[Habe77] R. A. Haberkorn, R. G. Griffin, M. D. Meadows, and E. Oldfield. "Deuterium nuclear magnetic resonance investigation of the dipalmitoyl lecithin-cholesterol-water system". *J. Am. Chem. Soc.*, Vol. 99, No. 22, pp. 7353–7355, 1977.

[Hail92] J. Haile. *Molecular dynamics simulation. Elementary methods*. Wiley, 1992.

[Hain01] T. H. Haines. "Do sterols reduce proton and sodium leaks through lipid bilayers?". *Prog. Lipid Res.*, Vol. 40, No. 4, pp. 299–324, July 2001.

[Hair97] E. Hairer and D. Stoffer. "Reversible Long-Term Integration with Variable Stepsizes". *SIAM J. Sci. Comput.*, Vol. 18, No. 1, pp. 257–269, 1997.

[Harv98] S. C. Harvey, R. K.-Z. Tan, and T. E. C. III. "The flying ice cube: Velocity rescaling in molecular dynamics leads to violation of energy equipartition". *J. Comput. Chem.*, Vol. 19, No. 7, pp. 726–740, 1998.

[Helm04] J. B. Helms and C. Zurzolo. "Lipids as Targeting Signals: Lipid Rafts and Intracellular Trafficking". *Traffic*, Vol. 5, No. 4, pp. 247–254, 2004.

[Hess02] B. Hess. "Determining the shear viscosity of model liquids from molecular dynamics simulations". *J. Chem. Phys.*, Vol. 116, No. 1, pp. 209–217, 2002.

[Hess97] B. Hess, H. Bekker, H. J. C. Berendsen, and J. G. E. M. Fraaije. "LINCS: A linear constraint solver for molecular simulations". *J. Comput. Chem.*, Vol. 18, No. 12, pp. 1463–1472, 1997.

[Hoch92] F. L. Hoch. "Cardiolipins and biomembrane function.". *Biochim. Biophys. Acta*, Vol. 1113, No. 1, pp. 71–133, Mar 1992.

[Hock70] R. W. Hockney. "The Potential Calculation and Some Applications". *Methods in Computational Physics*, Vol. 9, pp. 136–211, 1970.

[Hofs03] C. Hofsäß, E. Lindahl, and O. Edholm. "Molecular Dynamics Simulations of Phospholipid Bilayers with Cholesterol". *Biophys. J.*, Vol. 84, No. 4, pp. 2192–2206, Apr. 2003.

[Holt01] M. Höltje, T. Förster, B. Brandt, T. Engels, W. von Rybinski, and H.-D. Höltje. "Molecular dynamics simulations of stratum corneum lipid models: fatty acids and cholesterol". *Biochim. Biophys. Acta, Biomembr.*, Vol. 1511, No. 1, pp. 156–167, March 2001.

[Hook65] R. Hooke. *Micrographia, or, Some physiological descriptions of minute bodies made by magnifying glasses.* John Martyn and James Allestry, London, 1665.

[Hoov85] W. G. Hoover. "Canonical dynamics: Equilibrium phase-space distributions". *Phys. Rev. A*, Vol. 31, No. 3, pp. 1695–1697, March 1985.

[Horr99] D. F. Horrobin. "Lipid metabolism, human evolution and schizophrenia.". *Prostaglandins Leukot Essent Fatty Acids*, Vol. 60, No. 5-6, pp. 431–437, 1999.

[Hovi90] R. Hovius, H. Lambrechts, K. Nicolay, and B. de Kruijff. "Improved methods to isolate and subfractionate rat liver mitochondria. Lipid composition of the inner and outer membrane.". *Biochim. Biophys. Acta*, Vol. 1021, No. 2, pp. 217–226, Jan 1990.

[Hsu02] L.-Y. Hsu, J. W. Kampf, and C. E. Nordman. "Structure and pseudosymmetry of cholesterol at 310 K". *Acta Cryst. B*, Vol. 58, pp. 260–264, 2002.

[Huan01] C. hsien Huang. "Mixed-chain phospholipids: Structures and chain-melting behavior". *Lipids*, Vol. 36, pp. 1077–1097, 2001.

[Huan02] J. Huang. "Exploration of Molecular Interactions in Cholesterol Superlattices: Effect of Multibody Interactions". *Biophys. J.*, Vol. 83, No. 2, pp. 1014–1025, Aug. 2002.

[Huan06] K. C. Huang, R. Mukhopadhyay, and N. S. Wingreen. "A curvature-mediated mechanism for localization of lipids to bacterial poles.". *PLoS Comput Biol*, Vol. 2, No. 11, p. e151, Nov 2006.

[Huan77] C.-H. Huang. "A structural model for the cholesterol-phosphatidylcholine complexes in bilayer membranes". *Lipids*, Vol. 12, No. 4, pp. 348–356, Apr. 1977.

[Huan99] J. Huang and G. W. Feigenson. "A Microscopic Interaction Model of Maximum Solubility of Cholesterol in Lipid Bilayers". *Biophys. J.*, Vol. 76, No. 4, pp. 2142–2157, Apr. 1999.

[Hubb68] W. L. Hubbell and H. M. McConnell. "Spin-label studies of the excitable membranes of nerve and muscle". *Proc. Natl. Acad. Sci. U. S. A.*, Vol. 61, No. 1, pp. 12–16, Sep. 1968.

[Hui83] S. W. Hui and N. B. He. "Molecular organization in cholesterol-lecithin bilayers by x-ray and electron diffraction measurements". *Biochemistry*, Vol. 22, No. 5, pp. 1159–1164, 1983.

[Hulb03] A. J. Hulbert. "Life, death and membrane bilayers". *J. Exp. Biol.*, Vol. 206, No. 14, pp. 2303–2311, July 2003.

[Hung07] W.-C. Hung, M.-T. Lee, F.-Y. Chen, and H. W. Huang. "The Condensing Effect of Cholesterol in Lipid Bilayers". *Biophys. J.*, Vol. 92, No. 11, pp. 3960–3967, June 2007.

[Ichi99] H. Ichimori, T. Hata, H. Matsuki, and S. Kaneshina. "Effect of unsaturated acyl chains on the thermotropic and barotropic phase transitions of phospholipid bilayer membranes". *Chem. Phys. Lipids*, Vol. 100, No. 1-2, pp. 151 – 164, 1999.

[Inok78] Y. Inoko and T. Mitsui. "Structural Parameters of Dipalmitoyl Phosphatidylcholine Lamellar Phases and Bilayer Phase Transitions". *J. Phys. Soc. Jpn.*, Vol. 44, No. 6, pp. 1918–1924, 1978.

[Inou99] T. Inoue, T. Kitahashi, and Y. Nibu. "Phase behavior of hydrated bilayer of binary phospholipid mixtures composed of 1,2-distearoylphosphatidylcholine and 1-stearoyl-2-oleoylphosphatidylcholine or 1-oleoyl-2-stearoylphosphatidylcholine". *Chem. Phys. Lipids*, Vol. 99, pp. 103–109, 1999.

[Iske98] S. Isken and J. A. M. de Bont. "Bacteria tolerant to organic solvents". *Extremophiles*, Vol. 2, No. 3, pp. 229–238, Aug. 1998.

[Isra80] J. N. Israelachvili, S. Marcelja, and R. G. Horn. "Physical principles of membrane organization". *Q. Rev. Biophys.*, Vol. 13, pp. 121–200, 1980.

[Isra91] J. Israelachvili. *Intermolecular and surface forces.* ACADEMIC PRESS, University of California, Santa Barbara, second Ed., NOV 1991. ISBN-13: 978-0-12-375181-2 ISBN-10: 0-12-375181-0.

[Jaco79] R. Jacobs and E. Oldfield. "Deuterium nuclear magnetic resonance investigation of dimyristoyllecithin-dipalmitoyllecithin and dimyristoyllecithin-cholesterol mixtures". *Biochemistry*, Vol. 18, No. 15, pp. 3280–3285, 1979.

[Jaco95] K. Jacobson, E. D. Sheets, and R. Simson. "Revisiting the fluid mosaic model of membranes". *Science*, Vol. 268, pp. 1441–1442, 1995.

[Jame75] T. James. *Nuclear Magnetic Resonance in Biochemistry*, Chap. 8, p. 413. New York: Academic, 1975.

[Jani76] M. J. Janiak, D. M. Small, and G. G. Shipley. "Nature of the thermal pretransition of synthetic phospholipids: dimyristoyl- and dipalmitoyllecithin". *Biochemistry*, Vol. 15, No. 21, pp. 4575–4580, Oct. 1976.

[Jorg83] W. L. Jorgensen, J. Chandrasekhar, J. D. Madura, R. W. Impey, and M. L. Klein. "Comparison of simple potential functions for simulating liquid water". *J. Chem. Phys.*, Vol. 79, No. 2, pp. 926–935, 1983.

[Jorg84] W. L. Jorgensen, J. D. Madura, and C. J. Swenson. "Optimized intermolecular potential functions for liquid hydrocarbons". *J. Am. Chem. Soc.*, Vol. 106, No. 22, pp. 6638–6646, 1984.

[Jorg88] W. L. Jorgensen and J. Tirado-Rives. "The OPLS [optimized potentials for liquid simulations] potential functions for proteins, energy minimizations for crystals of cyclic peptides and crambin". *J. Am. Chem. Soc.*, Vol. 110, No. 6, pp. 1657–1666, 1988.

[Jorg96] W. L. Jorgensen, D. S. Maxwell, and J. Tirado-Rives. "Development and Testing of the OPLS All-Atom Force Field on Conformational Energetics and Properties of Organic Liquids". *J. Am. Chem. Soc.*, Vol. 118, No. 45, pp. 11225–11236, Jan. 1996.

[Kami01] G. A. Kaminski, R. A. Friesner, J. Tirado-Rives, and W. L. Jorgensen. "Evaluation and Reparametrization of the OPLS-AA Force Field for Proteins via Comparison with Accurate Quantum Chemical Calculations on Peptides". *J. Phys. Chem. B*, Vol. 105, No. 28, pp. 6474–6487, July 2001.

[Kane98] F. Kaneko, J. Yano, and K. Sato. "Diversity in the fatty-acid conformation and chain packing of cis-unsaturated lipids". *Curr. Opin. Struct. Biol.*, Vol. 8(4), pp. 417–425, 1998.

[Katz94] Y. Katz. "Anesthesia and the Meyer-Overton rule. I: Potencies and perturbations". *J. Theor. Biol.*, Vol. 167(2), pp. 93–97, 1994.

[Ke65] B. Ke. "Optical rotatory dispersion of chloroplast-lamellae fragments". *Arch. Biochem. Biophys.*, Vol. 112, No. 3, pp. 554–561, 1965.

[Kill98] J. A. Killian. "Hydrophobic mismatch between proteins and lipids in membranes.". *Biochim. Biophys. Acta*, Vol. 1376, No. 3, pp. 401–415, Nov 1998.

[Kino77] K. Kinosita, S. Kawato, and A. Ikegami. "A theory of fluorescence polarization decay in membranes". *Biophys. J.*, Vol. 20, No. 3, pp. 289–305, Dec. 1977.

[Kobe98] M. Köberl, H. J. Hinz, and G. Rapp. "Temperature scanning simultaneous small- and wide-angle X-ray scattering studies on glycolipid vesicles: areas, expansion coefficients and hydration". *Chem. Phys. Lipids*, Vol. 91, No. 1, pp. 13–37, 1998.

[Kol04] M. A. Kol, A. I. P. M. de Kroon, J. A. Killian, and B. de Kruijff. "Transbilayer Movement of Phospholipids in Biogenic Membranes". *Biochemistry*, Vol. 43, No. 10, pp. 2673–2681, 2004.

[Korl99] J. Korlach, P. Schwille, W. W. Webb, and G. W. Feigenson. "Characterization of lipid bilayer phases by confocal microscopy and fluorescence correlation spectroscopy". *Proc. Natl. Acad. Sci. U. S. A.*, Vol. 96, No. 15, pp. 8461–8466, July 1999.

[Korn69] E. D. Korn. "Cell Membranes: Structure and Synthesis". *Annu. Rev. Biochem.*, Vol. 38, No. 1, pp. 263–288, 1969.

[Koyn98] R. Koynova and M. Caffrey. "Phases and phase transitions of the phosphatidylcholines". *Biochim. Biophys. Acta, Rev. Biomembr.*, Vol. 1376, No. 1, pp. 91–145, 1998.

[Kraf02] E. Kraffe, P. Soudant, Y. Marty, N. Kervarec, and P. Jehan. "Evidence of a tetradocosahexaenoic cardiolipin in some marine bivalves.". *Lipids*, Vol. 37, No. 5, pp. 507–514, May 2002.

[Kraf06] M. L. Kraft, P. K. Weber, M. L. Longo, I. D. Hutcheon, and S. G. Boxer. "Phase Separation of Lipid Membranes Analyzed with High-Resolution Secondary Ion Mass Spectrometry". *Science*, Vol. 313, No. 5795, pp. 1948–1951, Sep. 2006.

[Krau04] F. Krause, N. H. Reifschneider, D. Vocke, H. Seelert, S. Rexroth, and N. A. Dencher. “"Respirasome"-like supercomplexes in green leaf mitochondria of spinach.”. *J. Biol. Chem.*, Vol. 279, No. 46, pp. 48369–48375, Nov 2004.

[Kuo79] A.-L. Kuo and C. G. Wade. “Lipid lateral diffusion by pulsed nuclear magnetic resonance”. *Biochemistry*, Vol. 18, No. 11, pp. 2300–2308, 1979.

[Kusu04] A. Kusumi, I. Koyama-Honda, and K. Suzuki. “Molecular Dynamics and Interactions for Creation of Stimulation-Induced Stabilized Rafts from Small Unstable Steady-State Rafts”. *Traffic*, Vol. 5, No. 4, pp. 213–230, 2004.

[Kusu93] A. Kusumi, Y. Sako, and M. Yamamoto. “Confined lateral diffusion of membrane receptors as studied by single particle tracking (nanovid microscopy). Effects of calcium-induced differentiation in cultured epithelial cells”. *Biophys. J.*, Vol. 65, No. 5, pp. 2021–2040, Nov. 1993.

[Kusu96] A. Kusumi and Y. Sako. “Cell surface organization by the membrane skeleton”. *Curr. Opin. Cell Biol.*, Vol. 8(4), pp. 566–574, 1996.

[Kuuc05a] N. Kučerka, Y. Liu, N. Chu, H. I. Petrache, S. Tristram-Nagle, and J. F. Nagle. “Structure of fully hydrated fluid phase DMPC and DLPC lipid bilayers using X-ray scattering from oriented multilamellar arrays and from unilamellar vesicles.”. *Biophys. J.*, Vol. 88, No. 4, pp. 2626–2637, Apr 2005.

[Kuuc05b] N. Kučerka, S. Tristram-Nagle, and J. Nagle. “Structure of Fully Hydrated Fluid Phase Lipid Bilayers with Monounsaturated Chains”. *J. Membr. Biol.*, Vol. 208, No. 3, pp. 193–202, Jan. 2005.

[Kuuc06] N. Kučerka, S. Tristram-Nagle, and J. F. Nagle. “Closer Look at Structure of Fully Hydrated Fluid Phase DPPC Bilayers”. *Biophys. J.*, Vol. 90, No. 11, pp. L83–L85, June 2006.

[Kuuc08a] N. Kučerka, J. F. Nagle, J. N. Sachs, S. E. Feller, J. Pencer, A. Jackson, and J. Katsaras. “Lipid Bilayer Structure Determined by the Simultaneous Analysis of Neutron and X-Ray Scattering Data”. *Biophys. J.*, Vol. 95, No. 5, pp. 2356–2367, Sep. 2008.

[Kuuc08b] N. Kučerka, J. D. Perlmutter, J. Pan, S. Tristram-Nagle, J. Katsaras, and J. N. Sachs. “The Effect of Cholesterol on Short- and Long-Chain Monounsaturated Lipid Bilayers as Determined by Molecular Dynamics Simulations and X-Ray Scattering”. *Biophys. J.*, Vol. 95, No. 6, pp. 2792–2805, Sep. 2008.

[Lako99] J. Lakowicz. *Principles of fluorescence spectroscopy.* Kluwer Academic-Plenum Publishers., 2 Ed., 1999.

[Leac01] A. R. Leach. *Molecular Modeling: Principles and applications.* Pearson, Prentice Hall, England, 2nd Ed., 2001.

[LeCo64] J. LeCocq and C. E. Ballou. “On the Structure of Cardiolipin”. *Biochemistry*, Vol. 3, No. 7, pp. 976–980, May 1964.

[Leeu80] S. W. de Leeuw, J. W. Perram, and E. R. Smith. “Simulation of Electrostatic Systems in Periodic Boundary Conditions. I. Lattice Sums and Dielectric Constants”. *P. R. Soc. London. A*, Vol. 373, No. 1752, pp. 27–56, Oct. 1980.

[Lena07] G. Lenaz and M. L. Genova. "Kinetics of integrated electron transfer in the mitochondrial respiratory chain: random collisions vs. solid state electron channeling.". *Am J Physiol Cell Physiol*, Vol. 292, No. 4, pp. C1221–C1239, Apr 2007.

[Lena66] J. Lenard and S. J. Singer. "Protein conformation in cell membranes preparations as studied by optical rotatory dispersion and circular dichroism". *Proc. Natl. Acad. Sci. U. S. A.*, Vol. 56, No. 6, pp. 1828–1835, Dec. 1966.

[Levy98] R. M. Levy and E. Gallicchio. "Computer simulations with explicit solvent: Recent Progress in the Thermodynamic Decomposition of Free Energies and in Modeling Electrostatic Effects". *Annu. Rev. Phys. Chem.*, Vol. 49, No. 1, pp. 531–567, 1998.

[Lewi88] R. N. A. H. Lewis, B. D. Sykes, and R. N. McElhaney. "Thermotropic phase behavior of model membranes composed of phosphatidylcholines containing cis-monounsaturated acyl chain homologs of oleic acid: differential scanning calorimetric and phosphorus-31 NMR spectroscopic studies". *Biochemistry*, Vol. 27, No. 3, pp. 880–887, 1988.

[Li03] X.-M. Li, M. M. Momsen, H. L. Brockman, and R. E. Brown. "Sterol Structure and Sphingomyelin Acyl Chain Length Modulate Lateral Packing Elasticity and Detergent Solubility in Model Membranes". *Biophys. J.*, Vol. 85, No. 6, pp. 3788–3801, Dec. 2003.

[Li07] Z. Li, T. K. Hailemariam, H. Zhou, Y. Li, D. C. Duckworth, D. A. Peake, Y. Zhang, M.-S. Kuo, G. Cao, and X.-C. Jiang. "Inhibition of sphingomyelin synthase (SMS) affects intracellular sphingomyelin accumulation and plasma membrane lipid organization". *Biochim. Biophys. Acta, Mol. Cell Biol. Lipids*, Vol. 1771, No. 9, pp. 1186–1194, 2007.

[Lind01a] E. Lindahl and O. Edholm. "Molecular dynamics simulation of NMR relaxation rates and slow dynamics in lipid bilayers". *J. Chem. Phys.*, Vol. 115, No. 10, pp. 4938–4950, 2001.

[Lind01b] E. Lindahl, B. Hess, and D. van der Spoel. "GROMACS 3.0: a package for molecular simulation and trajectory analysis". *J. Mol. Model.*, Vol. 7, No. 8, pp. 306–317, Aug. 2001.

[Lind81] G. Lindblom, L. B. A. Johansson, and G. Arvidson. "Effect of cholesterol in membranes. Pulsed nuclear magnetic resonance measurements of lipid lateral diffusion". *Biochemistry*, Vol. 20, No. 8, pp. 2204–2207, 1981.

[Lipa80] G. Lipari and A. Szabo. "Effect of librational motion on fluorescence depolarization and nuclear magnetic resonance relaxation in macromolecules and membranes". *Biophys. J.*, Vol. 30, No. 3, pp. 489–506, June 1980.

[Liu04] Y. Liu and J. F. Nagle. "Diffuse scattering provides material parameters and electron density profiles of biomembranes". *Phys. Rev. E*, Vol. 69, No. 4, p. 040901, Apr. 2004.

[Lohn91] K. Lohner. "Effects of small organic molecules on phospholidpid phase transitions". *Chem. Phys. Lipids*, Vol. 57, No. 2-3, pp. 341–362, 1991.

[Lope05] I. Lopez-Montero, N. Rodriguez, S. Cribier, A. Pohl, M. Velez, and P. F. Devaux. "Rapid Transbilayer Movement of Ceramides in Phospholipid Vesicles and in Human Erythrocytes". *J. Biol. Chem.*, Vol. 280, No. 27, pp. 25811–25819, July 2005.

[Lupi08] S. Lupi, A. Perla, P. Maselli, F. Bordi, and S. Sennato. "Infrared spectra of phosphatidylethanolamine-cardiolipin binary system". *Colloids Surf. B Biointerfaces*, Vol. 64, No. 1, pp. 56–64, 2008.

[Macd87] P. M. Macdonald and J. Seelig. "Calcium binding to mixed cardiolipin-phosphatidylcholine bilayers as studied by deuterium nuclear magnetic resonance". *Biochemistry*, Vol. 26, No. 19, pp. 6292–6298, May 1987.

[Mack04] A. D. Mackerell. "Empirical force fields for biological macromolecules: Overview and issues". *J. Comput. Chem.*, Vol. 25, No. 13, pp. 1584–1604, 2004.

[MacK98] A. D. MacKerell, D. Bashford, Bellott, R. L. Dunbrack, J. D. Evanseck, M. J. Field, S. Fischer, J. Gao, H. Guo, S. Ha, D. Joseph-McCarthy, L. Kuchnir, K. Kuczera, F. T. K. Lau, C. Mattos, S. Michnick, T. Ngo, D. T. Nguyen, B. Prodhom, W. E. Reiher, B. Roux, M. Schlenkrich, J. C. Smith, R. Stote, J. Straub, M. Watanabe, J. Wiorkiewicz-Kuczera, D. Yin, and M. Karplus. "All-Atom Empirical Potential for Molecular Modeling and Dynamics Studies of Proteins". *J. Phys. Chem. B*, Vol. 102, No. 18, pp. 3586–3616, 1998.

[Mara82] B. Maraviglia, J. H. Davis, M. Bloom, J. Westerman, and K. W. Wirtz. "Human erythrocyte membranes are fluid down to -5C". *Biochim. Biophys. Acta, Biomembr.*, Vol. 686, No. 1, pp. 137–140, 1982.

[Marr07] S. J. Marrink, H. J. Risselada, S. Yefimov, D. P. Tieleman, and A. H. de Vries. "The MARTINI force field: coarse grained model for biomolecular simulations.". *J Phys Chem B*, Vol. 111, No. 27, pp. 7812–7824, Jul 2007.

[Marr09] S. J. Marrink, A. H. de Vries, and D. P. Tieleman. "Lipids on the move: Simulations of membrane pores, domains, stalks and curves". *Biochim. Biophys. Acta, Biomembr.*, Vol. 1788, No. 1, pp. 149–168, Jan. 2009.

[Mars07] D. Marsh. "Lateral Pressure Profile, Spontaneous Curvature Frustration, and the Incorporation and Conformation of Proteins in Membranes". *Biophys. J.*, Vol. 93, No. 11, pp. 3884–3899, Dec. 2007.

[Mars08] D. Marsh. "Energetics of Hydrophobic Matching in Lipid-Protein Interactions". *Biophys. J.*, Vol. 94, No. 10, pp. 3996–4013, May 2008.

[Mars81] D. Marsh. *Membrane Spectroscopy*, Chap. Electron Spin Resonance: Spin Labels, pp. 51–142. Springer-Verlag, 1981.

[Mars99] D. Marsh. "Thermodynamic Analysis of Chain-Melting Transition Temperatures for Monounsaturated Phospholipid Membranes: Dependence on cis-Monoenoic Double Bond Position". *Biophys. J.*, Vol. 77, No. 2, pp. 953–963, Aug. 1999.

[Mart07] H. Martinez-Seara, T. Róg, M. Pasenkiewicz-Gierula, I. Vattulainen, M. Karttunen, and R. Reigada. "Effect of Double Bond Position on Lipid Bilayer Properties: Insight through Atomistic Simulations". *J. Phys. Chem. B*, Vol. 111, No. 38, pp. 11162–11168, 2007.

[Mart08a] H. Martinez-Seara, T. Róg, M. Karttunen, R. Reigada, and I. Vattulainen. "Influence of cis double-bond parametrization on lipid membrane properties: How seemingly insignificant details in force-field change even qualitative trends". *J. Chem. Phys.*, Vol. 129, No. 10, p. 105103, 2008.

[Mart08b] H. Martinez-Seara, T. Róg, M. Pasenkiewicz-Gierula, I. Vattulainen, M. Karttunen, and R. Reigada. "Interplay of Unsaturated Phospholipids and Cholesterol in Membranes: Effect of the Double-Bond Position". *Biophys. J.*, Vol. 95, No. 7, pp. 3295–3305, Oct. 2008.

[Mart09] H. Martinez-Seara, T. Róg, M. Karttunen, I. Vattulainen, and R. Reigada. "Why is the *sn*-2 Chain of Monounsaturated Glycerophospholipids Usually Unsaturated whereas the *sn*-1 Chain Is Saturated? Studies of 1-Stearoyl-2-oleoyl-*sn*-glycero-3-phosphatidylcholine (SOPC) and 1-Oleoyl-2-stearoyl-*sn*-glycero-3-phosphatidylcholine (OSPC) Membranes with and without Cholesterol". *J. Phys. Chem. B*, Vol. 113, No. 24, pp. 8347–8356, June 2009.

[Mash01] R. J. Mashl, H. L. Scott, S. Subramaniam, and E. Jakobsson. "Molecular Simulation of Dioleoylphosphatidylcholine Lipid Bilayers at Differing Levels of Hydration". *Biophys. J.*, Vol. 81, No. 6, pp. 3005–3015, Dec. 2001.

[Math08] J. C. Mathai, S. Tristram-Nagle, J. F. Nagle, and M. L. Zeidel. "Structural Determinants of Water Permeability through the Lipid Membrane". *J. Gen. Physiol.*, Vol. 131, pp. 69–73, 2008.

[Mats06] K. Matsumoto, J. Kusaka, A. Nishibori, and H. Hara. "Lipid domains in bacterial membranes.". *Mol. Microbiol.*, Vol. 61, No. 5, pp. 1110–1117, Sep 2006.

[Mayo04] S. Mayor and M. Rao. "Rafts: Scale-Dependent, Active Lipid Organization at the Cell Surface". *Traffic*, Vol. 5, No. 4, pp. 231–240, 2004.

[McCa94] J. L. McCauley. *Chaos, Dynamics, and Fractals: an Algorithmic Approach to Deterministic Chaos*. Cambridge University Press, Cambridge, 1994.

[McCo03] H. M. McConnell and A. Radhakrishnan. "Condensed complexes of cholesterol and phospholipids". *Biochim. Biophys. Acta, Biomembr.*, Vol. 1610, No. 2, pp. 159–173, 2003.

[McCo05] H. McConnell. "Complexes in Ternary Cholesterol-Phospholipid Mixtures". *Biophys. J.*, Vol. 88, No. 4, pp. L23–L25, Apr. 2005.

[McCo71a] H. M. McConnell and W. L. Hubbell. "Molecular motion in spin-labeled phospholipids and membranes". *J. Am. Chem. Soc.*, Vol. 93, No. 2, pp. 314–326, 1971.

[McCo71b] H. M. McConnell and R. D. Kornberg. "Inside-outside transitions of phospholipids in vesicle membranes". *Biochemistry*, Vol. 10, No. 7, pp. 1111–1120, 1971.

[McEl82] R. N. McElhaney. "Effects of Membrane Lipids on Transport and Enzymic Activities". *Curr. Top. Membr. Trans.*, Vol. 17, pp. 317–380, 1982.

[Meck03] K. R. Mecke, T. Charitat, and F. Graner. "Fluctuating Lipid Bilayer in an Arbitrary Potential: Theory and Experimental Determination of Bending Rigidity". *Langmuir*, Vol. 19, No. 6, pp. 2080–2087, 2003.

[Meer05] G. van Meer. "Cellular lipidomics". *EMBO J.*, Vol. 24, pp. 3159–3165, 2005.

[Meer08] G. van Meer, D. R. Voelker, and G. W. Feigenson. "Membrane lipids: where they are and how they behave". *Nat. Rev. Mol. Cell Biol.*, Vol. 9, No. 2, pp. 112–124, Feb. 2008.

[Meye09] F. de Meyer and B. Smit. "Effect of cholesterol on the structure of a phospholipid bilayer". *Proc. Natl. Acad. Sci. U. S. A.*, Vol. 106, No. 10, pp. 3654–3658, March 2009.

[Miao02] L. Miao, M. Nielsen, J. Thewalt, J. H. Ipsen, M. Bloom, M. J. Zuckermann, and O. G. Mouritsen. "From lanosterol to cholesterol: structural evolution and differential effects on lipid bilayers.". *Biophys. J.*, Vol. 82, No. 3, pp. 1429–1444, Mar 2002.

[Mile00] E. Mileykovskaya and W. Dowhan. "Visualization of phospholipid domains in Escherichia coli by using the cardiolipin-specific fluorescent dye 10-N-nonyl acridine orange.". *J. Bacteriol.*, Vol. 182, No. 4, pp. 1172–1175, Feb 2000.

[Mile05] E. Mileykovskaya and W. Dowhan. "Role of membrane lipids in bacterial division-site selection.". *Curr. Opin. Microbiol.*, Vol. 8, No. 2, pp. 135–142, Apr 2005.

[Mile09] E. Mileykovskaya and W. Dowhan. "Cardiolipin membrane domains in prokaryotes and eukaryotes.". *Biochim. Biophys. Acta*, Vol. 1788, No. 10, pp. 2084–2091, Oct 2009.

[Miya92] S. Miyamoto and P. A. Kollman. "Settle: An analytical version of the SHAKE and RATTLE algorithm for rigid water models". *J. Comput. Chem.*, Vol. 13, No. 8, pp. 952–962, 1992.

[Mour84] O. Mouritsen and M. Bloom. "Mattress model of lipid-protein interactions in membranes". *Biophys. J.*, Vol. 46, No. 2, pp. 141–153, Aug. 1984.

[Munr03] S. Munro. "Lipid Rafts: Elusive or Illusive?". *Cell*, Vol. 115, No. 4, pp. 377–388, Nov. 2003.

[Murt09] T. Murtola, A. Bunker, I. Vattulainen, M. Deserno, and M. Karttunen. "Multiscale modeling of emergent materials: biological and soft matter.". *Phys Chem Chem Phys*, Vol. 11, No. 12, pp. 1869–1892, Mar 2009.

[Murz01] K. Murzyn, T. Róg, G. Jezierski, Y. Takaoka, and M. Pasenkiewicz-Gierula. "Effects of Phospholipid Unsaturation on the Membrane/Water Interface: A Molecular Simulation Study". *Biophys. J.*, Vol. 81, No. 1, pp. 170–183, July 2001.

[Murz06] K. Murzyn, W. Zhao, M. Karttunen, M. Kurdziel, and T. Róg. "Dynamics of water at membrane surfaces: Effect of headgroup structure". *Biointerphases*, Vol. 1, No. 3, pp. 98–105, 2006.

[Murz99] K. Murzyn and M. Pasenkiewicz-Gierula. "Construction and optimisation of a computer model for a bacterial membrane". *Acta Biochim. Pol.*, Vol. 46(1), pp. 631–639, 1999.

[Nagl00] J. F. Nagle and S. Tristram-Nagle. "Structure of lipid bilayers". *Biochim. Biophys. Acta, Rev. Biomembr.*, Vol. 1469, No. 3, pp. 159–195, 2000.

[Nagl07] J. F. Nagle, J. C. Mathai, M. L. Zeidel, and S. Tristram-Nagle. "Theory of Passive Permeability through Lipid Bilayers". *J. Gen. Physiol.*, Vol. 131, No. 1, pp. 77–85, Dec. 2007.

[Need88] D. Needham, T. J. McIntosh, and E. Evans. "Thermomechanical and transition properties of dimyristoylphosphatidylcholine/cholesterol bilayers". *Biochemistry*, Vol. 27, No. 13, pp. 4668–4673, 1988.

[Nich05] S. Nichols-Smith and T. Kuhl. "Electrostatic interactions between model mitochondrial membranes.". *Colloids Surf. B Biointerfaces*, Vol. 41, No. 2-3, pp. 121–127, Mar 2005.

[Niel99] M. Nielsen, L. Miao, J. H. Ipsen, M. J. Zuckermann, and O. G. Mouritsen. "Off-lattice model for the phase behavior of lipid-cholesterol bilayers". *Phys. Rev. E*, Vol. 59, No. 5, pp. 5790–5803, May 1999.

[Niem06] P. S. Niemelä, M. T. Hyvönen, and I. Vattulainen. "Influence of Chain Length and Unsaturation on Sphingomyelin Bilayers". *Biophys. J.*, Vol. 90, No. 3, pp. 851–863, Feb. 2006.

[Niem07] P. S. Niemelä, M. T. Ollila, Samuli andD Hyvönen, M. Karttunen, and I. Vattulainen. "Assessing the Nature of Lipid Raft Membranes". *PLoS Comput. Biol.*, Vol. 3, No. 2, p. e34, 02 2007.

[Nose84] S. Nosé. "A unified formulation of the constant temperature molecular dynamics methods". *J. Chem. Phys.*, Vol. 81, No. 1, pp. 511–519, 1984.

[Ohvo02] H. Ohvo-Rekilä, B. Ramstedt, P. Leppimäki, and J. P. Slotte. "Cholesterol interactions with phospholipids in membranes". *Prog. Lipid Res.*, Vol. 41, No. 1, pp. 66–97, 2002.

[Oldf78] E. Oldfield, M. Meadows, D. Rice, and R. Jacobs. "Spectroscopic studies of specifically deuterium labeled membrane systems. Nuclear magnetic resonance investigation of the effects of cholesterol in model systems". *Biochemistry*, Vol. 17, No. 14, pp. 2727–2740, 1978.

[Olli07a] S. Ollila, M. T. Hyvonen, and I. Vattulainen. "Polyunsaturation in Lipid Membranes: Dynamic Properties and Lateral Pressure Profiles". *J. Phys. Chem. B*, Vol. 111, No. 12, pp. 3139–3150, 2007.

[Olli07b] S. Ollila, T. Róg, M. Karttunen, and I. Vattulainen. "Role of sterol type on lateral pressure profiles of lipid membranes affecting membrane protein functionality: Comparison between cholesterol, desmosterol, 7-dehydrocholesterol and ketosterol". *J. Struct. Biol.*, Vol. 159, No. 2, pp. 311–323, Aug. 2007.

[Olss96] N. U. Olsson, A. J. Harding, C. Harper, and N. Salem. "High-performance liquid chromatography method with light-scattering detection for measurements of lipid class composition: analysis of brains from alcoholics". *J. Chromatogr. B*, Vol. 681, No. 2, pp. 213–218, 1996.

[Olss97] N. U. Olsson and J. N. Salem. "Molecular species analysis of phospholipids". *J. Chromatogr. B*, Vol. 692, pp. 245–256, 1997.

[Oroz08] M. Orozco, A. Noy, and A. Pérez. "Recent advances in the study of nucleic acid flexibility by molecular dynamics.". *Curr Opin Struct Biol*, Vol. 18, No. 2, pp. 185–193, Apr 2008.

[Pan06] D. Pan, W. Wang, W. Liu, L. Yang, and H. W. Huang. "Chain Packing in the Inverted Hexagonal Phase of Phospholipids: A Study by X-ray Anomalous Diffraction on Bromine-labeled Chains". *J. Am. Chem. Soc.*, Vol. 128, No. 11, pp. 3800–3807, 2006.

[Pan08] J. Pan, S. Tristram-Nagle, N. Kucerka, and J. F. Nagle. "Temperature Dependence of Structure, Bending Rigidity, and Bilayer Interactions of Dioleoylphosphatidylcholine Bilayers". *Biophys. J.*, Vol. 94, pp. 117–124, 2008.

[Pan09] J. Pan, S. Tristram-Nagle, and J. F. Nagle. "Effect of cholesterol on structural and mechanical properties of membranes depends on lipid chain saturation". *Phys. Rev. E*, Vol. 80, No. 2, p. 021931, 2009.

[Pand04] S. A. Pandit, E. Jakobsson, and H. Scott. "Simulation of the Early Stages of Nano-Domain Formation in Mixed Bilayers of Sphingomyelin, Cholesterol, and Dioleylphosphatidylcholine". *Biophys. J.*, Vol. 87, No. 5, pp. 3312–3322, Nov. 2004.

[Pand09] S. A. Pandit and H. L. Scott. "Multiscale simulations of heterogeneous model membranes". *Biochim. Biophys. Acta, Biomembr.*, Vol. 1788, No. 1, pp. 136–148, Jan. 2009.

[Pang42] M. C. Pangborn. "Isolation and purification of a serologically active phospholipid from beef heart". *J. Biol. Chem.*, Vol. 143, pp. 247–256, 1942.

[Papa07] A. Papadopulos, S. Vehring, I. Lopez-Montero, L. Kutschenko, M. Stockl, P. F. Devaux, M. Kozlov, T. Pomorski, and A. Herrmann. "Flippase Activity Detected with Unlabeled Lipids by Shape Changes of Giant Unilamellar Vesicles". *J. Biol. Chem.*, Vol. 282, No. 21, pp. 15559–15568, May 2007.

[Parr81] M. Parrinello and A. Rahman. "Polymorphic transitions in single crystals: A new molecular dynamics method". *J. Appl. Phys.*, Vol. 52, No. 12, pp. 7182–7190, 1981.

[Pase00] M. Pasenkiewicz-Gierula, T. Róg, K. Kitamura, and A. Kusumi. "Cholesterol Effects on the Phosphatidylcholine Bilayer Polar Region: A Molecular Simulation Study". *Biophys. J.*, Vol. 78, No. 3, pp. 1376–1389, March 2000.

[Past02] R. W. Pastor, R. M. Venable, and S. E. Feller. "Lipid Bilayers, NMR Relaxation, and Computer Simulations". *Acc. Chem. Res.*, Vol. 35(6), pp. 438–446, April 2002.

[Patr03] M. Patra, M. Karttunen, M. Hyvönen, E. Falck, P. Lindqvist, and I. Vattulainen. "Molecular Dynamics Simulations of Lipid Bilayers: Major Artifacts Due to Truncating Electrostatic Interactions". *Biophys. J.*, Vol. 84, No. 6, pp. 3636–3645, June 2003.

[Patr04] M. Patra, M. Karttunen, M. T. Hyvonen, E. Falck, and I. Vattulainen. "Lipid Bilayers Driven to a Wrong Lane in Molecular Dynamics Simulations by Subtle Changes in Long-Range Electrostatic Interactions". *J. Phys. Chem. B*, Vol. 108, No. 14, pp. 4485–4494, 2004.

[Penc06] J. Pencer, S. Krueger, C. P. Adams, and J. Katsaras. "Method of separated form factors for polydisperse vesicles". *J. Appl. Cryst.*, Vol. 39, pp. 293–303, 2006.

[Petr00] H. I. Petrache, S. W. Dodd, and M. F. Brown. "Area per Lipid and Acyl Length Distributions in Fluid Phosphatidylcholines Determined by 2H NMR Spectroscopy". *Biophys. J.*, Vol. 79, No. 6, pp. 3172–3192, Dec. 2000.

[Petr04] H. I. Petrache, S. Tristram-Nagle, K. Gawrisch, D. Harries, V. A. Parsegian, and J. F. Nagle. "Structure and Fluctuations of Charged Phosphatidylserine Bilayers in the Absence of Salt". *Biophys. J.*, Vol. 86, No. 3, pp. 1574–1586, March 2004.

[Pinh94] T. J. Pinheiro, A. A. Duralski, and A. Watts. "Phospholipid headgroup-headgroup electrostatic interactions in mixed bilayers of cardiolipin with phosphatidylcholines studied by 2H NMR.". *Biochemistry*, Vol. 33, No. 16, pp. 4896–4902, Apr 1994.

[Pitm04] M. C. Pitman, F. Suits, A. D. MacKerell, and S. E. Feller. "Molecular-Level Organization of Saturated and Polyunsaturated Fatty Acids in a Phosphatidylcholine Bilayer Containing Cholesterol". *Biochemistry*, Vol. 43, No. 49, pp. 15318–15328, Dec. 2004.

[Plow05] S. J. Plowman, C. Muncke, R. G. Parton, and J. F. Hancock. "H-ras, K-ras, and inner plasma membrane raft proteins operate in nanoclusters with differential dependence on the actin cytoskeleton". *Proc. Natl. Acad. Sci. U. S. A.*, Vol. 102, No. 43, pp. 15500–15505, Oct. 2005.

[Pomo06] T. Pomorski and A. Menon. "Lipid flippases and their biological functions". *Cell. Mol. Life Sci.*, Vol. 63, No. 24, pp. 2908–2921, Dec. 2006.

[Powe85] G. L. Powell and D. Marsh. "Polymorphic phase behavior of cardiolipin derivatives studied by 31P NMR and X-ray diffraction.". *Biochemistry*, Vol. 24, No. 12, pp. 2902–2908, Jun 1985.

[Poyr08] S. Pöyry, T. Róg, M. Karttunen, and I. Vattulainen. "Significance of Cholesterol Methyl Groups". *J. Phys. Chem. B*, Vol. 112, No. 10, pp. 2922–2929, 2008.

[Pres82] F. T. Presti, R. J. Pace, and S. I. Chan. "Cholesterol-phospholipid interaction in membranes. 2. Stoichiometry and molecular packing of cholesterol-rich domains". *Biochemistry*, Vol. 21, No. 16, pp. 3831–3835, 1982.

[Pric01] M. L. P. Price, D. Ostrovsky, and W. L. Jorgensen. "Gas-phase and liquid-state properties of esters, nitriles, and nitro compounds with the OPLS-AA force field". *J. Comput. Chem.*, Vol. 22, No. 13, pp. 1340–1352, 2001.

[Prio03] I. A. Prior, C. Muncke, R. G. Parton, and J. F. Hancock. "Direct visualization of Ras proteins in spatially distinct cell surface microdomains". *J. Cell Biol.*, Vol. 160, No. 2, pp. 165–170, Jan. 2003.

[Priv88] P. L. Privalov and S. J. Gill. "Stability of Protein Structure and Hydrophobic Interaction". *Advances in Protein Chemistry*, Vol. 39, pp. 191–234, 1988.

[Qiu 90] W. Qiu-Dong. "The global solution of the N-body problem". *Celest. Mech. Dyn. Astr.*, Vol. 50, No. 1, pp. 73–88, March 1990.

[Radh00] A. Radhakrishnan, T. G. Anderson, and H. M. McConnell. "Condensed complexes, rafts, and the chemical activity of cholesterol in membranes". *Proc. Natl. Acad. Sci. U. S. A.*, Vol. 97, No. 23, pp. 12422–12427, Nov. 2000.

[Radh01] A. Radhakrishnan, X.-M. Li, R. E. Brown, and H. M. McConnell. "Stoichiometry of cholesterol-sphingomyelin condensed complexes in monolayers". *Biochim. Biophys. Acta, Biomembr.*, Vol. 1511, No. 1, pp. 1–6, 2001.

[Radh05] A. Radhakrishnan and H. McConnell. "Condensed complexes in vesicles containing cholesterol and phospholipids". *Proc. Natl. Acad. Sci. U. S. A.*, Vol. 102, No. 36, pp. 12662–12666, Sep. 2005.

[Radh99a] A. Radhakrishnan and H. M. McConnell. "Cholesterol–Phospholipid Complexes in Membranes". *J. Am. Chem. Soc.*, Vol. 121, No. 2, pp. 486–487, 1999.

[Radh99b] A. Radhakrishnan and H. M. McConnell. "Condensed Complexes of Cholesterol and Phospholipids". *Biophys. J.*, Vol. 77, No. 3, pp. 1507–1517, Sep. 1999.

[Rahm64] A. Rahman. "Correlations in the Motion of Atoms in Liquid Argon". *Phys. Rev.*, Vol. 136, No. 2A, pp. A405–A411, Oct. 1964.

[Rahm71] A. Rahman and F. H. Stillinger. "Molecular Dynamics Study of Liquid Water". *J. Chem. Phys.*, Vol. 55, No. 7, pp. 3336–3359, 1971.

[Rams02] B. Ramstedt and J. P. Slotte. "Membrane properties of sphingomyelins". *FEBS Lett.*, Vol. 531, No. 1, pp. 33–37, 2002.

[Ranc82] M. Rance, K. R. Jeffrey, A. P. Tulloch, K. W. Butler, and I. C. Smith. "Effects of cholesterol on the orientational order of unsaturated lipids in the membranes of Acholeplasma laidlawii: A 2H-NMR study". *Biochim. Biophys. Acta, Biomembr.*, Vol. 688, No. 1, pp. 191–200, 1982.

[Rand88] R. P. Rand, N. Fuller, V. A. Parsegian, and D. C. Rau. "Variation in hydration forces between neutral phospholipid bilayers: evidence for hydration attraction.". *Biochemistry*, Vol. 27, No. 20, pp. 7711–7722, Oct 1988.

[Rapa83] D. C. Rapaport. "Hydrogen bonds in water". *Mol. Phys.*, Vol. 50, No. 5, pp. 1151–1162, 1983.

[Rawi00] W. Rawicz, K. Olbrich, T. McIntosh, D. Needham, and E. Evans. "Effect of Chain Length and Unsaturation on Elasticity of Lipid Bilayers". *Biophys. J.*, Vol. 79, No. 1, pp. 328–339, July 2000.

[Reno89] J. P. Renou, J. B. Giziewicz, I. C. P. Smith, and H. C. Jarrell. "Glycolipid membrane surface structure: orientation, conformation, and motion of a disaccharide headgroup". *Biochemistry*, Vol. 28, No. 4, pp. 1804–1814, 1989.

[Repa05] J. Repáková, J. M. Holopainen, M. R. Morrow, M. C. McDonald, P. Capková, and I. Vattulainen. "Influence of DPH on the structure and dynamics of a DPPC bilayer.". *Biophys. J.*, Vol. 88, No. 5, pp. 3398–3410, May 2005.

[Riss08] H. J. Risselada and S. J. Marrink. "The molecular face of lipid rafts in model membranes.". *Proc. Natl. Acad. Sci. U. S. A.*, Vol. 105, No. 45, pp. 17367–17372, Nov 2008.

[Rizz99] R. C. Rizzo and W. L. Jorgensen. "OPLS All-Atom Model for Amines: Resolution of the Amine Hydration Problem". *J. Am. Chem. Soc.*, Vol. 121, No. 20, pp. 4827–4836, May 1999.

[Rog01] T. Róg and M. Pasenkiewicz-Gierula. "Cholesterol effects on the phosphatidylcholine bilayer nonpolar region: a molecular simulation study.". *Biophys J*, Vol. 81, No. 4, pp. 2190–2202, Oct 2001.

[Rog03] T. Róg, K. Murzyn, and M. Pasenkiewicz-Gierula. "Molecular dynamics simulations of charged and neutral lipid bilayers: treatment of electrostatic interactions.". *Acta Biochim. Pol.*, Vol. 50, pp. 789–798, 2003.

[Rog06] T. Róg and M. Pasenkiewicz-Gierula. "Cholesterol effects on a mixed-chain phosphatidylcholine bilayer: a molecular dynamics simulation study.". *Biochimie*, Vol. 88, No. 5, pp. 449–460, May 2006.

[Rog07a] T. Róg, M. Pasenkiewicz-Gierula, I. Vattulainen, and M. Karttunen. "What Happens if Cholesterol Is Made Smoother: Importance of Methyl Substituents in Cholesterol Ring Structure on Phosphatidylcholine–Sterol Interaction". *Biophys. J.*, Vol. 92, No. 10, pp. 3346–3357, May 2007.

[Rog07b] T. Róg, I. Vattulainen, A. Bunker, and M. Karttunen. "Glycolipid Membranes through Atomistic Simulations: Effect of Glucose and Galactose Head Groups on Lipid Bilayer Properties". *J. Phys. Chem. B*, Vol. 111, No. 34, pp. 10146–10154, Aug. 2007.

[Rog08a] T. Róg, L. M. Stimson, M. Pasenkiewicz-Gierula, I. Vattulainen, and M. Karttunen. "Replacing the Cholesterol Hydroxyl Group with the Ketone Group Facilitates Sterol Flip-Flop and Promotes Membrane Fluidity". *J. Phys. Chem. B*, Vol. 112, No. 7, pp. 1946–1952, 2008.

[Rog08b] T. Róg, I. Vattulainen, M. Jansen, E. Ikonen, and M. Karttunen. "Comparison of cholesterol and its direct precursors along the biosynthetic pathway: Effects of cholesterol, desmosterol and 7-dehydrocholesterol on saturated and unsaturated lipid bilayers". *J. Chem. Phys.*, Vol. 129, No. 15, p. 154508, 2008.

[Rog09a] T. Róg, H. Martinez-Seara, N. Munck, M. Orešič, M. Karttunen, and I. Vattulainen. "Role of Cardiolipins in the Inner Mitochondrial Membrane: Insight Gained through Atom-Scale Simulations". *J. Phys. Chem. B*, Vol. 113, No. 11, pp. 3413–3422, 2009.

[Rog09b] T. Róg, M. Pasenkiewicz-Gierula, I. Vattulainen, and M. Karttunen. "Ordering effects of cholesterol and its analogues". *Biochim. Biophys. Acta, Biomembr.*, Vol. 1788, No. 1, pp. 97–121, Jan. 2009.

[Romi72] J. C. Romijn, L. M. van Golde, R. N. McElhaney, and L. L. van Deenen. "Some studies on the fatty acid composition of total lipids and phosphatidylglycerol from Acholeplasma laidlawii B and their relation to the premeability of intact cells of this organism.". *Biochim. Biophys. Acta*, Vol. 280, No. 1, pp. 22–32, Sep 1972.

[Rott79a] S. Rottem and O. Markowitz. "Membrane lipids of Mycoplasma gallisepticum: a disaturated phosphatidylcholine and a phosphatidylglycerol with an unusual positional distribution of fatty acids.". *Biochemistry*, Vol. 18, No. 14, pp. 2930–2935, Jul 1979.

[Rott79b] S. Rottem and O. Markowitz. "Unusual positional distribution of fatty acids in phosphatidylglycerol of sterol-requiring mycoplasmas.". *FEBS Lett.*, Vol. 107, No. 2, pp. 379–382, Nov 1979.

[Rube79] J. L. Rubenstein, B. A. Smith, and H. M. McConnell. "Lateral diffusion in binary mixtures of cholesterol and phosphatidylcholines". *Proc. Natl. Acad. Sci. U. S. A.*, Vol. 76, No. 1, pp. 15–18, Jan. 1979.

[Ruiz07a] M. Ruiz Villarreal. "Cell membrane detailed diagram: English version (wikipedia)". http://commons.wikimedia.org/wiki/File:Cell_membrane_detailed_diagram_en.svg.

[Ruiz07b] M. Ruiz Villarreal. "Phospholipids aqueous solution structures (Wikipedia)". http://commons.wikimedia.org/wiki/File:Phospholipids_aqueous_solution_structures.svg.

[Ruja86] C. Rujanavech and D. Silbert. "LM cell growth and membrane lipid adaptation to sterol structure". *J. Biol. Chem.*, Vol. 261, No. 16, pp. 7196–7203, June 1986.

[Ruoc82] M. J. Ruocco and G. Shipley. "Characterization of the sub-transition of hydrated dipalmitoylphosphatidylcholine bi layers. Kinetic, hydration and structural study". *Biochim. Biophys. Acta, Biomembr.*, Vol. 691, No. 2, pp. 309–320, 1982.

[Ryck77] J.-P. Ryckaert, G. Ciccotti, and H. J. C. Berendsen. "Numerical integration of the cartesian equations of motion of a system with constraints: molecular dynamics of n-alkanes". *J. Comp. Phys.*, Vol. 23, pp. 327–341, 1977.

[Sait77] Y. Saito, J. R. Silvius, and R. N. McElhaney. "Membrane lipid biosynthesis in Acholeplasma laidlawii B. Relationship between fatty acid structure and the positional distribution of esterified fatty acids in phospho- and glycolipids from growing cells.". *Arch. Biochem. Biophys.*, Vol. 182, No. 2, pp. 443–454, Aug 1977.

[Sako94] Y. Sako and A. Kusumi. "Compartmentalized structure of the plasma membrane for receptor movements as revealed by a nanometer-level motion analysis". *J. Cell Biol.*, Vol. 125, No. 6, pp. 1251–1264, June 1994.

[Sala04] C. Salaün, D. J. James, and L. H. Chamberlain. "Lipid Rafts and the Regulation of Exocytosis". *Traffic*, Vol. 5, No. 4, pp. 255–264, 2004.

[Sams01] A. V. Samsonov, I. Mihalyov, and F. S. Cohen. "Characterization of Cholesterol-Sphingomyelin Domains and Their Dynamics in Bilayer Membranes". *Biophys. J.*, Vol. 81, No. 3, pp. 1486–1500, Sep. 2001.

[Sanz06] A. Sanz, R. Pamplona, and G. Barja. "Is the mitochondrial free radical theory of aging intact?". *Antioxid. Redox Sign.*, Vol. 8, No. 3-4, pp. 582–599, 2006.

[Sanz94] J. M. Sanz-Serna and M. P. Calvo. *Numerical Hamiltonian Problems.* Chapman & Hall, London, England, 1994.

[Sast00] J. Sastre, F. V. Pallardó, J. G. de la Asunción, and J. Viña. "Mitochondria, oxidative stress and aging.". *Free Radic. Res.*, Vol. 32, No. 3, pp. 189–198, Mar 2000.

[Schl00] M. Schlame, D. Rua, and M. L. Greenberg. "The biosynthesis and functional role of cardiolipin.". *Prog. Lipid Res.*, Vol. 39, No. 3, pp. 257–288, May 2000.

[Schl02] T. Schlick. *Molecular Modeling and Simulation: An Interdisciplinary Guide.* Springer Verlag, New York, 2002.

[Schl06] M. Schlame and M. Ren. "Barth syndrome, a human disorder of cardiolipin metabolism.". *FEBS Lett.*, Vol. 580, No. 23, pp. 5450–5455, Oct 2006.

[Schl08] M. Schlame. "Cardiolipin synthesis for the assembly of bacterial and mitochondrial membranes.". *J. Lipid Res.*, Vol. 49, No. 8, pp. 1607–1620, Aug 2008.

[Schr94] R. Schroeder, E. London, and D. Brown. "Interactions between saturated acyl chains confer detergent resistance on lipids and glycosylphosphatidylinositol (GPI)-anchored proteins: GPI-anchored proteins in liposomes and cells show similar behavior". *Proc. Natl. Acad. Sci. U. S. A.*, Vol. 91, No. 25, pp. 12130–12134, Dec. 1994.

[Schu04] S. Schuck and K. Simons. "Polarized sorting in epithelial cells: raft clustering and the biogenesis of the apical membrane". *J. Cell. Sci.*, Vol. 117, No. 25, pp. 5955–5964, 2004.

[Seel74] A. Seelig and J. Seelig. "Dynamic structure of fatty acyl chains in a phospholipid bilayer measured by deuterium magnetic resonance". *Biochemistry*, Vol. 13, No. 23, pp. 4839–4845, 1974.

[Seel77] A. Seelig and J. Seelig. "Effect of a single cis double bond on the structure of a phospholipid bilayer". *Biochemistry*, Vol. 16, No. 1, pp. 45–50, 1977.

[Seel78] J. Seelig and N. Waespe-Sarcevic. "Molecular order in cis and trans unsaturated phospholipid bilayers". *Biochemistry*, Vol. 17, No. 16, pp. 3310–3315, 1978.

[Senn05] S. Sennato, F. Bordi, C. Cametti, C. Coluzza, A. Desideri, and S. Rufini. "Evidence of Domain Formation in Cardiolipin-Glycerophospholipid Mixed Monolayers. A Thermodynamic and AFM Study". *J. Phys. Chem. B*, Vol. 109, No. 33, pp. 15950–15957, 2005.

[Shar04] P. Sharma, R. Varma, R. Sarasij, Ira, K. Gousset, G. Krishnamoorthy, M. Rao, and S. Mayor. "Nanoscale Organization of Multiple GPI-Anchored Proteins in Living Cell Membranes". *Cell*, Vol. 116(4), No. 4, pp. 577–589, Feb. 2004.

[Shie81] H.-S. Shieh, L. G. Hoard, and C. E. Nordman. "The structure of cholesterol". *Acta Cryst. B*, Vol. 37, pp. 1538–1543, 1981.

[Shir94] Y. Shiratori, A. K. Okwu, and I. Tabas. "Free cholesterol loading of macrophages stimulates phosphatidylcholine biosynthesis and up-regulation of CTP: phosphocholine cytidylyltransferase". *J. Biol. Chem.*, Vol. 269, No. 15, pp. 11337–11348, Apr. 1994.

[Shoe02] S. D. Shoemaker and T. K. Vanderlick. "Intramembrane electrostatic interactions destabilize lipid vesicles.". *Biophys. J.*, Vol. 83, No. 4, pp. 2007–2014, Oct 2002.

[Shou90] A. Shouffani and B. Kanner. "Cholesterol is required for the reconstruction of the sodium- and chloride-coupled, gamma-aminobutyric acid transporter from rat brain". *J. Biol. Chem.*, Vol. 265, No. 11, pp. 6002–6008, Apr. 1990.

[Silb67] D. F. Silbert and P. R. Vagelos. "Fatty acid mutant of E. coli lacking a beta-hydroxydecanoyl thioester dehydrase". *Proc. Natl. Acad. Sci. U. S. A.*, Vol. 58, No. 4, pp. 1579–1586, Oct. 1967.

[Silv77] J. R. Silvius, Y. Saito, and R. N. McElhaney. "Membrane lipid biosynthesis in Acholeplasma laidlawii B. Investigations into the in vivo regulation of the quantity and hydrocarbon chain lengths of de novo biosynthesized fatty aicds in response to exogenously supplied fatty acids.". *Arch. Biochem. Biophys.*, Vol. 182, No. 2, pp. 455–464, Aug 1977.

[Silv82] J. R. Silvius. "Thermotropic Phase Transitions of Pure Lipids in Model Membranes and Their Modifications by Membrane Proteins". In: *Lipid-Protein Interactions*, John Wiley & Sons, New York, 1982.

[Simi88] D. Siminovitch, P. Wong, R. Berchtold, and H. Mantsch. "A comparison of the effect of one and two mono-unsaturated acyl chains on the structure of phospholipid bilayers: a high pressure infrared spectroscopic study". *Chem. Phys. Lipids*, Vol. 46, No. 2, pp. 79–87, 1988.

[Simo00] K. Simons and E. Ikonen. "How Cells Handle Cholesterol". *Science*, Vol. 290, No. 5497, pp. 1721–1726, Dec. 2000.

[Simo02] K. Simons and R. Ehehalt. "Cholesterol, lipid rafts, and disease". *J. Clin. Invest.*, Vol. 110(5), pp. 597–603, 2002.

[Simo04] K. Simons and W. L. Vaz. "Model systems, lipid rafts, and cell membranes". *Annu. Rev. Biophys. Biomol. Struct.*, Vol. 33, No. 1, pp. 269–295, 2004.

[Simo97] K. Simons and E. Ikonen. "Functional rafts in cell membranes". *Nature*, Vol. 387, No. 6633, pp. 569–572, June 1997.

[Sing72] S. J. Singer and G. L. Nicolson. "The Fluid Mosaic Model of the Structure of Cell Membranes". *Science*, Vol. 175, No. 4023, pp. 720–731, Feb. 1972.

[Slot83] J. Slotte and B. Lundberg. "Effects of cholesterol surface transfer on cholesterol and phosphatidylcholine synthesis in cultured rat arterial smooth muscle cells.". *Med. Biol.*, Vol. 61(4), pp. 223–227, 1983.

[Smit82] T. L. Smith and M. J. Gerhart. "Alterations in brain lipid composition of mice made physically dependent to ethanol". *Life Sci.*, Vol. 31, No. 14, pp. 1419–1425, 1982.

[Smon99] A. M. Smondyrev and M. L. Berkowitz. "Structure of Dipalmitoylphosphatidylcholine/Cholesterol Bilayer at Low and High Cholesterol Concentrations: Molecular Dynamics Simulation". *Biophys. J.*, Vol. 77, No. 4, pp. 2075–2089, Oct. 1999.

[Some09] P. Somerharju, J. A. Virtanen, K. H. Cheng, and M. Hermansson. "The superlattice model of lateral organization of membranes and its implications on membrane lipid homeostasis". *Biochim. Biophys. Acta, Biomembr.*, Vol. 1788(1), pp. 12–23, 2009.

[Some85] P. J. Somerharju, J. A. Virtanen, K. K. Eklund, P. Vainio, and P. K. J. Kinnunen. "1-Palmitoyl-2-pyrenedecanoyl glycerophospholipids as membrane probes: evidence for regular distribution in liquid-crystalline phosphatidylcholine bilayers". *Biochemistry*, Vol. 24, No. 11, pp. 2773–2781, 1985.

[Some99] P. Somerharju, J. A. Virtanen, and K. H. Cheng. "Lateral organisation of membrane lipids: The superlattice view". *Biochim. Biophys. Acta, Mol. Cell Biol. Lipids*, Vol. 1440, No. 1, pp. 32–48, 1999.

[Sonn07] J. Sonne, M. O. Jensen, F. Y. Hansen, L. Hemmingsen, and G. H. Peters. "Reparameterization of all-atom dipalmitoylphosphatidylcholine lipid parameters enables simulation of fluid bilayers at zero tension.". *Biophys. J.*, Vol. 92, No. 12, pp. 4157–4167, Jun 2007.

[Spoe05a] D. V. D. Spoel, E. Lindahl, B. Hess, G. Groenhof, A. E. Mark, and H. J. C. Berendsen. "GROMACS: Fast, flexible, and free". *J. Comput. Chem.*, Vol. 26, No. 16, pp. 1701–1718, 2005.

[Spoe05b] D. van der Spoel, E. Lindahl, B. Hess, C. Kutzner, A. R. van Buuren, E. Apol, P. J. Meulenhoff, D. P. Tieleman, A. L. Sijbers, K. A. Feenstra, R. van Drunen, and H. J. Berendsen. *Gromacs User Manual version 4.0.* www.gromacs.org, 2005.

[Stec02] T. L. Steck, J. Ye, and Y. Lange. "Probing Red Cell Membrane Cholesterol Movement with Cyclodextrin". *Biophys. J.*, Vol. 83, No. 4, pp. 2118–2125, Oct. 2002.

[Stei69] J. M. Steim, M. E. Tourtellotte, J. C. Reinert, R. N. McElhaney, and R. L. Rader. "Calorimetric evidence for the liquid-crystalline state of lipids in biomembrane.". *Proc. Natl. Acad. Sci. U. S. A.*, Vol. 63, No. 1, pp. 104–109, May 1969.

[Stie73] A. Stier and E. Sackmann. "Spin labels as enzyme substrates Heterogeneous lipid distribution in liver microsomal membranes". *Biochim. Biophys. Acta, Biomembr.*, Vol. 311, pp. 400–408, 1973.

[Stim07] L. Stimson, L. Dong, M. Karttunen, A. Wisniewska, M. Dutka, and T. Róg. "Stearic Acid Spin Labels in Lipid Bilayers: Insight through Atomistic Simulations". *J. Phys. Chem. B*, Vol. 111, No. 43, pp. 12447–12453, 2007.

[Stot06] B. L. Stottrup and S. L. Keller. "Phase behavior of lipid monolayers containing DPPC and cholesterol analogs.". *Biophys. J.*, Vol. 90, No. 9, pp. 3176–3183, May 2006.

[Stub84] C. D. Stubbs and A. D. Smith. "The modification of mammalian membrane polyunsaturated fatty acid composition in relation to membrane fluidity and function". *Biochim. Biophys. Acta, Rev. Biomembr.*, Vol. 779, No. 1, pp. 89–137, 1984.

[Subc03] W. K. Subczynski and A. Kusumi. "Dynamics of raft molecules in the cell and artificial membranes: approaches by pulse EPR spin labeling and single molecule optical microscopy". *Biochim. Biophys. Acta, Biomembr.*, Vol. 1610, No. 2, pp. 231–243, 2003.

[Subc07] W. K. Subczynski, A. Wisniewska, J. S. Hyde, and A. Kusumi. "Three-Dimensional Dynamic Structure of the Liquid-Ordered Domain in Lipid Membranes as Examined by Pulse-EPR Oxygen Probing". *Biophys. J.*, Vol. 92, No. 5, pp. 1573–1584, March 2007.

[Subc89] W. K. Subczynski, J. S. Hyde, and A. Kusumi. "Oxygen permeability of phosphatidylcholine–cholesterol membranes". *Proc. Natl. Acad. Sci. U. S. A.*, Vol. 86, No. 12, pp. 4474–4478, June 1989.

[Subc91] W. K. Subczynski, J. S. Hyde, and A. Kusumi. "Effect of alkyl chain unsaturation and cholesterol intercalation on oxygen transport in membranes: a pulse ESR spin labeling study". *Biochemistry*, Vol. 30, No. 35, pp. 8578–8590, 1991.

[Subc94] W. K. Subczynski, A. Wisniewska, J.-J. Yin, J. S. Hyde, and A. Kusumi. "Hydrophobic Barriers of Lipid Bilayer Membranes Formed by Reduction of Water Penetration by Alkyl Chain Unsaturation and Cholesterol". *Biochemistry*, Vol. 33, No. 24, pp. 7670–7681, 1994.

[Suck76] K. Suckling and G. Boyd. "Interactions of the cholesterol side-chain with egg lecithin a spin label study". *Biochim. Biophys. Acta, Rev. Biomembr.*, Vol. 436, No. 2, pp. 295–300, 1976.

[Suck79] K. Suckling, H. Blair, G. Boyd, I. Craig, and B. Malcolm. "The importance of the phospholipid bilayer and the length of the cholesterol molecule in membrane structure". *Biochim. Biophys. Acta, Biomembr.*, Vol. 551, No. 1, pp. 10–21, 1979.

[Sud07] M. Sud, E. Fahy, D. Cotter, A. Brown, E. A. Dennis, C. K. Glass, J. Merrill, Alfred H., R. C. Murphy, C. R. H. Raetz, D. W. Russell, and S. Subramaniam. "LMSD: LIPID MAPS structure database". *Nucl. Acids Res.*, Vol. 35, No. suppl_1, pp. D527–532, Jan. 2007.

[Suga05] I. P. Sugar and R. L. Biltonen. "Lateral Diffusion of Molecules in Two-Component Lipid Bilayer: A Monte Carlo Simulation Study". *J. Phys. Chem. B*, Vol. 109, No. 15, pp. 7373–7386, 2005.

[Taba02] I. Tabas. "Consequences of cellular cholesterol accumulation: basic concepts and physiological implications". *J. Clin. Invest.*, Vol. 110(7), pp. 905–911, 2002.

[Tafe07] F. G. Tafesse, K. Huitema, M. Hermansson, S. van der Poel, J. van den Dikkenberg, A. Uphoff, P. Somerharju, and J. C. M. Holthuis. "Both Sphingomyelin Synthases SMS1 and SMS2 Are Required for Sphingomyelin Homeostasis and Growth in Human HeLa Cells". *J. Biol. Chem.*, Vol. 282, No. 24, pp. 17537–17547, June 2007.

[Taka00] Y. Takaoka, M. Pasenkiewicz-Gierula, H. Miyagawa, K. Kitamura, Y. Tamura, and A. Kusumi. "Molecular Dynamics Generation of Nonarbitrary Membrane Models Reveals Lipid Orientational Correlations". *Biophys. J.*, Vol. 79, No. 6, pp. 3118–3138, Dec. 2000.

[Tang92] D. Tang and P. Chong. "E/M dips. Evidence for lipids regularly distributed into hexagonal super-lattices in pyrene-PC/DMPC binary mixtures at specific concentrations". *Biophys. J.*, Vol. 63, No. 4, pp. 903–910, Oct. 1992.

[Tann72] M. J. Tanner and D. H. Boxer. "Separation and some properties of the major proteins of the human erythrocyte membrane.". *Biochem. J.*, Vol. 129, No. 2, pp. 333–347, 1972.

[Tiel02] D. P. Tieleman and J. Bentz. "Molecular Dynamics Simulation of the Evolution of Hydrophobic Defects in One Monolayer of a Phosphatidylcholine Bilayer: Relevance for Membrane Fusion Mechanisms". *Biophys. J.*, Vol. 83, No. 3, pp. 1501–1510, Sep. 2002.

[Tiel96] D. P. Tieleman and H. J. C. Berendsen. "Molecular dynamics simulations of a fully hydrated dipalmitoylphosphatidylcholine bilayer with different macroscopic boundary conditions and parameters". *J. Chem. Phys.*, Vol. 105, No. 11, pp. 4871–4880, Sep. 1996.

[Tiel97] D. P. Tieleman, S. J. Marrink, and H. J. C. Berendsen. "A computer perspective of membranes: molecular dynamics studies of lipid bilayer systems". *Biochim. Biophys. Acta, Rev. Biomembr.*, Vol. 1331, No. 3, pp. 235–270, 1997.

[Tiel99] H. J. Tieleman, D. P.and Berendsen and M. S. Sansom. "An Alamethicin Channel in a Lipid Bilayer: Molecular Dynamics Simulations". *Biophys. J.*, Vol. 76, No. 4, pp. 1757–1769, Apr. 1999.

[Tour70] M. E. Tourtellotte, D. Branton, and A. Keith. "Membrane Structure: Spin Labeling and Freeze Etching of Mycoplasma laidlawii". *Proc. Natl. Acad. Sci. U. S. A.*, Vol. 66, No. 3, pp. 909–916, July 1970.

[Tris02] S. Tristram-Nagle, Y. Liu, J. Legleiter, and J. F. Nagle. "Structure of Gel Phase DMPC Determined by X-Ray Diffraction". *Biophys. J.*, Vol. 83, No. 6, pp. 3324–3335, Dec. 2002.

[Tu95] K. Tu, D. J. Tobias, and M. L. Klein. "Constant pressure and temperature molecular dynamics simulation of a fully hydrated liquid crystal phase dipalmitoylphosphatidylcholine bilayer". *Biophys. J.*, Vol. 69, No. 6, pp. 2558–2562, Dec. 1995.

[Tuck92] M. Tuckerman, B. J. Berne, and G. J. Martyna. "Reversible multiple time scale molecular dynamics". *J. Chem. Phys.*, Vol. 97, No. 3, pp. 1990–2001, 1992.

[Vain06] S. Vainio, M. Jansen, M. Koivusalo, T. Róg, M. Karttunen, I. Vattulainen, and E. Ikonen. "Significance of Sterol Structural Specificity: Demosterol connot replace cholesterol in lipid rafts". *J. Biol. Chem.*, Vol. 281, No. 1, pp. 348–355, 2006.

[Van 65] L. L. M. Van Deenen. *Progress of Chemistry of Fats and Other Lipids*, Chap. 1, pp. 1–47. Vol. 1, Pergamon, New York, 1965.

[Vanc00] D. E. Vance and H. V. den Bosch. "Cholesterol in the year 2000". *Biochim. Biophys. Acta, Mol. Cell Biol. Lipids*, Vol. 1529, No. 1-3, pp. 1–8, 2000.

[Vand94] G. Vanderkooi. "Computation of mixed phosphatidylcholine-cholesterol bilayer structures by energy minimization". *Biophys. J.*, Vol. 66, No. 5, pp. 1457–1468, May 1994.

[Varm98] R. Varma and S. Mayor. "GPI-anchored proteins are organized in submicron domains at the cell surface". *Nature*, Vol. 394, No. 6695, pp. 798–801, Aug. 1998.

[Vaz89] W. L. Vaz, E. C. Melo, and T. E. Thompson. "Translational diffusion and fluid domain connectivity in a two-component, two-phase phospholipid bilayer". *Biophys. J.*, Vol. 56, No. 5, pp. 869–876, Nov. 1989.

[Vaz90] W. L. Vaz, E. C. Melo, and T. E. Thompson. "Fluid phase connectivity in an isomorphous, two-component, two-phase phosphatidylcholine bilayer". *Biophys. J.*, Vol. 58, No. 1, pp. 273–275, July 1990.

[Vaz91] W. Vaz and P. F. Almeida. "Microscopic versus macroscopic diffusion in one-component fluid phase lipid bilayer membranes". *Biophys. J.*, Vol. 60, pp. 1553–1554, 1991.

[Veat03] S. L. Veatch and S. L. Keller. "Separation of Liquid Phases in Giant Vesicles of Ternary Mixtures of Phospholipids and Cholesterol". *Biophys. J.*, Vol. 85, No. 5, pp. 3074–3083, Nov. 2003.

[Veat05a] S. L. Veatch and S. L. Keller. "Miscibility Phase Diagrams of Giant Vesicles Containing Sphingomyelin". *Phys. Rev. Lett.*, Vol. 94, No. 14, p. 148101, Apr 2005.

[Veat05b] S. L. Veatch and S. L. Keller. "Seeing spots: Complex phase behavior in simple membranes". *Biochim. Biophys. Acta, Mol. Cell Res.*, Vol. 1746, No. 3, pp. 172–185, 2005.

[Vemu89] R. Vemuri and K. D. Philipson. "Influence of sterols and phospholipids on sarcolemmal and sarcoplasmic reticular cation transporters". *J. Biol. Chem.*, Vol. 264, No. 15, pp. 8680–8685, May 1989.

[Vere03] G. Vereb, J. Szöllösi, J. Matkó, P. Nagy, T. Farkas, L. Vígh, L. Mátyus, T. A. Waldmann, and S. Damjanovich. "Dynamic, yet structured: The cell membrane three decades after the Singer-Nicolson model". *Proc. Natl. Acad. Sci. U. S. A.*, Vol. 100, No. 14, pp. 8053–8058, July 2003.

[Verl67] L. Verlet. "Computer "Experiments" on Classical Fluids. I. Thermodynamical Properties of Lennard-Jones Molecules". *Phys. Rev.*, Vol. 159, No. 1, pp. 98–103, July 1967.

[Virt95] J. Virtanen, M. Ruonala, M. Vauhkonen, and P. Somerharju. "Lateral Organization of Liquid-Crystalline Cholesterol-Dimyristoylphosphatidylcholine Bilayers. Evidence for Domains with Hexagonal and Centered Rectangular Cholesterol Superlattices". *Biochemistry*, Vol. 34, No. 36, pp. 11568–11581, 1995.

[Vist90] M. R. Vist and J. H. Davis. "Phase equilibria of cholesterol/dipalmitoylphosphatidylcholine mixtures: deuterium nuclear magnetic resonance and differential scanning calorimetry". *Biochemistry*, Vol. 29, No. 2, pp. 451–464, 1990.

[Von 78] P. H. Von Dreele. "Estimation of lateral species separation from phase transitions in nonideal two-dimensional lipid mixtures". *Biochemistry*, Vol. 17, No. 19, pp. 3939–3943, 1978.

[Wall66] D. F. Wallach and P. H. Zahler. "Protein conformations in cellular membranes". *Proc. Natl. Acad. Sci. U. S. A.*, Vol. 56, No. 5, pp. 1552–1559, Nov. 1966.

[Wang04] J. Wang, Megha, and E. London. "Relationship between Sterol/Steroid Structure and Participation in Ordered Lipid Domains (Lipid Rafts): Implications for Lipid Raft Structure and Function". *Biochemistry*, Vol. 43, No. 4, pp. 1010–1018, 2004.

[Wang95] G. Wang, H.-n. Lin, S. Li, and C.-h. Huang. "Phosphatidylcholines with sn-1 Saturated and sn-2 cis-Monounsaturated Acyl Chains". *J. Biol. Chem.*, Vol. 270, No. 39, pp. 22738–22746, Sep. 1995.

[Warr70] R. C. Warren and R. M. Hicks. "Structure of the Subunits in the Thick Luminal Membrane of Rat Urinary Bladder". *Nature*, Vol. 227, No. 5255, pp. 280–281, July 1970.

[Wars05] D. E. Warschawski and P. F. Devaux. "Order parameters of unsaturated phospholipids in membranes and the effect of cholesterol: a 1H-13C solid-state NMR study at natural abundance.". *Eur. Biophys. J.*, Vol. 34, No. 8, pp. 987–996, Nov 2005.

[Webe96] F. J. Weber and J. A. M. de Bont. "Adaptation mechanisms of microorganisms to the toxic effects of organic solvents on membranes". *Biochim. Biophys. Acta, Rev. Biomembr.*, Vol. 1286, pp. 225–245, March 1996.

[Wein84] S. J. Weiner, P. A. Kollman, D. A. Case, U. C. Singh, C. Ghio, G. Alagona, S. Profeta, and P. Weiner. "A new force field for molecular mechanical simulation of nucleic acids and proteins". *J. Am. Chem. Soc.*, Vol. 106, No. 3, pp. 765–784, 1984.

[Wenn77] H. Wennerström and G. Lindblom. "Biological and model membranes studied by nuclear magnetic resonance of spin one half nuclei". *Q. Rev. Biophys.*, Vol. 10, No. 01, pp. 67–96, 1977.

[Wien92] M. Wiener and S. White. "Structure of a fluid dioleoylphosphatidylcholine bilayer determined by joint refinement of x-ray and neutron diffraction data. III. Complete structure". *Biophys. J.*, Vol. 61, No. 2, pp. 434–447, Feb. 1992.

[Xu05] F. Xu, S. D. Rychnovsky, J. D. Belani, H. H. Hobbs, J. C. Cohen, and R. B. Rawson. "Dual roles for cholesterol in mammalian cells". *Proc. Natl. Acad. Sci. U. S. A.*, Vol. 102, No. 41, pp. 14551–14556, Oct. 2005.

[Yeag75] P. L. Yeagle, W. C. Hutton, C. H. Huang, and R. B. Martin. "Headgroup conformation and lipid–cholesterol association in phosphatidylcholine vesicles: a 31P(1H) nuclear Overhauser effect study". *Proc. Natl. Acad. Sci. U. S. A.*, Vol. 72, No. 9, pp. 3477–3481, Sep. 1975.

[Yu73] J. Yu, D. A. Fischman, and T. L. Steck. "Selective solubilization of proteins and phospholipids from red blood cell membranes by nonionic detergents". *J. Supramol. Struct.*, Vol. 1(3), pp. 233–248, 1973.

[Zhan08] Y.-M. Zhang and C. O. Rock. "Membrane lipid homeostasis in bacteria". *Nat. Rev. Micro.*, Vol. 6, No. 3, pp. 222–233, March 2008.

[Zhao07a] J. Zhao, J. Wu, F. A. Heberle, T. T. Mills, P. Klawitter, G. Huang, G. Costanza, and G. W. Feigenson. "Phase studies of model biomembranes: Complex behavior of DSPC/DOPC/Cholesterol". *Biochim. Biophys. Acta, Biomembr.*, Vol. 1768(11), pp. 2764–2776, 2007.

[Zhao07b] W. Zhao, T. Róg, A. A. Gurtovenko, I. Vattulainen, and M. Karttunen. "Atomic-Scale Structure and Electrostatics of Anionic Palmitoyloleoylphosphatidylglycerol Lipid Bilayers with Na^+ Counterions". *Biophys. J.*, Vol. 92, No. 4, pp. 1114–1124, Feb. 2007.

Part II

Catalan Summary

Índex

Índex de Figures

Índex de Taules

Llista d'Abreviatures

Abreviatures	**Detalls**
Card	Cardiolipine
CHOL	Colesterol
DCHOL	Colesterol Pla Sense els dos Metils del Anell
DOPC	1,2–dioleil–*sn*–glícero–3–fosfatidilcolina
DSPC	1,2–distearoil–*sn*–glícero–3–fosfatidilcolina
OSPC	1–oleil–2–estearoil–*sn*–glícero–3–fosfatidilcolina
Phd	Família Glícero–fosfolípid
PhdCho	Família Glícero–fosfatidilcolina
PhdEtn	Família Glícero–fosfatidiletanolamine
POPC	1–palmitoil–2–oleil–*sn*–glícero–3–fosfatidilcolina
SL	Esfingolípid
SOPC	1–estearoil–2–oleil–*sn*–glícero–3–fosfatidilcolina
T_m	Temperatura Transició de Fase

CAPÍTOL 1

Resum en Català

1.1 Membranes Biològiques

Les membranes biològiques són fonamentals per la vida. Constitueixen l'element físic que separa la cèl·lula del seu entorn, i també sovint els seus diferents orgànuls i compartiments. Les funcions de cadascuna d'aquestes membranes són diverses. Entre les principals, i al marge de la de frontera física, podem incloure el manteniment de gradients de determinades espècies químiques, el control del transport de molècules a través de la mateixa, l'ús com a plataforma d'ancoratge per enzims i altres proteïnes, la activació enzimàtica i el moviment cel·lular conjuntament amb el citoesquelet. Les membranes són elements molt prims (<10 nm) i estan constituïdes majoritàriament per lípids i proteïnes (Fig. 1.1). La seva estructura bàsica ve donada per la naturalesa amfifílica dels lípids, que origina la formació d'estructures autoorganitzades com a conseqüència de l'intent de la part hidrofílica de maximitzar el contacte amb el medi aquós mentre que la part hidrofòbica intenta minimitzar-lo [Cook06, Isra91]. Entre aquestes estructures trobem la de bicapa, que constitueix la matriu de les membranes biològiques.

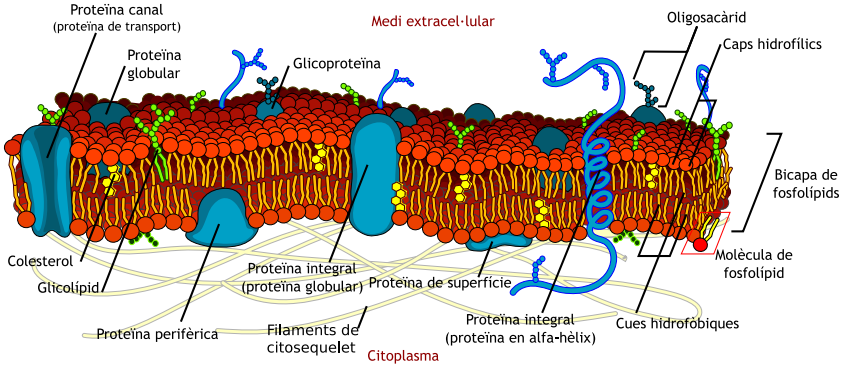

Figura 1.1: Representació esquemàtica de l'estructura de la membrana cel·lular. Figura adaptada de [Ruiz07].

Principalment, la idea que tenim sobre l'estructura i organització de les membranes és basa en el model de **mosaic fluid** [Sing72]. Aquest model introduït el 1972 descriu la membrana com una bicapa lipídica, on diferents proteïnes es troben inserides. Tant lípids com proteïnes presenten difusions lliures en el pla de la membrana, donant lloc a distribucions essencialment aleatòries d'aquests components. Tot i que aquest model encara constitueix la base conceptual de com entenem la membrana, diverses evidències experimentals recollides recentment han constatat que la distribució de lípids i proteïnes en el pla de la membrana no és ni molt menys aleatòria sinó que segueix una ordenació determinada en funció de l'estat de la cèl·lula, essencial pel seu correcte funcionament [Jaco95, Simo97]. La unificació d'aquestes observacions amb el model de mosaic fluid va ser plantejat per Vereb et al. en el seu model de **mosaic dinàmicament estructurat** que és sens dubte el referent actual en quant a l'estructura i organització de la membrana cel·lular[Vere03].

1.1.1 Estructura i Composició de les Membranes Biològiques

Les membranes cel·lulars presenten una composició que depèn fortament del seu origen (cèl·lula, orgànul, compartiment). De fet la immensa diversitat molecular de lípids i proteïnes, i les seves proporcions en diferents membranes complica el seu estudi i el correcte establiment de la relació entre composició i funcionalitat. En aquest sentit, per tal de reduir el grau de complexitat del problema que representa l'estudi de les membranes biològiques, aquesta Tesi es centra en l'estudi de membranes lipídiques model sense proteïnes.

En conjunt, els nombre de lípids identificats en membranes cel·lulars es comptabilitza en milers [Meer05, Sud07, Meer08]. Les proporcions en membrana d'aquests lípids confereixen a la cèl·lula un control específic de la funcionalitat de les seves membranes. Majoritàriament, els lípids que constitueixen les membranes es poden classificar en fosfolípids (Phd), glicolípids, esfingolípids (SL) i esterols. Tots ells presenten una part hidrofílica i una hidrofòbica. Deixant de banda els esterols, la resta de lípids de membrana difereixen entre sí majoritàriament en el grup polar (part hidrofílica) [Davi03]. En canvi, la part hidrofòbica en tots ells està constituïda fonamentalment per llargues cadenes alifàtiques lineals. Aquestes cadenes presenten llargades típiques d'entre C_{14} i C_{22} [Olss97], i poden presentar diferents graus d'insaturació [Hulb03]. Cal destacar que en cèl·lules de mamífers aquests dobles enllaços sempre tenen configuració *cis*, i són vitals en el manteniment de la fluïdesa de les membranes [McEl82, Lewi88], així com en diversos processos de reconeixement cel·lular i de regulació de la permeabilitat [Math08] i de l'activitat proteica. En general es pot assignar a cada classe lipídica una certa predilecció per un tipus cadenes. Per exemple, els SLs acostumen a presentar cadenes llargues i saturades, en contrast amb els Phds on abunden cadenes insaturades de llargades més moderades [Olss97]. Com a norma general aquests lípids estan formats per dues cadenes (Fig. 1.2a), que poden ser iguals entre elles (ex: DSPC, DPPC, DOPC) o diferents (ex: POPC). En el cas que les cadenes siguin diferents degut a què les posicions on s'enllacen no són equivalents (posicions *sn*–1 i *sn*–2), es poden tenir diferents isòmers posicionals (ex: SOPC, OSPC). L'anàlisi del rol de la insaturació i l'efecte de la isomeria en la funcionalitat de la membrana constituïda per fosfolípids és una part essencial d'aquesta Tesi.

En concret, en tots els treballs inclosos en aquesta Tesi la matriu lipídica estudiada conté íntegrament fosfolípids i, eventualment, esterols. Els fosfolípids estan formats per l'esterificació de un glicerol, amb dos àcids grassos i un grup fosfat (Fig. 1.2a). A la vegada diferents

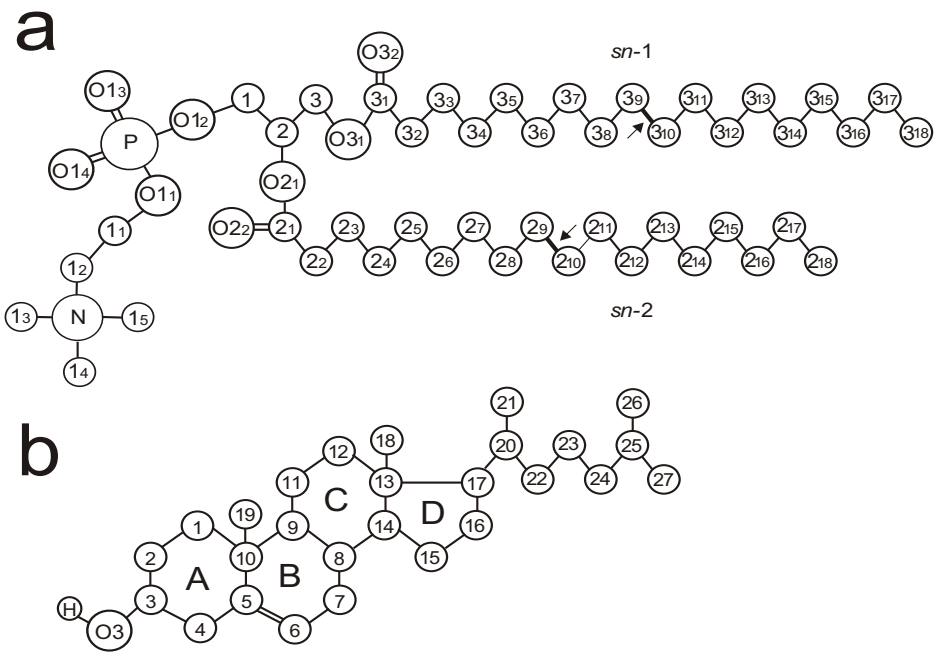

Figura 1.2: (a) Estructura molecular dels lípids DSPC i (b) colesterol amb la corresponent numeració dels àtoms emprada en aquesta Tesi. Les fletxes indican la posició del doble enllaç en el cas del fosfolípid doblement insaturat DOPC.

fragments moleculars es poden adherir al grup fosfat donant lloc a diferents caps polars, les propietats finals dels quals poden diferir substancialment (càrrega, volum, formació de ponts de hidrogen...) [Davi03]. En aquesta Tesi s'ha centrat en les fosfatidilcolines (PhdCho) per la seva abundància natural, tot i que fosfatidiletanolamines (PhdEtn) i cardiolipines (Card) s'han estudiat també en la darrera secció. Les PhdChos presenten una càrrega global neutra, de fet són Zwitteriòniques i a causa del voluminós cap polar la forma resultant de la molècula és esquemàticament cilíndrica, el que justifica el seu rol estabilitzador a les membranes amb poca curvatura. També convé assenyalar que només poden ser acceptors d'enllaços d'hidrogen. Això contrasta amb les Cards que són divalents (-2 e) o amb les PhdEtn que presenten hidròdgens capaços de formar enllaços d'hidrogen. La forma cònica d'aquests darrers lípids indica també el diferent rol estructural respecte a les PhdChos [Mars07]. Finalment destacar que els PhdCho de manera natural acostumen a tenir una cadena insaturada en la posició *sn*–2 mentre que en *sn*–1 la cadena és sovint saturada [Van 65, Romi72, Cron75, Sait77]. Concretament, en el cas que la cadena insaturada presenti un sol doble enllaç aquest es troba preferentment en el centre de la cadena (ex: àcid oleic). Aquestes darreres observacions han estat estudiades en detall en aquesta Tesi.

Finalment, i amb una gran rellevància en les membranes d'origen animal, trobem els esterols. Aquests compostos també són lípids tot i que exhibeixen estructures moleculars molt diferents a les descrites anteriorment. En particular quan ens referim a membranes animals podem restringir tots els comentaris al colesterol (CHOL), que és sens dubte un dels seus components principals [Meer08]. L'estructura del colesterol (Fig. 1.2b) es caracteritza per la presència d'una part rígida i força plana formada per quatre anells fusionats, que juntament amb una cadena alifàtica flexible enllaçada en un dels extrems constitueixen la

part hidrofòbica de la molècula. La part hidrofílica es concentra en el hidroxil que es troba a l'altre extrem de l'estructura d'anells. Cal destacar també la presència de dos metils en una de les cares de l'anell (C18 i C19), trencant la topologia plana de la cara en qüestió. O el que és el mateix, el colesterol presenta una cara llisa (cara α) i una rugosa (cara β) que conté els metils.

La presència de colesterol a les membranes té un impacte considerable en les seves propietats estructurals i dinàmiques. Entre d'altres efectes, és capaç de fluïdificar membranes que d'altre manera estarien en la seva fase gel, o d'induir ordre en membranes que es troben en una fase més líquida desordenada. Aquest darrer efecte és conegut com l'efecte condensació del colesterol. El colesterol també té una incidència fonamental en propietats com la rigidesa, permeabilitat, formació de dominis i organització lateral dels components moleculars. Aquesta gran quantitat d'efectes justifica el seu rol cabdal en multitud de funcions de membrana i el perquè la cèl·lula presenta un conjunt molt ampli de mecanismes per regular exquisidament el contingut de colesterol en les seves membranes [Simo00].

Com que la funcionalitat d'una membrana està estretament relacionada amb la seva composició i aquesta varia enormement depenent del seu origen, tots els estudis s'han d'acotar al tipus de membrana d'interès. Aquesta Tesi, per exemple, s'inspira en la composició de la matriu lipídica de la membrana plasmàtica externa de cèl·lules de mamífers. Aquesta està formada majoritàriament per Phds, SL i colesterol (fins al 40 mol% en alguns casos) [Dewe71], dels quals un 50% de les Phds corresponen a PhdChos.

Al final d'aquesta Tesi s'estudiarà també una membrana de composició totalment diferent: la membrana mitocondrial interna. Aquesta presenta una matriu lipídica formada essencialment per una mescla de PhdChos, PhdEtns i Card (5–20 mol%) [Daum85, Hovi90, Hoch92, Gome99]. Això darrer crida l'atenció ja que les Card són lípids fortament relacionats amb membranes bacterianes.

1.1.2 Termodinàmica de les Membranes Lipídiques

Atesa la complexitat inherent en les membranes biològiques, prèviament és fonamental estudiar sistemes amb nivells de complexitat força més reduïts. En aquest sentit les membranes més senzilles són les formades per un sol component (membranes pures), que poden presentar dues fases diferents. La fase gel que correspon a una fase sòlida i la fase L_α que correspon a una fase líquida coneguda també com a fase líquida desordenada i que trobem a temperatures més altes. En comparació la fase gel presenta difusions rotacionals i laterals significativament inferiors que la fase L_α [Suga05]. Una altra característica de la fase gel és que les cadenes lipídiques estan molt estirades o el que és el mateix presenten de forma quasi exclusiva conformacions *trans* (0°) dels díedres corresponents als enllaços C–C en el conjunt de les cadenes alifàtiques. En canvi, en la fase $L_\alpha$la probabilitat de conformacions *gauche* (120°) és força més elevada, i això es tradueix en membranes més primes [Dimo00, Rawi00, Meck03]i menys rígides [Kobe98, Tris02] respecte a la fase gel. La transició entre la fase gel a la $L_\alpha$és de primer ordre i a la temperatura que és produeix l'anomenarem T_m. La T_md'un lípid depèn del cap polar, la llargada de les cues i del nombre de dobles enllaços i la seva posició a les cadenes. En general lípids amb cadenes curtes i insaturades presenten $T_m$baixes (lípids de baix T_m), en canvi, aquells amb cadenes llargues i saturades presentes $T_m$altes (lípids d'elevat T_m) [Koyn98].

Per apropar-nos a la membrana plasmàtica de cèl·lules de mamífers, el següent pas és estudiar mescles binàries de lípids amb colesterol. El principal efecte de l'addició de colesterol a les membranes és l'aparició d'una nova fase líquida L_o, coneguda també com a fase líquida ordenada. Aquesta fase presenta d'alguna manera característiques intermèdies a les fases gel i L_α. Per exemple, les difusions laterals [Rube79, Lind81, Alec82] i rotacionals [Corn83] no estan gaire restringides, tot i que simultàniament la membrana és més rígida [Need88], més gruixuda [Hui83] i menys permeable [Deme72] que en la fase L_α. És important remarcar que totes aquestes característiques estan considerades com a essencials en les membranes corresponents a les cèl·lules eucariotes, posant de rellevància la importància del colesterol [Davi79, Davi80, Mara82, Ranc82, Bloo88].

S'ha de destacar també la importància dels models ternaris per capturar la fenomenologia bàsica de les membranes biològiques. Aquestes membranes models ja revelen una gran riquesa en el seu comportament fàsic, amb zones de coexistència i canvis de fase que en gran part depenen dels lípids escollits [Veat03, Veat05b, Veat05a, Feig06, Zhao07a, Feig09]. En particular, a la zona de coexistència de les fases L_α, rica en lípids de baixa T_m(insaturats i/o curts), i L_o, rica en lípids d'elevada T_m(saturats i/o llargs) i colesterol, se li atribueix una gran rellevància biològica.

1.1.3 Ordenaments Lipídics: Estructures Laterals

A aquestes alçades és important insistir en què les propietats de les membranes estan determinades per la interacció col·lectiva dels seus lípids constituents. És a dir, que no n'hi ha prou amb conèixer la composició d'una membrana, sinó que també és fonamental conèixer la distribució espacial dels components. Malauradament aquesta organització lipídica es desenvolupa a escales nanomètriques, on l'obtenció d'informació amb les actuals tècniques experimentals és en el la majoria dels casos impossible o, si més no, una font de controvèrsia en la seva interpretació. És per això que és molts casos aquest problema només és abordable des d'un punt de vista teòric, i en aquest sentit la proposició de models és una pràctica habitual. Aquests es validen en base a evidències experimentals i, si s'escau, són corregits o descartats. En aquest sentit quan parlen de membranes amb colesterol es pot pensar en quatre models límits: lípids distribuïts de forma aleatòria, lípids formant un xarxa regular, la formació de complexos entre els lípids i la formació de dominis amb diferents composicions (Fig. 1.3). Les darreres tres opcions poden tenir un sentit en un context biològic d'acord amb les evidencies experimentals de què disposem i per això seran discutits a continuació.

Entre els models disponibles per descriure l'organització dels lípids a les membranes amb colesterol trobem aquells que postulen arranjaments regulars dels lípids. El més general d'aquest models, ja que no és limita només a membranes amb colesterol, és l'anomenat **Superlattice** model o model de xarxa extensa que postula l'existència d'arranjaments regulars dels diferents lípids que formen la membrana. Cal clarificar que no postula una cobertura total de la membrana amb aquestes xarxes regulars sinó que més aviat la coexistència de regions no ordenades amb regions d'ordenament regular [Chon94b]. També conclou que per la compressibilitat dels lípids la xarxa regular és essencialment deformable i dinàmica (Fig. 1.3b). El mecanisme que justifica aquest model és la suposició que lípids semblants tendeixen a estar el més separats possible entre ells. Això condiciona l'aparició d'estructures regulars en proporcions lipídiques específiques. Excel·lents reculls sobre el model i les

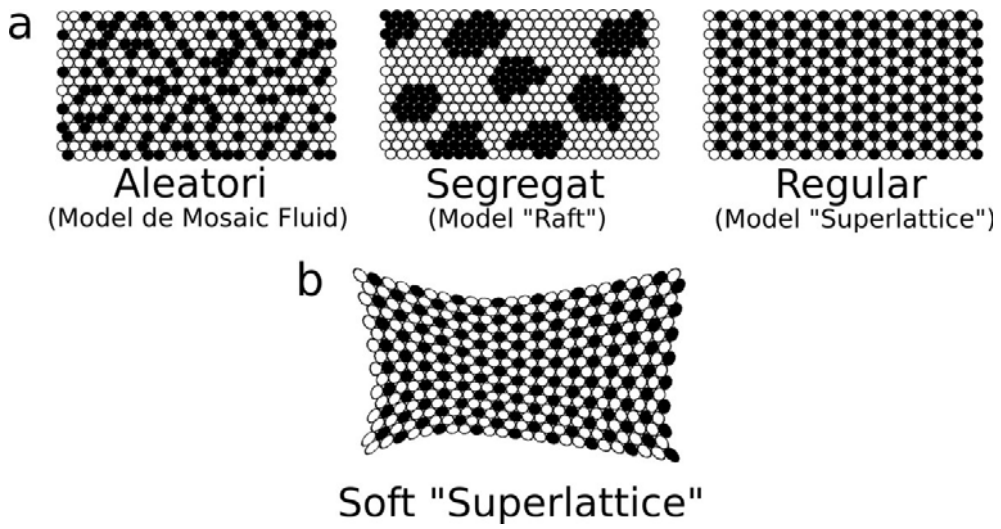

Figura 1.3: Models d'organització lateral dels lípids en membranes, on les partícules de cada color representen lípids diferents. Figura adaptada de [Some09].

evidencies experimentals que el recolzen es poden trobar a les Refs. [Some99, Some09].

Un altre model que treballa sobre la hipòtesi d'arranjaments regulars és l'**Umbrella** model o model de paraigües [Huan99]. A diferència del model anterior, aquest model es concentra majorment en les membranes amb colesterol. De fet, segons com, és pot entendre com una extensió del **Superlattice** model especialitzat en membranes amb colesterol, tot i que presenten certes diferències. Aquest model argumenta que la desigualtat entre el petit cap polar del colesterol i el seu esquelet hidrofòbic determina la relació entre el colesterol i els lípids que l'envolten. El petit cap polar del colesterol (grup hidroxil) no és prou gran per protegir la seva part hidrofòbica de l'exposició a l'aigua, el que resulta en una contribució desfavorable a la energia lliure [Priv88, Levy98]. Com a conseqüència, el colesterol tendeix a agrupar-se amb lípids que són capaços de protegir-lo del aigua [Huan02, Ali07], i a evitar agrupaments de colesterol que serien difícils de protegir. El model pronostica que els lípids que millor protegeixen els colesterols són aquells que presenten una proporció elevada entre els volums dels seus fragments hidrofílic i hidrofòbic. Entre els lípids que responen a aquestes característiques destaquen aquells que presenten grups colines com alguns Phds i SLs. És important ressaltar que tot i la simplicitat del model presenta una gran capacitat de pronòstic. Per exemple, és capaç de predir el límit de solubilitat del colesterol en PhdChos que se situa vora el 66,7 mol%. També explica entre altres la predilecció del colesterol per els lípids saturats respecte als insaturats en base a la major ràtio cap/cua dels primers, ja que són més compressibles com a conseqüència de l'absència de dobles enllaços rígids.

L'altre model plantejat per descriure l'ordenament lateral en membranes amb colesterol és el **Condensed Complex** model o model de complexos condensats que es basa especialment en el seu comportament fàsic[Radh99b, Radh99a, McCo03]. Aquest model difereix totalment dels dos anteriors, ja que proposa que l'ordenament causat pel colesterol així com l'efecte de condensació observats experimentalment són conseqüència directa de la formació de complexos amb estequiometria definida entre colesterol i lípids d'elevada T_m(R),

$$CHOL + R \leftrightarrows COMPLEX. \tag{1.1}$$

Aquests complexos se'ls hi suposa una àrea superficial menor que la suma dels seus components individuals per separat, i necessàriament, per tant, presenten un major ordenament. Quan els sistemes contenen simultàniament lípids de baixa T_m, als quals se'ls considera no reactius amb el colesterol i poc miscibles amb els complexos, el model és capaç d'explicar la coexistència de dominis rics en colesterols i lípids d'elevada $T_m(L_o)$ i dominis pobres en colesterol i rics en lípids de baixa $T_m(L_\alpha)$. Aquest model que ha provat ser molt efectiu en la descripció de monocapes, en el cas de bicapes no sembla tan encertat. En particular la impossibilitat d'aïllar aquests complexos sembla constituir el seu principal detractor [Vand94, Huan99, Niel99, Smon99].

Finalment, per concloure aquesta secció presentem la hipòtesi **raft** (nanodomini) lipídic [Simo97]. Aquesta postula l'existència de dominis nanomètrics rics en colesterol i lípids d'elevada T_m, envoltats per una matriu pobre en colesterol i rica en lípids de baixa T_m. Així doncs, els dominis raft se'ls pressuposa una naturalesa ordenada com la de la fase L_o, mentre que l'entorn és semblant a la fase desordenada L_α. Aquests rafts se'ls pot considerar com plataformes dinàmiques i on s'ancoren específicament diferents proteïnes dotant a aquests nanodominis d'una rellevància funcional extraordinària [Simo97, Simo04]. Per tant, el que conclou aquesta hipòtesi és que la distribució lipídica en membranes cel·lulars és força heterogènia en la escala nanomètrica on es formen dominis (rafts) que serien essencials pel funcionament de la membrana [Brow00, Doug05]. De fet, l'escala nanomètrica d'aquests dominis dificulta la confirmació d'aquesta hipòtesi, ja que les tècniques experimentals de què es disposen actualment no ofereixen la resolució adequada [Ande02].

1.1.4 Tècniques Experimentals

Tot i que en l'actualitat el nostre coneixement sobre les membranes biològiques és incomplet el desenvolupament constant de noves tècniques experimentals l'ha incrementat de forma considerable. Les escales temporals i espacials involucrades en l'estructura i els processos de membrana són tant dispars que constitueixen, sens dubte, un desafiament considerable per qualsevol tècnica experimental. Així doncs és natural que per l'estudi de membranes es faci ús no només d'una sinó d'un considerable nombre de tècniques que ens proporcionen la informació sobre com està estructurada una membrana i dels processos que en ella hi concorren. Malgrat que el contingut d'aquesta Tesi és bàsicament teòric/numèric, sovint es fan comparacions amb resultats de diverses tècniques experimentals, de les quals es fa aquí una petita selecció.

Les tècniques basades en el fenomen de la fluorescència són sens dubte responsables de l'actual concepció dinàmica de la membrana. El seu fonament és la luminescència originada en l'absorció-emissió fotònica fent ús d'estats moleculars singlet. La seva major limitació és que requereix la presència de compostos anomenats cromòfors que no són gens abundants en les membranes naturals. L'addició de cromòfors pertorba la membrana i conseqüentment afecta a la pròpia mesura. Malgrat això, atès que la tècnica de per si és molt sensible, petites addicions de cromòfors acostumen a ser suficients i per tant la membrana es pot suposar poc alterada. D'entre tots els mètodes basats en fluorescència per l'estudi de membranes destaca l'anisotropia de fluorescència en estat estacionari i/o amb resolució temporal. Aquest mètode proveeix d'informació sobre la fluïdesa, paràmetres d'ordre i moviment rotacional de la sonda fluorescent [Kino77, Lipa80], que està correlacionada amb l'entorn de la membrana on es troba. Aquesta tècnica és capaç de cobrir escales de temps d'entre picosegons a nanosegons.

Altres tècniques de fluorescència en canvi proveeixen informació sobre les difusions laterals, com són la microscòpia de recuperació de fluorescència després de fotoblanqueig (FRAP) [Vaz89] o l'espectroscòpia de correlació de fluorescència (FCS) [Eige94, Alme95, Korl99]. Finalment, esmentar la fluorescència de transferència d'energia de ressonància (FRET) que permet determinar la formació de clústers i agregats.

Una altre tècnica fonamental en l'estudi de membranes és la ressonància paramagnètica electrònica, que, al igual que la fluorescència, normalment requereix l'ús de sondes, i és per tant una tècnica invasiva. A diferència de la fluorescència, però, les sondes són bastant més petites i ben localitzades en el perfil transversal de la membrana, ja que s'introdueixen enllaçades covalentment a algun dels components de la membrana. L'alta sensibilitat de la tècnica ens permet obtenir dades sobre l'estructura interna de la membrana [McCo71a, Ge98], difusió d'oxigen a través de la mateixa [Subc89, Subc91], obtenció de perfils d'hidrofobicitat [Subc94], estudi canvis de fase [Subc07], caracterització de la probabilitat d'un lípid per canviar espontàniament d'una capa a una altra [McCo71b] i en alguns casos estudi de dominis nanoscòpics [Simo97].

L'única tècnica que a priori seria capaç de proveir simultàniament d'informació estructural i dinàmica precisa sense la necessitat d'introduir sondes és la ressonància magnètica nuclear (RMN), degut a l'existència natural de nuclis magnèticament actius en les membranes. Aquesta és basa en l'estudi de l'espectre produït per l'absorció d'aquests nuclis quan es troben immersos en un camp magnètic extern. Aplicada a membranes, per la seva naturalesa ordenada, s'obtenen espectres sense estructura clara (pics amples i superposats) [Boci78] típics de la RMN d'estat sòlid. Això és conseqüència de l'impossibilitat que en l'escala temporal de la mesura les interaccions dipolars inter- i intramoleculars es promitgin. Addicionalment, aquest moviment restringit del lípids en la membrana provoca l'aparició interessant de fenòmens de relaxació quadropolar. Actualment la RMN és capaç de determinar paràmetres d'ordre i calcular la mobilitat de cadascun dels diferents segments lipídics en les cadenes laterals. També cal destacar la possibilitat d'utilitzar-la per estimar contactes entre alguns àtoms concrets que a la vegada ens permet teoritzar sobre la seva posició relativa. Finalment, esmentar el seu ús en el càlcul de constants de difusió.

Una altra conjunt de tècniques d'importància cabdal pel coneixement de l'estructura de la membrana són les tècniques de dispersió. En el cas de les membranes, dos tipus de radiació presenten interès, els raigs-X (SAXS) i el feix de neutrons (SANS), ambdues fonamentalment en el context de dispersions en angles petits (SAS). La informació que proveeixen aquestes tècniques queda condensada en l'anomenat factor d'estructura que depèn de l'estructura transversal de la membrana. Mitjançant models, el factor d'estructura ens permet accedir a propietats tant diverses de les membranes com l'àrea per lípid, el gruix de la membrana i el volum efectiu dels lípids a la membrana. Tot i que aquestes mesures són de per si importants per la validació de models de membrana, el més rellevant és que el factor d'estructura també es pot obtenir en simulacions de membranes i per tant constitueix una de les poques mesures per comparar experiments i simulacions lliures de models intermedis. [Kuuc08a]

Finalment, per concloure el llistat, cal esmentar la calorimetria diferencial d'escombratge (DSC) que és una tècnica termoanalítica que mesura l'intercanvii d'energia al llarg d'un procés de canvi de fase. Aquesta tècnica d'alta precisió no només permet detectar amb precisió la temperatura a la que té lloc el canvi de fase, sinó que permet sovint descriure la naturalesa del mateix [Stei69].

1.2 Dinàmica Molecular

En el context clàssic, l'evolució temporal de qualsevol sistema es pot predir si es coneixen les forces que actuen en ell i, en un moment donat, les posicions de totes les partícules que el constitueixen. L'evolució temporal del sistema queda establerts per la Mecànica Newtoniana,

$$m_i \cdot \frac{d^2\mathbf{r_i}}{dt^2} = \mathbf{F_i} = -\nabla_{\mathbf{r_i}} U(\mathbf{r_1}, \mathbf{r_2}, \ldots, \mathbf{r_N}) \tag{1.2}$$

on N és el número de partícules, $\mathbf{r_i}$ representa les coordenades cartesianes de la partícula i, $\mathbf{F_i}$ és la força que actua sobre ella, i U és l'energia potencial del sistema.

La tècnica encarregada de l'estudi de sistemes moleculars mitjançant la resolució numèrica de les equacions de moviment dins d'aquest context clàssic és la Dinàmica Molecular (DM). En l'actualitat, l'ús d'aquesta tècnica és troba molt estesa ja que ha demostrat ser de gran utilitat, en particular aplicada a l'estudi de sistemes biològics. Aquesta metodologia proporciona tant informació temporal del processos estudiats com característiques mitjanes, el que la fa molt valuosa. L'estudi de membranes lipídiques que contempla aquesta Tesi s'ha dut a terme íntegrament mitjançant DM, mitjançant l'anàlisi de les trajectòries obtingudes.

En les següents seccions descriurem de forma resumida les parts essencials de la DM en membranes que inclouen la descripció de les forces del sistema ("camp de força"), alguns detalls tècnics rellevants de la tècnica i finalitzarem amb les seves limitacions.

1.2.1 Camp de Força

La correcta descripció del potencial d'interacció entre les partícules és bàsic per predir l'evolució del sistema en un context clàssic. La forma funcional d'aquest potencial és el que coneixem com a camp de força. De forma general un camp de forces pot ser atomístic o "coarse-grained" (de gra gros), on els primers són més acurats i els segons ho són menys però permeten estudiar processos a escales temporals i espacials més grans. Solucions on és combinen les dues variants també són possibles, com el cas de camps de forces d'àtoms units que es fa servir en aquesta Tesi, on determinats àtoms lleugers (ex: hidrògens) són inclosos amb els àtoms pesats amb els quals estan enllaçats (ex: carbonis). Existeixen diferents camps de força per sistemes biològics: AMBER [Corn83, Wein84], CHARM [Broo83, MacK98], GROMOS [Guns87, Guns98], OPLS [Jorg84, Jorg88].... En general l'òptima elecció dels camps de força es fonamenta en la seva capacitat de reproduir les característiques d'interès en base a experiències prèvies en sistemes el més semblants possible al que es vol estudiar. La majoria de camps de força es poden descriure com:

$$U = U_{enllaç} + U_{angle} + U_{torsió} + U_{vdw} + U_{coulomb} \tag{1.3}$$

on cadascun del termes té en consideració una part essencial de la física del sistema. En particular, els tres primers són els anomenats potencials enllaçants ja que contenen la informació de la interacció d'àtoms separats per 1, 2 ó 3 enllaços respectivament. La interacció entre la resta d'àtoms no considerats en ells s'inclouen en les dues darreres contribucions que corresponen a les forces de van der Waals i electrostàtiques, respectivament.

Un exemple de camp de forces senzill i àmpliament usat en sistemes biològics té la següent forma funcional:

$$U = \sum_{enllaços} \frac{k_i^b}{2}\left(\mathbf{r_i} - \mathbf{r_i^{eq}}\right)^2 + \sum_{angles} \frac{k_i^\alpha}{2}\left(\theta_i - \theta_i^{eq}\right)^2 + \\ + \sum_{torsions} \sum_{n} k_{\phi,n}\Big(1 + \cos\left(n\phi - \phi^{ref}\right)\Big) + \\ + \sum_{parelles} \left(\left\{ \frac{C_{ij}^{(12)}}{r_{ij}^{12}} - \frac{C_{ij}^{(6)}}{r_{ij}^{6}} \right\}_{vdw} + \left\{ k_e \frac{q_i q_j}{r_{ij}} \right\}_{coul} \right) \tag{1.4}$$

Aquí, tant els enllaços com els angles estan descrits per oscil·ladors harmònics. Els díedres o torsions venen representades per expansions en sèrie de cosinus que són de vital importància en sistemes amb cadenes flexibles com les que presenten els lípids i que requereix d'un nombre elevat de termes en l'expansió per ser acurats. Finalment les forces de van der Waals estan representades per potencials de *Lennard-Jones*, i la força electrostàtica per la llei de Coulomb.

L'obtenció dels paràmetres del camp de forces per un sistema és una feina complexa d'ajust respecte a dades experimentals i/o altres fonts teòriques, que s'optimitzen per reproduir un conjunt determinat de propietats. La bondat dels paràmetres obtinguts determinen inequívocament la qualitat dels resultats que se'n deriven.

1.2.2 Implementació Pràctica

A banda del camp de forces i dels seus paràmetres, per tal de simular qualsevol sistema amb Dinàmica Molecular requerim d'un conjunt d'algoritmes que integrin les equacions de moviment dins del col·lectiu estadístic pertinent. En aquesta secció repassarem alguns d'aquests algoritmes més importants concentrant-nos en aquells que s'han utilitzat en aquesta Tesi.

L'algoritme clau que constitueix el cor d'un programa de DM és l'integrador. Aquest és essencial ja que no existeix una solució analítica de les equacions de moviment per un sistema si conte més de dos partícules [Qiu 90]. Així doncs, l'única manera de tractar un problema real és mitjançant la integració numèrica de les equacions de moviment. És a dir, l'integrador partint del conjunt de posicions $\mathbf{r}_{i=1,N}$ i velocitats $\mathbf{v}_{i=1,N}$ a temps t, genera una nova configuració a un temps $t + \Delta t$, on Δt és el pas de temps. Existeixen diversos integradors amb característiques diferents: simplicitat o estabilitat, tenir alta precisió, ser simplèctics.... La seva elecció sovint depèn del problema en qüestió. En aquesta Tesi s'ha fet ús d'una variació del algoritme de Verlet [Verl67]: l'algoritme "leap-frog" [Hock70]. Aquest presenta un excel·lent rendiment computacional i és força robust, tot i que al presentar un asincronisme temporal entre les posicions i velocitats generades no és capaç de calcular de forma precisa l'energia total del sistema. L'esquema bàsic del algoritme és el següent:

$$r(t+\Delta t) = r(t) + \Delta t\ v(t+\frac{1}{2}\Delta t) \tag{1.5}$$

$$v(t+\frac{1}{2}\Delta t) = v(t-\frac{1}{2}\Delta t) + \Delta t\ a(t). \tag{1.6}$$

L'elecció del pas de temps a emprar en una simulació és complicada. Per una banda, si el temps és molt petit es necessiten un nombre molt elevat d'iteracions per explorar la totalitat

de l'espai de fases. Per l'altre, si és massa gran les trajectòries poden ser poc acurades i, fins i tot, poden presentar inestabilitats numèriques davant de la impossibilitat de descriure acuradament aquells moviments amb freqüències elevades. Com a solució de compromís s'escullen passos de temps de l'ordre d'un desè de la freqüència més elevada present al sistema. En sistemes biològics això implica passos de temps de $\sim$1 fs.

La multitud d'escales temporals que presenten els diferents processos biològics i l'existència d'un límit raonable d'iteracions per a una simulació, determinat per la potència de càlcul de què es disposa, restringeix l'ús de la DM a certs processos biològics. Tot i que l'increment constant de la potència de càlcul millora poc a poc aquest problema, sovint la única solució efectiva consisteix en incrementar el pas de temps. En sistemes biològics això es pot fer sense alterar significativament la correcta evolució temporal mitjançant la imposició de restriccions en els graus de llibertat que presentes freqüències més altes (enllaços, i angles). Tot i que existeixen diverses formes de restringir un grau de llibertat, el mètode més emprat consisteix en aplicar restriccions holonòmiques als graus de llibertat a restringir. La seva aplicació permet increments de fins a quatre vegades el pas de temps [Hess97, Bere98]. Per tal de resoldre el conjunt de restriccions imposat a un sistema existeixen diversos mètodes. Els més comuns són "LINCS" i "SHAKE" i una variant del darrer per petites molècules (ex: aigua) "SETTLE". La seva utilització permet, per exemple, l'ús de passos de temps de 2 fs en sistemes biològics.

La limitació en la grandària dels sistemes simulats, actualment de forma efectiva a l'escala nanomètrica, introdueix els anomenats efectes de grandària finita. Aquests es deuen a l'elevada proporció de partícules que es troben en els límits del sistema simulat. Aquestes partícules frontereres presenten entorns i per tant interaccions que difereixen de les que realment volem simular. Això produeix que les propietats d'un sistema variïn de forma poc realista amb la seva grandària. Per tal d'evitar parcialment aquest problema, es poden aplicar condicions periòdiques de contorn (CPC) a les simulacions. Aquest senzill mètode basat en la replicació infinita del sistema simulat (caixa de simulació) en totes direccions de l'espai aconsegueix que cap partícula sigui limítrofa. Cal tenir en compte que l'aplicació d'aquest mètode es restringeix a sistemes simètrics respecte als seus límits, com són les membranes, i per evitar ordenaments artificials a aquells que no presentin correlacions espacials més enllà de la grandària original [Leac01].

Un altre punt important és el que fa referència al tractament de les interaccions no enllaçants o de llarg abast (forces de van der Waals i electrostàtiques). El problema radica principalment en què el nombre d'aquestes interaccions augmenta de forma quadràtica amb el número de partícules $O(N^2)$ (Eq. 1.4), el que resulta en un notable alentiment de les simulacions per poc que es vulgui simular un nombre moderat d'àtoms. Per tal de minimitzar aquest problema s'apliquen diverses estratègies de les quals descriurem les dos més emprades en la simulació de membranes. La primera redueix el número de parelles a tenir en compte a aquelles que es troben dins d'una certa distància, "cutoff", en base a què les forces en qüestió tendeixen a zero amb la distància. Aquest mètode s'ha demostrat que produeix artefactes per el truncament del potencial en el radi de "cutoff" i que resulta en l'aparició de tensions inter- i intramoleculars [Patr03, Patr04, Baum05]. Això, en el cas de les interaccions electrostàtiques, és pràcticament inevitable a causa de la seva dependència asimptòtica d'1/r i, per tant, redueix la seva estricta validesa al tractament de les forces de van der Waals sempre que s'esculli un "cutoff" prou gran. La segona inclou aquells mètodes derivats de

les sumes d'Ewald [Ewal21], en especial per les interaccions electrostàtiques. En aquest mètode cada partícula interacciona amb totes aquelles situades dins de la caixa simulada, més totes aquelles situades dins les caixes periòdiques. Aquest mètode reescriu la dependència coulòmbica (1/r) en la suma de dos series amb millors propietats de convergència en els espais real i recíproc, respectivament. Tot i que el mètode en la seva formulació original no millora gaire la dependència quadràtica amb el número de partícules $O(N^2 - N^{3/2})$, sí evita la majoria dels artefactes provinents de l'ús de "cutoffs" [Patr03, Patr04, Baum05]. Addicionalment, modificacions del mètode com "particle mesh Ewald" (PME) milloren substancialment el rendiment amb dependències de l'ordre $O(N \log N)$ [Dard93], i constitueixen en l'actualitat la millor opció per la simulació de membranes.

Per concloure aquest llistat de parts bàsiques per la preparació d'una simulació, s'introduieix la necessitat d'algoritmes de control de la temperatura i la pressió. Aquest control és fonamental ja que el col·lectiu natural de les DMs amb condicions periòdiques de contorn és el microcanònic. És a dir, el volum, el nombre de partícules i l'energia total del sistema simulat es mantenen constants. Aquest entorn difereix del que trobem habitualment en sistemes biològics on les variables fixades acostumen a ser la temperatura i la pressió. La simulació d'aquestes condicions s'aconsegueix mitjançant la introducció dels anomenats banys de temperatura i pressió. Ja que la temperatura d'un sistema depèn de l'energia cinètica de les partícules, i aquesta de la seva velocitat, podem alterar la temperatura d'un sistema mitjançant la variació de la velocitat de les partícules que el formen. Això és el que fan els diferents algoritmes disponibles per aquest fi. Els que tenen una major aplicabilitat són els anomenat d'acoblament dèbil. Aquests no forcen el sistema a mantenir la temperatura constant en tot moment, sinó que corregeixen les desviacions respecte a la temperatura de referència de manera gradual. Entre ells destaquen els banys de Berendsen [Bere84] i Nosé-Hoover [Nose84, Hoov85]. De la mateixa manera, la pressió d'un sistema es pot conèixer a partir del teorema del virial de Clausius. Això permet desenvolupar banys de pressió fonamentats en l'ajust de les posicions de les partícules del sistema. Els bany de pressió més emprats són els de Berendsen [Bere84] i Parrinello-Rahman [Parr81] que són anàlegs als de temperatura anteriorment citats.

1.2.3 Limitacions

Tot i que la Dinàmica Molecular ha demostrat ser una tècnica ben desenvolupada i reeixida, presenta les seves limitacions. Les escales de treball, algoritmes i implementacions tècniques limiten la seva aplicació, tal i com succeeix en tota tècnica computacional. La limitació principal és deu a la necessitat d'un correcte mostreig de l'espai de fases, que directament limita la grandària del sistema simulat per tal de garantir arribar a temps prou llargs. Aquest és un punt clau en la simulació de sistemes biològics, tot i que avenços constants en tot aquest aspectes limitadors allunyen cada cop més el sostre dels sistemes que es poden tractar.

D'altra banda existeixen limitacions intrínseques a la tècnica, les quals restringeixen el seu àmbit d'aplicació. Per exemple, la descripció de l'evolució del sistema és purament clàssica, i això implica que processos on intervinguin forts rearranjaments electrònics no poden ser estudiats (ex: formació/destrucció d'enllaços). Per tal de superar aquesta restricció s'han desenvolupat tècniques híbrides de DM i mecànica quàntica on aquesta darrera s'aplica selectivament a parts concretes del sistema [AAqv93, Bako96, Gao96]. Una altra d'aquestes

limitacions és la naturalesa caòtica inherent a les equacions de moviment, que fa que simulacions de sistemes amb configuracions inicials lleugerament diferents divergeixin de forma exponencial [McCa94]. Això restringeix la validesa dels processos singulars observats, limitant el sentit físic a descripcions resultants de fer la mitjana temporal de les trajectòries individuals [Elof93, Daur96].

Una altre limitació important, és la imposada per la forma i qualitat del camp de forces escollit. Tot i que sovint basada en criteris de rendiment computacional, la forma funcional limita la qualitat descriptiva del sistema (ex: no permeten la introducció de la polaritzabilitat), així com la portabilitat de paràmetres entre diferents camps de forces. No és doncs d'estranyar que tenint en compte que l'exactitud de la descripció emprada marca els resultats obtinguts, els caps de forces es troben immersos en constants processos de revisió.

1.3 Motivació, Protocol i Eines Analítiques

1.3.1 Motivació de la Tesi

L'objectiu d'aquesta Tesi és l'estudi de com la composició d'una membrana lipídica afecta les seves propietats. L'elevat nombre d'espècies moleculars presents en les membranes cel·lulars, i les seves diferents distribucions de composició, depenent de l'organisme i tipus de membrana, reflecteixen la seva complexitat d'aquesta relació.

Les membranes cel·lulars actuen com a barreres físiques però també estan activament involucrades en innombrables funcions cel·lulars. La majoria d'aquestes funcions requereixen la combinació de propietats, funcionalitats i interaccions tant individuals com col·lectives dels diferents constituents de la membrana. Per tant, la diversitat de components en una membrana és responsable de la complexa però precisa estructura, funcionalitat i comportament dinàmic de la mateixa.

Paral·lelament als avenços experimentals, la modelització teòrica de les membranes multicomponents ha reportat grans progressos. De fet, l'ús de models i simulacions computacionals s'ha convertit en una eina important i necessària per la interpretació d'observacions experimentals i, en general, per entendre el comportament de la membrana cel·lular. La DM és en aquest sentit l'eina numèrica més comú en aquest tipus d'estudi a escala molecular, tot i que no és capaç d'abordar sistemes de la complexitat de les membranes biològiques reals. És per això que en l'actualitat es concentra en membranes amb un màxim de tres lípids, tot i que evidentment aquestes no exhibeixen la riquesa de comportament de les membranes biològiques. La comprensió del comportament d'aquests sistemes de complexitat reduïda és capaç de treure l'entrellat de la complexa relació entre funció i composició. De fet, una estratègia basada en l'increment progressiu del nombre d'espècies moleculars simulades pot eventualment fer-nos entendre el rol de cadascun dels elements de la membrana cel·lular en la seva funcionalitat. És per això que al llarg d'aquesta Tesi sempre simularem primer sistemes d'un sol component (sistemes purs), i només llavors introduirem un segon o un tercer component (sistemes mesclats).

En aquest treball s'ha estudiat a nivell molecular l'estructura i comportament dinàmic de bicapes formades per PhdChos i eventualment colesterol. Les composicions escollides

responen a la voluntat de millorar la comprensió que es té de la membrana plasmàtica de cèl·lules de mamífers formada majoritàriament per aquests lípids. En especial s'ha centrat l'atenció en l'estudi de la presència i posició del doble enllaç en les cadenes de les PhdChos i l'efecte del colesterol en les propietats físiques de les membranes i l'ordenament del seu entorn.

En la Sec. 1.4 s'han tractat amb membranes composades per PhdChos formats per cadenes monoinsaturades on la posició del doble enllaç s'ha anat variant al llarg de les mateixes. En aquest cas, el rol de la posició del doble enllaç lipídic en l'estructura de la membrana resultant s'ha analitzat, tant en absència com en presència de colesterol. En elles observem que interaccions especifiques entre el doble enllaç i el colesterol donen lloc a interessants comportaments no monòtons en diferents propietats estudiades en funció de la posició del doble enllaç. Això és tradueix en una maximització del desordre de la membrana quan el doble enllaç s'emplaça en el centre de la cadena alifàtica. Aquest comportament, en canvi, no és tan clar en absència de colesterol. Aquesta observació suggereix que la raó de la preferència natural per PhdChos amb el doble enllaç al mig de les cadenes en les membranes plasmàtiques està determinada per la presència de colesterol.

En la Sec. 1.5 s'adreça l'interessant problema dels lípids amb una cadena monoinsaturada i l'altra saturada (isòmers posicionals). Aquests lípids presenten dos possibles llocs d'ancoratge no equivalents del glicerol; *sn*–1 i *sn*–2 (Fig. 1.2. Tot i que a priori la diferència entre ambdues configuracions sembla menor, la majoria dels Phds naturals presenten una clara preferència per les cadenes insaturades enllaçades en la posició *sn*–2 mentre que la cadena *sn*–1 acostuma a presentar-se saturada. La raó d'aquesta preferència és desconeguda. Per estudiar-la s'han efectuat simulacions de membranes amb diferents isòmers posicionals, i es van trobar petites però sistemàtiques diferències tant en propietats estructurals com dinàmiques. També va quedar palès que la presència de colesterol amplifica aquestes diferències, suggerint un altre cop un mecanisme de selecció basat en la interacció amb colesterol.

El camp de forces usat per descriure el doble enllaç de les cadenes lipídiques és examinat a la Sec. 1.6. La comparació entre els paràmetres estàndards presents en el camp de forces GROMOS87 [Tiel02] i la versió corregida per Bachar et al. [Bach04] (la usada en aquesta Tesi) evidencia que la parametrització és un tema força delicat. Així es veurà que canvis de paràmetres, a priori menors, es tradueixen en alteracions no només quantitatives, com és d'esperar, sinó també qualitatives que alterarien els resultats de les seccions anteriors.

La interacció del colesterol i les PhdCho és sens dubte l'objectiu principal de la nostra recerca. En la Sec. 1.7 s'ha estudiat amb molt detall la capacitat del colesterol per ordenar i condensar la membrana. S'ha examinat com la particular estructura del colesterol i en especial la presència dels dos metils en la cara β de l'anell rígid indueixen un ordre molt concret als lípids que l'envolten, ja siguin PhdChos com altres colesterols. Aquest ordenament mostra una simetria fonamentalment trigonal i es causada pel colesterol de forma quasi exclusiva en la membrana, justificant la seva nul·la variabilitat estructural en cèl·lules eucariotes.

Finalment la Sec. 1.8 recull la recerca que s'ha dut a terme sobre membranes que contenen cardiolipines. En cèl·lules de mamífers aquests components són constituents comuns dels mitocondris, al igual que passa en els bacteris amb els que sembla tenir un llunyà parentiu. Les característiques úniques i particulars d'aquestes membranes dins de les membranes presents en cèl·lules eucariotes atragueren la nostre atenció i seran estudiades en aquesta darrera secció.

1.3.2 Protocol i Camp de Forces Emprat

En aquesta secció descriurem tant el protocol com el camp de forces emprat en les nostres simulacions. En tots dos casos, per tal de garantir la validesa dels resultats, únicament s'han utilitzat combinacions àmpliament provades i de validesa reconeguda. A més a més, com que aquest treball fa un ús intensiu de la comparativa entre simulacions s'ha procurat que les úniques diferències entre els sistemes simulats provinguin de la composició de les membranes i no de les peculiaritats del protocol, camp de forces o disposicions inicials del sistema. Així doncs, tots els sistemes comparteixen el mateix, protocol, plataforma de computació, tipus de distribució inicial i camp de forces. A continuació descriurem l'estructura d'una bicapa simulada i les característiques comunes de les simulacions. Posteriorment detallarem el protocol i camp de forces corresponents a les Secs. 1.4 to 1.7. Finalment farem algun comentari sobre el camp de forces particular emprat en la secció 1.8.

Totes les membranes simulades tenen la mateixa estructura. El cor lipídic el formen dues monocapes invertides esteses en el pla xy que s'emplacen una sobre l'altre formant una bicapa. Aquesta queda a continuació intercalada per dues capes d'aigua en la direcció z. Aquesta membrana es simula fent ús de condicions periòdiques de contorn (CPC) en les tres direccions. El nombre d'aigües escollit, per sobre de 0.36 % en pes [Inok78, Ruoc82], minimitza la interacció entre el caps lipídics polars com a conseqüència de les CPC imposades en la direcció z.

Totes les simulacions s'han dut a terme amb el paquet de Dinàmica Molecular GROMACS en la seva versió 3.3.1 citeLindahl2001a, Spoel2005. S'ha fet ús del col·lectiu NPT que simula el col·lectiu natural de les membranes. Tant la temperatura com la pressió s'han controlat mitjançant l'ús de banys d'acoblament feble (Berendsen [Bere84]) on les constants d'acoblament s'han fixat en 0.6 i 1.0 ps respectivament. La temperatura de la bicapa i de la capa aquosa s'han controlat de forma independent [Spoe05]. La pressió d'1 bar usada en totes les simulacions s'ha aplicat de forma independent en el pla xy i en la direcció perpendicular a la membrana (z). Per tal de permetre la utilització d'un pas de temps de 2 fs s'han fixat tots els enllaços dels sistemes mitjançant els algoritmes "LINCS" [Hess97] i "SETTLE" [Miya92]. En el capítol de les interaccions de llarg abast esmentar l'ús que s'ha fet de "cutoffs" d'1 nm per descriure les interaccions de van de Waals [Patr04], i de PME per descriure les electrostàtiques [Essm95]. Els paràmetres d'aquest darrer han estat: 1.0 nm de "cutoff" en el espai real, ordre 6 de la interpolació amb β-spline, 10^{-5} tolerància en la suma directa. Cal destacar que aquest protocol ha estat aplicat amb èxit anteriorment [Rog01, Falc04, Aitt06, Niem06, Niem07].

Els sistemes estudiats en les seccions 1.4, 1.5, 1.6 i 1.7 estan constituïts per PhdChos amb cadenes laterals de 18 metils cadascuna i formen membranes pures o mescles binàries amb colesterol. Per descriure els PhdChos s'ha fet ús del camp de forces d'àtoms units desenvolupat pel DPPC (Dipalmitoil–fosfatidilcolina), els detalls del qual es poden consultar a les Refs. [Tiel96, Berg97, Patr04] i les referències que contenen. El model emprat per la descripció dels dobles enllaços és el desenvolupat per Bachar et al. [Bach04], amb l'excepció de la Sec. 1.6 on a més s'ha fet servir una segona parametrització corresponent a l'estàndard en GROMACS87 [Tiel99, Tiel02] per tal de comparar els resultats amb el primer. El model d'aigua emprat és el "Simple Point Charge" (SPC) [Bere81]. Per all colesterols es va fer servir la descripció de Holtje et al. [Holt01] tal i com es descriu a la Ref. [Rog07a]. En la majoria

dels casos les simulacions s'han dut a terme a 338 K, que està per sobre de la $T_m$màxima d'entre els lípids simulats corresponent al DSPC (T_m= 328 K) [Koyn98].

En la Sec. 1.8 descriurem membranes amb Cardiolipines, que són lípids altament carregats, immersos en matrius lipídiques que simulen les mitocondrials (PhdChos i PhdEtns) [Daum85]. En aquest cas s'ha fet ús d'un camp de forces totalment atòmic (OPLS [Jorg96, Rizz99, Kami01, Pric01]), on les càrregues emprades s'han extret pel PhdChos de la Ref. [Taka00] i pel PhdEtns de la Ref. [Murz99]. Les mateixes càrregues s'han fet servir per la descripció dels grups carbonil i fosfat de les Cards. Pel glicerol pont i el seu hidroxil, en canvi, s'ha fet ús de les càrregues estàndards oferides en l'OPLS. Aquesta parametrització ha estat validada prèviament en membranes amb PhdChos, PhdEtns i glicolípids [Rog07b]. El model d'aigües que s'ha emprat és el TIP3P que és el compatible amb el camp de forces emprat per als lípids [Jorg83]. En aquest cas, el banys de temperatura i pressió escollits han estat els de Nosé-Hoover [Nose84, Hoov85] i Parrinello-Rahaman [Parr81] respectivament, i la temperatura de simulació ha estat fixada a 310 K.

En totes les simulacions l'equilibrament del sistema s'ha monitoritzat mitjançant el seguiment de l'evolució temporal de les àrees per lípid, la temperatura i l'energia. En la majoria dels casos 20 ns han demostrat ser suficients. S'ha de tenir en compte que en els estudis que presentarem l'extensió de les simulacions és crítica. Això és deu, a banda de garantir l'equilibri del sistema, a què una part important de les propietats mesurades requereixen d'una elevada estadística per tal de ser realment representatives. En aquest sentit, les membranes pures s'han simulat per un mínim de 100 ns. En el cas de les mescles amb colesterol aquest mínim s'ha ampliat a 150 ns per assegurar una correcta barreja dels dos components. En els casos en què les difusions dels components lipídics foren molt lentes, com en el cas d'alguns sistemes de la Sec. 1.7, aquests s'han simulat per més de 300 ns. Per tal de permetre aquests temps de simulació s'ha limitat la grandària del sistema simulat. Tot i que en tots els casos aquest nombre està per sobre del 64 lípids per capa, que ha demostrat ser més que suficient per minimitzar els efectes de grandària finita [Tiel97].

1.3.3 Propietats de les Membranes: Tècniques d'Anàlisis

En aquesta secció descriurem breument les propietats generals de la membrana obtingudes de les simulacions. Aquestes inclouen propietats tant estructurals com dinàmiques, i s'han calculat en tots els sistemes que s'han simulat en aquest treball. L'error associat als valors numèrics de les propietats mesurades s'ha avaluat mitjançant el mètode d'anàlisi de blocs [Hess02].

L'àrea per lípid és sens dubte una de les propietats fonamentals en una membrana, tant per la informació que proporciona com per la possibilitat de ser comparada amb resultats experimentals. Aquesta mesura també dóna una idea del nivell de desordre dels lípids de la membrana: quan més gran és l'àrea per lípid major és el desordre. En el cas de sistemes purs el càlcul de l'àrea per lípid és trivial, ja que, tan sols s'ha de dividir l'àrea total de sistema en el pla xy entre el nombre de lípids d'una capa. En el cas de sistemes amb més d'un component el càlcul és força més complicat i deixa de ser unívoc [Chiu02, Hofs03, Falc04, Edho05]. El problema radica en el criteri utilitzat per distribuir l'àrea entre els diferents components. En el cas de sistemes binaris amb colesterol s'han fet servir dos mètodes que són complementaris. El primer és equivalent al cas dels sistemes purs ignorant la presència de colesterols. El segon

és el mètode desenvolupat per Hofsäß et al. on sí es té en compte l'àrea per molècula ocupada pel colesterol [Hofs03]. En essència aquest mètode suposa que l'àrea ocupada per un lípid dividida pel seu volum equival a l'àrea ocupada per una de les capes de la membrana dividida pel seu volum.

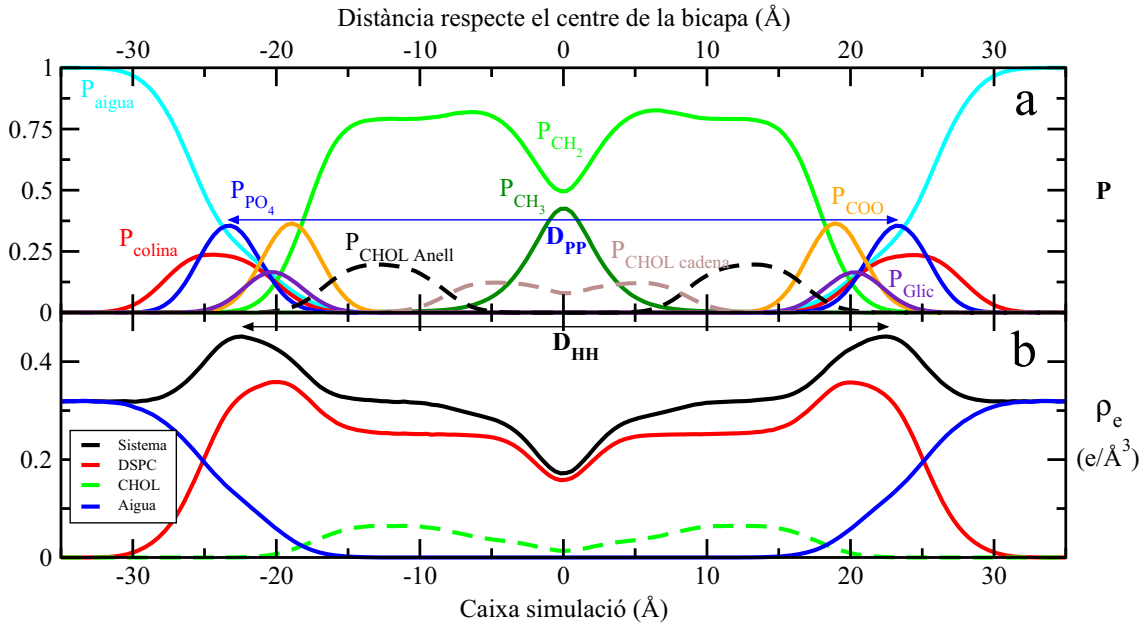

Figura 1.4: Representacions esquemàtiques de la estructura transversal d'una bicapa formada per la mescla binaria de DSPC i un 20 mol% de colesterol a 338 K. El panell (a) presenta la probabilitat de distribució, P=(ρ_e^X/ρ_e), per diferents grups atòmics del sistema corresponent tant al DSCP, colesterol i aigua. En el panell (b) veiem diferents perfils de densitat electrònica del sistema (global, DSPC, colesterol i aigua), ρ_e. L'eix de les x està en Å i representa la direcció normal a la bicapa i **D** correspon a la separació de repetició entre les capes contingudes en les vesícules multilamel·lars o bicapes apilades que s'utilitzen normalment en els experiments. Adaptat de Ref. [Nagl00] amb dades pròpies [Mart07].

Una altra característica essencial d'una membrana és el seu gruix, que s'ha comprovat que és clau per modular la seva funcionalitat [Mour84]. El valor del gruix ens dóna informació sobre l'ordenament de les cadenes, tot i que evidentment depenen de la llargada d'aquestes i la presència de dobles enllaços. Aquesta propietat com moltes altres que es revisan presenta el problema de què la seva definició no és única. Això és deu a què el límit d'on comença i on acaba la membrana en l'eix normal al seu pla pot estar definit de maneres diverses. En aquest treball s'han fet ús de dos gruixos diferents. El primer s'obté de fer la mitjana temporal de la distancia mitjana entre els fòsfors en capes oposades a cada temps, D_{PP} (Fig. 1.4a).

$$\mathbf{D_{PP}} = \langle \langle z_{P_i} \rangle_{n_1} - \langle z_{P_j} \rangle_{n_2} \rangle_t \tag{1.7}$$

on n_1 i n_2 corresponen als fòsfors de cada capa i z és la direcció normal al pla de la bicapa. La segona, s'obté del càlcul de la distància entre els dos pics obtinguts en els perfils de densitat electrònica, D_{HH} (Fig. 1.4b). Tot i que el primer mètode resulta ser més sensible que el segon, aquest darrer té l'avantatge que es pot comparar amb mesures experimentals. Tot i això, com que la majoria dels gruixos de membrana reportats experimentalment és

fonamenten en models volumètrics poc reproduïbles, la comparació dels mateixos amb els resultats de simulacions és complicada. Una discussió interessant referent als gruixos i al seu càlcul experimental es pot trobar a la Ref. [Nagl00].

Sovint és interessant conèixer el posicionament d'un grup molecular en la direcció normal al pla de la membrana. Per obtenir aquesta informació s'utilitzen els perfils de densitat electrònica (Fig. 1.4). Es calculen fent la mitjana temporal de la densitat electrònica de cada àtom de la membrana (on els electrons continguts en cada àtom se suposen concentrats en el centre del mateix) en funció de la posició en l'eix z perpendicular a la bicapa. Aquests perfils poden ser globals, per molècules (Fig. 1.4b) o representar algun fragment o grup atòmic concret que sigui d'interès (Fig. 1.4a). La importància d'aquests perfils radica en què es poden obtenir modelant els factors d'estructura obtinguts en experiments de difracció.

Una altra propietat interessant de les membranes és la inclinació que presenten certs segments moleculars respecte a l'eix z. En general, quan més propera és aquesta inclinació a 90°(paral·lel a la membrana) més fluida i desordenada es considera que és la membrana. Entre el segments més representatius en les PhdChos trobem les inclinacions de les cadenes alifàtiques (t_{sn-1} i t_{sn-2}), representades pel vector que uneix el primer i darrer metil de cada cadena. També podem calcular la inclinació del cap polar mitjançant el vector que uneix el fòsfor i nitrogen, $t_{P\mapsto N}$. En el cas del colesterol, al ser el seu anell fonamentalment rígid, podem definir la seva inclinació mitjançant el vector entre els àtoms C3 i C17 (Fig. 1.2), t_{CHOL}. De forma similar, la seva cadena flexible queda ben caracteritzada en referència al vector que uneix els àtoms C18 i C25 (Fig. 1.2), t^t_{CHOL}.

Una de les eines a la nostra disposició per estudiar sistemes fluids la trobem en les funcions de correlació espacial entre parelles de grups atòmics o de molècules que ens permeten detectar ordenaments espacials existents tot i la naturalesa fluida del sistema. L'anàlisi d'aquest ordre ens permet identificar i descriure les interaccions fonamentals entre els diferents components de la membrana que són responsables de la seva estructura final. En general, aquestes funcions descriuen la probabilitat de trobar una partícula (entesa com grup atòmic o centre de masses de diversos grups atòmics o de la molècula) en una posició determinada $\mathbf{r}$, respecte una altra que considerem de referència. Això és pot expressar com:

$$g(\mathbf{r}) = \frac{V}{N_1 N_2} \left\langle \sum_{i=1}^{N_1} \sum_{j=1}^{N_2} \delta(\mathbf{r} - \mathbf{r}_{ij}) \right\rangle \tag{1.8}$$

on N_1 i N_2 corresponen al nombre de partícules de referència i aquelles de què vole conèixer la seva distribució, respectivament [Alle90]. L'ús de parèntesis angulars significa que es fa la mitjana temporal. Aquestes funcions de correlació s'acostumen a normalitzar de manera que quan la densitat de les partícules analitzades en un punt és igual a la seva densitat mitjana el seu valor és la unitat. Generalment ens interessarà conèixer la distància respecte a la partícula de referència i així doncs normalment usarem funcions de distribució radial. Aquestes funcions ens mostren pics de correlació que reflecteixen l'existència de distàncies preferents entre els fragments considerats. L'alçada d'aquest pics indiquen la probabilitat d'aquest posicionament. Si hi ha pics que es repeteixen indiquen la presència d'ordenaments de llarg abast. Finalment, l'existència de zones on el valor de la correlació és molt baix indiquen l'existència de zones d'exclusió on per algun motiu les partícules considerades no hi poden accedir.

Un altre paràmetre fonamental a l'hora de comparar les nostres simulacions amb dades experimentals és l'anomenat paràmetre d'ordre. El càlcul per un segment determinat es fa en base a la següent relació:

$$S_{mol} = \frac{1}{2} \left\langle 3\cos^2\theta - 1 \right\rangle_{t,mol} \tag{1.9}$$

on θ correspon a l'angle del segment considerat respecte a l'eix z, i els parèntesis angulars corresponen a fer la mitjana temporal i entre molècules. Un dels segment calculats habitualment és C–H de les cadenes lipídiques. Això es deu a la seva accessibilitat mitjançant mesures de RMN prèvia deuteració del segment a estudiar, d'aquí que se'l conegui com S_{CD}. Tot i que les nostres simulacions no consideren explícitament els àtoms d'hidrogen perquè estan incorporats als carbonis, el càlcul del S_{CD} es pot fer suposant geometries ideals pels enllaços C–H. Aquest paràmetre tal i com el seu nom indica és un indicador de l'ordre de les cadenes lipídiques. Si presenta un valor proper a $-S_{CD} \sim 1/2$ significa que el fragment estarà perfectament ordenat (configuració *trans*) i perpendicular a la membrana. Valors inferiors del $-S_{CD}$, com els que trobarem en fases líquides, indiquen menor ordenament (Fig. 1.5). Per tal d'obtenir una idea de l'ordre global de la cadena s'acostuma a fer la mitjana al llarg de la cadena de tot els seus $-S_{CD}$, l'anomenat $\langle -S_{CD} \rangle$. En aquest punt cal destacar que si el segment estudiat conté un doble enllaç, aquest presenta una geometria diferent i per tant dóna lloc a valors de $-S_{CD}$ diferents, que no tenen el mateix significat que l'exposat anteriorment per cadenes saturades (Fig. 1.5). És per aquest motiu que els segments que contenen el doble enllaç no es faran servir per al càlcul de $\langle -S_{CD} \rangle$.

Les simulacions atomístiques amb DM permeten també l'estudi a nivell molecular de la interfase membrana-solvent. En aquesta té lloc un delicat equilibri de interaccions entre lípids, i lípids i solvent crucial en l'estabilitat de la membrana. Entre les interaccions més rellevants que actuen estabilitzant la interfase trobem els ponts d'hidrogen i les interaccions entre grups carregats. A nivell de DM, aquestes interaccions es poden predir en base a la posició dels grups susceptibles de formar-les ja que es coneixen per cada instant de temps. Per exemple, si un àtom donador de ponts d'hidrogen es troba a prop d'un acceptor es podrà suposar la formació d'un enllaç d'hidrogen. De forma similar, si els metils de la colina amb una càrrega efectiva positiva estan suficientment a prop d'un grup carregat negativament, s'establirà una interacció entre els dos grups carregats. Els criteris geomètrics exactes emprats per definir aquestes interaccions al llarg d'aquest treball poden trobar-se en la Ref. [Murz01].

Per concloure aquest repàs, cal destacar que la DM permet estudiar també processos dinàmics, els quals són d'especial rellevància en el context de les membranes com a conseqüència de la seva naturalesa fluida. En particular, l'anàlisi dels nostres sistemes ens permet obtenir dades tan rellevants com la difusió lateral dels lípids i la dinàmica rotacional de molècules o d'alguns dels seus segments. La difusió lateral en el pla de la bicapa es caracteritza mitjançant la següent relació:

$$D_i = \lim_{\tau\to\infty} \left[\frac{1}{4t} \langle |\mathbf{r}(t+\tau) - \mathbf{r}(t)|^2 \rangle_{i,t} \right] \tag{1.10}$$

on $\langle |\mathbf{r}(t+\tau) - \mathbf{r}(t)|^2 \rangle$ és el desplaçament quadràtic mitjà en el pla xy del centre de masses del lípid i estudiat. Aquesta mesura presenta a temps llarg un règim lineal d'on extraurem el coeficient de difusió, D_i, que per altra banda també són accessibles experimentalment

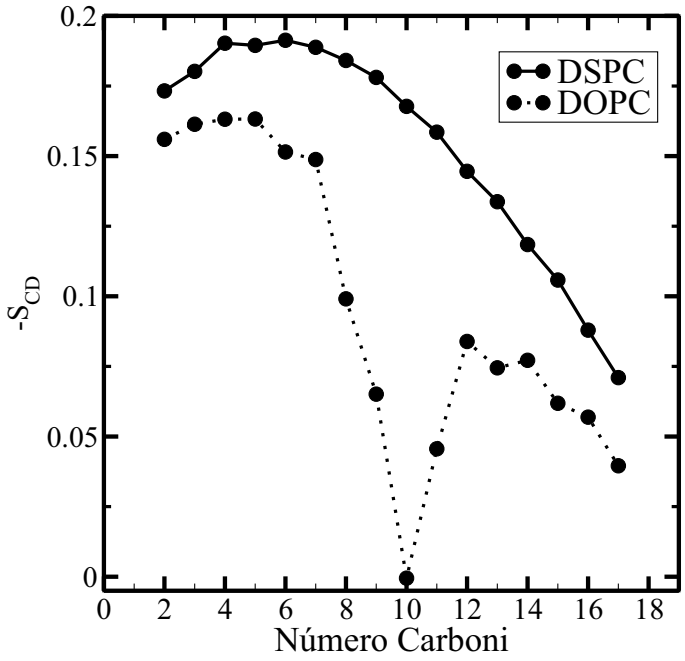

Figura 1.5: Perfils corresponents al paràmetre d'ordre S_{CD} per les cadenes *sn*–2 del DSPC (d18:0) i DOPC (18:1c9) a 338 K. "Número carboni" fa referència a la numeració dels grups metils tal i com s'observa a la Fig. 1.2. Els perfils mostren les característiques típiques del S_{CD} en el cas d'una cadena saturada (DSPC) i en una insaturada (DOPC). Ambdues ensenyen el típic màxim al voltant del 6è metil que correspon a la regió més ordenada de la capa. S'observa també que el segments pròxims al centre de la bicapa són els més desordenats. La comparació entre les cadenes del DOPC i DSPC permet dues ràpides observacions. La primera és que el DSPC és més ordenat ja que el seu perfil està sempre a valors superiors. La segona és la presència del doble enllaç que es fa evident per l'abrupte decaïment que s'observa en els segments implicats.

L'altre conjunt de propietats dinàmiques que són accessibles amb DM són els modes de moviment rotacional. Aquests poden fer referència a qualsevol segment interlipídic en funció de quina part de la molècula es vulgui analitzar. Una vegada escollit el segment d'interès, aquests poden ser caracteritzats mitjançant les anomenades funcions d'autocorrelació (ACF). Aquestes poden ser calculades de forma diversa però totes comparteixen la mateixa idea bàsica: fer una estimació de la memòria posicional del segment estudiat. Quan més trigui la funció d'autocorrelació en decaure al seu valor mínim, més memòria tindrà el procés o, el que és equivalent, més lent serà. Les funcions de correlació temporal utilitzades en aquesta Tesi són les funcions associades de Legendre de primer i segon ordre:

$$C_1(\tau) = \langle \mathbf{f}(t) \cdot \mathbf{f}(t+\tau) \rangle_{t,mol}. \tag{1.11}$$

$$C_2(\tau) = \frac{1}{2} \left\langle 3[\mathbf{f}(t) \cdot \mathbf{f}(t+\tau)]^2 - 1 \right\rangle_{t,mol} \tag{1.12}$$

on $\mathbf{f}(t)$ és el vector estudiat en la seva versió unitària.

1.4 Efecte Estructural en les Membranes de la Posició del Doble Enllaç en les Cadenes de les PhdChos: L'Efecte Selectiu del Colesterol

Les PhdChos són els lípids més abundants en membranes cel·lulars animals [Olss97]. Tal i com ja s'ha descrit en la Sec. 1.1.1 les seves cadenes poden presentar diferents llargades, graus d'insaturació i posicions dels dobles enllaços. És interessant, però, constatar que quan els lípids presenten cadenes monoinsaturades, els dobles enllaços acostumen a trobar-se al voltant del centre de la cadena en configuració *cis* [Seel77]. Acceptant que la membrana cel·lular requereixen elements constituents, varietats lipídiques, que li confereixin propietats suficientment diferents per tal de poder dur a terme una gran varietat de funcions, no existeix en la actualitat cap explicació per aquesta preferència. Tot i que existeixen diversos estudis experimentals i teòrics en referència a l'efecte de la llargada [Avel87, Cevc88, Wang95, Koyn98, Petr00, Rawi00, Huan01, Kuuc08b] i el grau d'insaturació [Di95, Koyn98, Rawi00, Bach04, Olli07] de les cadenes en les propietats de les membranes que constitueixen, el nombre d'estudis centrats en l'efecte de la posició del doble enllaç són escassos i focalitzats en l'efecte de la posició en la $T_m$de la membrana i no en les propietats generals de la mateixa [Seel77, Wang95, Kane98, Mars99, Rawi00].

Per clarificar aquesta qüestió s'han simulat onze membranes pures (només un component lipídic, 128 molècules) en la seva fase fluida. Tots els lípids simulats presenten cadenes de la mateixa llargada: 18 carbonis. La longitud seleccionada es basa en la presència natural en biomembranes de les cadenes oleiques (18:1c9) a les PhdCho [Olss97]. De la mateixa manera, la igualtat imposada a la longitud de les dues cadenes permet aïllar els efectes provinents de la presència i posició del doble enllaç d'aquells provinents de l'asimetria en la llargada de les cadenes. Amb aquestes simulacions es pretén veure si existeix alguna connexió entre la posició del doble enllaç i les propietats del sistema que justifiqui la preferència natural per cadenes on el doble enllaç es troba al centre. Una de les bicapes simulades està formada per PhdChos on les dues cadenes són saturades i corresponen a l'àcid esteàric (diestearoil–fosfatidilcolina; DSPC: *d*18:0), que es podria considerar com el sistema de referència. Tots els altres sistemes simulats tenen almenys una cadena *cis*-monoinsaturada, 18:1cX (on X marca la posició del doble enllaç, vegis Fig. 1.6). Set d'aquests sistemes presenten les dues cadenes idèntiques monoinsaturades (*d*18:1cX on X=3, 5, 7, 9, 11, 13, 15) i els tres sistemes restants presenten només insaturada la cadena *sn*–2 (*m*18:1cX on X=5, 9, 13). D'aquesta manera s'ha pretès aconseguir una variació de la posició del doble enllaç sistemàtica capaç de mostrar, un cop analitzades les simulacions pertinents, la importància de la presència i posició del doble enllaç.

En base a aquestes simulacions podem concloure que s'aconsegueix el màxim desordre en la bicapa quan el doble enllaç està situat al mig de la cadena, dioleil–fosfatidilcolina (DOPC:*d*18:1c9) en el cas dels diinsaturats i estearoil–oleil–fosfatidilcolina (SOPC: *m*18:1c9) en el cas del monoinsaturats. Això es veu tant en els màxims assolits en àrea per lípid i angle d'inclinació de les cues, com en els mínims complementaris trobats en el gruix de la membrana i el paràmetre d'ordre per aquests lípids (vegis Fig. 1.7). Així mateix, com és d'esperar, les PhdChos diinsaturades conformen membranes més desordenades que les seves anàlogues monoinsaturades. Per altra banda, l'absència de dobles enllaços porta a les membranes de diestearoil–fosfatidilcolina (DSPC:*d*18:0) a ser el sistema més ordenat. O el que

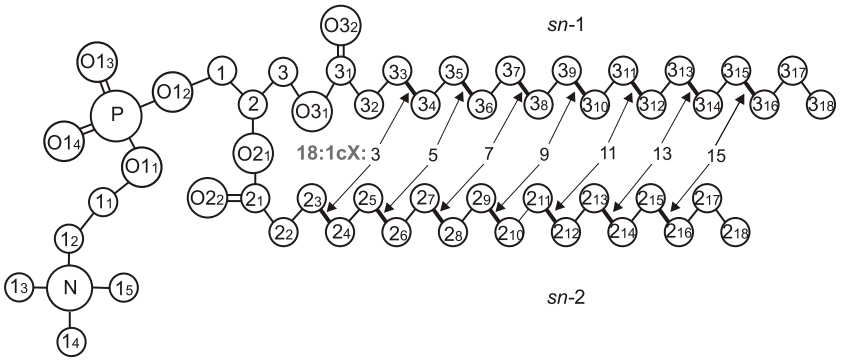

Figura 1.6: Estructura molecular de les PhdChos estudiades inclosa la numeració atòmica. Les posicions corresponents als dobles enllaços dels lípids simulats s'han marcat i numerat en les dues cadenes. El símbol químic, C, corresponent als carbonis s'ha elidit per claredat.

és el mateix, aquest sistema presenta la menor àrea per lípid i angle d'inclinació de les seves cadenes, així com el major gruix de la bicapa i paràmetre d'orde. A més a més, s'ha detectat un decaïment de l'ordre de les membranes quan el doble enllaç s'ha traslladat respecte a la posició central tant en direcció al cap polar com al final de la cua. Experimentalment, mesures de T_md'aquests mateixos sistemes corroboren aquesta observació [Wang95, Mars99]. La $T_m$per les PhdChos presenta una relació inversa amb l'àrea per lípid de les membranes que formen[Mart08], observant-se una $T_m$mínima pel DOPC i una $T_m$màxima pel DSPC. Aquest comportament és per tant no monòton en funció de la posició del doble enllaç i també s'ha detectat que és bastant asimètric. Això significa que el trasllat del doble enllaç en direcció al cap polar produeix un lleuger, tot i que estadísticament significatiu, decaïment de l'ordre de les membranes. En canvi, el trasllat en direcció al final de la cadena produeix un decaïment de l'ordre quantitativament superior fins arribar al comportament extrem del lípid saturat (DSPC). Resulta doncs evident que les PhdChos insaturades mostren una diferència major en les seves propietats respecte al lípid saturat quan el doble enllaç és troba en el mig de les cadenes (DOPC i SOPC). Tot i que aquest raonament és clar per les PhdChos amb dobles enllaços propers al centre de la bicapa, s'ha d'anar amb cura amb aquelles on el doble enllaç es troba a prop del cap ja que les diferències són substancialment menors.

El resultat anterior constitueix per si sol un avenç significatiu en la comprensió de la importància de la posició del doble enllaç en els lípids de membrana. La rellevància d'aquesta observació en membranes naturals està, però, supeditada a què el comportament descrit es mantingui en sistemes multicomponents que defineixen millor la verdadera natura de les biomembranes. El colesterol, també component majoritari en les membranes plasmàtiques de les cèl·lules de mamífers, és el candidat perfecte per dur a terme aquest estudi de mescles binàries. En aquest treball s'ha conjecturat que el posicionament del doble enllaç i per tant la selecció natural de lípids a les membranes està condicionada, almenys en part, per les interaccions específiques entre PhdCho i el colesterol.

Per comprovar aquesta hipòtesi, s'han dut a terme les mateixes simulacions descrites anteriorment però aquest cop afegint-hi un 20 mol% de colesterol en cadascuna de les membranes, que correspon a una concentració fisiològica típica [Olss96]. Com a efecte general, la incorporació de colesterol a les membranes indueix ordre en els lípids, l'anomenat efecte de condensació. Observis per exemple la una caiguda de l'àrea per molècula (Fig. 1.7a) i

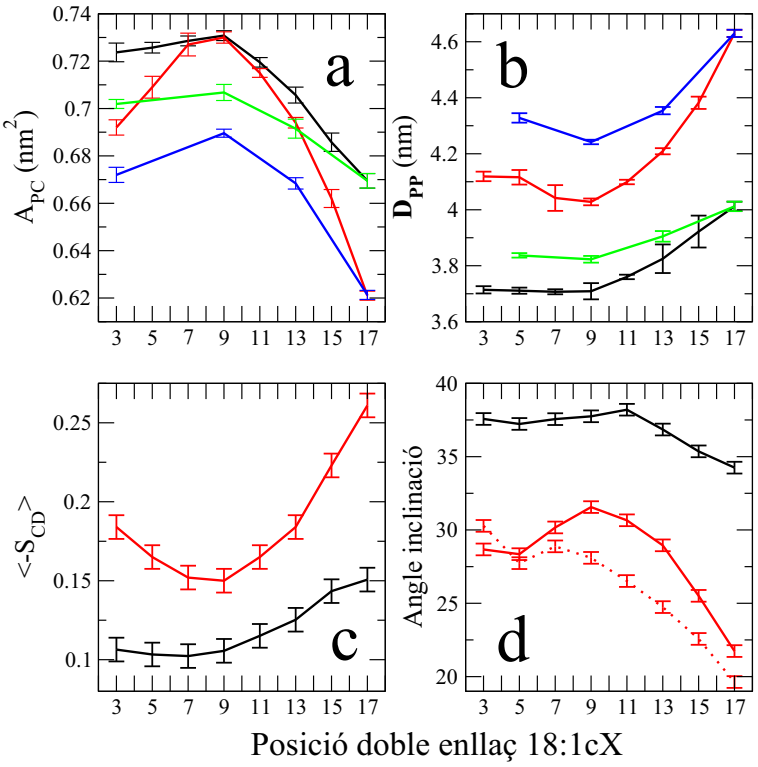

Figura 1.7: (a) Àrea per lípid, (b) gruix de la membrana, (c) paràmetre d'ordre mitjà i (d) angle d'inclinació en funció de la posició del doble enllaç en les PhdChos. S'ha representat en negre i verd els sistemes purs de les bicapes constituïdes per lípids di- i monoinsaturats respectivament. Els sistemes mixtes amb 20% de colesterol prenen en canvi els colors vermell i blau respectivament. La corba de punts en el panell (d) es refereix a l'angle d'inclinació dels colesterols. La posició 17 correspon al lípid saturat DSPC.

de la inclinació de les cadenes (Fig. 1.7d) en membranes amb colesterol en comparació als respectius sistemes purs, així com un augment generalitzat del gruix de la bicapa (Fig. 1.7b) i del paràmetre d'ordre (Fig. 1.7c). Aquestes simulacions també mostren que l'efecte de condensació està fortament influenciat per la posició del doble enllaç. Com a conseqüència, les diferències reportades anteriorment per als sistemes purs s'observen magnificades quan el colesterol es troba present. El colesterol, per tant, augmenta el comportament no monòton anteriorment observat pels sistemes purs: el trasllat del doble enllaç cap al cap polar i cap al final de la cua augmenta visiblement l'ordre del sistema respecte el DOPC i SOPC. En aquest sentit veiem que les bicapes mixtes amb DOPC i el SOPC són, ara amb més claredat, les més desordenades comparades amb aquelles formades per altres PhdChos amb el mateix número de cadenes monoinsaturades. Tanmateix, les diferències de comportament entre aquests i el DSPC es veuen ampliades considerablement respecte les membranes pures. Conseqüentment, es pot conjecturar sobre que la incorporació de PhdChos insaturats a les membranes constitueix un mecanisme simple per promoure la fluïdesa en les biomembrana, especialment quan els dobles enllaços es troben a prop del centre de la cadena (posició 9–10 Fig. 1.6) i en presència de colesterol. Això es pot interpretar com que el colesterol contribueix decisivament en la heterogeneïtat natural en les PhdChos de les seves cadenes monoinsaturades i possiblement constitueix el mecanisme bàsic en la formació de **rafts** o

nanodominis lipídics [Simo97].

Aquest treball, a banda d'obtenir dades sobre la variació del comportament macroscòpic de la membrana en funció de la posició del doble enllaç, també permet indagar sobre l'origen microscòpic d'aquest comportament. El comportament no monòton i asimètric observat en les propietats estructurals és pot racionalitzar mitjançant l'estudi de les interaccions entre PhdChos i colesterols a nivell atòmic. En els sistemes purs, l'origen d'aquest comportament es troba parcialment en què el màxim ordenament d'un segment de la cadena lateral d'una PhdCho varia en funció de la seva profunditat en la membrana, tal i com s'observa en el $-S_{CD}$ pel DSPC (Fig. 1.5). Cal tenir en compte, aleshores, que la capacitat per desordenar inherent al doble enllaç està directament relacionada amb l'ordre de l'entorn on es situa. En el cas de sistemes amb colesterol, apareixen noves interaccions que acabaran essent les responsables de les clares variacions de comportament. D'entrada s'observa que el colesterol ordena notablement la membrana, en especial en la zona on es troba situada l'estructura d'anells. També s'ha constatat que la presència d'un doble enllaç limita l'efecte de condensació del colesterol en comparació amb l'observat en les membranes saturades. També s'ha vist que la presència de colesterol magnifica el comportament no monòton i asimètric observat en els sistemes purs, fins el punt que la posició del doble enllaç pot induir més desordre que el número de dobles enllaços. L'origen de tot plegat es troba en la particular interacció del doble enllaç amb l'anell rígid del colesterol, i de forma notòria amb el metils que aquest presenta a la cara β (metils C18 i C19, vegis Fig. 1.2). Els motius que han permès identificar aquestes interaccions com a fonamentals són els següents. Primer, s'observa que la profunditat del colesterol en la membrana roman pràcticament inalterada independentment de la posició del doble enllaç del lípid que forma la membrana, ja que aquesta està bàsicament determinada pel pont d'hidrogen que es forma entre l'hidroxil del colesterol i l'oxigen del carbonil a la cadena *sn*–2. O el que és el mateix, el doble enllaç interaccionarà amb una part concreta del colesterol que dependrà únicament de la posició del doble enllaç a la cadena. Segon, els sistemes que presenten un major desordre mostren distàncies menors entre els seus dobles enllaços i el metil C18 del colesterol. La proximitat dels dobles enllaços al metil C19 també promou desordre però en menor grau que el C18. La combinació d'aquest dos factors (profunditat constant dels carbonis C18 i C19 en totes les membranes i el fet que la interacció entre aquests metils i el doble enllaç promouen el desordre) és suficient per explicar les diferències observades en les propietats estructurals de la membrana en funció de la posició del doble enllaç. S'ha observat que la interacció entre el C18 i el doble enllaç és màxima quan aquest es troba al mig de la cadena (DOPC/SOPC, posicions 9–10). Quan el doble enllaç es trasllada cap al final de la cadena, redueix la seva interacció amb el C18, afavorint l'empaquetament entre PhdChos i colesterols, i per tant l'àrea per molècula decreix i l'ordre dels lípids augmenta. En canvi, quan el doble enllaç es mou en direcció al cap polar tot i que la interacció d'aquest amb el C18 també es redueix, la creixent interacció amb el C19 resulta en un ordenament global menor de la membrana que en el cas anterior. Aquest descobriment suggereix que la interacció entre el C18 i el fragment semirígid del doble enllaç afecta l'angle d'inclinació del colesterol i aquest, a la seva vegada, el de les cadenes al seu voltant [Aitt06, Rog07a, Rog08a], explicant les variacions no monòtones observades. En canvi, la presència del C19 és responsable de l'asimetria reportada respecte la posició central (9–10, vegis Fig. 1.6).

En la mesura del possible, les simulacions aquí presentades s'han comparat de forma exhaustiva amb les dades experimentals disponibles. Cal destacar que aquesta comparativa

ha posat de manifest no només que ambdues estan d'acord des d'un punt de vista qualitatiu [Wang95, Mars99], sinó que en la majoria dels casos els sistemes són comparables també quantitativament [Nagl00, Petr00, Liu04, Kuuc05, Math08, Pan09].

1.5 Estudi de la Preferència Biològica per PhdChos on *sn*–1 és Saturada i *sn*–2 Insaturada com a Constituents de les Membranes: Diferències entre els Isòmers Posicionals SOPC i OSPC en Membranes amb i sense Colesterol

En aquesta secció es continuarà amb l'estudi de la preferència natural per determinats lípids com a constituents bàsics de les biomembranes. En particular centrarem l'atenció en una preferència que concerneix un altre cop a les cadenes laterals de les PhdChos. Donat un fosfoglícerolípid que presenti dues cadenes diferents, aquest podrà tenir isòmers posicionals ja que cada cadena té dos punts d'ancoratge no equivalents, *sn*–1 o *sn*–2 (la cadena *sn*–1 s'enllaça en el carboni 3 i la *sn*–2 en el carboni 2 del grup glicerol, vegis Fig. 1.6). Per tot els fosfoglícerolípids presents en les membranes cel·lulars, la cadena *sn*–1 és més comunament saturada, sent la *sn*–2 la que normalment es presenta mono- o poliinsaturada. Dit d'una altre manera, s'observa una clara preferència per situar els dobles enllaços a la cadena *sn*–2 [Van 65, Romi72, Cron75, Sait77]. Aquesta preferència s'observa tant en membranes provinents de cèl·lules eucariotes [Bare99, Rams02, Meer05] com procariotes [Rott79b, Iske98]. La raó d'aquesta preferència és desconeguda.

Fins al moment, tan sols un conjunt reduït d'articles han abordat aquest problema [Davi81, Davi83, Davi84, Simi88, Ichi99, Inou99]. Aquests estudis han mostrat mitjançant calorimetria que $T_m$depèn lleugerament de la cadena lipídica on és situa el doble enllaç. En el cas dels isòmers que estudiarem en aquesta secció SOPC (1–estearoil–2–oleil–sn–glícero–3–fosfatidilcolina, *m*18:0/1) i OSPC (1–oleil–2–estearoil–sn–glícero–3–fosfatidilcolina, *m*18:1/0)) la diferència és de 2–4 K, essent el SOPC qui té la T_m menor i que correspon al lípid amb la disposició de les cadenes d'acord a la preferència natural [Davi81, Davi83, Ichi99, Inou99]. Sistemes mixtes amb colesterol d'aquests isòmers posicionals també mostren que la interacció del colesterol amb la PhdCho depèn de la cadena on es troba la insaturació [Huan77, Davi83, Davi84]. A l'incomplet coneixement de les característiques estructurals i propietats físiques de membranes constituïdes per aquests tipus d'isòmers posicionals, se li ha d'afegir la manca d'informació sobre l'efecte fisiològic que permeti entendre el motiu final de l'observada preferència en les membranes cel·lulars [Cron74, Cron75]. Per exemple, s'ha documentat la pèrdua de la preferència posicional de les cadenes insaturades en membranes provinents de cèl·lules d'hepatomes s'associa a les elevades concentracions de colesterol presents [Dyat74]. En condicions similars d'elevat contingut de colesterol, aquest cop en micoplasmas, s'ha observat un increment de la concentració de lípids amb la cadena *sn*–1 insaturada i la *sn*–2 saturada [Rott79a, Davi81].

En aquesta secció emprem simulacions amb DM per considerar els isòmers posicionals *sn*–1/*sn*–2 en bicapes pures i en mescles binàries amb colesterol al 20 mol%. Els isòmers

seleccionats són PhdChos amb cadenes laterals de 18 carbonis amb una cadena saturada i l'altra monoinsaturada (SOPC i OSPC). On el SOPC presenta la configuració que representa la preferència natural. S'ha fet ús també de dos lípids de referència, DSCP (di-saturat) i DOPC (di-monoinsaturat), també amb cadenes de 18 carbonis.

Com a resultat d'aquestes simulacions es veuen petites, però consistents diferències entre els dos isòmers posicionals que van en la direcció de les dades experimentals disponibles. El lípid SOPC que té el doble enllaç en la cadena *sn*–2 és més desordenat que el OSPC que té el doble enllaç en la cadena *sn*–1. Totes les propietats calculades –estructurals i dinàmiques– confirmen aquesta observació, vegis Taula 1.1. Tot i que les diferències reportades són petites, en la literatura diferències d'aquestes magnituds, fins i tot inferiors, han demostrat ser suficients per alterar el comportament final de les membranes. Més encara, quan el colesterol es troba present, les diferències de comportament entre SOPC i OSPC s'amplifiquen, fet que suggereix que la localització del doble enllaç en glícero–fosfatidilcolines realment constitueix un element diferencial. Cal destacar que aquests resultats són a priori contraintuïtius ja que les diferències entre ambdós isòmers semblen menyspreables en base a la seva estructura on tan sols el doble enllaç canvia de cadena.

Els resultats de les nostres simulacions suggereixen que la diferència en la penetració o inserció dins de les membranes entre les cadenes *sn*–1 i *sn*–2 és el factor revelant a tenir en compte. El paràmetre que ens permet avaluar aquest fenomen és l'anomenat "desajust de cues" que expressa la distància en la direcció z entre el darrer metil de la cadena *sn*–1 i el darrer de la *sn*–2. Aquest paràmetre és positiu quan la cadena *sn*–1 s'endinsa més que la *sn*–2. En aquest treball observem que aquesta propietat és no nul·la fins i tot en lípids simètrics com poden ser el DSPC i el DOPC, que presenten valors de 0.40 i 0.28 Å respectivament (vegis Taula 1.1). El desajust de les cues varia més apreciablement en els isòmers per causa bàsicament de dos efectes. Primer, el punt d'ancoratge del glicerol de la cadena *sn*–1 es troba més inserida dins la membrana. Segon, la cadena insaturada és més curta. Com a resultat, el OSPC reporta valors negatius però propers en magnitud al dels lípids simètrics perquè els efectes es compensen (cua curta en la posició *sn*–1 que està més inserida, cua llarga en posició *sn*–2 que és la més superficial), -0.56 Å en la membrana pura. El SOPC, en canvi, presenta un valor de 1.32 Åja que en aquest cas tots dos efectes van en la mateixa direcció, maximitzant la distància d'inserció. És a dir, la diferència entre els dos isòmers és de quasi 2 Åtot i ser lípids idèntics llevat de la posició d'ancoratge de les cadenes saturada i monoinsaturada. Per comparar, la distància carboni-carboni en un cadena alifàtica és de 1.5 Å. Estudis experimentals en monocapes amb lípids asimètrics, des de 18:0-8:0 fins 18:0-18:0, han identificat el desajust entre les cues com a factor important per la promoció de desordre [Ali98] i, per tant, justifiquen el perquè les membranes de SOPC són més desordenades que les d'OSPC.

Una de les qüestions més importants sorgides arran d'aquest treball és per què la presència del colesterol incrementa les diferències observades entre el SOPC i OSPC en les bicapes pures. En la secció anterior s'ha vist que la capacitat del doble enllaç per desordenar depèn de la seva posició en la cadena en especial quan el colesterol està present. En particular s'ha identificat que quan el doble enllaç es troba al mig de la cadena, l'efecte de condensació induït pel colesterol és menor perquè la interacció del doble enllaç amb el metil C18 del colesterol és màxima ja que ambdós es troben al mateix nivell dins la bicapa. En el cas dels isòmers posicionals trobem que el SOPC té el doble enllaç a una distància mitjana respecte la posició

	DSPC	OSPC	SOPC	DOPC
T_m ($L_\beta \mapsto L_\alpha$) (K)	328.80	281.90	279.90	232.90
A^*_{PC} (Å^2)	66.95±0.31	70.21±0.19	70.67±0.34	73.08±0.21
	56.39±0.19	**61.88±0.31**	**62.63±0.17**	**66.25±0.24**
	NA	**3.27**	**3.73**	**3.06**
$\mathbf{D_{PP}}$ (nm)	4.63	4.28	4.25	4.04
±0.01 nm	**4.01**	**3.84**	**3.82**	**3.71**
$\langle -S_{CD} \rangle$ (±0.003)				
sn–1	0.261	0.177	0.208	0.150
	0.151	**0.114**	**0.136**	**0.106**
sn–2	0.262	0.217	0.172	0.152
	0.154	**0.140**	**0.113**	**0.106**
Angle inclinació (deg)				
t_{sn-1}	21.74	28.53	26.72	31.56
	34.25	**37.36**	**35.76**	**37.75**
t_{sn-2}	21.06	25.34	28.64	30.65
	33.46	**34.73**	**37.08**	**36.59**
$t_{P \mapsto N}$	98.90	99.30	99.51	100.49
	100.24	**100.81**	**100.80**	**101.50**
t_{CHOL}	19.63	24.29	25.91	26.52
t^t_{CHOL}	28.70	34.93	37.17	37.89
$\langle d_{centre\ bicapa} \rangle$ (Å± 0.1)				
sn–1	2.06	2.75	1.72	2.33
	2.17	**2.72**	**1.72**	**2.24**
sn–2	2.62	2.16	3.11	2.66
	2.57	**2.16**	**3.04**	**2.52**
Desajust cues	0.56	-0.59	1.39	0.33
	0.40	**-0.56**	**1.32**	**0.28**
$\langle d_{C18} \rangle$ (Å± 0.1)				
sn–1 ($C3_9$-$C3_{10}$)	0.07	<u>0.36</u>	0.70	<u>-0.06</u>
sn–2 ($C2_9$-$C2_{10}$)	-0.70	-0.37	<u>-0.02</u>	<u>-0.65</u>

Taula 1.1: Propietats estructurals caracteritzades de les membranes DSPC, OSPC, SOPC i DOPC. En negreta s'han marcat els valors per als sistemes purs, mentre que els altres corresponen als sistemes amb un 20 mol% colesterol. NA: no aplicable. Els valors subratllats indiquen la posició del doble enllaç. Els valors de T_m s'han extret de la Ref. [Ichi99].

del C18 molt inferior al OSPC (vegis $\langle d_{C18} \rangle$ en la Taula 1.1). Això explica el perquè el SOPC és troba més desordenat que el OSPC quan el colesterol està present en la membrana i, per tant, justifica l'augment de les diferències observades respecte els sistemes purs.

En conclusió, els resultats de les nostres simulacions suggereixen que la preferència natural pels isòmers posicionals —*sn*–1 saturada i *sn*–2 monoinsaturada— és el resultat evolutiu cap a l'obtenció de lípids que maximitzin el desordre de la membrana. Més encara, aquesta preferència està basada no només en les propietats dels lípids per si mateixos, sinó també en la seva interacció diferencial amb altres components de les membranes, en particular amb el colesterol.

1.6 Influència de la Parametrització del Doble Enllaç *Cis* en les Propietats de les Membranes Lipídiques

A les dues darreres dècades s'han dut a terme simulacions de DM d'una gran varietat de membranes composades per diferents lípids i proporcions dels mateixos. Malgrat això, el nombre d'estudis centrats en garantir la qualitat de les descripcions moleculars utilitzades (camps de forces) és força més limitada. En general, la gran majoria de la comunitat que treballa amb DM de membranes cel·lulars dirigeixen les seves investigacions en funció de la disponibilitat de camps de forces pels lípids simulats provinent d'uns pocs però excel·lents treballs de parametrització. Aquests han proveït d'un conjunt de paràmetres optimitzats per un conjunt de lípids molt limitat. A causa de la complexitat i temps requerit per fer una parametrització des de zero aquesta no és normalment una opció viable. En canvi, la majoria dels investigadors assumeixen un cert grau de portabilitat dels paràmetres entre lípids amb canvis estructurals menors, el que permet expandir de forma notòria el nombre de lípids a l'abast per simular en base als ja parametritzats. Aquest ha estat el cas del present treball on el camp de forces que s'ha fet servir per les PhdChos es basa parcialment en un treball on els paràmetres van ser optimitzats únicament pel lípid saturat dipalmitoil–fosfatidilcolina (DPPC) [Tiel96].

Tal i com s'ha vist en la Sec. 1.2.1 el camp de forces emprat per descriure un sistema determina unívocament el seu comportament. Així doncs, la qualitat del camp de forces és un factor decisiu en la fiabilitat d'una simulació. Com que les dues seccions anteriors descriuen amb gran detall l'efecte del doble enllaç de les cadenes laterals en la membrana, convé preguntar-se si aquests estaven descrits adequadament. O millor encara, si els resultats obtinguts són sensibles a la parametrització del doble enllaç. Tot i que és d'esperar que diferents parametritzacions del doble enllaç donin lloc a resultats quantitativament diferents, especialment en la regió hidrofòbica [Niem06, Olli07], el fet realment interessant és si els canvis produïts són també qualitatius. Això darrer indicaria un canvi dràstic en la física del sistema i posaria en dubte els resultats obtinguts amb el camp de forces que resultés erroni.

En aquesta secció s'estudia la importància de la parametrització del doble enllaç *cis* i s'ha comprovat que és un tema força subtil. Per això utilitzarem simulacions amb DM per determinar l'efecte de la descripció del doble enllaç en membranes constituïdes per PhdCho amb cadenes di-monoinsaturades. S'han considerat per això tant membranes pures com mescles amb un 20 mol% de colesterol. S'han comparat dos camps de força diferents pel doble enllaç mitjançant l'estudi de la variació sistemàtica de la posició del doble enllaç en la cadena lipídica tal i com es descriu en la Sec. 1.4. Totes les simulacions s'han efectuat per duplicat: Les primeres presenten la parametrització desenvolupada per Bachar et al. [Bach04] que té en compte les conformacions *skew* en els díedres immediatament adjacents al doble enllaç (Perfil amb dos màxims a -120° i 120°) i correspon a l'emprada en les Secs. 1.4, 1.5 i 1.7. Les segones utilitzen la parametrització "GROMOS87" per la descripció del doble enllaç [Tiel02].

El camp de forces que té en compte la població de les conformacions *skew* prediu que la membrana és més desordenada quan el doble enllaç es troba en el mig de la membrana tal i com a estat prèviament descrit a la Sec. 1.4. Això és visualitza en el màxim en l'àrea per lípid i en els mínims en el gruix de la membrana i en el paràmetre d'ordre mig trobats pel DOPC

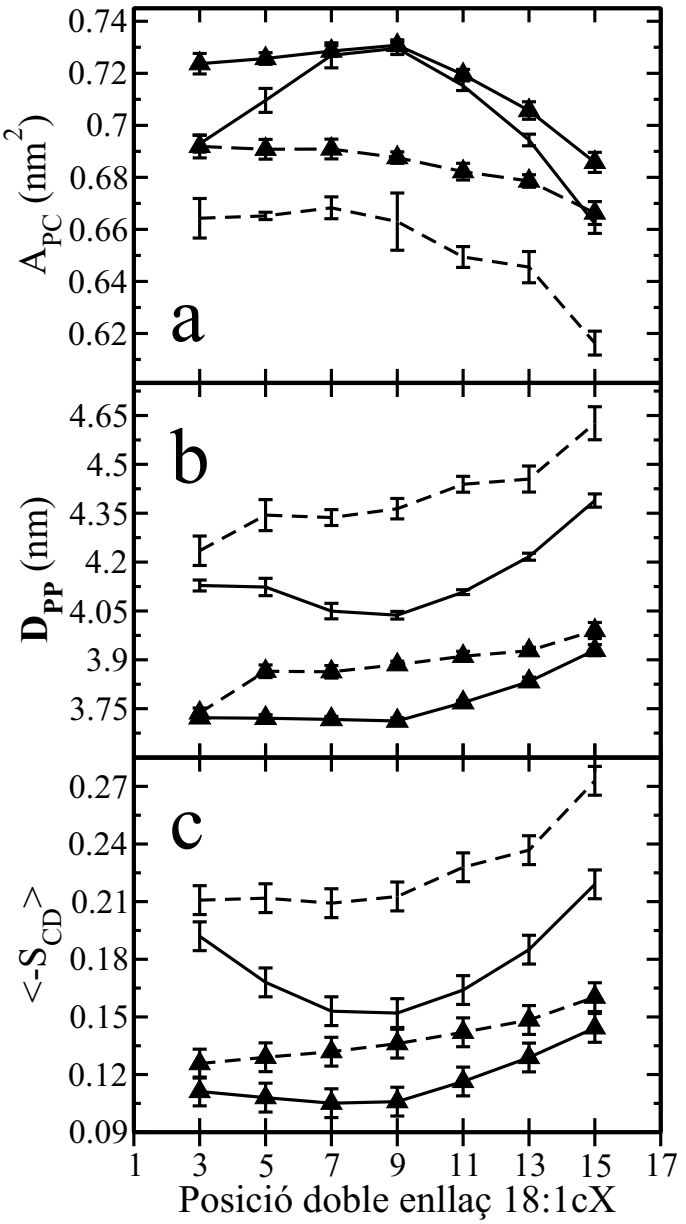

Figura 1.8: (a) Àrea per molècula de PhdCho, (b) gruix de la bicapa, i (c) valors del paràmetre d'ordre $\langle -S_{CD} \rangle$ en funció de la posició del doble enllaç. La línia sòlida correspon a la parametrització per Bachar et al. mentre que la línia discontinua correspon a la parametrització que no té en compte les conformacions *skew* dels díedres. Es mostren resultats tant pels sistemes purs (triangles), com per les mescles que contenen un 20 mol% de colesterol (línies sense símbols).

(*d*18:1c9), vegis Fig. 1.8. La descripció que no té en compte els estats *skew* prediu que l'àrea per lípid, a banda de ser sensiblement menor en temes absoluts, decreix monòtonament quan el doble enllaç es mou des de el cap polar cap al final de la cadena (vegis Fig. 1.8). Les altres propietats calculades són consistents amb aquesta observació. Això implica la desaparició dels màxims i mínims predits per la parametrització del Bachar et al. En conclusió, s'observa no només un canvi quantitatiu en els valors de les propietats calculades, sinó també en el comportament o tendència d'aquestes variables quan es varia la posició del doble enllaç.

Quan s'afegeix colesterol, les diferències discutides pel sistemes purs es fan encara més evidents. Això suggereix que en el context de sistemes multicomponents la importància d'una correcta parametrització del doble enllaç és fins i tot més important, perquè la interacció entre els diferents components pot agreujar les deficiències dels paràmetres emprats.

La comparació quantitativa dels resultats de les simulacions amb dades experimentals és complicada degut a què no hi ha dades disponibles per a tots els lípids simulats. El DOPC és, de fet, l'únic on és factible una comparació detallada. Quan comparem els resultats obtinguts de les simulacions del DOPC amb les dues parametritzacions i les dades experimentals disponibles s'observa que la parametrització per Bachar et al. les reprodueix substancialment millor. Àrea per lípid, gruix de la bicapa, paràmetres d'ordre, i fins i tot factors d'estructura són exemples on aquesta comparativa resulta millor.

En conclusió, els resultats obtinguts posen de manifest la importància de descriure correctament el doble enllaç a les cadenes lipídiques. Trobem que el comportament entre models varia no només quantitativament com és d'esperar sinó que també qualitativament modificant tendències el que sens dubte li dóna més importància a aquest tema. Per exemple, el comportament no monòton en l'àrea per lípid ques s'observa majorment en els sistemes mixtes amb colesterol i que en aquesta Tesi s'han fet servir per explicar la preferència natural per lípids amb el doble enllaç al mig de la cadena, no s'observa quan es fa ús de models més simplistes. Així doncs, quan és simulin membranes amb lípids insaturats, on el doble enllaç pugui tenir un cert rol rellevant, convé fer ús d'una parametrització que tingui en compte les conformacions *skew* per millorar la seva fiabilitat.

1.7 El Colesterol Indueix un Específic Ordre Espacial i Orientacional en Membranes Constituïdes per la Mescla Colesterol/Fosfolípid

El colesterol és el lípid més comú en les membranes cel·lulars animals [Ohvo02]. Estudis experimentals i teòrics mostren com el colesterol té una tendència natural a formar estructures ordenades en les membranes [Ali07, Chon09]. Des del punt de vista macroscòpic aquestes ordenacions es poden relacionar amb la fase L_o(Sec. 1.1.2), si be a nivell microscòpic l'organització lipídica i els mecanismes responsables d'aquests ordenaments romanen sense clarificar. Models conceptuals com el **Condensed Complex** model [Radh05] (basat en la formació complexes Phd–CHOL), el **Superlattice** model [Chon94a] (basat en l'existència de distribucions ordenades esteses) i l'**Umbrella** model [Huan99] (basat en el fet que el petit cap polar no pot protegir el gran anell hidrofòbic de l'aigua) han estat proposats per explicar la formació d'aquestes estructures ordenades (Sec. 1.1.3). Tot i la capacitat de predicció

demostrada per alguns d'ells, cap és capaç de justificar la singular capacitat del colesterol d'entre tots els esterols per organitzar lateralment la membrana. Aquest argument queda recolzat, per exemple, pel fet que el colesterol i l'ergosterol, d'estructura semblant al colesterol, són coneguts per la seva capacitat de formar **rafts** (nanodominis) lipídics, mentre que molts altres esterols no presenten aquesta capacitat [Li03, Wang04, Aitt06, Vain06, Rog08b].

Malgrat els nombrosos estudis que reporten l'habilitat única del colesterol per induir ordre en la membrana preservant la seva naturalesa fluida, no hi ha cap estudi que caracteritzi els mecanismes moleculars darrera d'aquesta habilitat. Per aquest motiu, aquesta secció es centre en l'estudi de l'organització lateral a escala nanoscòpica en membranes que contenen colesterol que ha resultat en un substancial avenç en el tema.

Per tal de descriure amb precisió l'entorn del colesterol i analitzar la seva dependència amb la concentració, s'han efectuat un total de 13 simulacions mitjançant DM a nivell atòmic de membranes en la seva fase fluida (338K). Les 10 primeres contenen o bé el PhdCho totalment saturat DSPC (5), o l'alternativa di-monoinsaturada DOPC (5) mesclats amb un 10, 20, 30, 40 i 50 mol% de colesterol. Per comparar s'han efectuat també tres simulacions amb un 20 i 40 mol% de colesterol pla (DCHOL) amb DSPC (2) i DOPC (1). L'estructura del DCHOL és idèntica a la del colesterol on el metils perpendiculars al pla de l'esterol, C18 i C19, s'han eliminat (vegis Fig. 1.2), obtenint un esterol amb dues cares planes. Cadascun dels sistemes conté 128 PhdChos, el corresponent nombre de esterols (14, 32, 56, 86 i 122) i 6186 aigües. Tots ells han estat simulats entre 200–300 ns.

D'aquestes simulacions s'han recollit diverses evidències de l'extraordinària capacitat del colesterol per ordenar/organitzar el seu entorn en les membranes i s'ha identificat la particular estructura del colesterol com a últim responsable d'aquesta capacitat. Primer de tot observem que les molècules de colesterol tendeixen a situar-se en la segona esfera de coordinació d'altres molècules de colesterol (vegis Figs. 1.9 i 1.10). Això es pot entendre com que el seu petit cap polar i gran anell alifàtic eviten, en la mesura del possible, contactes directes entre colesterols per tal d'evitar l'exposició de parts hidrofòbiques de la membrana a l'aigua i la conseqüent penalització energètica. En conseqüència, entre dues molècules d'esterol normalment hi ha PhdChos, posició que correspon a la primera esfera de coordinació (vegis Figs. 1.9 i 1.10). Això es produeix com a resultat de què el gran cap polar de les PhdChos (colina) és capaç de protegir eficaçment el colesterol de l'aigua. Només a concentracions de colesterol elevades la presència de colesterols en la primera esfera de coordinació es fa evident (vegis Fig. 1.9). En essència el descrit fins al moment constitueix la hipòtesi bàsica de l'**Umbrella** model [Ali07], que es troba totalment recolzada pels resultats aquí presentats.

En segon lloc s'han identificat patrons en el posicionament, en el pla de la membrana, de lípids i colesterols al voltant dels colesterols. Aquest fet no deixa de ser remarcable degut a la fluïdesa lateral de la membrana. Concretament s'ha vist com la presència del metils fora del pla de l'anell del colesterol (C18 i C19) indueixen en les cadenes de les PhdChos cinc posicions preferents en la primera esfera de coordinació (Fig. 1.10a), que a la vegada provoquen una simetria trigonal en el posicionament dels colesterols en la segona esfera de coordinació (Fig. 1.10b). L'efecte dels metils C18 i C19 provoca que la cara rugosa es subdivideixi en dues regions que resulten fonamentals en les capacitats organitzatives del colesterol i justifica la posició finals dels pics ($\beta 1$, α i $\beta 2$). Totes les membranes analitzades en aquest treball presenten les característiques aquí descrites encara que amb matisos. Per exemple, en el cas de les membranes amb DOPC els pics observats són sempre més difuminats que pel cas amb

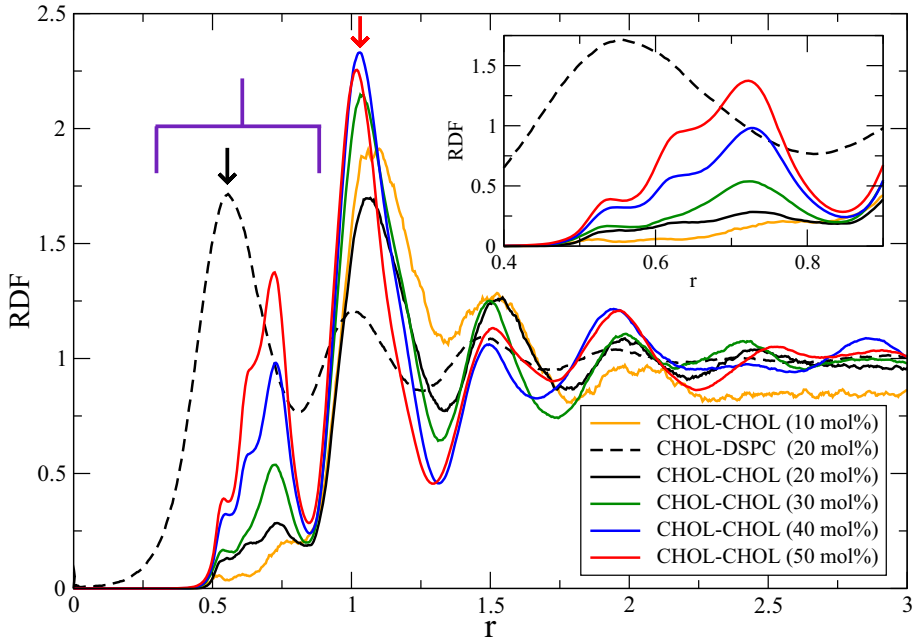

Figura 1.9: Funcions de distribució radial, RDF, per les parelles CHOL-CHOL (línia continua) i CHOL-DSPC (línia discontinua) per membranes DSPC/CHOL amb diferents concentracions de colesterol. Els colors utilitzats indiquen la concentració de colesterol: 10 mol% (taronja), 20 mol% (negre), 30 mol% (verd), 40 mol% (blau) i 50 mol% (vermell). Només s'inclou la informació corresponent a les parelles CHOL-DSPC pel sistema amb un 20 mol% de colesterol. La distància radial en el pla xy respecte el centre de masses de la molècula de colesterol s'ha representat amb r. Al requadre s'ha magnificat la primera esfera de coordinació on s'exhibeix un increment de l'ocurrència de les parelles CHOL-CHOL a concentracions elevades de colesterol.

DSPC, reflectint la menor capacitat del colesterol per ordenar lípids insaturats.

Aquest tipus d'ordenament és sens dubte una característica particular del colesterol. Això s'observa en la comparació de les propietats del colesterol i el DCHOL, el qual no presenta els metils C18 i C19. Els mapes de distribució pel DCHOL demostren que l'absència d'aquests metils dóna lloc a un comportament totalment diferent. Mentre els colesterols es posicionen al votant dels altres colesterols amb una simetria trigonal ($\beta 1$, α i $\beta 2$), el DCHOL ho fa en dos pics, un a cada cara (α i β) respecte els altres DCHOLs. Això en darrer terme es tradueix en una organització preferencial (si be dinàmica) en el pla de la membrana en triangles pel colesterol i fileres pel DCHOL (vegis Fig. 1.11). Això, entre altres, permet al colesterol expandir la seva organització en dues dimensions mentre que el DCHOL es limita a una, i aquest podria ser el motiu pel qual el colesterol condensa més la membrana que el DCHOL tot i tenir un volum major per la presència dels metils C18 i C19 en concentracions moderades.

L'organització que es troba en la segona esfera de coordinació dels colesterols va més enllà de ser posicional, ja que també apareix si s'analitza l'orientació relativa entre colesterols. Els colesterols corresponents als pics observats en el mapa de probabilitat CHOL-CHOL mostren orientacions preferencials. Aquestes s'han d'entendre dins d'un context dinàmic on el pes d'algunes orientacions és substancialment superior. Aquestes orientacions preferencials són tan sols sis, vegis Fig. 1.12.

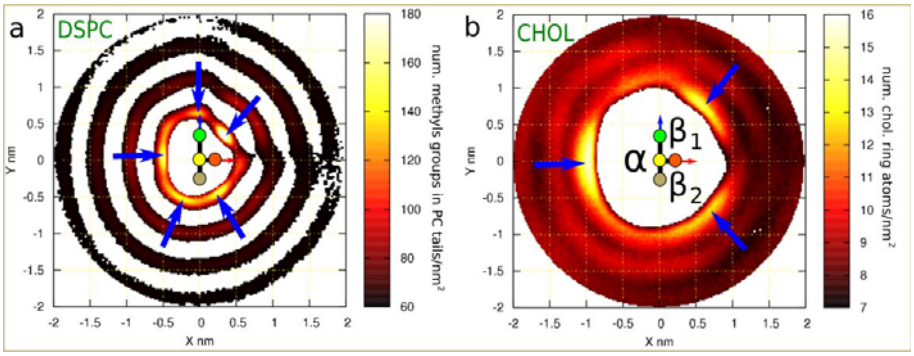

Figura 1.10: Mapa de la probabilitat de trobar una molècula determinada (a: PhdChos, b: colesterols) al voltant d'un colesterol escollit com a referència. Ambdós panells contenen informació referent a la membrana del DSPC amb 20% de colesterol, tot i que els altres sistemes presenten característiques similars. Al mig de cada panell s'observa una figura esquemàtica del colesterol de referència, on es distingeixen les cares llisa (α) i rugosa (β). La regió corresponent a la cara llisa està doncs orientada segons x <0, deixant la cara rugosa orientada a x >0. S'observa també que la cara β es pot tanmateix dividir en dues subregions: $\beta 1$ per y >0 i $\beta 2$ per y <0. El panell (a) mostra la densitat de distribució dels PhdChols on s'observa una primera esfera de coordinació a 0.5 nm del centre del colesterol de referència. Les zones amb major probabilitat de trobar PhdChos, cinc en total, s'han marcat amb fletxes blaves. La capacitat del colesterol per ordenar s'observa clarament en la presència de tres esferes de coordinació addicionals. El panell (b) mostra la densitat de distribució dels colesterols on s'observa que el colesterol evita estar en la primera esfera de coordinació d'un altre colesterol situant-se preferencialment en la segona (∼1 nm). A aquesta distància trobem tres pics clarament definits que s'han marcat amb fletxes blaves. Cadascun d'aquests pics es troba en una regió diferent (α, $\beta 1$ i $\beta 2$) evidenciant una clara simetria triangular.

Finalment, un dels resultats més importants d'aquest treball ha estat la identificació d'un mecanisme d'acció col·lectiva entre colesterols, responsable directe de l'efecte de condensació/ordenament que aquesta espècie indueix a les membranes. L'anàlisi de les orientacions dels lípids al voltant del colesterol ha revelat l'existència de certes configuracions necessàries per l'observació d'aquests efectes organitzadors. La més important és la que consisteix en un lípid intercalat entre dues molècules de colesterol. Aquesta configuració s'assoleix prèvia orientació de les cues de manera que aquestes es trobin equidistants al colesterol. S'observa que aquest arranjament molecular és més abundant en el cas que els lípids siguin saturats (DSPC), d'acord amb què aquests són més sensibles a l'ordenament per colesterols que els lípids insaturats (DOPC). També s'observa que la presència d'aquest arranjament augmenta amb la concentració de colesterol, tot i que no linealment. Aquests resultats relacionen la presència d'aquest arranjament amb la formació de la fase L_o, i explica perquè aquesta no s'observa en concentració molt baixes de colesterol on el comportament col·lectiu d'aquesta espècie no pot tenir lloc.

En conclusió, el colesterol prefereix estar en la segona esfera de coordinació d'altres colesterols, evitant contactes directes. Per tant la primera esfera de coordinació està bàsicament poblada per PhdChos. També s'ha vist que tant lípids com colesterols presenten una estructura definida, tant posicional com orientacional en les seves respectives esferes de coordinació. Aquests resultats troben el seu origen en la particular estructura del colesterol i molt es-

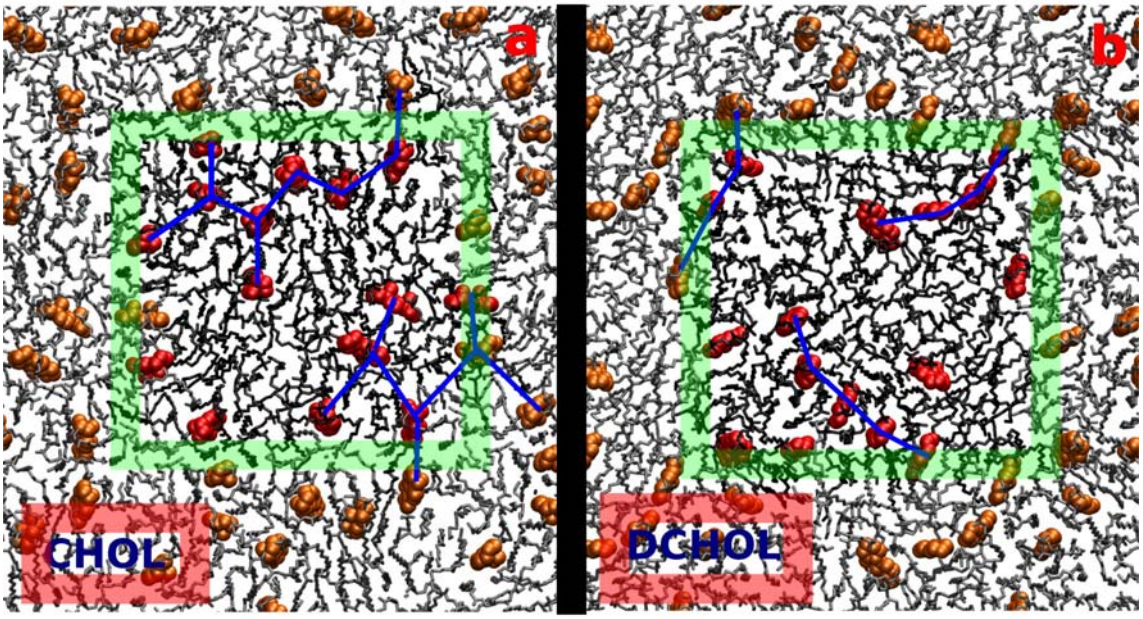

Figura 1.11: Vista superior d'una configuració de les membranes amb un 20 mol% d'esterol: (a) DSPC/CHOL i (b) DSPC/DCHOL. Només és presenta una de les capes per claredat. Les PhdChos s'han representat amb línies negres mentre que els esterols mitjançant boles vermelles. La grandària real del box de simulació està delimitat amb un requadre verd l'exterior del qual correspon a imatges periòdiques. Els esterols en les imatges periòdiques s'han representat en taronja i els PhdCho en gris. El panell (a) mostra clarament connexions laterals triangulars entre colesterols (línies blaves). El panell (b) mostra connexions lineals entre molècules DCHOL (línies blaves). Aquesta diferència fonamental es deu a l'absència dels metils C18 i C19 en el DCHOL.

pecialment en la presència dels metils C18 i C19 perpendiculars al pla de la molècula. El treball ha permès treure l'entrellat a nivell molecular del perquè el colesterol és tan particular i insubstituïble per altres esterols, tot i que presenten estructures a priori molt semblants.

1.8 El Rol de les Cardiolipines en les Membranes Mitocondrials

A la natura algunes membranes contenen lípids específics que rarament trobem en altres. Aquest és el cas de la membrana bacteriana interna o altres amb una relació evolutiva directe com serien les membranes mitocondrials que contenen cardiolipines (Card) en concentracions molars entre el 5 i el 20 mol% [Daum85, Hovi90, Hoch92, Gome99].

Les Cards constitueixen una classe lipídica amb trets característics força excepcionals. A diferència de molts altres tipus de lípids, les Cards tenen un cap aniònic divalent i una part hidrofòbica constituïda per quatre cadenes (vegis Fig. 1.13). Aquesta estructura tan inusual és el resultat de la seva naturalesa dimèrica corresponent a dos fosfolípids enllaçats mitjançant un glicerol central. Com a conseqüència, les Cards tenen típicament quatre cadenes, normalment insaturades, les característiques de les quals sovint depèn de l'origen de la membrana estudiada. Per exemple, en les cèl·lules del cor dels mamífers, els àcids grassos en

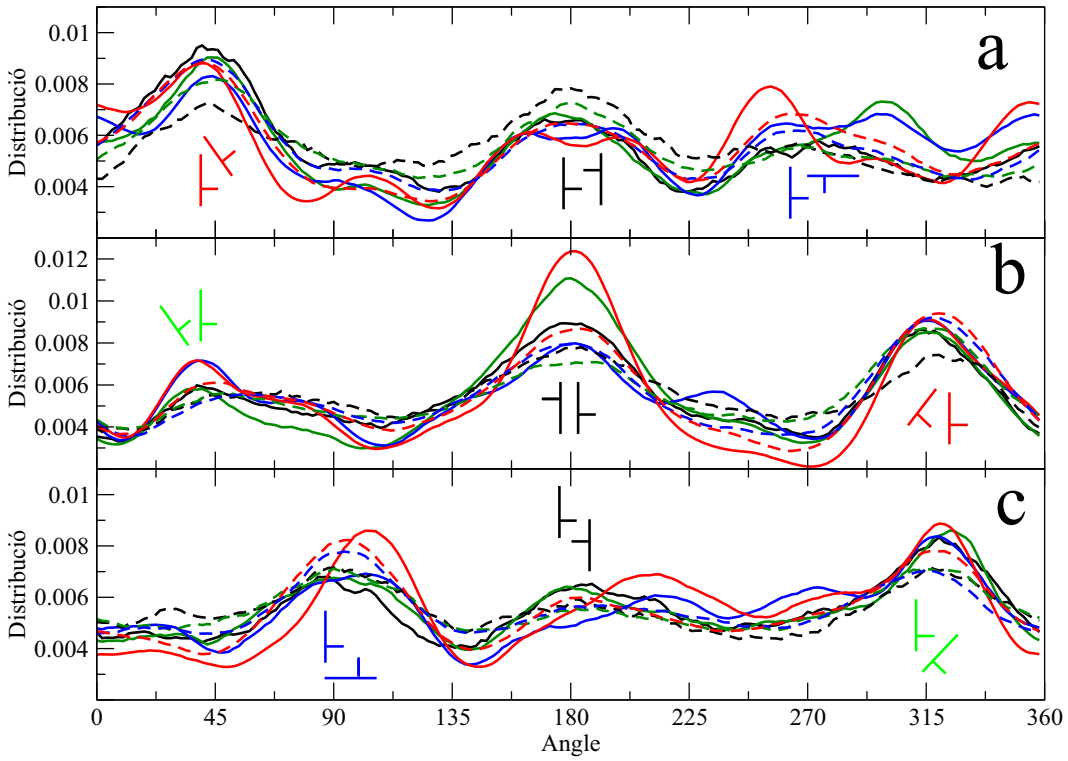

Figura 1.12: Distribució angular entre colesterols corresponent a les tres posicions preferents mostrades en el mapa de distribució CHO-CHOL. L'angle en l'eix de les xs és el format entre els vector C6-C11 de cada molècula de colesterol en la parella (Fig. 1.2). Cal destacar que les corbes dins d'un mateix panell presenten un comportament semblant, el que permet definir comportaments generals. El panell (a) fa referència al pic que es troba en la regió $\beta 1$. El panell (b) correspon al pic en α. El panell (c) correspon al pic en $\beta 2$. Les línies continues corresponen a les membranes amb DSPC mentre que les discontinues a les de DOPC. Els colors indiquen el contingut de colesterol: 20 mol% (negre), 30 mol% (verd), 40 mol% (blau), i 50 mol% (vermell). Les orientacions preferides s'han dibuixat esquemàticament a sobre del màxim corresponent. Les configuracions equivalents s'han dibuixat en un mateix color excepte les negres que no són equivalents entre elles.

les Cards són fonamentalment àcid linoleic, en canvi, en alguns organismes marins l'àcid gras més abundant és l'àcid docosahexanoic [Kraf02]. En conseqüència, l'estructura de les Cards està marcada per una gran regió hidrofòbica i un petit cap polar altament carregat. Ambdós factors porten a les Cards a afavorir curvatures negatives [Powe85, Ales07, Dahl07]. Encara més, l'elevada càrrega de les Cards, atès que les interaccions electrostàtiques entre espècies carregades és molt forta, fa que puguin actuar tant com estabilitzadors com desestabilitzadors de la membrana depenent del context en què es trobin [Shoe02, Nich05, Zhao07b]. En particular, tot i que típicament hi ha nombrosos lípids carregats negativament en la majoria de les membranes de les cèl·lules eucariotes, les Cards són els únics lípids carregats presents en els mitocondris [Hovi90].

Les Cards estan involucrades en una excepcional varietat de funcions. Entre elles destaquen l'estabilització de proteïnes de membrana i complexes respiratoris [Krau04, Lena07]; la transferència de protons i electrons [Hoch92, Gome99, Lena07]; la síntesi de l'ATP i la translocació ADP-ATP [Lena07], mort cel·lular programada [Gonz07], processos d'envelliment

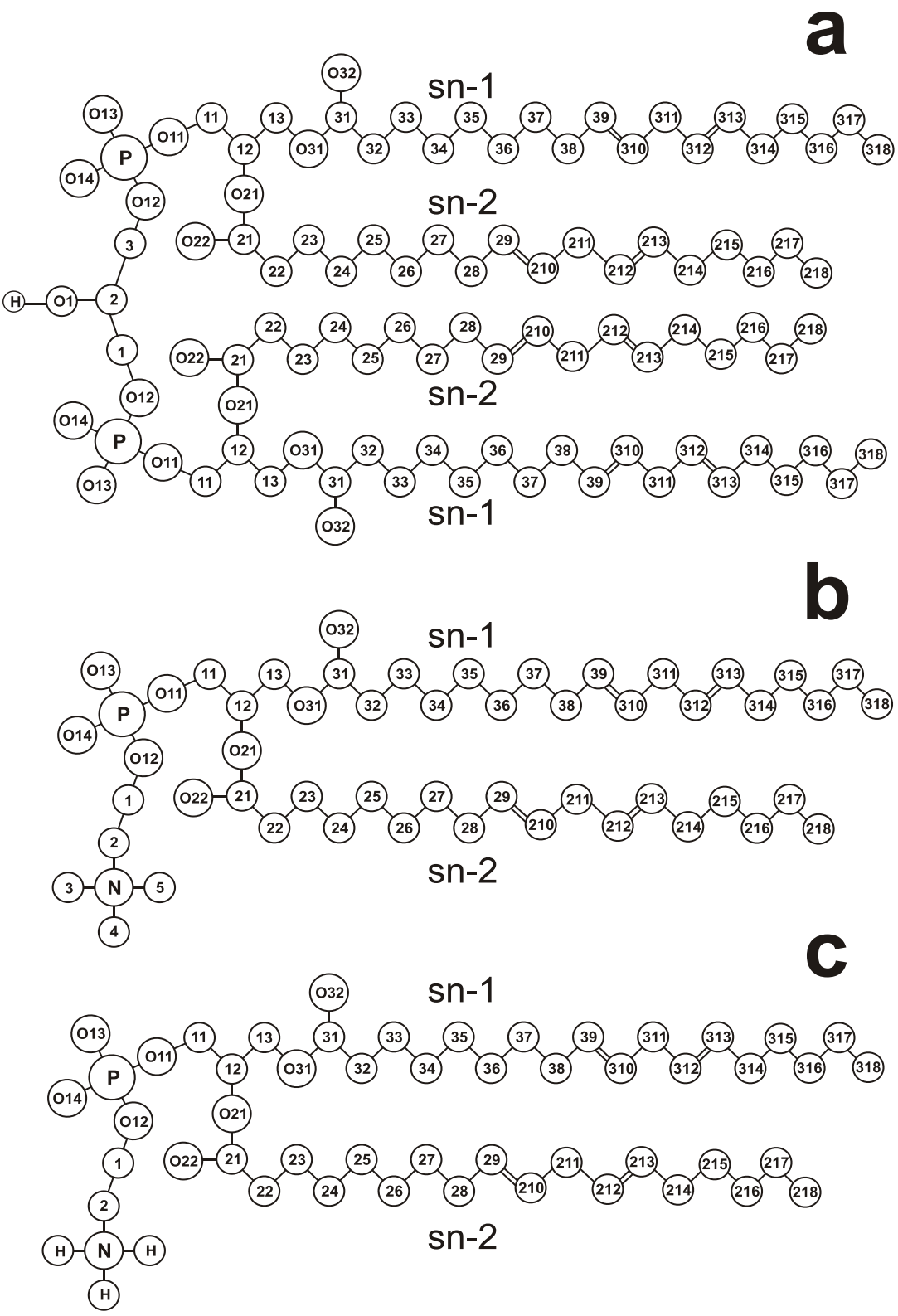

Figura 1.13: Estructures moleculars i numeració dels àtoms pels lípids simulats: (a) Card, (b) PhdCho, i (c) PhdEtn.

i estrès oxidatiu [Sast00, Sanz06], i malalties metabòliques com el síndrome de Barth o la disfunció tiroïdal [Schl06]. A la Ref. [Schl00] es pot trobar una descripció de les diferents funcions de les Cards. Aquesta multifuncionalitat justifica de per si la importància de l'estudi d'aquests lípids.

La principal finalitat d'aquesta secció és investigar el mecanismes moleculars per mitjà dels quals les Cards modifiquen les propietats de la membrana i afecten l'estructura de la mateixa. Això és essencial per comprendre el processos d'estabilització, transport i senyalització en el mitocondri, tot i que també és necessari per estendre el actuals models per tal d'incloure noves característiques com poden ser transport de càrregues on les Cards estan involucrades. Per tal de dur a terme aquest estudi, s'ha centrat l'interès en una membrana de composició semblant a la trobada en la membrana mitocondrial interna (50 mol% PhdCho, 40 mol% PhdEtn i 10 mol% Card; vegis Ref. [Daum85]) on tots els lípids presenten les mateixes cadenes laterals: l'àcid linoleic. Malauradament, la quantitat de dades experimentals disponible per la validació d'unes simulacions d'aquestes característiques és força incompleta. Això en combinació amb què aquest treball constitueix un dels primers que intenta estudiar aquest tipus de membranes ternàries [Dahl07, Dahl08] ha dut a focalitzar aquest estudi en la comparació d'aquesta membrana model amb membranes de referència de complexitat més reduïda: sistemes purs o mescles binaries dels components de la membrana model.

Membranes	PhdCho (PC)	PhdEtn (PE)	Card (CL)	aigua	Na^+
PC	128			3614	
PC-CL*	100		14	3586	28
PC-PE	70	58		3614	
PC-PE-CL*	54	46	14	3586	28
PE		128		3614	
PE-CL*		100	14	3586	28

Taula 1.2: Nombre de molècules de cada tipus en cada membrana simulada. *Dues simulacions amb la mateixa composició però diferents estructures inicials s'han dut a terme per tal d'estudiar la tendència de les Cards a agregar.

Així doncs, s'ha desenvolupat un model atòmic de la membrana mitocondrial interna (PC-PE-CL), les propietats del qual s'han caracteritzat mitjançant l'anàlisi de les trajectòries obtingudes de la seva simulació amb Dinàmica Molecular en escales temporals de l'ordre de 130 ns. La composició exacta d'aquesta membrana així com de les membranes de referència pures (PC, PE) i les binàries (PC-PE, PC-CL, PE-CL) es troben en la Taula 1.2. Els noms PC, PC-CL, PC-PE, PC-PE-CL, PE i PE-CL corresponen als emprats per referir-se a cadascuna de les membranes simulades, on PC, PE i CL són acrònims que corresponen a PhdCho, PhdEtn i Card. L'elevat nombre de sistemes de referència emprats està justificat ja que es vol (a) caracteritzar les interaccions de les Cards en els típics sistemes binaris, i (b) estudiar el sistema ternari de forma que es pugui detectar si alguna de les seves propietats es pot deduir en base a aquelles obtingudes pels sistemes binaris. A més a més, per tal d'esbrinar si els Cards tenen tendència a agregar-se s'han efectuat dues simulacions independents per cada membrana amb Cards amb dues configuracions inicials diferents. En la primera, la

Membrana	area[nm^2]	gruix [nm]
PC	0.340±0.001	4.1
PC-CL	0.318±0.001	4.1
PC-PE	0.318±0.001	4.2
PC-PE-CL	0.308±0.001	4.2
PE	0.299±0.003	4.4
PE-CL	0.296±0.001	4.3

Taula 1.3: Àrea per cadena lateral i gruix mitjà de les membranes simulades.

disposició de les Cards en el pla de la membrana és aleatòria; en la segona, en canvi, les Cards es troben formant un únic agregat. De manera general, a causa que aquest sistema ternari no havia estat simulat anteriorment i les dades experimentals disponibles són limitades, l'estudi s'ha centrat en la comparativa entre els sistemes i en especial en com les Cards alteren el comportament de les membranes.

Per començar, el nostre model ternari (PC-PE-CL) mostra que les Cards no tendeixen a agregar-se de forma espontània quan el sistema assoleix l'equilibri, vegis Fig. 1.14. La mateixa observació es manté en les membranes PC-CL i PE-CL. Aquesta observació redueix la possibilitat d'existència d'interaccions atractives de curt abast entre les Cards i recolza els mecanismes mediats per curvatura [Huan06] com a única força motriu en la formació dels dominics rics en les Cards que normalment s'observen *in vivo* [Mile09]. També trobem que l'efecte dels Cards en les tres matrius simulades és diferent, vegis Taula 1.3. En conseqüència, queda palès que els efectes de les Cards en la membrana PC-PE-CL no poden ser deduïts dels observats en les membranes PC-CL i PE-CL. Per tant, la inusual estructura de les Cards i el seu efecte en les interaccions amb els lípids del seu entorn semblen no ser additives.

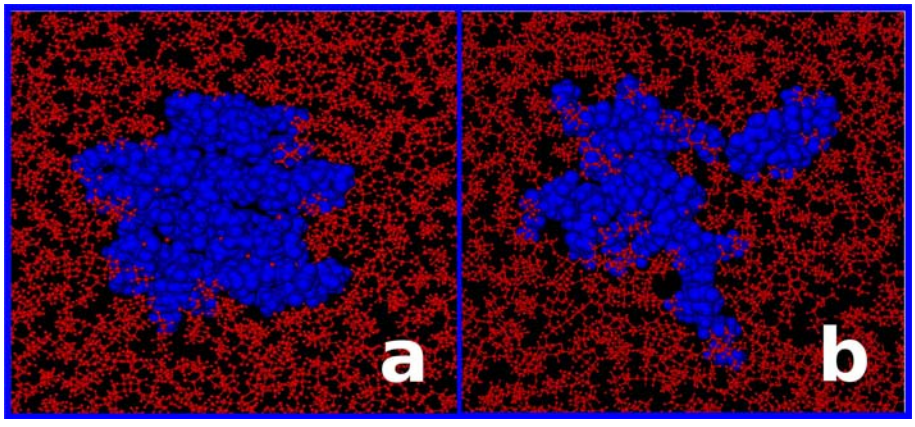

Figura 1.14: El panell (a) mostra l'estat inicial de la simulació de la membrana PC-PE-CL amb configuració agregada, mentre que el panell (b) mostra la darrera configuració (130 ns) del mateix sistema. PhdCho i PhdEtn es mostren amb línies vermelles, les cardiolipines, en canvi, s'han representat amb boles de color blau. La comparació dels dos panells suggereix que l'estat agregat no constitueix una configuració energètica òptima i per tant d'equilibri del sistema. Les altres membranes amb Cards PC-CL i PE-CL mostren el mateix comportament.

L'efecte de les Cards en les membranes composades per PhdChos sembla ser particularment significatiu. L'addició de molècules de Cards en la matriu pura de PhdCho dóna lloc a una petita però evident, condensació de la membrana i, com a conseqüència, d'un augment de l'ordre de les cadenes lateral. Aquest resultat està d'acord amb dades experimentals i estudis computacionals en els quals observen un minvament de la permeabilitat de les membranes de PhdChos acompanyat per un augment de l'estabilitat de les mateixes quan les Cards es troben presents [Macd87]. A la interfase veiem que les PhdChos formen preferentment interaccions entre càrregues amb les Cards que demostren ser considerablement més estables que les formades entre les pròpies PhdChos. Aquest sembla ser el principal motiu de l'alentiment observat en el moviment rotacional dels caps polars en les PhdChos. Tot i això, el nombre total d'interaccions de càrregues quan les Cards estan presents (PC-CL) és inferior en comparació amb els sistemes purs (PC), fet que queda compensat amb enllaços a contraions.

En el cas de la bicapa que conté tan sols PhdEtn, a l'afegir-li Cards no s'observa cap efecte ni en l'àrea per cadena lateral (Taula 1.3) ni en l'ordre de les mateixes. En general, els enllaços d'hidrogen entre PhdEtn i Cards són menys freqüents i estables que els que es donen entre PhdEtns. També romanen inalterats tant el nombre total d'enllaços d'hidrogen entre les membranes pura (PE) i mixta (PE-CL), com la rotació dels caps polars de les PhdEtn, la qual cosa suggereix que els enllaços d'hidrogen intramoleculars dominen sobre els intermoleculars. L'única interacció addicional en el sistema PE-CL respecte el PE a la interfase correspon a la formació de ponts iònics.

El comportament de la membrana PC-PE, tot i que no constitueix l'objectiu prioritari d'aquest estudi, és força interessant ja que tant el PhdCho com el PhdEtn modifiquen mútuament les seves propietats. Això s'observa clarament en el fet que l'àrea per molècula que s'obté en la membrana PC-PE (0.635 nm^2) és inferior a la que seria d'esperar per simple mitjana de les pures (0.643 nm^2) tenint en compte que està constituïda per 70 PhdChos i 58 PhdEtns. El nombre d'enllaços d'hidrogen intermoleculars per molècula de PhdEtn entre PhdEtns-PhdEtns (1.80), és superior al nombre d'enllaços d'hidrogen PhdEtn-PhdCho (0.89), tot i que la proporció de PhdChos en la membrana és superior. En canvi, el nombre de interaccions de càrrega és superior en parelles PhdCho-PhdCho que en parelles PhdCho-PhdEtn.

Quan afegim les Cards a la matriu PC-PE, l'àrea superficial roman pràcticament inalterada (Taula 1.3) tot i que la regió interficial esdevé força menys dinàmica. Les rotacions dels caps polars tant pels PhdChos com PhdEtns s'alenteixen. De fet la rotació dels caps polars de les PhdChos en el sistema PC-PE-CL és la més lenta en comparació a les reportades pels sistemes PC i PC-CL. Les rotacions dels caps polars de les PhdEtn, en canvi, són més semblants en tots els sistemes. D'acord amb les dades experimentals disponibles [Pinh94], es troba que l'angle d'inclinació del vector PN, $t_{P\mapsto N}$, de les PhdChos en el sistema ternari (PC-PE-CL) augmenta 9°en comparació al de la membrana pura (PC). En els experiments per Pinheiro et al., el canvi d'orientació del dipol PN observat és de 6°, tot i que augmenta incrementant la concentració de Cards. En general, l'efecte de les Cards en la membrana PC-PE-CL és complex i no pot ser explicat en base a l'addició del comportament observat en els sistemes binaris (PC-CL i PE-CL).

A nivell molecular, s'observa que els enllaços d'hidrogen entre PhdEtns són més habituals i estables que els constituïts entre PhdEtn-PhdCho i PhdEtn-Card. En el cas de les interaccions de càrrega, les PhdCho-Card són les més freqüents i estables. Cal ressaltar que en el sistema

ternari, el nombre total d'enllaços d'hidròdgens és el més gran de tots, mentre que el nombre d'interaccions de càrrega és el més petit de tots. Com que en general els ponts d'hidrogen són interaccions més fortes, implica que la membrana PC-PE-CL, de composició semblant a la mitocondrial, és la que presenta globalment les interaccions interlípides més importants.

En conclusió, la influència de les Cards en les propietats de les membranes es troben principalment en la interfície membrana-aigua i depenen fortament de la composició de la membrana. Per una banda, les Cards alteren significativament les propietats de les PhdChos a les que confereixen un estat força més ordenat. Això és conseqüència de la formació d'interaccions de càrrega estables entre els dos lípids en la interfase Per altra banda, les Cards pràcticament no alteren el comportament de les PhdEtn. També s'observa que la membrana PC-PE-CL presenta el major nombre de enllaços d'hidrogen i el menor nombre d'interaccions de càrrega interlípida. Finalment, no observem cap tendència en les Cards a agregar-se. Encara més, quan es força les Cards a estar agregades el sistema esdevé clarament inestable. Això evidencia la necessitat de mecanismes alternatius a la simple interacció entre les Cards per explicar la formació dels dominis rics en Cards observats en membranes naturals [Mile00, Mats06, Mile09].

Bibliografia

[AAqv93] J. Åqvist and A. Warshel. "Simulation of enzyme reactions using valence bond force fields and other hybrid quantum/classical approaches". *Chem. Rev.*, Vol. 93, No. 7, pp. 2523–2544, 1993.

[Aitt06] J. Aittoniemi, T. Róg, P. Niemela, M. Pasenkiewicz-Gierula, M. Karttunen, and I. Vattulainen. "Tilt: Major Factor in Sterols' Ordering Capability in Membranes". *J. Phys. Chem. B*, Vol. 110, No. 51, pp. 25562–25564, 2006.

[Alec82] M. R. Alecio, D. E. Golan, W. R. Veatch, and R. R. Rando. "Use of a fluorescent cholesterol derivative to measure lateral mobility of cholesterol in membranes". *Proc. Natl. Acad. Sci. U. S. A.*, Vol. 79, No. 17, pp. 5171–5174, Sep. 1982.

[Ales07] A. Alessandrini, G. Valdrè, U. Valdrè, and U. Muscatello. "Defects in ordered aggregates of cardiolipin visualized by atomic force microscopy.". *Chem. Phys. Lipids*, Vol. 146, No. 2, pp. 111–124, Apr 2007.

[Ali07] M. R. Ali, K. H. Cheng, and J. Huang. "Assess the nature of cholesterol–lipid interactions through the chemical potential of cholesterol in phosphatidylcholine bilayers". *Proc. Natl. Acad. Sci. U. S. A.*, Vol. 104, No. 13, pp. 5372–5377, March 2007.

[Ali98] S. Ali, J. M. Smaby, M. M. Momsen, H. L. Brockman, and R. E. Brown. "Acyl chain-length asymmetry alters the interfacial elastic interactions of phosphatidylcholines.". *Biophys. J.*, Vol. 74, No. 1, pp. 338–348, Jan 1998.

[Alle90] M. P. Allen and D. J. Tildesley. *Computer Suimulation of Liquids*. Oxford University Press, New York, 1990.

[Alme95] P. F. F. Almeida and V. W. L. C. "Lateral diffusion in membranes". In: *Structure and Dynamics of Membranes: From Cells to Vesicles*, pp. 305–357, Elsevier, Amsterdam, The Netherlands, 1995.

[Ande02] R. G. W. Anderson and K. Jacobson. "A Role for Lipid Shells in Targeting Proteins to Caveolae, Rafts, and Other Lipid Domains". *Science*, Vol. 296, No. 5574, pp. 1821–1825, June 2002.

[Avel87] M. Aveldano and H. Sprecher. "Very long chain (C24 to C36) polyenoic fatty acids of the n-3 and n-6 series in dipolyunsaturated phosphatidylcholines from bovine retina". *J. Biol. Chem.*, Vol. 262, No. 3, pp. 1180–1186, Jan. 1987.

[Bach04] M. Bachar, P. Brunelle, D. P. Tieleman, and A. Rauk. "Molecular Dynamics Simulation of a Polyunsaturated Lipid Bilayer Susceptible to Lipid Peroxidation". *J. Phys. Chem. B*, Vol. 108, No. 22, pp. 7170–7179, 2004.

[Bako96] D. Bakowies and W. Thiel. "Hybrid Models for Combined Quantum Mechanical and Molecular Mechanical Approaches". *J. Phys. Chem.*, Vol. 100, No. 25, pp. 10580–10594, 1996.

[Bare99] Y. Barenholz and T. E. Thompson. "Sphingomyelin: biophysical aspects". *Chem. Phys. Lipids*, Vol. 102, pp. 29–34, 1999.

[Baum05] A. Baumketner and J.-E. Shea. "The Influence of Different Treatments of Electrostatic Interactions on the Thermodynamics of Folding of Peptides?". *J. Phys. Chem. B*, Vol. 109, No. 45, pp. 21322–21328, Nov. 2005.

[Bere81] H. J. C. Berendsen, J. P. M. Postma, W. F. van Gunsteren, and J. Hermans. *Intermolecular Forces*, Chap. Interaction models for water in relation to protein hydration, pp. 331–342. Reidel, Dordrecht, The Netherlands, 1981.

[Bere84] H. J. C. Berendsen, J. P. M. Postma, W. F. van Gunsteren, A. DiNola, and J. R. Haak. "Molecular dynamics with coupling to an external bath". *J. Chem. Phys.*, Vol. 81, No. 8, pp. 3684–3690, 1984.

[Bere98] H. J. C. Berendsen. *Computational Molecular Dynamics: Challenges, Methods, Ideas*, Chap. Molecular Dynamics Simulations: The Limits and Beyond, pp. 3–36. Vol. 4 of *Lecture Notes in Computational Science and Engineering*, Springer Verlag, 1998.

[Berg97] O. Berger, O. Edholm, and F. Jähnig. "Molecular dynamics simulations of a fluid bilayer of dipalmitoylphosphatidylcholine at full hydration, constant pressure, and constant temperature". *Biophys. J.*, Vol. 72, No. 5, pp. 2002–2013, May 1997.

[Bloo88] M. Bloom and O. G. Mouritsen. "The evolution of membranes". *Can. J. Chem.*, Vol. 66, pp. 706–712, 1988.

[Boci78] D. F. Bocian and S. I. Chan. "NMR Studies of Membrane Structure and Dynamics". *Annu. Rev. Phys. Chem.*, Vol. 29, No. 1, pp. 307–335, 1978.

[Broo83] B. R. Brooks, R. E. Bruccoleri, B. D. Olafson, D. J. States, S. Swaminathan, and M. Karplus. "CHARMM: A program for macromolecular energy, minimization, and dynamics calculations". *J. Comput. Chem.*, Vol. 4, No. 2, pp. 187–217, 1983.

[Brow00] D. A. Brown and E. London. "Structure and Function of Sphingolipid- and Cholesterol-rich Membrane Rafts". *J. Biol. Chem.*, Vol. 275, No. 23, pp. 17221–17224, June 2000.

[Cevc88] G. Cevc, J. M. Seddon, R. Hartung, and W. Eggert. "Phosphatidylcholine-fatty acid membranes. I. Effects of protonation, salt concentration, temperature and chain-length on the col loidal and phase properties of mixed vesicles, bilayers and nonlamellar structures". *Biochim. Biophys. Acta, Biomembr.*, Vol. 940, No. 2, pp. 219–240, 1988.

[Chiu02] S. Chiu, E. Jakobsson, R. J. Mashl, and H. L. Scott. "Cholesterol-Induced Modifications in Lipid Bilayers: A Simulation Study". *Biophys. J.*, Vol. 83, No. 4, pp. 1842–1853, Oct. 2002.

[Chon09] P. L.-G. Chong, W. Zhua, and B. Venegas. "On the lateral structure of model membranes containing cholesterol". *Biochim. Biophys. Acta, Biomembr.*, Vol. 1788(1), pp. 2–11, 2009.

[Chon94a] P. L. Chong. "Evidence for regular distribution of sterols in liquid crystalline phosphatidylcholine bilayers.". *Proc. Natl. Acad. Sci. U. S. A.*, Vol. 91, No. 21, pp. 10069–10073, Oct 1994.

[Chon94b] P. L. Chong, D. Tang, and I. P. Sugar. "Exploration of physical principles underlying lipid regular distribution: effects of pressure, temperature, and radius of curvature on E/M dips in pyrene-labeled PC/DMPC binary mixtures". *Biophys. J.*, Vol. 66, No. 6, pp. 2029–2038, June 1994.

[Cook06] I. R. Cooke and M. Deserno. "Coupling between Lipid Shape and Membrane Curvature". *Biophys. J.*, Vol. 91, No. 2, pp. 487–495, July 2006.

[Corn83] B. Cornell and M. Keniry. "The effect of cholesterol and gramicidin A' on the carbonyl groups of dimyristoylphosphatidylcholine dispersions". *Biochim. Biophys. Acta, Biomembr.*, Vol. 732, No. 3, pp. 705–710, 1983.

[Cron74] J. E. Cronan. "Regulation of the fatty acid composition of the membrane phospholipids of Escherichia coli.". *Proc. Natl. Acad. Sci. U. S. A.*, Vol. 71, No. 9, pp. 3758–3762, Sep 1974.

[Cron75] J. Cronan, J. E. and E. P. Gelmann. "Physical properties of membrane lipids: biological relevance and regulation.". *Bacteriol. Rev.*, Vol. 39, pp. 232–256, 1975.

[Dahl07] M. Dahlberg. "Polymorphic Phase Behavior of Cardiolipin Derivatives Studied by Coarse-Grained Molecular Dynamics". *J. Phys. Chem. B*, Vol. 111, No. 25, pp. 7194–7200, 2007.

[Dahl08] M. Dahlberg and A. Maliniak. "Molecular dynamics simulations of cardiolipin bilayers.". *J. Phys. Chem. B*, Vol. 112, No. 37, pp. 11655–11663, Sep 2008.

[Dard93] T. Darden, D. York, and L. Pedersen. "Particle mesh Ewald: An N [center-dot] log(N) method for Ewald sums in large systems". *J. Chem. Phys.*, Vol. 98, No. 12, pp. 10089–10092, 1993.

[Daum85] G. Daum. "Lipids of mitochondria". *Biochim. Biophys. Acta, Rev. Biomembr.*, Vol. 822, No. 1, pp. 1–42, 1985.

[Daur96] X. Daura, B. Oliva, E. Querol, F. X. Avilés, and O. Tapia. "On the sensitivity of MD trajectories to changes in water-protein interaction parameters: The potato carboxypeptidase inhibitor in water as a test case for the GROMOS force field". *Proteins*, Vol. 25, No. 1, pp. 89–103, 1996.

[Davi03] U. David Metzler, Iowa State University. *Biochemistry (2 volume set), 1 & 2The Chemical Reactions of Living Cells.* ACADEMIC PRESS, second Ed., april 2003.

[Davi79] J. Davis, B. Maraviglia, G. Weeks, and D. Godin. "Bilayer rigidity of the erythrocyte membrane 2H-NMR of a perdeuterated palmitic acid probe". *Biochim. Biophys. Acta, Biomembr.*, Vol. 550, No. 2, pp. 362–366, 1979.

[Davi80] J. H. Davis, M. Bloom, K. W. Butler, and I. C. Smith. "The temperature dependence of molecular order and the influence of cholesterol in Acholeplasma laidlawii membranes". *Biochim. Biophys. Acta, Biomembr.*, Vol. 597, No. 3, pp. 477–491, 1980.

[Davi81] P. J. Davis, B. D. Fleming, K. P. Coolbear, and K. M. W. Keough. "Gel to liquid-crystalline transition temperatures of water dispersions of two pairs of positional isomers of unsaturated mixed-acid phosphatidylcholines". *Biochemistry*, Vol. 20, No. 12, pp. 3633–3636, 1981.

[Davi83] P. J. Davis and K. M. W. Keough. "Differential scanning calorimetric studies of aqueous dispersions of mixtures of cholesterol with some mixed-acid and single-acid phosphatidylcholines". *Biochemistry*, Vol. 22, No. 26, pp. 6334–6340, 1983.

[Davi84] P. Davis and K. Keough. "Scanning calorimetric studies of aqueous dispersions of bilayers made with cholesterol and a pair of positional isomers of 3-sn-phosphatidylcholine". *Biochim. Biophys. Acta, Biomembr.*, Vol. 778, No. 2, pp. 305–310, 1984.

[Deme72] R. Demel, K. Bruckdorfer, and L. V. Deenen. "The effect of sterol structure on the permeability of lipomes to glucose, glycerol and Rb^+". *Biochim. Biophys. Acta, Biomembr.*, Vol. 255, No. 1, pp. 321–330, 1972.

[Dewe71] M. M. Dewey and L. Barr. "Some Considerations About the Structure of Cellular Membranes". In: F. Bronner and A. Kleinzeller, Eds., *Current Topics in Membranes and Transport*, pp. 1 – 33, Academic Press, 1971.

[Di95] L. Di and D. M. Small. "Physical Behavior of the Hydrophobic Core of Membranes: Properties of 1-Stearoyl-2-linoleoyl-sn-glycerol". *Biochemistry*, Vol. 34, No. 51, pp. 16672–16677, 1995.

[Dimo00] R. Dimova, B. Pouligny, and C. Dietrich. "Pretransitional Effects in Dimyristoylphosphatidylcholine Vesicle Membranes: Optical Dynamometry Study". *Biophys. J.*, Vol. 79, No. 1, pp. 340–356, July 2000.

[Doug05] A. D. Douglass and R. D. Vale. "Single-Molecule Microscopy Reveals Plasma Membrane Microdomains Created by Protein-Protein Networks that Exclude or Trap Signaling Molecules in T Cells". *Cell*, Vol. 121, No. 6, pp. 937–950, June 2005.

[Dyat74] E. V. Dyatlovitskaya, G. V. Yanchevskaya, and L. D. Bergelson. "Molecular species and membrane forming properties of lecithins in normal liver and hepatoma.". *Chem. Phys. Lipids*, Vol. 12, No. 2, pp. 132–149, Apr 1974.

[Edho05] O. Edholm and J. F. Nagle. "Areas of Molecules in Membranes Consisting of Mixtures". *Biophys. J.*, Vol. 89, No. 3, pp. 1827–1832, Sep. 2005.

[Eige94] M. Eigen and R. Rigler. "Sorting single molecules: application to diagnostics and evolutionary biotechnology". *Proc. Natl. Acad. Sci. U. S. A.*, Vol. 91, No. 13, pp. 5740–5747, June 1994.

[Elof93] A. Elofsson and L. Nilsson. "How Consistent are Molecular Dynamics Simulations? : Comparing Structure and Dynamics in Reduced and Oxidized Escherichia coli Thioredoxin". *J. Mol. Biol.*, Vol. 233, No. 4, pp. 766–780, 1993.

[Essm95] U. Essmann, L. Perera, M. L. Berkowitz, T. Darden, H. Lee, and L. G. Pedersen. "A smooth particle mesh Ewald method". *J. Chem. Phys.*, Vol. 103, No. 19, pp. 8577–8593, 1995.

[Ewal21] P. P. Ewald. "Die berechnung optischer und elektrostatischer gitterpotentiale". *Ann. Phys.*, Vol. 64, pp. 253–287, 1921.

[Falc04] E. Falck, M. Patra, M. Karttunen, M. T. Hyvnen, and I. Vattulainen. "Lessons of Slicing Membranes: Interplay of Packing, Free Area, and Lateral Diffusion in Phospholipid/Cholesterol Bilayers". *Biophys. J.*, Vol. 87, No. 2, pp. 1076–1091, Aug. 2004.

[Feig06] G. W. Feigenson. "Phase behavior of lipid mixtures". *Nature Chem. Biol.*, Vol. 2, pp. 560–563, 2006.

[Feig09] G. W. Feigenson. "Phase diagrams and lipid domains in multicomponent lipid bilayer mixtures". *Biochim. Biophys. Acta, Biomembr.*, Vol. 1788(1), pp. 47–52, 2009.

[Gao96] J. Gao. *Reviews in Computational Chemistry*, Chap. Methods and applications of combined quantum mechanical and molecular mechanical potentials, pp. 119–185. Vol. 7, VCH Publishers, New York, 1996.

[Ge98] M. Ge and J. H. Freed. "Polarity Profiles in Oriented and Dispersed Phosphatidylcholine Bilayers Are Different: An Electron Spin Resonance Study". *Biophys. J.*, Vol. 74, No. 2, pp. 910–917, Feb. 1998.

[Gome99] B. Gomez and N. C. Robinson. "Quantitative determination of cardiolipin in mitochondrial electron transferring complexes by silicic acid high-performance liquid chromatography.". *Anal Biochem*, Vol. 267, No. 1, pp. 212–216, Feb 1999.

[Gonz07] F. Gonzalvez and E. Gottlieb. "Cardiolipin: setting the beat of apoptosis.". *Apoptosis*, Vol. 12, No. 5, pp. 877–885, May 2007.

[Guns87] W. F. van Gunsteren and H. J. C. Berendsen. *Gromos-87 manual*. Biomos BV, Nijenborgh 4, 9747 AG Groningen, The Netherlands, 1987.

[Guns98] W. F. van Gunsteren, X. Daura, and A. E. Mark. *Encyclopedia of Computational Chemistry*, Chap. Gromos force field, pp. 1211–1216. Wiley, 1998.

[Hess02] B. Hess. "Determining the shear viscosity of model liquids from molecular dynamics simulations". *J. Chem. Phys.*, Vol. 116, No. 1, pp. 209–217, 2002.

[Hess97] B. Hess, H. Bekker, H. J. C. Berendsen, and J. G. E. M. Fraaije. "LINCS: A linear constraint solver for molecular simulations". *J. Comput. Chem.*, Vol. 18, No. 12, pp. 1463–1472, 1997.

[Hoch92] F. L. Hoch. "Cardiolipins and biomembrane function.". *Biochim. Biophys. Acta*, Vol. 1113, No. 1, pp. 71–133, Mar 1992.

[Hock70] R. W. Hockney. "The Potential Calculation and Some Applications". *Methods in Computational Physics*, Vol. 9, pp. 136–211, 1970.

[Hofs03] C. Hofsäß, E. Lindahl, and O. Edholm. "Molecular Dynamics Simulations of Phospholipid Bilayers with Cholesterol". *Biophys. J.*, Vol. 84, No. 4, pp. 2192–2206, Apr. 2003.

[Holt01] M. Höltje, T. Förster, B. Brandt, T. Engels, W. von Rybinski, and H.-D. Höltje. "Molecular dynamics simulations of stratum corneum lipid models: fatty acids and cholesterol". *Biochim. Biophys. Acta, Biomembr.*, Vol. 1511, No. 1, pp. 156–167, March 2001.

[Hoov85] W. G. Hoover. "Canonical dynamics: Equilibrium phase-space distributions". *Phys. Rev. A*, Vol. 31, No. 3, pp. 1695–1697, March 1985.

[Hovi90] R. Hovius, H. Lambrechts, K. Nicolay, and B. de Kruijff. "Improved methods to isolate and subfractionate rat liver mitochondria. Lipid composition of the inner and outer membrane.". *Biochim. Biophys. Acta*, Vol. 1021, No. 2, pp. 217–226, Jan 1990.

[Huan01] C. hsien Huang. "Mixed-chain phospholipids: Structures and chain-melting behavior". *Lipids*, Vol. 36, pp. 1077–1097, 2001.

[Huan02] J. Huang. "Exploration of Molecular Interactions in Cholesterol Superlattices: Effect of Multibody Interactions". *Biophys. J.*, Vol. 83, No. 2, pp. 1014–1025, Aug. 2002.

[Huan06] K. C. Huang, R. Mukhopadhyay, and N. S. Wingreen. "A curvature-mediated mechanism for localization of lipids to bacterial poles.". *PLoS Comput Biol*, Vol. 2, No. 11, p. e151, Nov 2006.

[Huan77] C.-H. Huang. "A structural model for the cholesterol-phosphatidylcholine complexes in bilayer membranes". *Lipids*, Vol. 12, No. 4, pp. 348–356, Apr. 1977.

[Huan99] J. Huang and G. W. Feigenson. "A Microscopic Interaction Model of Maximum Solubility of Cholesterol in Lipid Bilayers". *Biophys. J.*, Vol. 76, No. 4, pp. 2142–2157, Apr. 1999.

[Hui83] S. W. Hui and N. B. He. "Molecular organization in cholesterol-lecithin bilayers by x-ray and electron diffraction measurements". *Biochemistry*, Vol. 22, No. 5, pp. 1159–1164, 1983.

[Hulb03] A. J. Hulbert. "Life, death and membrane bilayers". *J. Exp. Biol.*, Vol. 206, No. 14, pp. 2303–2311, July 2003.

[Ichi99] H. Ichimori, T. Hata, H. Matsuki, and S. Kaneshina. "Effect of unsaturated acyl chains on the thermotropic and barotropic phase transitions of phospholipid bilayer membranes". *Chem. Phys. Lipids*, Vol. 100, No. 1-2, pp. 151 – 164, 1999.

[Inok78] Y. Inoko and T. Mitsui. "Structural Parameters of Dipalmitoyl Phosphatidylcholine Lamellar Phases and Bilayer Phase Transitions". *J. Phys. Soc. Jpn.*, Vol. 44, No. 6, pp. 1918–1924, 1978.

[Inou99] T. Inoue, T. Kitahashi, and Y. Nibu. "Phase behavior of hydrated bilayer of binary phospholipid mixtures composed of 1,2-distearoylphosphatidylcholine and 1-stearoyl-2-oleoylphosphatidylcholine or 1-oleoyl-2-stearoylphosphatidylcholine". *Chem. Phys. Lipids*, Vol. 99, pp. 103–109, 1999.

[Iske98] S. Isken and J. A. M. de Bont. "Bacteria tolerant to organic solvents". *Extremophiles*, Vol. 2, No. 3, pp. 229–238, Aug. 1998.

[Isra91] J. Israelachvili. *Intermolecular and surface forces*. ACADEMIC PRESS, University of California, Santa Barbara, second Ed., NOV 1991. ISBN-13: 978-0-12-375181-2 ISBN-10: 0-12-375181-0.

[Jaco95] K. Jacobson, E. D. Sheets, and R. Simson. "Revisiting the fluid mosaic model of membranes". *Science*, Vol. 268, pp. 1441–1442, 1995.

[Jorg83] W. L. Jorgensen, J. Chandrasekhar, J. D. Madura, R. W. Impey, and M. L. Klein. "Comparison of simple potential functions for simulating liquid water". *J. Chem. Phys.*, Vol. 79, No. 2, pp. 926–935, 1983.

[Jorg84] W. L. Jorgensen, J. D. Madura, and C. J. Swenson. "Optimized intermolecular potential functions for liquid hydrocarbons". *J. Am. Chem. Soc.*, Vol. 106, No. 22, pp. 6638–6646, 1984.

[Jorg88] W. L. Jorgensen and J. Tirado-Rives. "The OPLS [optimized potentials for liquid simulations] potential functions for proteins, energy minimizations for crystals of cyclic peptides and crambin". *J. Am. Chem. Soc.*, Vol. 110, No. 6, pp. 1657–1666, 1988.

[Jorg96] W. L. Jorgensen, D. S. Maxwell, and J. Tirado-Rives. "Development and Testing of the OPLS All-Atom Force Field on Conformational Energetics and Properties of Organic Liquids". *J. Am. Chem. Soc.*, Vol. 118, No. 45, pp. 11225–11236, Jan. 1996.

[Kami01] G. A. Kaminski, R. A. Friesner, J. Tirado-Rives, and W. L. Jorgensen. "Evaluation and Reparametrization of the OPLS-AA Force Field for Proteins via Comparison with Accurate Quantum Chemical Calculations on Peptides". *J. Phys. Chem. B*, Vol. 105, No. 28, pp. 6474–6487, July 2001.

[Kane98] F. Kaneko, J. Yano, and K. Sato. "Diversity in the fatty-acid conformation and chain packing of cis-unsaturated lipids". *Curr. Opin. Struct. Biol.*, Vol. 8(4), pp. 417–425, 1998.

[Kino77] K. Kinosita, S. Kawato, and A. Ikegami. "A theory of fluorescence polarization decay in membranes". *Biophys. J.*, Vol. 20, No. 3, pp. 289–305, Dec. 1977.

[Kobe98] M. Köberl, H. J. Hinz, and G. Rapp. "Temperature scanning simultaneous small- and wide-angle X-ray scattering studies on glycolipid vesicles: areas, expansion coefficients and hydration". *Chem. Phys. Lipids*, Vol. 91, No. 1, pp. 13–37, 1998.

[Korl99] J. Korlach, P. Schwille, W. W. Webb, and G. W. Feigenson. "Characterization of lipid bilayer phases by confocal microscopy and fluorescence correlation spectroscopy". *Proc. Natl. Acad. Sci. U. S. A.*, Vol. 96, No. 15, pp. 8461–8466, July 1999.

[Koyn98] R. Koynova and M. Caffrey. "Phases and phase transitions of the phosphatidylcholines". *Biochim. Biophys. Acta, Rev. Biomembr.*, Vol. 1376, No. 1, pp. 91–145, 1998.

[Kraf02] E. Kraffe, P. Soudant, Y. Marty, N. Kervarec, and P. Jehan. "Evidence of a tetradocosahexaenoic cardiolipin in some marine bivalves.". *Lipids*, Vol. 37, No. 5, pp. 507–514, May 2002.

[Krau04] F. Krause, N. H. Reifschneider, D. Vocke, H. Seelert, S. Rexroth, and N. A. Dencher. ""Respirasome-like supercomplexes in green leaf mitochondria of spinach.". *J. Biol. Chem.*, Vol. 279, No. 46, pp. 48369–48375, Nov 2004.

[Kuuc05] N. Kučerka, S. Tristram-Nagle, and J. Nagle. "Structure of Fully Hydrated Fluid Phase Lipid Bilayers with Monounsaturated Chains". *J. Membr. Biol.*, Vol. 208, No. 3, pp. 193–202, Jan. 2005.

[Kuuc08a] N. Kučerka, J. F. Nagle, J. N. Sachs, S. E. Feller, J. Pencer, A. Jackson, and J. Katsaras. "Lipid Bilayer Structure Determined by the Simultaneous Analysis of Neutron and X-Ray Scattering Data". *Biophys. J.*, Vol. 95, No. 5, pp. 2356–2367, Sep. 2008.

[Kuuc08b] N. Kučerka, J. D. Perlmutter, J. Pan, S. Tristram-Nagle, J. Katsaras, and J. N. Sachs. "The Effect of Cholesterol on Short- and Long-Chain Monounsaturated Lipid Bilayers as Determined by Molecular Dynamics Simulations and X-Ray Scattering". *Biophys. J.*, Vol. 95, No. 6, pp. 2792–2805, Sep. 2008.

[Leac01] A. R. Leach. *Molecular Modeling: Principles and applications.* Pearson, Prentice Hall, England, 2nd Ed., 2001.

[Lena07] G. Lenaz and M. L. Genova. "Kinetics of integrated electron transfer in the mitochondrial respiratory chain: random collisions vs. solid state electron channeling.". *Am J Physiol Cell Physiol*, Vol. 292, No. 4, pp. C1221–C1239, Apr 2007.

[Levy98] R. M. Levy and E. Gallicchio. "Computer simulations with explicit solvent: Recent Progress in the Thermodynamic Decomposition of Free Energies and in Modeling Electrostatic Effects". *Annu. Rev. Phys. Chem.*, Vol. 49, No. 1, pp. 531–567, 1998.

[Lewi88] R. N. A. H. Lewis, B. D. Sykes, and R. N. McElhaney. "Thermotropic phase behavior of model membranes composed of phosphatidylcholines containing cis-monounsaturated acyl chain homologs of oleic acid: differential scanning calorimetric and phosphorus-31 NMR spectroscopic studies". *Biochemistry*, Vol. 27, No. 3, pp. 880–887, 1988.

[Li03] X.-M. Li, M. M. Momsen, H. L. Brockman, and R. E. Brown. "Sterol Structure and Sphingomyelin Acyl Chain Length Modulate Lateral Packing Elasticity and Detergent Solubility in Model Membranes". *Biophys. J.*, Vol. 85, No. 6, pp. 3788–3801, Dec. 2003.

[Lind81] G. Lindblom, L. B. A. Johansson, and G. Arvidson. "Effect of cholesterol in membranes. Pulsed nuclear magnetic resonance measurements of lipid lateral diffusion". *Biochemistry*, Vol. 20, No. 8, pp. 2204–2207, 1981.

[Lipa80] G. Lipari and A. Szabo. "Effect of librational motion on fluorescence depolarization and nuclear magnetic resonance relaxation in macromolecules and membranes". *Biophys. J.*, Vol. 30, No. 3, pp. 489–506, June 1980.

[Liu04] Y. Liu and J. F. Nagle. "Diffuse scattering provides material parameters and electron density profiles of biomembranes". *Phys. Rev. E*, Vol. 69, No. 4, p. 040901, Apr. 2004.

[Macd87] P. M. Macdonald and J. Seelig. "Calcium binding to mixed cardiolipin-phosphatidylcholine bilayers as studied by deuterium nuclear magnetic resonance". *Biochemistry*, Vol. 26, No. 19, pp. 6292–6298, May 1987.

[MacK98] A. D. MacKerell, D. Bashford, Bellott, R. L. Dunbrack, J. D. Evanseck, M. J. Field, S. Fischer, J. Gao, H. Guo, S. Ha, D. Joseph-McCarthy, L. Kuchnir, K. Kuczera, F. T. K. Lau, C. Mattos, S. Michnick, T. Ngo, D. T. Nguyen, B. Prodhom, W. E. Reiher, B. Roux, M. Schlenkrich, J. C. Smith, R. Stote, J. Straub, M. Watanabe, J. Wiorkiewicz-Kuczera, D. Yin, and M. Karplus. "All-Atom Empirical Potential for Molecular Modeling and Dynamics Studies of Proteins". *J. Phys. Chem. B*, Vol. 102, No. 18, pp. 3586–3616, 1998.

[Mara82] B. Maraviglia, J. H. Davis, M. Bloom, J. Westerman, and K. W. Wirtz. "Human erythrocyte membranes are fluid down to -5C". *Biochim. Biophys. Acta, Biomembr.*, Vol. 686, No. 1, pp. 137–140, 1982.

[Mars07] D. Marsh. "Lateral Pressure Profile, Spontaneous Curvature Frustration, and the Incorporation and Conformation of Proteins in Membranes". *Biophys. J.*, Vol. 93, No. 11, pp. 3884–3899, Dec. 2007.

[Mars99] D. Marsh. "Thermodynamic Analysis of Chain-Melting Transition Temperatures for Monounsaturated Phospholipid Membranes: Dependence on cis-Monoenoic Double Bond Position". *Biophys. J.*, Vol. 77, No. 2, pp. 953–963, Aug. 1999.

[Mart07] H. Martinez-Seara, T. Róg, M. Pasenkiewicz-Gierula, I. Vattulainen, M. Karttunen, and R. Reigada. "Effect of Double Bond Position on Lipid Bilayer Properties: Insight through Atomistic Simulations". *J. Phys. Chem. B*, Vol. 111, No. 38, pp. 11162–11168, 2007.

[Mart08] H. Martinez-Seara, T. Róg, M. Karttunen, R. Reigada, and I. Vattulainen. "Influence of cis double-bond parametrization on lipid membrane properties: How seemingly insignificant details in force-field change even qualitative trends". *J. Chem. Phys.*, Vol. 129, No. 10, p. 105103, 2008.

[Math08] J. C. Mathai, S. Tristram-Nagle, J. F. Nagle, and M. L. Zeidel. "Structural Determinants of Water Permeability through the Lipid Membrane". *J. Gen. Physiol.*, Vol. 131, pp. 69–73, 2008.

[Mats06] K. Matsumoto, J. Kusaka, A. Nishibori, and H. Hara. "Lipid domains in bacterial membranes.". *Mol. Microbiol.*, Vol. 61, No. 5, pp. 1110–1117, Sep 2006.

[McCa94] J. L. McCauley. *Chaos, Dynamics, and Fractals: an Algorithmic Approach to Deterministic Chaos.* Cambridge University Press, Cambridge, 1994.

[McCo03] H. M. McConnell and A. Radhakrishnan. "Condensed complexes of cholesterol and phospholipids". *Biochim. Biophys. Acta, Biomembr.*, Vol. 1610, No. 2, pp. 159–173, 2003.

[McCo71a] H. M. McConnell and W. L. Hubbell. "Molecular motion in spin-labeled phospholipids and membranes". *J. Am. Chem. Soc.*, Vol. 93, No. 2, pp. 314–326, 1971.

[McCo71b] H. M. McConnell and R. D. Kornberg. "Inside-outside transitions of phospholipids in vesicle membranes". *Biochemistry*, Vol. 10, No. 7, pp. 1111–1120, 1971.

[McEl82] R. N. McElhaney. "Effects of Membrane Lipids on Transport and Enzymic Activities". *Curr. Top. Membr. Trans.*, Vol. 17, pp. 317–380, 1982.

[Meck03] K. R. Mecke, T. Charitat, and F. Graner. "Fluctuating Lipid Bilayer in an Arbitrary Potential: Theory and Experimental Determination of Bending Rigidity". *Langmuir*, Vol. 19, No. 6, pp. 2080–2087, 2003.

[Meer05] G. van Meer. "Cellular lipidomics". *EMBO J.*, Vol. 24, pp. 3159–3165, 2005.

[Meer08] G. van Meer, D. R. Voelker, and G. W. Feigenson. "Membrane lipids: where they are and how they behave". *Nat. Rev. Mol. Cell Biol.*, Vol. 9, No. 2, pp. 112–124, Feb. 2008.

[Mile00] E. Mileykovskaya and W. Dowhan. "Visualization of phospholipid domains in Escherichia coli by using the cardiolipin-specific fluorescent dye 10-N-nonyl acridine orange.". *J. Bacteriol.*, Vol. 182, No. 4, pp. 1172–1175, Feb 2000.

[Mile09] E. Mileykovskaya and W. Dowhan. "Cardiolipin membrane domains in prokaryotes and eukaryotes.". *Biochim. Biophys. Acta*, Vol. 1788, No. 10, pp. 2084–2091, Oct 2009.

[Miya92] S. Miyamoto and P. A. Kollman. "Settle: An analytical version of the SHAKE and RATTLE algorithm for rigid water models". *J. Comput. Chem.*, Vol. 13, No. 8, pp. 952–962, 1992.

[Mour84] O. Mouritsen and M. Bloom. "Mattress model of lipid-protein interactions in membranes". *Biophys. J.*, Vol. 46, No. 2, pp. 141–153, Aug. 1984.

[Murz01] K. Murzyn, T. Róg, G. Jezierski, Y. Takaoka, and M. Pasenkiewicz-Gierula. "Effects of Phospholipid Unsaturation on the Membrane/Water Interface: A Molecular Simulation Study". *Biophys. J.*, Vol. 81, No. 1, pp. 170–183, July 2001.

[Murz99] K. Murzyn and M. Pasenkiewicz-Gierula. "Construction and optimisation of a computer model for a bacterial membrane". *Acta Biochim. Pol.*, Vol. 46(1), pp. 631–639, 1999.

[Nagl00] J. F. Nagle and S. Tristram-Nagle. "Structure of lipid bilayers". *Biochim. Biophys. Acta, Rev. Biomembr.*, Vol. 1469, No. 3, pp. 159–195, 2000.

[Need88] D. Needham, T. J. McIntosh, and E. Evans. "Thermomechanical and transition properties of dimyristoylphosphatidylcholine/cholesterol bilayers". *Biochemistry*, Vol. 27, No. 13, pp. 4668–4673, 1988.

[Nich05] S. Nichols-Smith and T. Kuhl. "Electrostatic interactions between model mitochondrial membranes.". *Colloids Surf. B Biointerfaces*, Vol. 41, No. 2-3, pp. 121–127, Mar 2005.

[Niel99] M. Nielsen, L. Miao, J. H. Ipsen, M. J. Zuckermann, and O. G. Mouritsen. "Off-lattice model for the phase behavior of lipid-cholesterol bilayers". *Phys. Rev. E*, Vol. 59, No. 5, pp. 5790–5803, May 1999.

[Niem06] P. S. Niemelä, M. T. Hyvönen, and I. Vattulainen. "Influence of Chain Length and Unsaturation on Sphingomyelin Bilayers". *Biophys. J.*, Vol. 90, No. 3, pp. 851–863, Feb. 2006.

[Niem07] P. S. Niemelä, M. T. Ollila, Samuli andD Hyvönen, M. Karttunen, and I. Vattulainen. "Assessing the Nature of Lipid Raft Membranes". *PLoS Comput. Biol.*, Vol. 3, No. 2, p. e34, 02 2007.

[Nose84] S. Nosé. "A unified formulation of the constant temperature molecular dynamics methods". *J. Chem. Phys.*, Vol. 81, No. 1, pp. 511–519, 1984.

[Ohvo02] H. Ohvo-Rekilä, B. Ramstedt, P. Leppimäki, and J. P. Slotte. "Cholesterol interactions with phospholipids in membranes". *Prog. Lipid Res.*, Vol. 41, No. 1, pp. 66–97, 2002.

[Olli07] S. Ollila, M. T. Hyvonen, and I. Vattulainen. "Polyunsaturation in Lipid Membranes: Dynamic Properties and Lateral Pressure Profiles". *J. Phys. Chem. B*, Vol. 111, No. 12, pp. 3139–3150, 2007.

[Olss96] N. U. Olsson, A. J. Harding, C. Harper, and N. Salem. "High-performance liquid chromatography method with light-scattering detection for measurements of lipid class composition: analysis of brains from alcoholics". *J. Chromatogr. B*, Vol. 681, No. 2, pp. 213–218, 1996.

[Olss97] N. U. Olsson and J. N. Salem. "Molecular species analysis of phospholipids". *J. Chromatogr. B*, Vol. 692, pp. 245–256, 1997.

[Pan09] J. Pan, S. Tristram-Nagle, and J. F. Nagle. "Effect of cholesterol on structural and mechanical properties of membranes depends on lipid chain saturation". *Phys. Rev. E*, Vol. 80, No. 2, p. 021931, 2009.

[Parr81] M. Parrinello and A. Rahman. "Polymorphic transitions in single crystals: A new molecular dynamics method". *J. Appl. Phys.*, Vol. 52, No. 12, pp. 7182–7190, 1981.

[Patr03] M. Patra, M. Karttunen, M. Hyvönen, E. Falck, P. Lindqvist, and I. Vattulainen. "Molecular Dynamics Simulations of Lipid Bilayers: Major Artifacts Due to Truncating Electrostatic Interactions". *Biophys. J.*, Vol. 84, No. 6, pp. 3636–3645, June 2003.

[Patr04] M. Patra, M. Karttunen, M. T. Hyvonen, E. Falck, and I. Vattulainen. "Lipid Bilayers Driven to a Wrong Lane in Molecular Dynamics Simulations by Subtle Changes in Long-Range Electrostatic Interactions". *J. Phys. Chem. B*, Vol. 108, No. 14, pp. 4485–4494, 2004.

[Petr00] H. I. Petrache, S. W. Dodd, and M. F. Brown. "Area per Lipid and Acyl Length Distributions in Fluid Phosphatidylcholines Determined by 2H NMR Spectroscopy". *Biophys. J.*, Vol. 79, No. 6, pp. 3172–3192, Dec. 2000.

[Pinh94] T. J. Pinheiro, A. A. Duralski, and A. Watts. "Phospholipid headgroup-headgroup electrostatic interactions in mixed bilayers of cardiolipin with phosphatidylcholines studied by 2H NMR.". *Biochemistry*, Vol. 33, No. 16, pp. 4896–4902, Apr 1994.

[Powe85] G. L. Powell and D. Marsh. "Polymorphic phase behavior of cardiolipin derivatives studied by 31P NMR and X-ray diffraction.". *Biochemistry*, Vol. 24, No. 12, pp. 2902–2908, Jun 1985.

[Pric01] M. L. P. Price, D. Ostrovsky, and W. L. Jorgensen. "Gas-phase and liquid-state properties of esters, nitriles, and nitro compounds with the OPLS-AA force field". *J. Comput. Chem.*, Vol. 22, No. 13, pp. 1340–1352, 2001.

[Priv88] P. L. Privalov and S. J. Gill. "Stability of Protein Structure and Hydrophobic Interaction". *Advances in Protein Chemistry*, Vol. 39, pp. 191–234, 1988.

[Qiu 90] W. Qiu-Dong. "The global solution of the N-body problem". *Celest. Mech. Dyn. Astr.*, Vol. 50, No. 1, pp. 73–88, March 1990.

[Radh05] A. Radhakrishnan and H. McConnell. "Condensed complexes in vesicles containing cholesterol and phospholipids". *Proc. Natl. Acad. Sci. U. S. A.*, Vol. 102, No. 36, pp. 12662–12666, Sep. 2005.

[Radh99a] A. Radhakrishnan and H. M. McConnell. "Cholesterol–Phospholipid Complexes in Membranes". *J. Am. Chem. Soc.*, Vol. 121, No. 2, pp. 486–487, 1999.

[Radh99b] A. Radhakrishnan and H. M. McConnell. "Condensed Complexes of Cholesterol and Phospholipids". *Biophys. J.*, Vol. 77, No. 3, pp. 1507–1517, Sep. 1999.

[Rams02] B. Ramstedt and J. P. Slotte. "Membrane properties of sphingomyelins". *FEBS Lett.*, Vol. 531, No. 1, pp. 33–37, 2002.

[Ranc82] M. Rance, K. R. Jeffrey, A. P. Tulloch, K. W. Butler, and I. C. Smith. "Effects of cholesterol on the orientational order of unsaturated lipids in the membranes of Acholeplasma laidlawii: A 2H-NMR study". *Biochim. Biophys. Acta, Biomembr.*, Vol. 688, No. 1, pp. 191–200, 1982.

[Rawi00] W. Rawicz, K. Olbrich, T. McIntosh, D. Needham, and E. Evans. "Effect of Chain Length and Unsaturation on Elasticity of Lipid Bilayers". *Biophys. J.*, Vol. 79, No. 1, pp. 328–339, July 2000.

[Rizz99] R. C. Rizzo and W. L. Jorgensen. "OPLS All-Atom Model for Amines: Resolution of the Amine Hydration Problem". *J. Am. Chem. Soc.*, Vol. 121, No. 20, pp. 4827–4836, May 1999.

[Rog01] T. Róg and M. Pasenkiewicz-Gierula. "Cholesterol effects on the phosphatidylcholine bilayer nonpolar region: a molecular simulation study.". *Biophys J*, Vol. 81, No. 4, pp. 2190–2202, Oct 2001.

[Rog07a] T. Róg, M. Pasenkiewicz-Gierula, I. Vattulainen, and M. Karttunen. "What Happens if Cholesterol Is Made Smoother: Importance of Methyl Substituents in Cholesterol Ring Structure on Phosphatidylcholine–Sterol Interaction". *Biophys. J.*, Vol. 92, No. 10, pp. 3346–3357, May 2007.

[Rog07b] T. Róg, I. Vattulainen, A. Bunker, and M. Karttunen. "Glycolipid Membranes through Atomistic Simulations: Effect of Glucose and Galactose Head Groups on Lipid Bilayer Properties". *J. Phys. Chem. B*, Vol. 111, No. 34, pp. 10146–10154, Aug. 2007.

[Rog08a] T. Róg, L. M. Stimson, M. Pasenkiewicz-Gierula, I. Vattulainen, and M. Karttunen. "Replacing the Cholesterol Hydroxyl Group with the Ketone Group Facilitates Sterol Flip-Flop and Promotes Membrane Fluidity". *J. Phys. Chem. B*, Vol. 112, No. 7, pp. 1946–1952, 2008.

[Rog08b] T. Róg, I. Vattulainen, M. Jansen, E. Ikonen, and M. Karttunen. "Comparison of cholesterol and its direct precursors along the biosynthetic pathway: Effects of cholesterol, desmosterol and 7-dehydrocholesterol on saturated and unsaturated lipid bilayers". *J. Chem. Phys.*, Vol. 129, No. 15, p. 154508, 2008.

[Romi72] J. C. Romijn, L. M. van Golde, R. N. McElhaney, and L. L. van Deenen. "Some studies on the fatty acid composition of total lipids and phosphatidylglycerol from Acholeplasma laidlawii B and their relation to the premeability of intact cells of this organism.". *Biochim. Biophys. Acta*, Vol. 280, No. 1, pp. 22–32, Sep 1972.

[Rott79a] S. Rottem and O. Markowitz. "Membrane lipids of Mycoplasma gallisepticum: a disaturated phosphatidylcholine and a phosphatidylglycerol with an unusual positional distribution of fatty acids.". *Biochemistry*, Vol. 18, No. 14, pp. 2930–2935, Jul 1979.

[Rott79b] S. Rottem and O. Markowitz. "Unusual positional distribution of fatty acids in phosphatidylglycerol of sterol-requiring mycoplasmas.". *FEBS Lett.*, Vol. 107, No. 2, pp. 379–382, Nov 1979.

[Rube79] J. L. Rubenstein, B. A. Smith, and H. M. McConnell. "Lateral diffusion in binary mixtures of cholesterol and phosphatidylcholines". *Proc. Natl. Acad. Sci. U. S. A.*, Vol. 76, No. 1, pp. 15–18, Jan. 1979.

[Ruiz07] M. Ruiz Villarreal. "Cell membrane detailed diagram: Catalan version (wikipedia)". http://commons.wikimedia.org/wiki/File:Cell_membrane_detailed_diagram_cat.svg.

[Ruoc82] M. J. Ruocco and G. Shipley. "Characterization of the sub-transition of hydrated dipalmitoylphosphatidylcholine bi layers. Kinetic, hydration and structural study". *Biochim. Biophys. Acta, Biomembr.*, Vol. 691, No. 2, pp. 309–320, 1982.

[Sait77] Y. Saito, J. R. Silvius, and R. N. McElhaney. "Membrane lipid biosynthesis in Acholeplasma laidlawii B. Relationship between fatty acid structure and the positional distribution of esterified fatty acids in phospho- and glycolipids from growing cells.". *Arch. Biochem. Biophys.*, Vol. 182, No. 2, pp. 443–454, Aug 1977.

[Sanz06] A. Sanz, R. Pamplona, and G. Barja. "Is the mitochondrial free radical theory of aging intact?". *Antioxid. Redox Sign.*, Vol. 8, No. 3-4, pp. 582–599, 2006.

[Sast00] J. Sastre, F. V. Pallardó, J. G. de la Asunción, and J. Viña. "Mitochondria, oxidative stress and aging.". *Free Radic. Res.*, Vol. 32, No. 3, pp. 189–198, Mar 2000.

[Schl00] M. Schlame, D. Rua, and M. L. Greenberg. "The biosynthesis and functional role of cardiolipin.". *Prog. Lipid Res.*, Vol. 39, No. 3, pp. 257–288, May 2000.

[Schl06] M. Schlame and M. Ren. "Barth syndrome, a human disorder of cardiolipin metabolism.". *FEBS Lett.*, Vol. 580, No. 23, pp. 5450–5455, Oct 2006.

[Seel77] A. Seelig and J. Seelig. "Effect of a single cis double bond on the structure of a phospholipid bilayer". *Biochemistry*, Vol. 16, No. 1, pp. 45–50, 1977.

[Shoe02] S. D. Shoemaker and T. K. Vanderlick. "Intramembrane electrostatic interactions destabilize lipid vesicles.". *Biophys. J.*, Vol. 83, No. 4, pp. 2007–2014, Oct 2002.

[Simi88] D. Siminovitch, P. Wong, R. Berchtold, and H. Mantsch. "A comparison of the effect of one and two mono-unsaturated acyl chains on the structure of phospholipid bilayers: a high pressure infrared spectroscopic study". *Chem. Phys. Lipids*, Vol. 46, No. 2, pp. 79–87, 1988.

[Simo00] K. Simons and E. Ikonen. "How Cells Handle Cholesterol". *Science*, Vol. 290, No. 5497, pp. 1721–1726, Dec. 2000.

[Simo04] K. Simons and W. L. Vaz. "Model systems, lipid rafts, and cell membranes". *Annu. Rev. Biophys. Biomol. Struct.*, Vol. 33, No. 1, pp. 269–295, 2004.

[Simo97] K. Simons and E. Ikonen. "Functional rafts in cell membranes". *Nature*, Vol. 387, No. 6633, pp. 569–572, June 1997.

[Sing72] S. J. Singer and G. L. Nicolson. "The Fluid Mosaic Model of the Structure of Cell Membranes". *Science*, Vol. 175, No. 4023, pp. 720–731, Feb. 1972.

[Smon99] A. M. Smondyrev and M. L. Berkowitz. "Structure of Dipalmitoylphosphatidylcholine/Cholesterol Bilayer at Low and High Cholesterol Concentrations: Molecular Dynamics Simulation". *Biophys. J.*, Vol. 77, No. 4, pp. 2075–2089, Oct. 1999.

[Some09] P. Somerharju, J. A. Virtanen, K. H. Cheng, and M. Hermansson. "The superlattice model of lateral organization of membranes and its implications on membrane lipid homeostasis". *Biochim. Biophys. Acta, Biomembr.*, Vol. 1788(1), pp. 12–23, 2009.

[Some99] P. Somerharju, J. A. Virtanen, and K. H. Cheng. "Lateral organisation of membrane lipids: The superlattice view". *Biochim. Biophys. Acta, Mol. Cell Biol. Lipids*, Vol. 1440, No. 1, pp. 32–48, 1999.

[Spoe05] D. van der Spoel, E. Lindahl, B. Hess, C. Kutzner, A. R. van Buuren, E. Apol, P. J. Meulenhoff, D. P. Tieleman, A. L. Sijbers, K. A. Feenstra, R. van Drunen, and H. J. Berendsen. *Gromacs User Manual version 4.0.* www.gromacs.org, 2005.

[Stei69] J. M. Steim, M. E. Tourtellotte, J. C. Reinert, R. N. McElhaney, and R. L. Rader. "Calorimetric evidence for the liquid-crystalline state of lipids in biomembrane.". *Proc. Natl. Acad. Sci. U. S. A.*, Vol. 63, No. 1, pp. 104–109, May 1969.

[Subc07] W. K. Subczynski, A. Wisniewska, J. S. Hyde, and A. Kusumi. "Three-Dimensional Dynamic Structure of the Liquid-Ordered Domain in Lipid Membranes as Examined by Pulse-EPR Oxygen Probing". *Biophys. J.*, Vol. 92, No. 5, pp. 1573–1584, March 2007.

[Subc89] W. K. Subczynski, J. S. Hyde, and A. Kusumi. "Oxygen permeability of phosphatidylcholine–cholesterol membranes". *Proc. Natl. Acad. Sci. U. S. A.*, Vol. 86, No. 12, pp. 4474–4478, June 1989.

[Subc91] W. K. Subczynski, J. S. Hyde, and A. Kusumi. "Effect of alkyl chain unsaturation and cholesterol intercalation on oxygen transport in membranes: a pulse ESR spin labeling study". *Biochemistry*, Vol. 30, No. 35, pp. 8578–8590, 1991.

[Subc94] W. K. Subczynski, A. Wisniewska, J.-J. Yin, J. S. Hyde, and A. Kusumi. "Hydrophobic Barriers of Lipid Bilayer Membranes Formed by Reduction of Water Penetration by Alkyl Chain Unsaturation and Cholesterol". *Biochemistry*, Vol. 33, No. 24, pp. 7670–7681, 1994.

[Sud07] M. Sud, E. Fahy, D. Cotter, A. Brown, E. A. Dennis, C. K. Glass, J. Merrill, Alfred H., R. C. Murphy, C. R. H. Raetz, D. W. Russell, and S. Subramaniam. "LMSD: LIPID MAPS structure database". *Nucl. Acids Res.*, Vol. 35, No. suppl_1, pp. D527–532, Jan. 2007.

[Suga05] I. P. Sugar and R. L. Biltonen. "Lateral Diffusion of Molecules in Two-Component Lipid Bilayer: A Monte Carlo Simulation Study". *J. Phys. Chem. B*, Vol. 109, No. 15, pp. 7373–7386, 2005.

[Taka00] Y. Takaoka, M. Pasenkiewicz-Gierula, H. Miyagawa, K. Kitamura, Y. Tamura, and A. Kusumi. "Molecular Dynamics Generation of Nonarbitrary Membrane Models Reveals Lipid Orientational Correlations". *Biophys. J.*, Vol. 79, No. 6, pp. 3118–3138, Dec. 2000.

[Tiel02] D. P. Tieleman and J. Bentz. "Molecular Dynamics Simulation of the Evolution of Hydrophobic Defects in One Monolayer of a Phosphatidylcholine Bilayer: Relevance for Membrane Fusion Mechanisms". *Biophys. J.*, Vol. 83, No. 3, pp. 1501–1510, Sep. 2002.

[Tiel96] D. P. Tieleman and H. J. C. Berendsen. "Molecular dynamics simulations of a fully hydrated dipalmitoylphosphatidylcholine bilayer with different macroscopic boundary conditions and parameters". *J. Chem. Phys.*, Vol. 105, No. 11, pp. 4871–4880, Sep. 1996.

[Tiel97] D. P. Tieleman, S. J. Marrink, and H. J. C. Berendsen. "A computer perspective of membranes: molecular dynamics studies of lipid bilayer systems". *Biochim. Biophys. Acta, Rev. Biomembr.*, Vol. 1331, No. 3, pp. 235–270, 1997.

[Tiel99] H. J. Tieleman, D. P.and Berendsen and M. S. Sansom. "An Alamethicin Channel in a Lipid Bilayer: Molecular Dynamics Simulations". *Biophys. J.*, Vol. 76, No. 4, pp. 1757–1769, Apr. 1999.

[Tris02] S. Tristram-Nagle, Y. Liu, J. Legleiter, and J. F. Nagle. "Structure of Gel Phase DMPC Determined by X-Ray Diffraction". *Biophys. J.*, Vol. 83, No. 6, pp. 3324–3335, Dec. 2002.

[Vain06] S. Vainio, M. Jansen, M. Koivusalo, T. Róg, M. Karttunen, I. Vattulainen, and E. Ikonen. "Significance of Sterol Structural Specificity: Demosterol connot replace cholesterol in lipid rafts". *J. Biol. Chem.*, Vol. 281, No. 1, pp. 348–355, 2006.

[Van 65] L. L. M. Van Deenen. *Progress of Chemistry of Fats and Other Lipids*, Chap. 1, pp. 1–47. Vol. 1, Pergamon, New York, 1965.

[Vand94] G. Vanderkooi. "Computation of mixed phosphatidylcholine-cholesterol bilayer structures by energy minimization". *Biophys. J.*, Vol. 66, No. 5, pp. 1457–1468, May 1994.

[Vaz89] W. L. Vaz, E. C. Melo, and T. E. Thompson. "Translational diffusion and fluid domain connectivity in a two-component, two-phase phospholipid bilayer". *Biophys. J.*, Vol. 56, No. 5, pp. 869–876, Nov. 1989.

[Veat03] S. L. Veatch and S. L. Keller. "Separation of Liquid Phases in Giant Vesicles of Ternary Mixtures of Phospholipids and Cholesterol". *Biophys. J.*, Vol. 85, No. 5, pp. 3074–3083, Nov. 2003.

[Veat05a] S. L. Veatch and S. L. Keller. "Miscibility Phase Diagrams of Giant Vesicles Containing Sphingomyelin". *Phys. Rev. Lett.*, Vol. 94, No. 14, p. 148101, Apr 2005.

[Veat05b] S. L. Veatch and S. L. Keller. "Seeing spots: Complex phase behavior in simple membranes". *Biochim. Biophys. Acta, Mol. Cell Res.*, Vol. 1746, No. 3, pp. 172–185, 2005.

[Vere03] G. Vereb, J. Szöllösi, J. Matkó, P. Nagy, T. Farkas, L. Vígh, L. Mátyus, T. A. Waldmann, and S. Damjanovich. "Dynamic, yet structured: The cell membrane three decades after the Singer-Nicolson model". *Proc. Natl. Acad. Sci. U. S. A.*, Vol. 100, No. 14, pp. 8053–8058, July 2003.

[Verl67] L. Verlet. "Computer "Experiments"on Classical Fluids. I. Thermodynamical Properties of Lennard-Jones Molecules". *Phys. Rev.*, Vol. 159, No. 1, pp. 98–103, July 1967.

[Wang04] J. Wang, Megha, and E. London. "Relationship between Sterol/Steroid Structure and Participation in Ordered Lipid Domains (Lipid Rafts): Implications for Lipid Raft Structure and Function". *Biochemistry*, Vol. 43, No. 4, pp. 1010–1018, 2004.

[Wang95] G. Wang, H.-n. Lin, S. Li, and C.-h. Huang. "Phosphatidylcholines with sn-1 Saturated and sn-2 cis-Monounsaturated Acyl Chains". *J. Biol. Chem.*, Vol. 270, No. 39, pp. 22738–22746, Sep. 1995.

[Wein84] S. J. Weiner, P. A. Kollman, D. A. Case, U. C. Singh, C. Ghio, G. Alagona, S. Profeta, and P. Weiner. "A new force field for molecular mechanical simulation of nucleic acids and proteins". *J. Am. Chem. Soc.*, Vol. 106, No. 3, pp. 765–784, 1984.

[Zhao07a] J. Zhao, J. Wu, F. A. Heberle, T. T. Mills, P. Klawitter, G. Huang, G. Costanza, and G. W. Feigenson. "Phase studies of model biomembranes: Complex behavior of DSPC/DOPC/Cholesterol". *Biochim. Biophys. Acta, Biomembr.*, Vol. 1768(11), pp. 2764–2776, 2007.

[Zhao07b] W. Zhao, T. Róg, A. A. Gurtovenko, I. Vattulainen, and M. Karttunen. "Atomic-Scale Structure and Electrostatics of Anionic Palmitoyloleoylphosphatidylglycerol Lipid Bilayers with Na^+ Counterions". *Biophys. J.*, Vol. 92, No. 4, pp. 1114–1124, Feb. 2007.